Fusogenic membrane glycoproteins as a gene therapy for cancer

Thesis

FUSOGENIC MEMBRANE GLYCOPROTEINS AS A GENE THERAPY FOR CANCER

ANDREW R. BATEMAN

MB BS, MRCP, FRCR

A thesis submitted in partial fulfilment of the requirements of the Open University for the degree of Doctor of Philosophy

September 2002

Molecular Medicine Program
Mayo Foundation
200 First street SW
Rochester Minnesota

DATE OF SUBMISSION: 27 MARCH 2003
DATE OF AWARD: 11 DECEMBER 2003

ProQuest LLC.
789 East Eisenhower Parkway
P.O. Box 1346
Ann Arbor, MI 48106 – 1346

Abstract

Gene therapy strategies hold great promise for the treatment of cancer. This work tests the hypothesis that viral fusogenic membrane glycoproteins (FMG) have potential as cytotoxic gene therapy agents. The truncated, hyperfusogenic form of a C-type retrovirus envelope gene: the Gibbon ape leukaemia virus envelope (GALV), and the F and H genes of the paramyxovirus Measles, were the predominate FMG investigated. Initial studies demonstrated the cytotoxicicty of expressing FMG in tumour cells *in vitro*. Extensive cell death occured following cell-cell fusion and syncitia formation. Comparison with suicide genes indicated superior cell killing with FMG due to a greater bystander effect. FMG killing induced a stress response with induction and upregulation of heat shock proteins. Detailed analysis of cell death following FMG expression and syncitia formation suggested a non-apoptotic, necrotic mechanism. This was independent of the cell cycle.

Viral vectors expressing FMG were developed. There was inefficient production of retroviral vectors based on the Moloney murine leukaemia virus expressing GALV. Improved titre was seen from a lentiviral vector expressing GALV. This vector, when injected intratumourally, was able to eradicate small tumours in nude mice.

Adenoviral vectors expressing F and H were produced. Intratumoural injection of these vectors resulted in syncitia formation in vivo. Direct intratumoural injection of an H expressing adenoviral vector into human xenograft tumours expressing Measles F resulted in tumour eradication in 30% of mice. Production of an adenoviral vector expressing GALV required a strategy involving Cre recombinase and a transcriptional silencer to overcome the direct cytotoxicity to producer cells.

Co-expression of granulocyte-macrophage colony-stimulating factor (GM-CSF) with FMG by a number of mechanisms was developed. Their particular in vitro properties were analysed in detail.

In summary this thesis represents the initial studies of a group of genes with their novel application as gene therapy agents for the treatment of cancer. Incorporation of FMG in the development of cytotoxic and immunomodulatory gene therapy strategies hold significant promise and merit further development.

ACKNOWLEDGEMENTS

First and foremost I would like to thank Dr Richard Vile for being everything a supervisor should be and more. As well as taking me on a tour of the world his lab provided such a great environment for scientific endeavour that it was a pleasure to be a part of. His energy and enthusiasm for cancer research is infectious and I feel priviliged to have been guided by such a teacher. I am indebted to him for giving me such a fantastic PhD subject and developing my scientific career. Of course one of the lasting lessons and skills learnt will be how to throw a tight spiral in confined spaces.

I would like to thank my lab mates who taught me a great deal, laughed a lot and helped make the Vile lab what it was and is: they were in chronological order Alan, Smurph, Nicki, Todders, Emma, Lisa, Michael, Anja, Atique, David, Marka, Vy, Kevin, Heung, Bernard.

I would also like to thank Dr Steve Russell not only for his help and enthusiasm with regards to my project, but also as Director of the MMP for making it such a stimulating and friendly place to work.

Thanks also goes to colleagues who helped with various aspects of the project and includes Dimitri, Del, Dr Jeff Salisbury, Dr Scott Kauffman, Tim, John.

The Mayo Graduate school and Cathy Chellgren in particular deserve many thanks for help in setting up the link with the Open University and allowing me the opportunity to study for a PhD.

Finally I would like to thank my family: my grandfather who set me out on this road, my parents who provided me with the where for all to make the trip and my wife, Peta who sustained me on the journey. Particular thanks goes to Lauren who delayed her birth so I could finish making an adenovirus, and Joshua who managed to cry just enough so his Mother would wake but not his Father.

TABLE OF CONTENTS

LIST OF ILLUSTRATIONS Page

Chapter 1

Chapter 3

LIST OF TABLES **Page**

CHAPTER 1:INTRODUCTION TO GENE THERAPY AND FUSOGENIC MEMBRANE GLYCOPROTEINS

1.1 Introduction

There remains a pressing need for novel cancer therapies. Cancer continues to increase in terms of its percentage of all causes of death and despite much effort five year survival rates are extremely poor for a significant number of solid tumours. For example, of the projected 28,300 new cases of pancreatic cancer diagnosed in the US in 2000, there will be an estimated 28,200 deaths (SEER 1997 overview). This stark outlook for patients and inferred failure of current mainstream therapies is not confined to the minority of solid tumour types, but a wide variety of tumour types have a survival of less than 30% (SEER projected survival 2000). In the past 20 years enhancement of traditional therapies such as radiation (Saunders et al., 1999) or addition of novel chemotherapeutic agents (McGuire et al., 1997), has only had a modest impact on subsets of patients. The greatest gains appear to have been made through early detection e.g. cervical and breast cancer screening. Indeed the greatest gains in terms of reduction in cancer deaths would come from prevention; specifically cessation of smoking – not a new idea!

In terms of novel therapies there have been a number of notable successes which have made the transition from basic science to mainstream clinical usage (Cobleigh et al., 1999; Coiffier et al., 2002; Kantarjian et al., 2002; Savage and Antman, 2002; Vogel et al., 2002). The benefit of these newer therapies is not only their therapeutic efficacy but also their reduced side effect profile compared to traditional anti-cancer modalities. An additional benefit is that these successes of 'targeted' therapy leave room for tempered optimism that further research will lead to improved treatments for cancer. Balanced against these successes there have been a number of strategies heralded as potential 'wonder' treatments which as of yet have not performed in clinical trials; most notably matrix metalloproteinase inhibitors and anti-angiogenic therapies.

A novel therapy that holds great promise but as yet has not delivered significant therapeutic benefit is gene therapy. The continued increased understanding of cancer at the molecular level (Hanahan and Weinberg, 2000) enhances the view that gene therapy is an attractive proposition for treating cancer. In considering any gene therapy two components need to be assessed: the therapeutic genetic material and the means to deliver this to target

cells. For gene therapy to show clinical efficacy both these components will need to be optimised.

1.2 Gene therapy strategies

Transfer of genetic material to accomplish a therapeutic intervention in cancer patients can be achieved by a number of strategies. They include:

1. Genetic sequence-targeted therapies e.g. antisense therapy, ribozymes.
2. Tumour suppressor gene therapy
3. Cytoreductive gene therapy
4. Immunomodulation
5. Antiangiogenic gene therapy

Cytoreductive gene therapy will be discussed in detail, the remainder will be briefly outlined. Genetic sequence-targeted therapies and tumour suppressor gene therapy target specific mutations within tumour cells: antisense is the production of an oligodeoxynucleotide capable of binding a specific target mRNA sequence (usually of an 'oncogene') which results in inhibition of translation or transcription. Ribozymes, enzymatic RNA molecules, also can be designed to target specific mRNA for degradation. Tumour suppressor gene therapy acts to replace a key gene function lost in the malignant transformation, such as p53. These approaches have undergone marked development and are currently being explored in the clinical setting (Clayman et al., 1999; Cunningham et al., 2000; Roth et al., 1996; Schuler et al., 1998; Swisher et al., 1999; Tait et al., 1999; Webb et al., 1997) and detailed reviews are indicated (Cotter, 1999; Marcusson et al., 1999; Turner, 2000). However, at the present time, these agents may not be the most attractive for tackling cancer in patients for a number of reasons including: a) tumours are heterogeneous and these therapies are highly specific; b) these strategies would require a very high percentage, if not all, of the tumour cell population to be successfully transduced, a goal which is currently not achieveable; c) the complexity of the mutations within cancer cells may cause an ineffective result even with successful delivery e.g transferred wild type p53 being 'knocked out' by dominant negative mutants.

Gene therapy strategies aimed specifically at inducing an anti-tumour immune response can be grouped under the heading: Immunomodulation. The immune system has the

ability to be highly specific and systemic in its effects. Coupled with this is the potential for massive amplification of response and the production of long lasting memory. It is not surprising therefore that at present approximately two-thirds of current cancer gene therapy clinical trials registered on the NIH RAC database are for immunotherapies (Diaz and Vile, 1999). A detailed review of present developments in this field is (Davis, 2000).

Antiangiogenic therapy has grown out of the realisation of the critical role host stromal cells, and endothelial cells in particular, play in the development of tumours (Hanahan and Weinberg, 2000). For tumours to develop beyond a 1-2mm size and metastasise it is an essential requirement that they develop the ability to induce angiogenesis (Hanahan and Folkman, 1996). Angiogenesis is under complex control with both proangiogenic factors - including basic fibroblast growth factor (bFGF) and vascular endothelial growth factor (VEGF), and inhibitory factors - including angiostatin, endostatin, reviewed in detail in (Desai and Libutti, 1999). The process of tumour angiogenesis occurs via a series of steps including endothelial cell migration, proliferation and maturation. This results in a diverse group of potential targets for intervention (Bergers et al., 1999; Harris and Thorgeirsson, 1998). Importantly, in the adult, physiological angiogenesis is confined to pregnancy and the normal female reproductive cycle. (Pathologically it plays a role in wound healing and disease states other than malignancy such as diabetic retinopathy and rheumatoid arthritis.) This means that antiangiogenic therapy is likely to have little direct toxicity. Another key benefit is that the target cell, the endothelial cell, has normal physiology and should respond in a predictable manner without the development of a resistant phenotype (Boehm et al., 1997). However there have been problems bringing antiangiogenic agents into the clinic, these include problems with production of recombinant forms of endogenous inhibitors of angiogenesis, high dose requirements and the probable need for longterm administration. Despite these issues antiangiogenic gene therapy remains an attractive alternative approach and a detailed review of current developments can be seen in (Feldman and Libutti, 2000).

1.2.1 Cytoreductive gene therapy (CGT)

This category of gene therapy strategies includes those genes that when expressed will lead to the death of the cell. At present the major group of genes within this category are

the suicide genes. Replication competent viruses will also be discussed in this group as they have primarily been investigated due to their direct cytotoxic effects. The novel fusogenic membrane glycoproteins (FMG) should be classified in this group and will be introduced.

1.2.1.1 Suicide genes

Suicide genes are the most widely utilised and studied cytoreductive genes. These are genes which, when expressed in a target population, induce sensitivity to a specific prodrug. Metabolism of this prodrug by the therapeutic gene product produces a significantly more toxic drug resulting in target cell death (Moolten, 1986). The most commonly used suicide gene to date is Herpes Simplex Virus type 1 thymidine kinase (HSVtk). Additional suicide genes under development are listed in **Table 1**. The HSVtk gene product phosphorylates purine analogs (e.g. ganciclovir, acyclovir) approximately 1,000 times more efficiently than mammalian enzymes. The monophosphate is then further phosphorylated by cellular kinases to generate the triphosphate form. This is incorporated into DNA in S phase of the cell cycle, resulting in chain termination and DNA α-polymerase inhibition, and cell death. Preclinical studies showed the efficacy of this approach (Moolten, 1994), and also identified a critical component of any cytoreductive gene therapy, namely the bystander effect (BE). This relates to the observation that the number of killed cells is significantly greater than the number expressing the transgene (Freeman et al., 1993). In vitro, this phenomenon is due to the cell expressing the suicide gene converting the prodrug and releasing the toxic drug locally to its neighbours either via gap junctions or apoptotic vesicles in the case of HSVtk / ganciclovir, or by free diffusion in the case of Cytosine Deaminase (CD)/ 5-Fluorocytosine (5FC). In vivo, the more significant mediator of BE is via immune mechanisms (Gagandeep et al., 1996; Vile et al., 1994). Thus with only 10% of a target population expressing HSVtk, significant tumour responses can be seen in immunocompetent animals, which are lost in immunodeficient mice. These observations led to clinical trials, a number of which have been published.

The first reported clinical trial was in recurrent malignant brain tumours (Ram et al., 1997). Patients received intratumoural implantation of $1x10^8$-$1x10^9$ murine HSVtk

Table 1.1: Examples of GDEPT systems which are currently the subject of preclinical and clinical investigation. (Modified from Connors 1995).

Enzyme	Prodrug	Active Drug	Ref
HSVtk	Ganciclovir	Ganciclovir triphosphate	Moolten86
Cytosine deaminase	5-fluorocytosine	5-fluorouracil	Mullen92
DT diaphorase	CB 1954	5-(aziridin-1-yl)-4-hydroxylamino-2-nitrobenzamide	Anlezark92
Nitroreductase	CB 1954	5-(aziridin-1-yl)-4-hydroxylamino-2-nitrobenzamide	Anlezark92
Guanine phosphoribosyl tarnsferase	6-thioxanthine	6-thioxanthine monophosphate	Mroz 93
Purine nucleoside phosphorylase	6-methyl-purine-2'-deoxynucleoside	6-methylpurine	Sorscher94
Thymidine phosphorylase	5'-deoxy-5-fluorouridine	5-fluorouracil	Patterson 95
Carboxylesterase	Irinotecan (CPT-11)	SN-38	Danks98
Folylpolyglutamyl synthetase	Edatrexate	Edatrexate polyglutamate	Aghi99
Carboxypeptidase A1	Methotrexate-α-peptides	Methotrexate	Hamstra00
Carboxypeptidase G2	Benzoic acid mustard glutamates	Benzoic acid mustards	Marais 96
Cytochrome P-450 (CYP2B1)	Cyclophosphamide, Ifosfamide	Phosphoramide mustard	ChenL96

retroviral producing cells via closely spaced (5-10mm) needle tracts. Seven days after implantation patients received i.v. ganciclovir and 5 small tumours showed radiologically detectable responses. Two patients had further surgical intervention prior to ganciclovir at day 7 which allowed an assessment of in vivo transfer of the transgene: Immunohistochemistry revealed very low transduction efficiency confined to the immediate collar of cells around needle tracts and a prefential transduction of endothelial cells in tumour neovasculature. There appeared to be no added toxicity of this gene therapy approach above neurosurgical intervention. The conclusions from this study and additional trials (Klatzmann et al., 1998a; Klatzmann et al., 1998b; Shand et al., 1999; Sterman et al., 1998) identify a possible therapeutic benefit of HSVtk / ganciclovir therapy, low toxicity profile, but the most striking finding is the poor transduction efficiency. Assessment of superficial malignant melanoma nodules directly injected with murine HSVtk retroviral vector-producer cells suggested a transduction efficiency of tumour cells of less than 1% (Klatzmann et al., 1998a). Equally adenoviral delivery of HSVtk in malignant mesothelioma again showed poor transduction efficiency although there was a dose dependent relationship (Sterman et al., 1998). Better vectors for gene delivery are needed before a meaningful analysis of suicide genes as therapy can be made (Vile et al., 2000). Toxicity will also have to be carefully monitored should the HSVtk system be utilised in a more systemic approach or with adenoviral vectors following preclinical data identifying the potential for significant hepatotoxicity (van der Eb et al., 1998).

That said, developments have occurred to enhance the therapeutic benefit of HSVtk. Through random sequence mutagenesis, more active thymidine kinases have been produced which may lead to greater activity or a substrate preference for acyclovir over ganciclovir, which would yield benefits due to the better toxicity profile of the former (Kokoris et al., 2000). Other groups have looked to combine suicide genes to exploit multiple mechanisms of action, in a similar way to the development of multiagent systemic chemotherapy. The combination of HSVtk with CD has proven synergistic (Aghi et al., 1998) and an attractive agent is the development of a CD/HSVtk fusion gene (Rogulski et al., 1997). Similarly, utilising suicide gene therapy as a radiation sensitizer has produced enhanced therapeutic effects in murine models (Hanna et al., 1997;

Kawashita et al., 1999; Pederson et al., 1997; Rogulski et al., 1997). The later study also sought to increase the specificity of the HSVtk/GCV system by placing gene expression under the control of the radiation-responsive early growth response gene 1 (Egr-1) promoter; thereby combining the spatial control achieveable with radiation, and exploiting the markedly increased Egr-1 promoter response to radiation in hepatocellular carcinoma cells compared to normal hepatocytes.

To overcome the previously identified major limitation of vector delivery a number of groups have sought to incorporate suicide genes into replication competent viruses (Rogulski et al., 2000; Wildner et al., 1999). These strategies will be discussed in the next section.

In summary, a number of suicide gene strategies have been developed to the point of clinical trials. Deficiencies in gene delivery have hampered assessment of this approach and its utility in multimodality cancer therapy, but there is optimism that with improved vectors it will play a role in clinical therapy; whether these genes are expressed from a replication competent vector or co-expressed with other genes (Lambin et al., 2000). Tempered with this is the knowledge that to be effective suicide gene therapy requires: a) the efficient delivery of both transgene and prodrug to target cells; b) cancer cell mechanisms involved in resistance to systemic chemotherapy may also affect this "molecular chemotherapy"; c) the critical BE is only in the order of one log in most models; d) many of the strategies are cell cycle dependent.

1.2.1.2 Replication Competent Viruses

A number of viruses are lytic in their release phase from host cells and consequently are cytotoxic. This led to to the concept of using replication competent viruses (RCV) to treat cancer and, indeed, trials were conducted in the 1950's-1970's with limited success and toxicity (Russell, 1994). Greater understanding of viral biology and our improved ability to manipulate and manufacture recombinant viruses, coupled with the poor transduction efficiency of replication incompetent vectors, has led to a re-evaluation of RCV. Indeed, the concept remains an attractive one and the subject of intense research activity (Peng and Vile, 1999; Pennisi, 1998; Russell, 1994). Clearly, the objective would be to develop systems in which recombinant viruses (with or without therapeutic transgenes) are

selectively replication competent in cancer cells (a property called oncolysis). Since carcinogenesis and efficient viral replication require similar changes to occur in normal cells, such as dysregulation of cell cycle control and circumvention of normal apoptotic signalling pathways, this provides the basis for selective viral targeting of malignant cells. The replication competent adenovirus (RCA) Onyx-015 has led the way in pre-clinical and clinical testing. Onyx-015 contains a deletion of the viral E1b gene. The normal function of E1b 55k protein is to bind p53 and prevent apoptosis in infected cells, complementing the E1a functions of forcing the cell into S phase of the cell cycle and the E1b 19k protein which also suppresses apoptosis. p53 is one of the most commonly mutated genes in a wide variety of tumour types and it was initially proposed that Onyx-015 would only replicate in p53 deficient cells. This has been the subject of controversy (Hall et al., 1998) but through pre-clinical and clinical testing it is clear that normal human cells are poorly permissive to Onyx-015 replication, whereas tumour cells are permissive (Heise et al., 1997; Khuri et al., 2000). The Onyx strategy relies on the lytic activity of the adenovirus to mediate its cytotoxicity. An attractive application for this vector is in combination with chemotherapy, targeting those tumour cells relatively resistant to chemotherapy, namely p53 deficient/mutated cells. Clinical phase 2 data are now available on this application; 37 patients with recurrent head and neck cancer were enrolled to receive cisplatin and 5-fluorouracil in conjunction with direct intratumoural injection of Onyx-015 (Khuri et al., 2000). Nineteen of 30 evaluable patients had objective responses, 8 complete and 11 partial, with prolonged time to progression. Interestingly there was no correlation between response and tumour p53 status, nor baseline neutralizing antibody titre to the adenovirus. Equally important was the lack of major toxicity attributable to Onyx-015, apart from pain at the injection site. These data are very encouraging for a therapeutic role for this agent (Anderson, 2000) and phase 3 studies are ongoing.

A clear extension of replication competent vectors is to modify them to deliver a transgene, and/or to increase specificity with transcriptional control of the E1 genes (Hermiston, 2000). To date, suicide genes have been the transgene of choice for incorporation into replication competent vectors. This combination would be expected to be beneficial due to the increased cytotoxicity of 'molecular chemotherapy' and viral lysis. In addition, during the adenoviral life cycle, cells are driven into S phase to enable viral

replication thus making them sensitive to the effects of HSVtk/ganciclovir or CD/5FC. This combination also provides a potential safety mechanism since replication can be terminated by the addition of prodrug to destroy the producer cells. Indeed, there is a fine balance in this system between allowing replication and spread of the virus and administering prodrug for enhanced killing of target cells and BE, thereby terminating viral replication (McCart et al., 2000; Rogulski et al., 2000; Wildner et al., 1999). These studies showed in a number of models the enhanced efficacy of RCV plus suicide gene/prodrug over either alone, with Rogulski et al showing a further additional benefit with adding in radiation.

Specificity of replication can also be obtained through transcriptional control of the E1 genes. This has been demonstrated in hepatocelluar carcinoma using the α-fetoprotein gene promoter (Hallenbeck et al., 1999). Prostate specific RCA have also been developed, initially with just the E1A gene under the control of a tissue specific enhancer/promoter (Rodriguez et al., 1997). This gave an approximate 400 fold greater cytotoxicity in prostate specific antigen $(PSA)^+$ cell lines compared to PSA^- lines. Improved selectivity to 10,000-100,000 fold was achieved by placing both E1A and E1B genes under tissue specific control (and restoring E3 function), resulting in eradication of LNCaP xenografts following a single i.v. dose of $1x10^{11}$ viral particles (Yu et al., 1999).

Conditionally replicating herpesviruses have also been developed (Martuza, 2000). Two have reached the stage of phase 1 clinical trial (Markert et al., 2000; Rampling et al., 2000). Both viruses used in these studies are deleted in the γ_1 34.5 loci and have been shown to replicate specifically in dividing cells (tumours), being avirulent in normal cells/tissues. G207 has an additional deletion affecting the ribonucleotide reductase gene. Both studies were conducted in patients with malignant glioma. There was no significant toxicity identified in either study. However, it was not possible to identify whether there was active viral replication in tumours and meaningful response data will require further studies (Kirn, 2000). Herpes simplex viruses have the added benefit of already carrying the HSVtk gene, allowing for prodrug delivery. Again, there is the issue of favouring viral replication over additional cytotoxicity, however it does add a specific safety feature. To overcome the limitation in viral replication posed by HSVtk/ganciclovir, additional suicide genes can be inserted (Pawlik et al., 2000). This group expressed cytochrome P450, a

normal mammalian enzyme expressed in liver and not normally in tumour cells, in a replication competent herpesvirus and showed enhanced cytotoxicity with cyclophosphamide in vitro. Intravenous administration of the virus in a hepatocellular model showed a significant reduction in tumour burden.

Reovirus, generally considered non-pathogenic in humans, is also being developed as a novel cancer therapeutic agent. Replication competence is dependent on an activated ras signalling pathway, either through mutation of ras itself or upstream receptor tyrosine kinases e.g. erbB2/Her2/neu. Again the cytotoxicity is due to direct cell lysis. Normal untransformed cells are resistant to viral replication. Encouraging in vivo results were seen in human xenografts grown in an immunodeficient mouse model and in an immunocompetent model using ras transformed fibroblasts (Coffey et al., 1998). In the latter this was independent of neutralising antibodies to reovirus, an important concern considering 50% of adults carry antibodies following prior subclinical infection.

Detailed knowledge of viral life cycles, coupled with understanding of the key processes in malignant transformation allow novel vectors to be considered for therapeutic application. This is demonstrated by the development of replication competent vesicular stomatitis virus (VSV) in the treatment of interferon non-responsive tumours (Stojdl et al., 2000). VSV infection normally induces interferon production in non-transformed cells, preventing further VSV production through inhibition of viral mRNA synthesis. Many tumours have evolved defects in the interferon pathway, resulting in their susceptibility to VSV infection and oncolysis.

RCV, following on from the results with Onyx-015, have moved on considerably from being an attractive propositon to a very real potential therapy. The developments detailed above outline the scope and variety of vectors currently under consideration. Through these vectors gene therapy may overcome the problem of vector titre and targeting.

However even with these potential advances considerable difficulties do remain with the biodistribution of therapeutic viruses despite retargeting to tumour cells. In a rat model of colorectal cancer direct intratumoural injection of an adenoviral vector expressing LacZ indicated low levels of tumour cell infection (Kuppen et al., 2001). This tumour model is composed of tumour cells mixed with supporting stromal cells and extracellular matrix (ECM); more closely resembling human colon adenocarcinomas. The hypothesis is that

the ECM in these tumours is a significant barrier for the spread of viral vectors. If systemic administration is preferred then problems of sequestration by nontarget tissues remain: Bernt et al. investigated the efficacy of a targeted replication competent adenovirus in eradicating human tumour metasteses in mouse liver (Bernt et al., 2003). In vitro there was selective oncolysis of tumour cells by the targeted vector without infection of hepatocytes. In vivo although there was significantly less hepatotoxicity from the targeted vector compared to nontargeted, there was no improvement in tumour cell transduction. They found that stability of the virus in the blood as well as entrapment within the liver sinusoids proved major impediments to virus transduction of tumour cells. These studies highlight some of the remaining problems faced by the field of cancer gene therapy (Ross et al., 2003).

1.2.1.3 Fusogenic Membrane Glycoproteins

The purpose of this thesis is to consider the potential of fusogenic membrane glycoproteins (FMG) as a potential cytotoxic gene therapy for cancer. FMG are derived from viral genes, the protein products mediating viral binding and subsequent internalisation via viral particle fusion with the cell membrane. In vitro, when FMG are expressed in cell populations containing the requisite receptor, massive cell–cell fusion occurs and syncitia are formed. The proposal to be tested is that if tumour cells form syncitia secondary to FMG gene expression, then their clonogenic potential will be blocked, the syncitia will likely go on and die; resulting in a desired cytoreductive effect. The general structure and function of FMGs and specific details of the Gibbon ape leukaemia virus (GALV), Measles F and H FMG will be discussed.

1.3 VIRAL FUSOGENIC MEMBRANE GLYCOPROTEINS

Membrane fusion occurs in a wide array of biological processes and has been a recognised feature of some viral proteins for a long time (Poste, 1970). In fact all enveloped viruses enter cells by protein mediated membrane fusion. This includes viruses from diverse groups such as retroviruses, paramyxoviruses and orthomyxoviruses to name a few. The mechanism of viral entry is mediated by the viral envelope glycoprotein. In general these proteins are expressed as precursors which are endoproteolytically cleaved by cellular

proteases to form a receptor binding domain/protein and a membrane-anchored fusion domain/protein. These two domains can be non-covalently associated as in the case of C-type retroviruses and HIV-1, or covalently linked as in the case of influenza (Weissenhorn et al., 1999). An exception to this structural arrangement is in the case of paramyoviruses which express two separate proteins: for example measles virus expresses the haemagglutinin (H) protein which has a receptor binding function and the fusion protein (F).

Despite significant evolutionary diversity it has become increasingly recognised that there is significant similarity between the structure of proteins involved in membrane fusion, both viral proteins and mammalian vesicle fusion proteins, suggesting a common mechanism of membrane fusion (Poumbourios et al., 1999).

1.3.1 General structure of viral fusion proteins

The crystal structure of a number of viral fusion proteins has been ellucidated most notably for influenza virus HA_2, HIV-1 gp41 and the TM protein of Moloney murine leukaemia virus, and has aided the investigation of the fusion process (Bullough et al., 1994; Fass et al., 1996; Weissenhorn et al., 1997; Wilson et al., 1981). The crystal structure data for influenza shows two states; a neutral pH conformation, the metastable pre-fusion confirmation (Wilson et al., 1981), and the low pH, stable membrane fusion conformation (Bullough et al., 1994) (see **Figure 1.1**). The remaining crystal structures mentioned are thought to represent the stable membrane fusion conformation alone.

The N-terminus of each fusion protein contains a hydrophobic sequence, the 'fusion peptide', which in the stable conformation inserts into the target membrane during membrane fusion. Within the N-terminal segment is a region composed of heptad repeats of hydrophobic residues; this region forms α-helical coiled coils. Within the C-terminal sequences is another region that forms coiled coils, shown to pack in the reverse, anti-parallel direction to the N-terminal coils. This places both fusion peptide and transmembrane region on the same side of the molecule and is the conformation seen in the stable, membrane fusion conformation. It is this structural feature of a rod-shaped complex formed by alpha helices that unites the diverse group of proteins involved in membrane fusion and suggests a conserved mechanism (Poumbourios et al., 1999).

1.3.2 Proposed mechanisms of FMG mediated membrane fusion

Enveloped viruses enter cells primarily by one of two routes: entry following direct fusion between the viral and cell membranes at the cell surface or entry following endocytosis and fusion between the viral and endosomal membrane. The former mechanism being pH independent, the later pH dependent (Schneider-Schaulies, 2000). Both routes of entry require initial binding via the receptor binding domain to a cellular receptor. The pH independent mechanism then predicts that the receptor binding domain triggers a conformational change leading to the fusion event. Whereas in the pH dependent mechanism it is the lowering of the pH within the endosome which triggers the conformational changes. In each entry mechanism the precipitating event is the exposure of the fusion peptide from its position close to and parrallel to the viral membrane allowing it to be propelled outwards to become embedded in the cellular membrane (See **Figure 1.1**). It is at this point that the N-terminal and C-terminal helices have extended. It is this configuration that it is thought allows certain inhibitory peptides to bind and block completion of the fusion event, as described for gp41 and peptides DP-107 and DP-178 (Weissenhorn et al., 1999). Further conformational change then occurs in the C-terminal region allowing the C-terminal coiled coils to pack anti-parrallel to the N-terminal helices, producing the stable fusion conformation seen in the crystal stuctures, with both hydrophobic domains in close association. This close association would then be predicted to bring close apposition of both membranes and permit fusion and pore formation. Various models have been proposed to explain the mechanism of fusion and pore formation and are illustrated in **Figure 1.2**.

1.3.3 FMGs as potential therapeutic agents

The prospect of using FMG as a therapeutic agent relies on the induction of extensive cell-cell fusion of tumour cells to induce non-viable syncitia. For this to occur it is more likely to be effective using those FMG that undergo pH independent fusion at the cell surface. This is a feature of retroviruses and paramyxoviruses amongst others. An example of a C-type retroviral envelope (GALV) and a paramyxovirus envelope (Measles F and H) will form the basis of future studies conducted in this thesis: they will be detailed here.

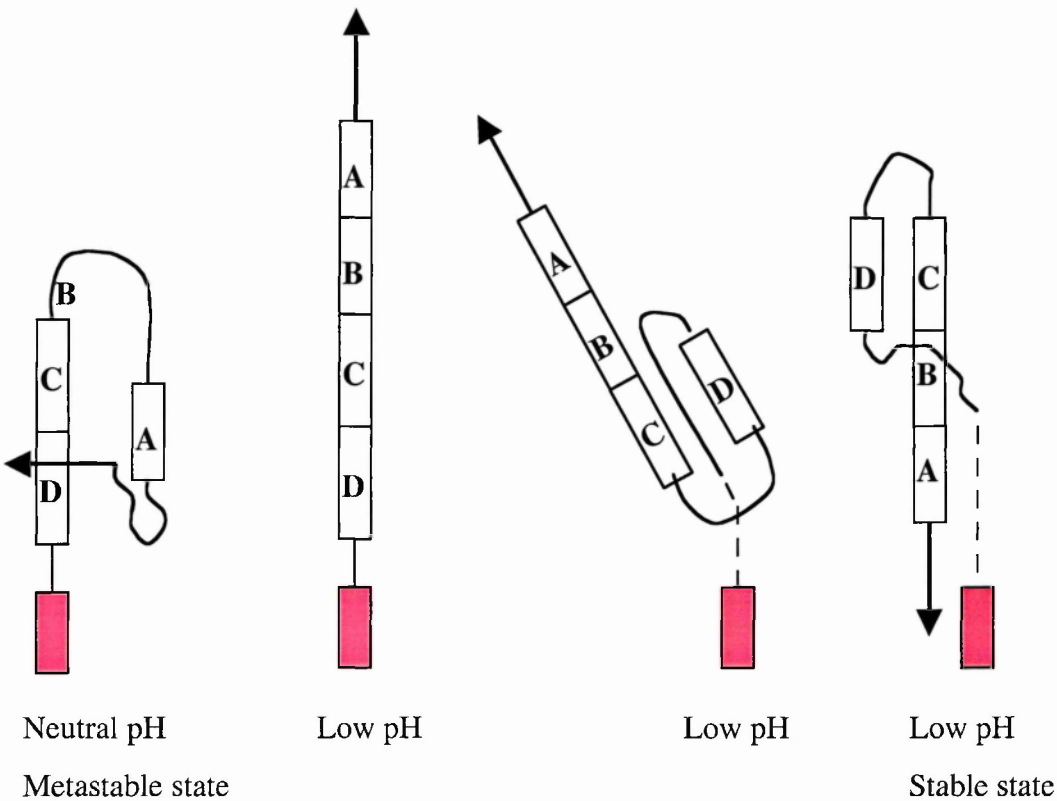

Figure 1.1: Proposed conformational changes in a viral fusogenic membrane glycoprotein.

The elucidation of the structure of influenza HA at normal pH (Wilson 1981) and low pH (Bullough 1994) has allowed a model of fusion to be proposed. Important regions have been designated A-D, fusion peptide (FP) is represented as an arrow and the membrane spanning region is coloured pink.

Activation of the fusion process (by low pH in the case of HA) produces a conformational change in loop B transforming it into an α-helix. This propels the N-terminal towards the target membrane. Then residues at the N-terminal end of D convert from a helical form to a loop. This causes D to flip 180^0 and pack anti-parrallel to the C helix. This results in both FP and the membrane spanning region becoming closely associated (modified from Hernandez '96).

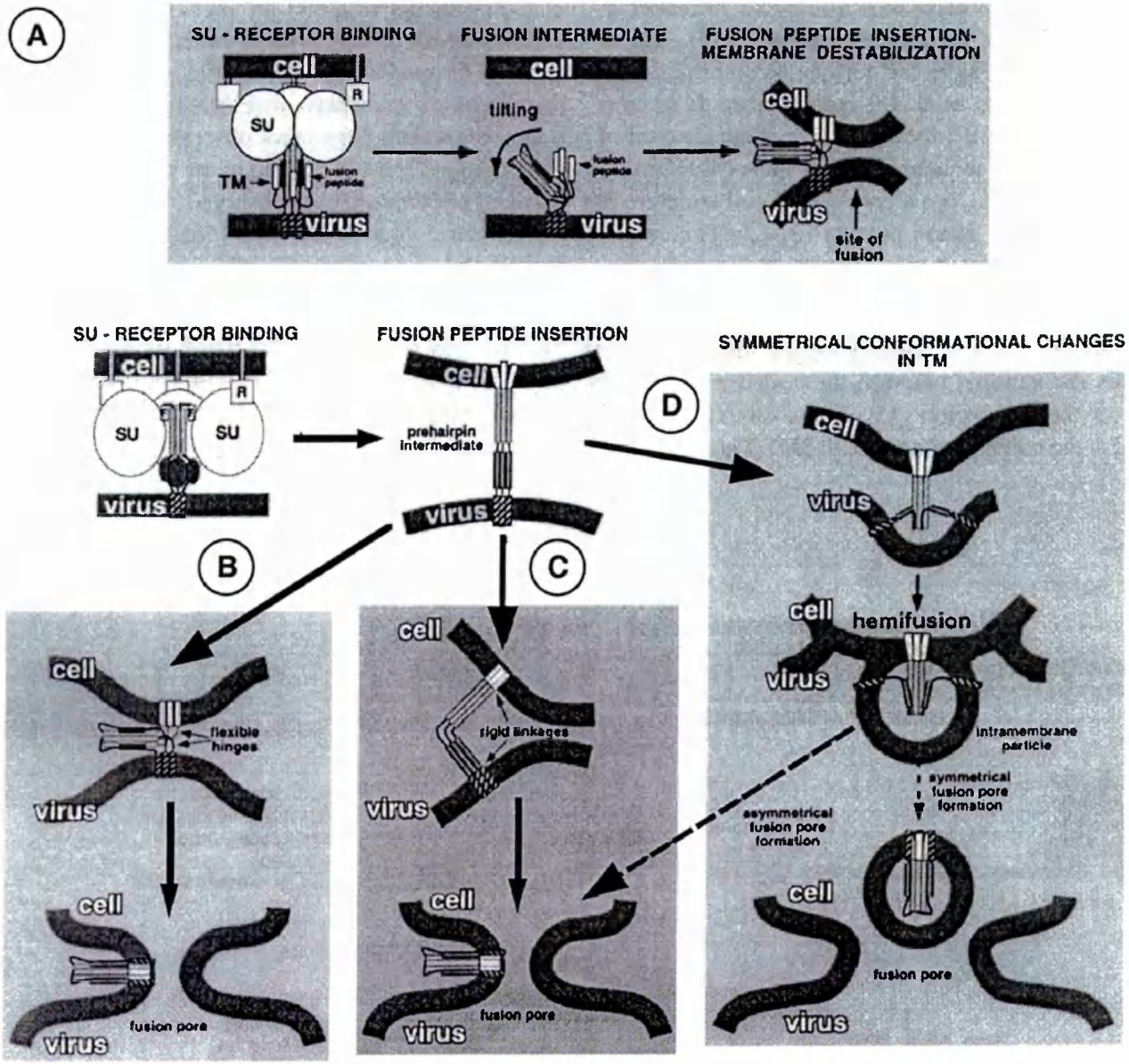

Figure 1.2: Models for the mechanism of membrane fusion induced by TM. The models illustrated (A-D) are depicted for retroviral membrane fusion but apply equally for other viruses. In the TM the fusion peptide (FP) is indicated by white cylinders, the N-terminal coiled-coil by light grey cylinders, the C-terminal segment is dark grey and the transmembrane domain is hatched. Model A (Caffrey et al. '98) assumes no conformational change occurs during fusion; insertion of FP occurs by random Brownian motion after SU dissociation. The remaining models incorporate the need for conformational change. Model B (Weissenhorn et al. '97) requires substantial flexibility of the polypeptide segments linking FP and the TM domain, and requires a breakdown in trimeric symmetry. Model C (Baker et al. '99) requires an assymetric bending which would be difficult to achieve in a trimeric structure. Model D (Kobe et al. '99) does not require significant flexibility or assymetric bending but embedding of the TM in the cell membrane. Modified from Poumbouris et al., '99.

1.4 Gibbon Ape Leukaemia Virus

Gibbon ape leukaemia viruses (GALV) are classified as one of the C-type retroviruses (Murphy et al., 1995). They were initially isolated from a group of captive baboons (Reitz et al., 1980) and a number of strains have been identified. The SEATO strain was isolated from gibbons with lymphosarcoma (Kawakami et al., 1972). The genetic organisation of GALV is identical to that of the other C-type retroviruses including the murine retroviruses and feline leukaemia viruses (Delassus et al., 1989). Indeed pseudotyping using the GALV envelope of MoMLV core particles has been developed for gene therapy purposes as in the retroviral packaging cell line PG13 (Miller et al., 1991). This approach found favour due to the broad number of human cell lines capable of being infected, in particular human haemopoietic cells (von Kalle et al., 1994). This broad infectivity range is due to the wide expression of the GALV receptor, PiT 1.

1.4.1 The GALV receptor, PiT 1

The primary determinant of the host range for a specific retrovirus is its choice of cell-surface target protein (receptor) (Miller, 1996). As a group retroviruses use a wide range of cell-surface proteins as receptors, but individually a single or rarely two distinct receptors allow for retroviral entry. It appears that for the majority of retroviruses binding of this single receptor is sufficient to precipitate the entry process but there are exceptions: for example HIV-1 binds CD4 as its primary cell-surface receptor but requires the co-receptors CCR5 or CXCR4.

The GALV receptor is a sodium-dependent phosphate symporter, PiT 1 (Kavanaugh et al., 1994; O'Hara et al., 1990) and is widely expressed in many tissues. PiT 1 is an integral membrane protein with 5 extracellular loops and 10 transmembrane regions. Transfer of region A, a 9 amino acid sequence in the C-terminal part of the fourth extracellular loop (positions 550-558), was able to convert the closely related fungal phosphate transporter Pho-4 (from Neurospora crassa) to be a permissive receptor for GALV (Pedersen et al., 1997). Across mammalian species there is highly conserved sequence homology of the whole PiT 1 protein, however there is significant variation in region A. This variation is thought to be a significant determinating factor in the permissivity of infection, resulting in human and rat cell lines being permissive and most murine species being resistant

(Weiss and Tailor, 1995). The closely related sodium-dependent phosphate symporter PiT 2 is the receptor for amphotropic MLV. PiT 2 has a very similar sequence and structure compared to PiT 1. Hamster PiT 2 (HaPiT2) is not only permissive to amphotropic MLV but also GALV due to a single amino acid change in region A compared to the human sequence, glutamic acid for lysine at position 522 (Eiden et al., 1996). Further work by this group identified the inhibitory effect to GALV infection of having lysine in one of the first two positions of region A in PiT 1. They also indicated regions outside region A in PiT 1 are important for permissivity to GALV infection (Chaudry and Eiden, 1997). Interestingly inhibitory mechanisms to GALV and A-MLV infection via HaPiT2 have been indicated in chinese hamster ovary (CHO) cells. CHO cells are resistant to GALV/ A-MLV infection unless they are pretreated with tunicamycin, an inhibitor of N-linked glycosolation, suggesting CHO cells secrete an inhibitory protein that can interfere with receptor function (Miller and Miller, 1993; Tailor et al., 2000).

1.4.2 GALV envelope

The structure of retroviral envelopes show many similarities across the *genus*. The GALV envelope shows very close homology to other C- type retrovirus envelopes such as those of MLV and Feline Leukaemia virus (FeLV). Due to this close similarity many of the characteristics of the heavily investigated MLV family are felt to be applicable to the GALV envelope. The domain organisation of GALV envelope can be seen in **Figure 1.3**. The envelope is composed of two polypeptides formed following the cleavage of the 85 kDa precursor protein. The larger 70 kDa SU (surface or gp70) polypeptide is completely extracellular and corresponds to the N-terminal region of the precursor. The smaller 15 kDa TM (transmembrane or p15E) polypeptide corresponds to the C-terminal region of the precursor. The major features consistent with other retroviral envelopes include:

- The signal peptide at the N-terminus ensures entry into the secretory pathway
- N-glycosylation of a number of asparagine residues within the SU
- A cleavage signal between the SU and TM domains which corresponds to a R/K-X-R/K-R concensus sequence for cellular furins
- A hydrophobic region at the N-terminal of the TM: the fusion peptide
- Regions within the TM capable of forming α-helices

Figure 1.3: Diagramatic representation of the three dimensional structure of a C-type retroviral envelope. The mature envelope is a trimer. SU includes the receptor binding domain (RBD), proline rich region (PRR) and C-terminal domain (C). TM includes the fusion peptide (FP), heptad repeats (HR), transmemebrane region (tm) and cytoplasmic region (cyt) which includes the R peptide ●.
Reproduced by kind permission of Dr D. Lavillette and Dr F-L. Cosset.

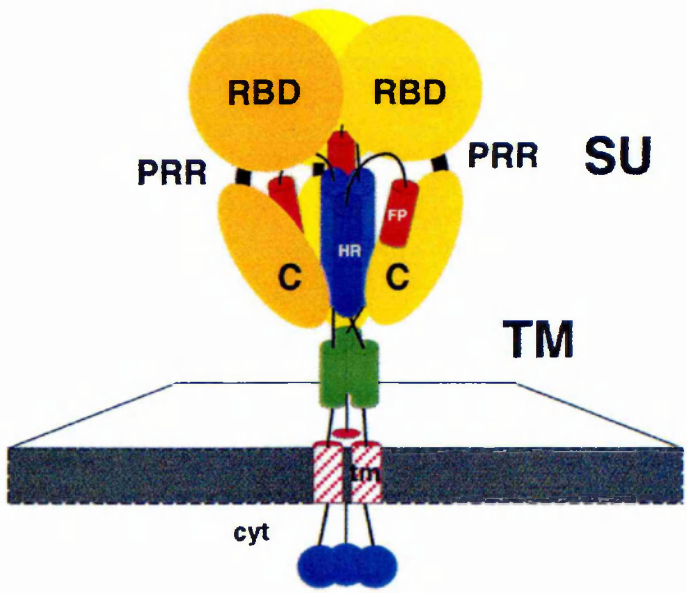

Figure 1.4: Comparison of MoMLV and GALV TM sequences. The hyperfusogenic GALV is truncated: direct comparison with the MoMLV sequence indicates it is lacking the terminal 19 amino acids including the R peptide (underlined).
MS - membrane spanning, C - Cytoplasmic Domains.

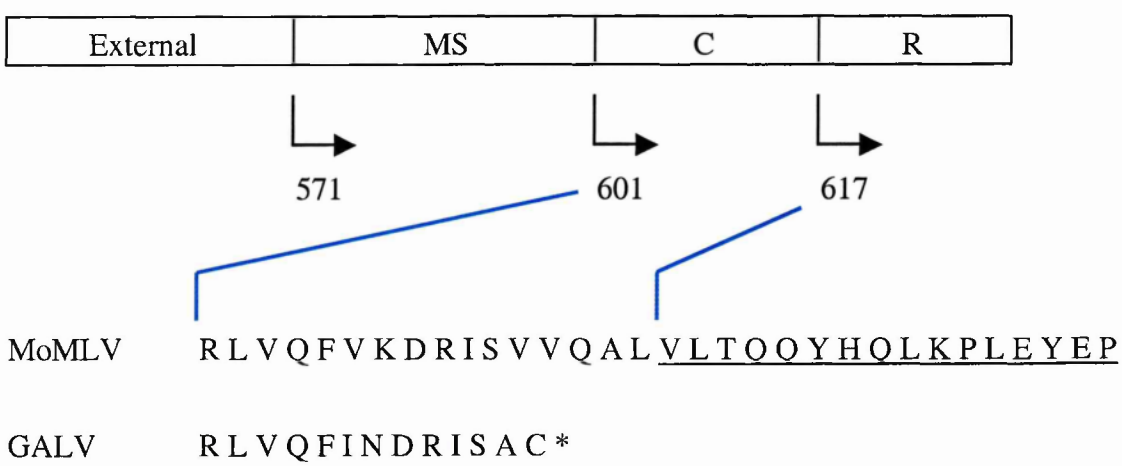

- A region of the TM which contains a number of cysteine residues
- A C-terminal region of the TM which represents the transmembrane region
- An intracytoplasmic region which contains a cleavage site for the viral protease resulting in the formation of the R peptide: the C-terminal 16 amino acid sequence

Following transcription, the spliced env mRNA is translated on nuclear membrane bound endoplasmic reticulum (ER). The signal peptide ensures targeting of the nascent polypeptide chain to the ER lumen with the hydrophobic transmembrane domain becoming anchored in the ER membrane. Within the ER lumen the newly synthesised polypeptide is modified by N-linked glycosylation, disulfide bond formation and assembled into trimers. After transport to the golgi the envelope precursor is cleaved into the SU and TM peptides which remain non-covalently associated. Also in the golgi the newly added sugars are modified. The mature protein is then transported to the cell surface and incorporated into budding virions. The envelope protein is not fully functional until, during the budding/release process, the viral protease cleaves the R peptide (Brody et al., 1994). A model for the fusion process mediated by a C-type retroviral envelope is illustrated in **Figure 1.5**.

SU (gp70)

The SU can be considered to be composed of a number of regions: the N-terminal receptor binding domain (RBD), a proline rich region (PRO), and the C-terminal domain (**Figure 1.3**). The RBD region is responsible for the recognition of the receptor (Battini et al., 1995). Within the RBD sequence, alignments between C-type retroviruses identified regions which vary with tropism, these varible regions have been termed VRA and VRB. The crystal structure of a C-type retrovirus RBD region identified the core to be an antiparrallel β sandwich with two interstrand loops representing VRA and VRB forming a helical subdomain. It is this helical subdomain that determines the receptor specificity (Fass et al., 1997). An additional function of SU is that following receptor recognition a signal needs to be transmitted that results in conformational changes within TM, precipitating fusion (**Figure 1.5**). Regions that have been shown to be important in post binding events in the SU are PRO (Lavillette et al., 1998) and extreme N-terminus of the RBD (Bae et al., 1997).

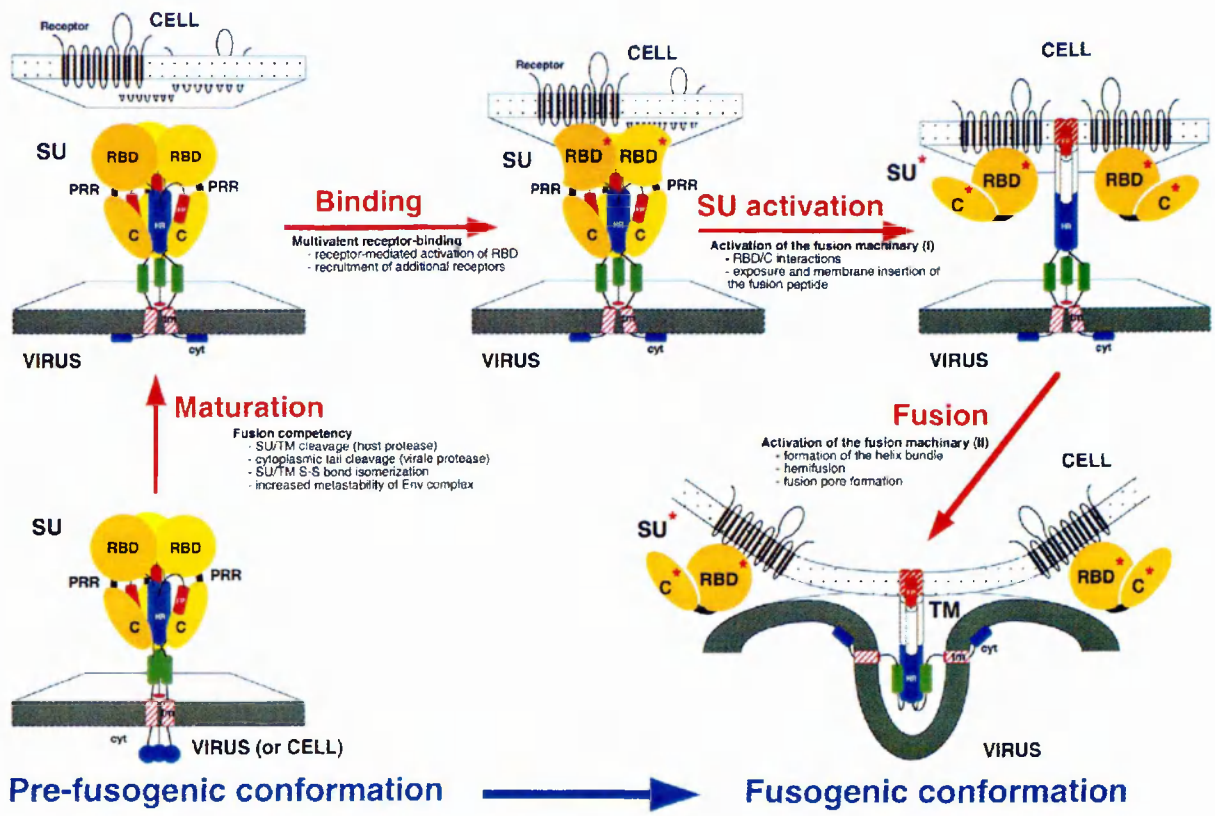

Figure 1.5: Model for the activation and fusion process for C-type retroviruses including GALV.

Envelope maturation includes cleavage of the R peptide. The hyperfusogenic GALV does not require this step to be fusion competent. Following receptor-SU binding conformational change occurs which exposes the fusion peptide. The fusion process then proceeds in a similar manner to that illustrated for influenza HA.
Reproduced by kind permission of Dr D. Lavillette and Dr F-L. Cosset.

TM (p15E)

The TM region contains the critical regions required and apparently conserved amongst diverse fusion proteins as discussed in Poumbourios et al.(1999). The specific functional domains for a C-type retrovirus can be seen in **Figure 1.3**. The TM is also thought to contain the domain important for trimerisation (Einfeld and Hunter, 1988). Mutational analysis has identified a number of regions which are important in the fusion process including the fusion peptide, heptad repeats and transmembrane domain (Denesvre et al., 1995; Taylor and Sanders, 1999; Zhao et al., 1998; Zhu et al., 1998). A particular region of focus has been the cytoplasmic domain and specifically the R peptide (the C-terminal 16 amino acid sequence). As previously indicated for the formation of fully mature virions capable of infection the R peptide is cleaved by the viral protease at or shortly after budding. Mutational analysis has identified that truncations in the cytoplasmic tail produces an envelope that is highly fusogenic in cell-cell fusion assays but is poorly incorporated into virions (Januszeski et al., 1997; Yang and Compans, 1997). Introduction of an R peptide from another retrovirus was capable of reverting the hyperfusogenic state of a truncated envelope (Yang and Compans, 1996). Thus the R peptide has an inhibitory role in fusion but is an important factor in the efficient incorporation of the envelope into budding virions. How it mediates these functions is still unclear.

We received a construct containing the GALV SEATO envelope (a kind gift of Dr S.J.Russell) which sequence analysis compared to MoMLV showed was terminally truncated, **Figure 1.4**. As predicted from the sequence this construct was hyperfusogenic in cell-cell fusion assays. This envelope would be studied in depth as a potential gene therapy agent in this thesis and will be referred to as GALV.

1.5 Measles Virus

Measles virus (MV) is a nonsegmented negative sense RNA virus classified in the *paramyxoviridae* family. It is a member of the *morbillivirus* genus which also includes the related Rinderpest and canine distemper viruses. Six genes (single mRNAs) are encoded by the genome as illustrated in **Figure 1.6**.

Figure 1.6: Genome arrangement of measles virus. MV is a negative-sense RNA virus. The genome is composed of 6 genes which encode 6 major structural proteins and 2 nonstructural proteins from the P gene (V and C proteins).

Leader sequence

Noncoding region

Gene	Protein
N	Nucleoprotein
P	Phosphoprotein \ C \ V
M	Matrix
F	Fusion (F)
H	Haemagluttinin (H)
L	Large

Figure 1.7: Schematic representation of the active, cleaved F protein

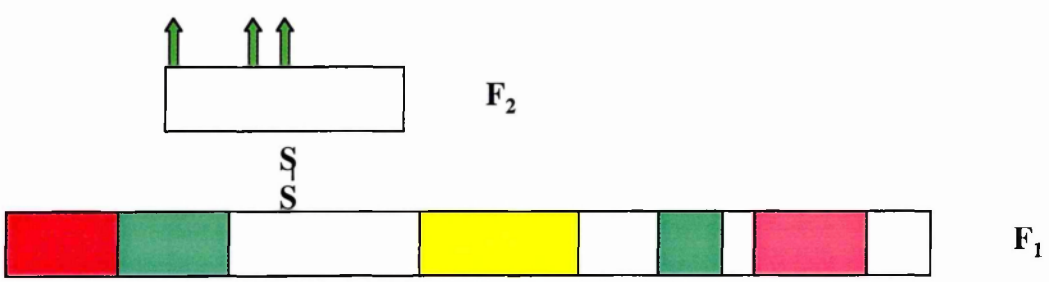

Fusion peptide

Heptad repeats

Transmembrane domain

Cysteine rich region

Glycosylation sites

1.5.1 Clinical features

Measles virus infects humans, usually children, producing a characteristic clinical pattern of prodromal fever, cough, coryza, and conjunctivitis, followed 2-3 days later by the appearance of a generalized maculopapular rash (Griffin D.E and Bellini W.J, 1996). Viral entry is by aerosol to the lower respiratory tract where initial viral replication occurs. This is followed by spread to the local lymphatics (replication here results in the characteristic Warthin-Finkeldey or multinucleated giant cells). Amplification of the virus occurs in the lymph nodes followed by viraemia. This permits MV to infect both blood monocytes and endothelial cells throughout the body. Infection to epithelial cells occurs in a wide variety of organs including the skin producing the characteristic rash and the oral mucosa producing Koplik's spots. The development of the rash is usually temporally related to the development of the immune response resulting in resolution of the rash over 5-7 days and a general clinical improvement. As well as a specific cell mediated immune responses to MV a state of immunosuppression arises secondary to MV infection. It is this immunosuppression which accounts for the approximate one million deaths in children of developing countries annually attributed to measles virus.

Well documented neurological complications are associated with MV infection. The complications include postinfectious encephalomyelitis which is an autoimmune demyelinating condition, inclusion body encephalitis seen in immunosuppressed individuals, and subacute sclerosing panencephalitis where persistant measles virus can be identified in the central nervous system many years after primary infection.

Measles virus was first isolated and grown in tissue culture in 1954. The source of the virus was blood from David Edmonston, a child with measles. Primary human kidney cells were then used to propogate the "Edmonston" strain. Subsequently the virus has been able to propogate in a number of both primate and nonprimate cell lines (Griffin D.E and Bellini W.J, 1996). The first receptor identified for MV was for the Edmonston strain and was CD 46 (Dorig et al., 1993; Naniche et al., 1993). CD 46, also known as human membrane cofactor protein, is expressed on the cell surface of all nucleated cells (Manchester et al., 2000; Seya et al., 1999). It is a member of a family of complement-binding proteins and specifically inactivates C3b/C4b, preventing complement attack of

host cells. Despite this association with the innate immune system it was not clear how MV could induce immunosuppression.

1.5.2 Measles virus receptors and immunosuppression

The immunosuppression induced by MV has been shown to be due primarily to suppression of cell-mediated immunity (Bhardwaj, 1997). Primary blood monocytes infected with MV show a marked impairment in IL-12 production upon stimulation (Karp et al., 1996). Dendritic cells can be infected with MV (Bhardwaj, 1997). When infected DC are co-cultured with syngeneic activated T cells there is a significant increase in MV production and marked increase in syncitia formation. This effect seemed to be mediated through CD40 - CD40L interactions. Associated with the increase in MV replication was massive apoptosis of both the highly infected DC and also the poorly infected T cells. IL-12 production by DC infected with MV was markedly impaired (Fugier-Vivier et al., 1997). The ability of MV infected DC to activate naïve T cells in the allogeneic mixed leukocyte reaction was lost even if only a small percentage of DC were actually infected (Grosjean et al., 1997).

Recent studies have indicated a more likely receptor for wild type MV. The identification of signalling lymphocytic activation molecule (SLAM) (CDw150) as a measles virus receptor eventuated from the observation that MV clinical isolates are readily isolated on an EBV transformed marmoset B-cell line, B95a (Kobune et al., 1990). These isolated MV strains were then noted to retain their pathogenicity for monkeys and were also able to infect non B-cell and T-cell lines expressing CD46. A cDNA library of B95a was made and divided into pools (Tatsuo et al., 2000). These were then transfected into a cell line non-permissive to B95a – isolated MV. These cells were then exposed to a VSV expressing GFP and deleted of its envelope (VSVΔG) but expressing the H of a B95a – isolated MV, and F of the Edmonston strain. A single pool of cells was identified expressing significant amounts of GFP. Further analysis indicated the clone permissive to the mutant VSV contained cDNA encoding the SLAM gene. In addition further investigation of other members of the morbillivirus family has shown they too utilise SLAM as a receptor (Tatsuo et al., 2001). The identification of SLAM as a receptor aids in the understanding of the known pathogenesis of MV. SLAM was first identified as a

receptor on T cells (Cocks et al., 1995). Engagement of SLAM on CD4+ T cells enhanced proliferation and promoted cytokine production, particularly IFN-γ. Subsequent studies indicated that SLAM is also a B cell growth and differentiation promoting molecule (Punnonen et al., 1997), and is expressed on dendritic cells (Polacino et al., 1996).

The tissue distribution of SLAM expression (lymphoid organs) is more in keeping with the sites of MV replication compared to CD46. Equally the immunosuppresssion seen with MV can be readily explained by destruction of infected SLAM expressing cells. Therefore it appears that wild type MV uses SLAM as the primary receptor with CD46 usage arising out of in vitro adaptation (Yanagi, 2001). A single mutation at position 481 to tyrosine (Xie et al., 1999) or 546 to glycine (Rima et al., 1997) may permit MV strains to interact with CD46.

1.5.3 Measles F and H

Three proteins participate in the formation of MV envelope: Matrix, H and F. H and F together are required for receptor binding and fusion (Wild et al., 1991) and will be detailed.

The Haemagglutinin (H) protein mediates binding to the MV receptor. H is a type 2 membrane protein of 617 amino acids. In the ER glycosylation occurs at 4 sites prior to H forming disulphide-linked dimers. At the cell surface the dimers dimerise forming a tetramer (Ogura et al., 1991). As well as binding the receptor, H is also required to interact with F.

The fusion (F) protein is responsible for membrane fusion. F is a type 1 membrane protein and is synthesised as the inactive polyprotein F_0 of approximately 60 kd. It is glycosylated in the ER, forms an homotrimer and is transported to the plasma membrane. In the trans golgi, host furin cleaves F_0 yielding two disulfide-linked polypeptides, F_1 (41 kd) and F_2 (18 kd) (Scheid and Choppin, 1977). As can be seen in **Figure 1.7** F_1 contains the hydrophobic carboxy-terminus of F_0 which serves to anchor the protein into the membrane, with a further 14 amino acid intracellular cytoplasmic tail. At the amino terminus of F_1 is another hydrophobic region, the 'fusion peptide'. Adjacent to both these areas are heptad repeats capable of forming α-helical coiled coils (Lamb et al., 1999). This structural arrangement conforms to the general structure of viral fusion proteins previously

described. In keeping with this, studies on the closely related paramyxovirus simian virus 5 (SV5) F protein have shown close similarities to influenza HA and HIV Env. The final stable state formed following conformational changes is a core trimer (Lamb et al., 1999). Towards the centre of F_1 is a cysteine rich region thought to be important for interaction with H.

We received separate constructs containing measles F and H genes (a kind gift of Dr R.Cattaneo, Mayo). In parallel to GALV these genes were studied for their fusogenic activity and suitability as potential gene therapy agents.

1.6 Viral vectors

1.6.1 Introduction

The development of clinically applicable gene therapy protocols is equally dependent on the means of delivering the gene as it is on the actual gene itself. The development of vectors that are safe and result in high levels of gene expression in target cells is critical for the field of gene therapy. Presently vectors can be broadly divided into non-viral and viral. Non-viral vectors will not be detailed in this discussion.

A number of candidate viral vectors for cancer gene therapy are being used in clinical trials or are under development and include retroviruses, lentiviruses, adenoviruses, adeno-associated viruses and herpesviruses amongst others (Kay et al., 2001). Each of these viral vector systems have specific characteristics which affect their suitability for a particular application. The genetic engineering employed to allow the use of viruses as vectors has been similar. Coding genes and *cis*-acting sequences are separated to prevent recombinantion and the production of wild type virus, see **Figure 1.8**. The coding sequences work in *trans* and can be expressed from heterologous plasmids or be incorporated into the genome of producer cells. The viral *cis*-acting sequences are linked to the therapeutic gene. When this construct is introduced into producer cells replication-defective vector particles are produced. Maintaining the separation of coding and *cis*-acting sequences aims to ensure no replication competent virus is produced; an important safety feature. However by disrupting the wild type viral genome some of the complex

Figure 1.8: Strategy for engineering a virus into a vector. The helper DNA contains viral genes essential for viral replication and structural genes. These can be contained in a heterologous plasmid or stably inserted into the host chromosomal DNA of the packaging cell. The helper DNA lacks the packaging domain (ψ). The vector DNA contains the therapeutic expression cassette and non-coding viral *cis*-acting elements that include a packaging domain. This ensures only vector genome is packaged into a particle. Modified from Kay '01.

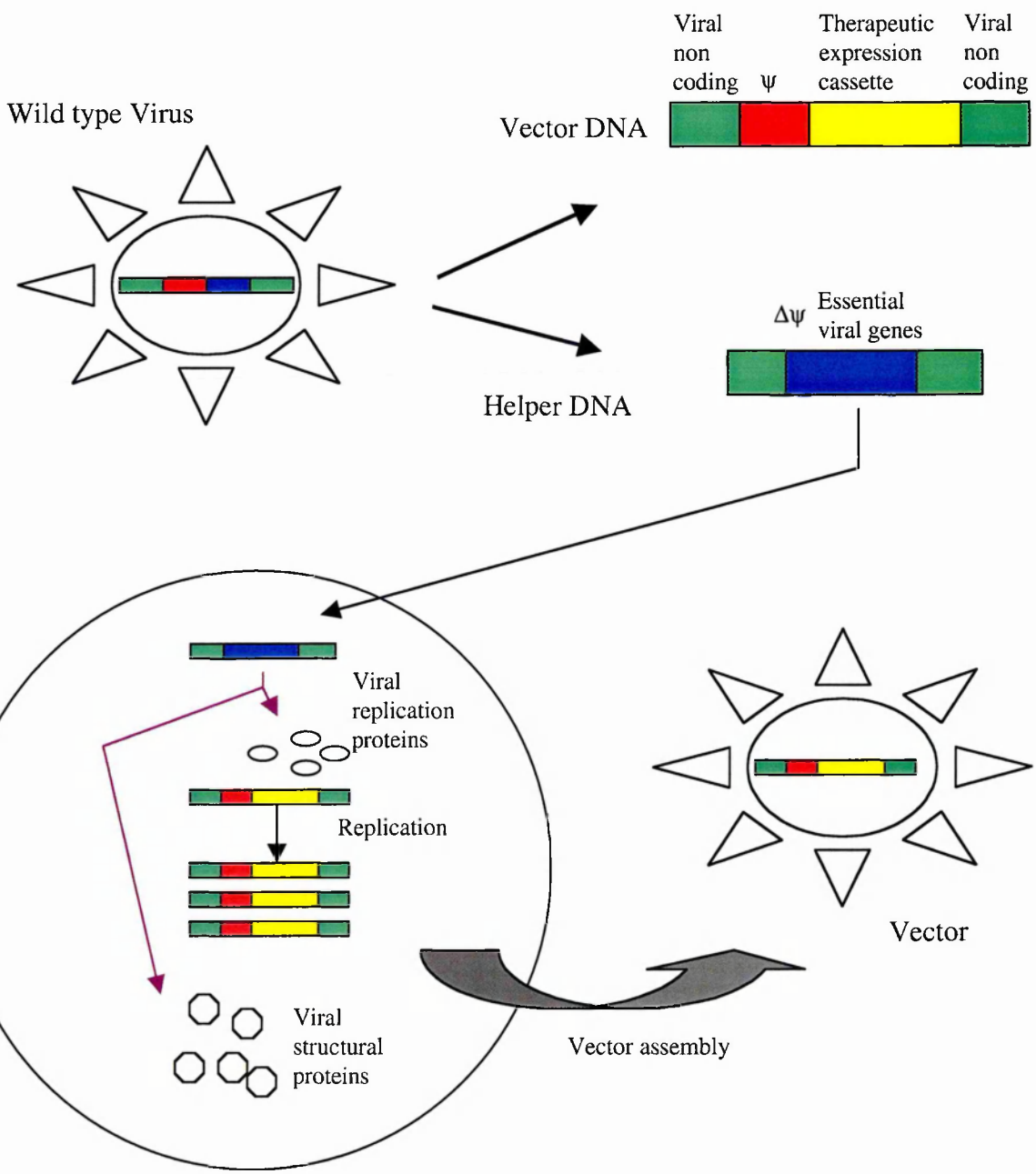

regulatory interactions are lost and the production of fully functional vector will be less efficient than seen with wild type virus (Kay et al., 2001).
The specific features of retroviral, lentiviral and adenoviral vectors will be detailed.

1.6.2 Retroviral Vectors

Retroviral vectors were really the first viral vectors adapted for gene therapy and consequently have gained widespread use both in pre-clinical and clinical studies (Hu and Pathak, 2000; Vile and Russell, 1995). Retroviruses have been classified into 7 genera based on their pathogenicity, morphology, genome organisation and nucleotide sequence relationships (Murphy et al., 1995). An alternative classification can be made based on genome structure alone: simple retroviruses encode gag, pro, pol and env genes where as complex retroviruses encode these genes plus several accessory genes. One unifying feature is that they all possess two molecules of single stranded RNA and upon entry into host cells utilise a reverse transcriptase to form double stranded DNA. Mammalian C type retroviruses, an example of a simple retrovirus, have been the most studied and developed for gene therapy; in particular vectors derived from Moloney murine leukaemia virus (MoMLV). More recent vector systems from Lentiviruses, a complex retrovirus, have been developed and are finding application as delivery vehicles.

1.6.2.1 Retroviral structure

Retroviruses are enveloped viruses ~ 90-140nm in diameter. The virion consists of a an inner core separated from a phospholipid envelope by matrix protein. The core is made up of a icosahedral protein shell, capsid, enclosing the two positive sense RNA strands. These strands have a 5' cap of m7G5'ppp5'G_{m}p and 3' poly(A) of approximately 200 A residues. Towards the 5' end of the genome a tRNA molecule is associated by its 3' terminal 18 nucleotides; these are base paired to a specific sequence (the primer binding site) of the retroviral RNA. Also found within the capsid are the retroviral reverse transcriptase, protease and integrase enzymes. The phospholipid envelope is derived from the plasma membrane of the virus-producing cell, is roughly spherical and has oligomeric viral glycoproteins projecting as spikes on electron microscopy from the surface.

1.6.2.2 Moloney murine leukaemia virus genome

The RNA genome consists of central coding regions with non-coding sequences at each end. In the RNA genome these non-coding regions differ at either end and will form the long terminal repeat sequences (LTR) at each end of the proviral DNA. After the 5' cap is found the terminally redundant sequence termed 'R'. This plays an important role in reverse transcription by allowing transfer of the nascent DNA strand from one end to the other as there is a identical R sequence at the extreme 3'end of the molecule preceding the poly(A). The 5' untranslated region (U5) contains sequences that facilitate the initiation of reverse transcription and will form the 3' end of the LTR. Downstream from this is the primer binding site followed by the leader sequence. The leader sequence contains a splice donor site for mRNA, which is usually only utilised for env, and the packaging signal. This signal specifies genomic RNA to be packaged into newly formed virions and in MLV enhanced efficiency of packaging occurs from sequences extending into the gag open reading frame (Hu and Pathak, 2000). The coding sequence consisting of gag, pol and env then follows. The gag (group specific antigen) encodes a precursor protein which is proteolytically cleaved to form the matrix, capsid and nucleocapsid proteins and an additional protein p12 which has not been assigned a function. Both the pro and pol genes are translated as C-terminal extensions of a fraction of the gag mRNA. The pro gene encodes the viral protease which cleaves viral precursor proteins and pol encodes the reverse transcriptase and integrase enzymes. The 3' end of pol overlaps the start of env in a different reading frame so there is no intervening sequence. The env gene codes for the retroviral envelope glycoprotein which is translated from a spliced subgenomic RNA. Beyond the coding region is the poly purine tract, a series of A and G residues, which contains the initiation site for synthesis of the plus strand of viral DNA as it escapes digestion by Rnase H (Coffin. J, 1996). Next is the U3 region which will form the 5' portion of the LTR and as such will be the region recognised by the cellular transcription machinery (viral promoter). It also contains transcriptional enhancer sequences and cis acting sequences necessary for virus replication. In addition both the U3 and U5 regions contain att (attachment) sites which are recognised by integrase and are necessary for efficient integration of the viral DNA. At the 3' end of the genome is the other copy of R which contains the polyadenylation signal.

1.6.2.3 Retrovirus life cyle

The life cycle can be thought to commence when the viral envelope binds the cell surface receptor and fuses with the target membrane, releasing the viral core into the cytoplasm of the target cell, see **Figure 1.9**. Synthesis of viral DNA then begins within 4-8 hours of infection, see **Figure 1.10**. Reverse transcription is initiated from the primer tRNA, usually $tRNA^{Pro}$ in MLV, and proceeds until the 5'end of the genome is reached. To this point a molecule termed 'strong stop DNA' has been formed (termed as it represents a pause in reverse transcription). This molecule and the reverse transcriptase then perform a 'jump' to the 3' end of the viral RNA. It is able to perform this transfer due to the repeated R sequence at each end of the genome which allows complementary base pairing and the RNase H activity of reverse transcriptase removes the RNA which has just been copied. Elements of the capsid structure also make this jump efficient. Synthesis then continues to the 5' end of the template which is now the 5' end of the primer binding site as RNase H has removed R and U5. During this synthesis process the RNA continues to be degraded, approximately 18 bases behind the point of synthesis, except at the polypurine tract. The sequence of the polypurine tract is then able to act as the primer for the DNA plus-strand synthesis by reverse transcriptase. This proceeds towards the 5' end of the minus strand. When this end is reached another jump occurs, this time with the primer binding sequence copied in both strands which allows complementary base pairing. The formation of double stranded DNA can now be completed and the primer tRNA removed from the 5' ends of each strand using RNase H activity.

The newly formed double stranded DNA now needs to be transported into the nucleus, which in the case of C-type retroviruses requires the cell to undergo mitosis. Once in the nucleus integration can occur. This is a highly specific process and is initiated by integrase removing the terminal two bases at each 3'end of the viral DNA, leaving a 3' hydroxyl group. This free hydroxyl group is then able to permit strand transfer, joining the two ends of the viral DNA to cellular DNA. Cellular DNA repair mechanisms then fill in the gap in the molecule by displacing the two mismatched bases at the 5' end of the provirus, ligate the remaining ends, and in doing so produce a characteristic duplication of 4-6 base pairs of cellular DNA flanking the provirus.Following integration all further viral replication occurs using cellular systems. Transcription of the viral genome is driven from the

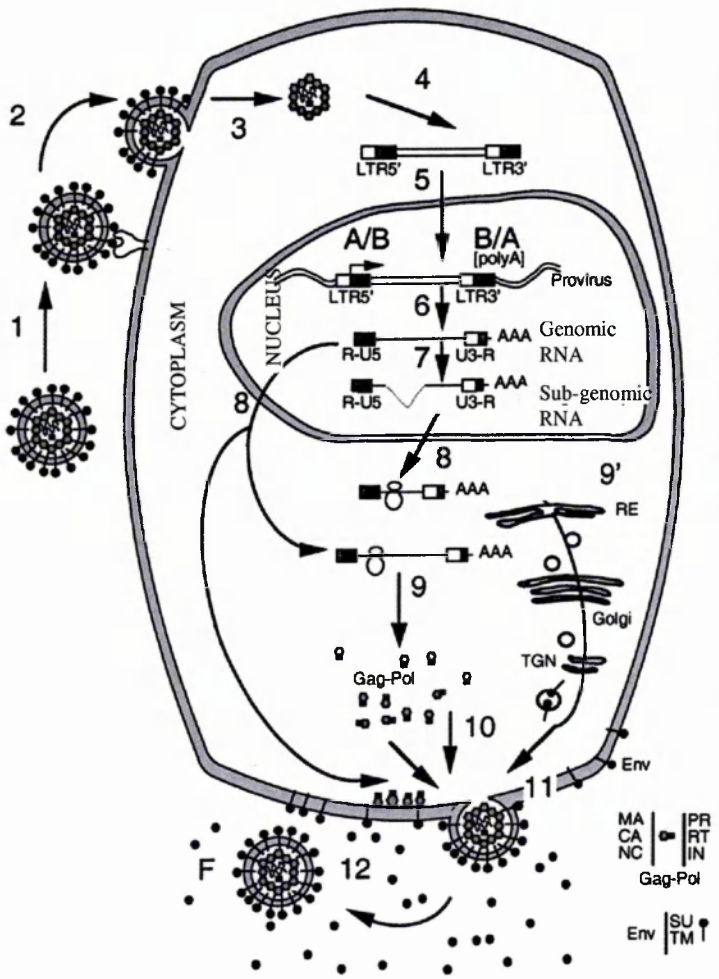

Principle characteristics of retroviral replication:

1 Binding of receptor

2 Fusion of cell and viral membranes

3 Entry of the capsid and partial uncoating

4 Reverse transcription

5 Transport into the nucleus and integration into cellular DNA

6 Transcription

7 Splicing

8 Passage of mRNA into the cytoplasm

9 Translation of Gag-Pro-Pol

9' Translation of Env and maturation in the trans golgi network

10 Assembly of genomic RNA and Gag -Pol precursors

11 Budding and incorporation of envelope

12 Release of viral particles and soluble SU

Figure 1.9 : Stylised life cycle of a retrovirus (modified from F. Mallet).

Figure 1.10: Schematic representation of viral DNA synthesis. See text for full details.

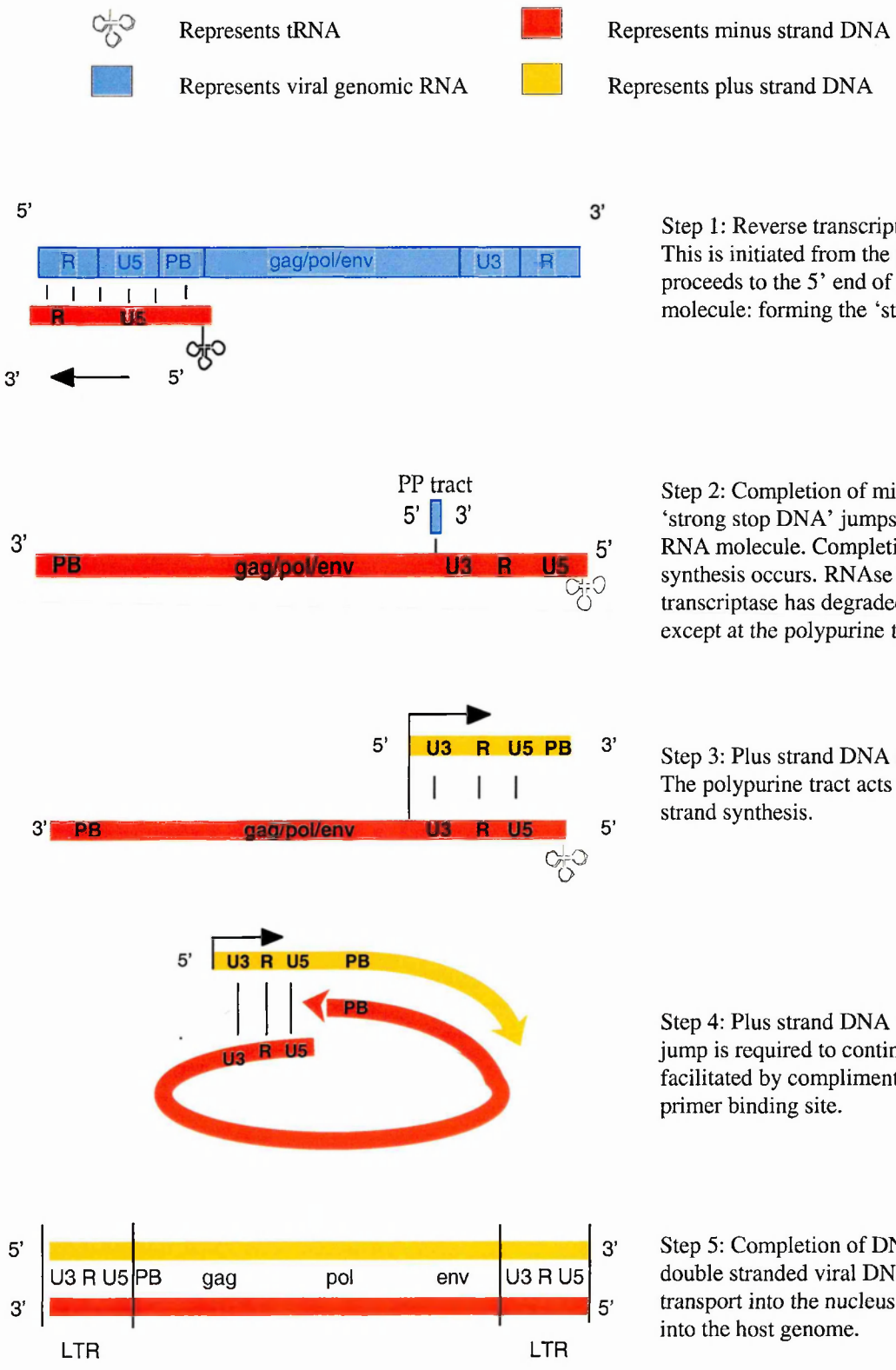

Step 1: Reverse transcription commences. This is initiated from the primer tRNA and proceeds to the 5' end of the RNA molecule: forming the 'strong stop DNA'.

Step 2: Completion of minus strand synthesis. 'strong stop DNA' jumps to the 3' end of the RNA molecule. Completion of minus strand synthesis occurs. RNAse H activity of reverse transcriptase has degraded the viral RNA except at the polypurine tract.

Step 3: Plus strand DNA synthesis commences. The polypurine tract acts as a primer for the plus strand synthesis.

Step 4: Plus strand DNA synthesis. Another jump is required to continue synthesis, this is facilitated by complimentary pairing of the primer binding site.

Step 5: Completion of DNA synthesis. The double stranded viral DNA now requires transport into the nucleus to allow intergration into the host genome.

transcription and enhancer elements in the U3 region of the LTR. Transcription produces a single RNA precursor some of which is spliced to produce env mRNA and transported to membrane bound polyribosomes. The remainder is transported to the cytoplasm where a small fraction is reserved as RNA genome for the new virions, the remainder being used as mRNA for gag, pro and pol and translated on free polyribosomes. Gag proteins are produced at a ratio of 10:1 due to a translational stop sequence in the 3' region of gag.
In the cytoplasm the gag and gag-pro-pol polyproteins oligomerise and begin forming viral core particles on the inner face of the cell membrane. This coincides with budding: invaginations of the cell membrane which at this time is studded with viral envelope glycoproteins. The full length mRNA binds through its packaging signal to the gag polyprotein as the particle assembles. Eventually the budding produces a fully closed sphere releasing the newly formed virions which do not become fully infectious until the protease cleaves the gag and pol polyproteins.

1.6.2.4 Recombinant retroviral vectors

The development of retroviral vectors has come from the understanding of retroviral biology. In particular vectors based on the Murine Leukaemia viruses have been the most studied and developed. For safety reasons replication defective vectors have been produced. The standard procedures have utilised the DNA form of the virus which allows for ease of manipulation. Essentially the coding sequence of the virus is replaced with the therapeutic gene, with necessary cis-acting elements retained. This vector is then transfected into helper or packaging cells which provide additional viral genes lacking from the vector and to support replication of the recombinant virus. The necessary cis-acting elements are listed (Vile and Russell, 1995):

- Packaging signal – ensures encapsidation of the vector RNA
- Elements required for reverse transcription – primer binding site, terminal repeat sequences (R) and the polypurine tract
- att sequences necessary for integration

An additional constraint on the vector is that the total vector sequence has to be $\leq$ 8kb, any greater and it will not be adequately packaged.

1.6.2.5 Packaging cell lines

The function of packaging cell lines is to support the propagation of the retroviral vector by providing in *trans* additional components necessary for assembly of vector particles: primarily the gag, pro, pol and env products. The first generation of cell lines were stable transfectants containing the proviral DNA from which the packaging signal had been removed (Mann et al., 1983). These produced recombinant retrovirus but despite not having the packaging signal helper RNA could still be packaged into virions albeit at a very low efficiency. Then through recombination events during reverse transcription significant numbers of replication competent retrovirus (RCR) could be produced. Therefore second generation packaging cell lines (such as PA317) were constructed in which further deletions of the helper DNA included parts of the 3' and 5' LTR (Miller and Buttimore, 1986). This resulted in less homology and decreased the likelihood of recombination events. To further reduce the likelihood of RCR 'split-genome' packaging cell lines were subsequently produced. These cell lines have viral gag/gag-pol polyproteins expressed from one plasmid and the env proteins expressed from another (Markowitz et al., 1988). This increases further the number of recombination events required to reconstitute RCR; however this has still been demonstrated in one of these cell lines (Chong et al., 1998).

Additional modifications of packaging cell lines have been to produce virions which incorporate the viral genome of one virus and contain proteins from a different virus, pseudotyping. This most commonly involves one virus using the envelope of another virus, either the envelope of a different retrovirus e.g. the PG13 cell line which expressess MLV gag-pol and the GALV envelope (Miller et al., 1991) or the envelope of a different viral family e.g. the G protein of vesicular stomatitis virus (Burns et al., 1993). This alteration in envelope may allow for different target cells to be infected e.g. improved infection of haemopoietic stem cells with a GALV envelope pseudotyped virus (Miller et al., 1991).

C type recombinant retroviruses produced from murine packaging cells are rapidly inactivated in human serum by the complement system. This is due to both viral and packaging cell factors (Takeuchi et al., 1994). Therefore for potential human in vivo

protocols human packaging lines pseudotyped with envelopes less susceptible to inactivation have been produced (Cosset et al., 1995).

1.6.2.6 Utility of retroviral vectors for gene therapy

Retroviral vectors were one of the first vector systems developed for gene therapy and still remain the most common agent used in human gene therapy trials (Weber et al., 2001). The benefits of using retroviral vectors is that the biology of RV is well understood, there are established methods for large-scale manufacturing with the use of constitutive producer cell lines, RV permanently integrate into the host cell genome and there is a good safety record in human clinical trials. In fact two successful gene therapy protocols to date have involved retroviral vectors. Both protocols involved *ex vivo* transduction: HSVtk was transferred into donor lymphocytes to control graft-versus-host disease in an allogeneic graft-versus-leukaemia response (Bonini et al., 1997), and the cDNA of the common cytokine receptor γ-chain was transduced into the bone marrow stem cells of children affected by severe combined immunodificiency (SCID)-X1 (Cavazzana-Calvo et al., 2000).

On the negative side is that the clinical studies conducted have generally shown a low level of transduction e.g. the glioma – HSVtk protocol conducted by Ram et al., (1997). There are a number of reasons for this but a major factor is the necessity for cells to be dividing for retroviral vectors to integrate. Appreciation of this feature has led to the development of lentiviral based vectors.

Initially titres obtainable from retroviral vectors with, for instance, MLV envelope proteins were in the order of 10^7-10^8; compounding the problem of low transduction efficiency. Pseudotyping with VSV-G allows greater concentration of virus leading to titres of 10^{10} (Yee et al., 1994). As well as improvements in titre focus has been given to targeting RV vectors. A number of strategies are being explored including tethering (Gordon et al., 2001), inverse targeting (Fielding et al., 2000), adaptor proteins (Snitkovsky and Young, 1998) and trans-complementation of fusion (Lin et al., 2001).

A further problem with the use of RV vectors in gene therapy protocols requiring prolonged transgene expression is the phenomenon of transcriptional silencing. This is

particularly pronounced in stem cells and is only in part due to cytosine methylation of CpG sequences (Pannell and Ellis, 2001).

1.6.3 Lentiviral vectors

Development of vectors from lentiviruses has been driven by the inability of C-type retroviruses to infect non-dividing cells. The capacity of lentiviruses to infect non-replicating or post mitotic cells have made them attractive vehicles for gene delivery and vectors from a number of different lentiviral species have been developed (Federico, 1999). Human immunodeficiency virus type 1(HIV-1) based vectors have been the most investigated and utilised.

1.6.3.1 HIV-1 genome and accessory proteins

As a complex retrovirus, in addition to the gag, pro, pol and env gene products, 6 accessory proteins are encoded. Three of these proteins are found in the viral particle: Vif, Vpr and Nef; Tat and Rev provide essential gene regulatory functions; and Vpu indirectly assists in the assembly of the virion (Frankel and Young, 1998). HIV-1 genome encodes 9 open reading frames and spliced mRNAs are used to express all of the accessory proteins.
Tat is a transcriptional activator that increases the production of viral mRNA ~ 100-fold and is therefore essential for viral replication. Without Tat polymerases do not transcribe more than the first few hundred nucleotides of the proviral DNA. Tat binds to the TAR (trans-activating response element) located at the 5' end of the nascent viral mRNA transcripts.
Rev regulates transport of unspliced or single spliced viral mRNA from the nucleus to the cytoplasm. It does this by binding to the Rev responsive element (RRE), located within the env coding region, contained within the viral mRNA transcripts. Without Rev the default pathway would be to produce multiply spliced mRNA which does not require Rev for export.
Vpu promotes degradation of CD4 in the endoplasmic reticulum when it clusters with env glycoproteins. This allows the envelope to transport to the cell surface and assemble into

viral particles. Vpu also enhances release of the viral particle, this is a nonspecific action as it can also promote release of heterologous retroviral particles (Lamb and Pinto, 1997). Nef also interacts with CD4, this time promoting its recycling from the cell surface and golgi to traffic to lysosomes and degradation (Kerkau et al., 1997). Nef also plays a role in viral reverse transcription but the exact mechanism is unclear.

Vif is important for the production of highly infectious particles from T lymphocytes in vivo. Some cell lines in vitro are able to produce highly infectious particles from Vif mutant viruses. It was therefore assumed Vif may counteract a negative host factor found in some cells (Cohen et al., 1996). This has now been identified to be the case. APOBEC3G is a cytidine deaminase nucleic acid-editing enzyme which has antiviral activity: incorporation of this enzyme into HIV-1 virions severely inhibits reverse transcription. Vif has now been shown to bind to APOBEC3G and induce its rapid degradation, thus preventing APOBEC3G incorporation and antiviral activity (Marin et al., 2003).

Vpr is important for nuclear localisation of the viral core following entry into the cytoplasm. Gag matrix and integrase have also been demonstrated to have nuclear localising activity. Vpr can also induce G2 cell cycle arrest (Emerman, 1996).

1.6.3.2 HIV-1 based vectors

The first generation vector design involved the use of packaging cell lines containing the whole HIV genome under heterologous transcriptional control, lacking the packaging signal and deleted in env (Naldini et al., 1996). The VSV-G envelope was provided in trans. The transfer vector contained the transgene under the transcriptional control of the HIV-1 LTRs, the packaging signal (including the first few bases of the gag open reading frame for optimal packaging) and the RRE. Subsequently it was found that effective packaging cells could be produced with the deletion of Vif, Vpr, Vpu and Nef and in so doing reduced the risk of RCR production, see **Figure 1.11** (Zufferey et al., 1997). The lentiviral vectors are produced by transient three plasmid transfection of producer cells. This strategy can yield titres of $>10^9$ (Kafri, 2001). Further gains in biosafety have been achieved by the generation of self inactivating vectors. The enhancer and promoter sequences from the vector's 3' LTR have been deleted. Following reverse transcription

Figure 1.11: Comparison of the HIV-1 proviral DNA with a multiply deleted packaging plasmid. The viral envelope and four accessory proteins are deleted in the packaging construct. Lentiviral vector is produced by transient transfection of 293T cells with this plasmid, vector plasmid containing the *cis*-acting elements and the transgene expression cassette, and an envelope expressing plasmid (usually VSV-G) (Zufferey '97).

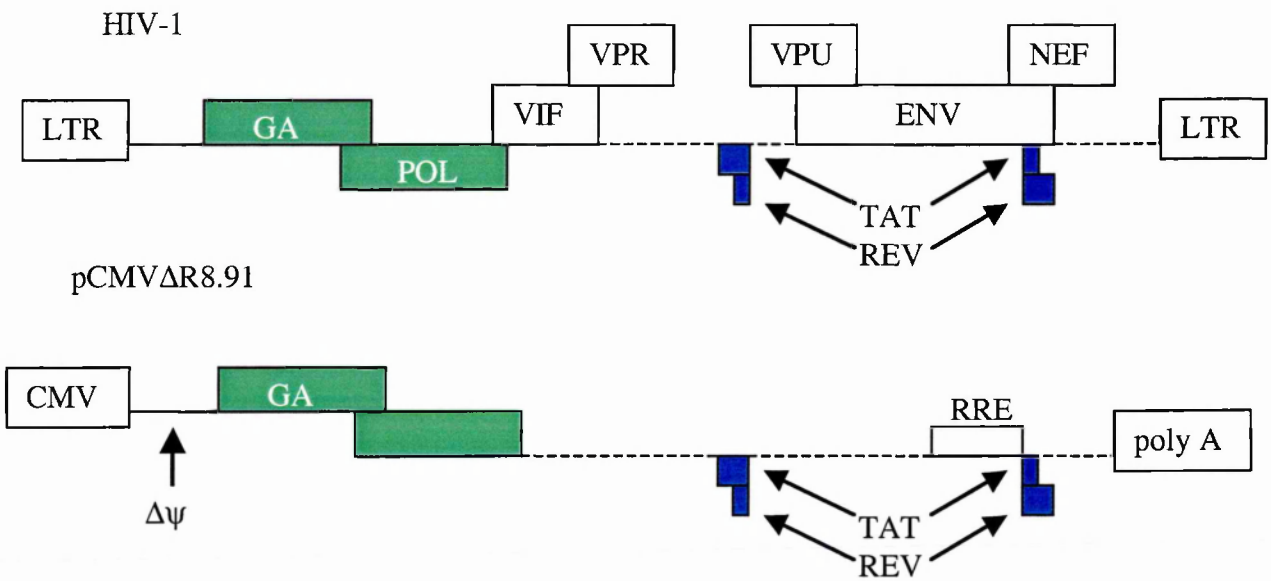

Figure 1.12: Ad5 genome structure. The ~36 kb genome is divided into 100 mu. The LTRs are demonstrated at each end of the double stranded DNA genome. The Early (E) and Late (L) regions with their direction of transcription are indicated. MLP/TP - major late promoter/tripartite leader. Dotted lines represent sequences spliced out during mRNA maturation, modified from Zhang '99.

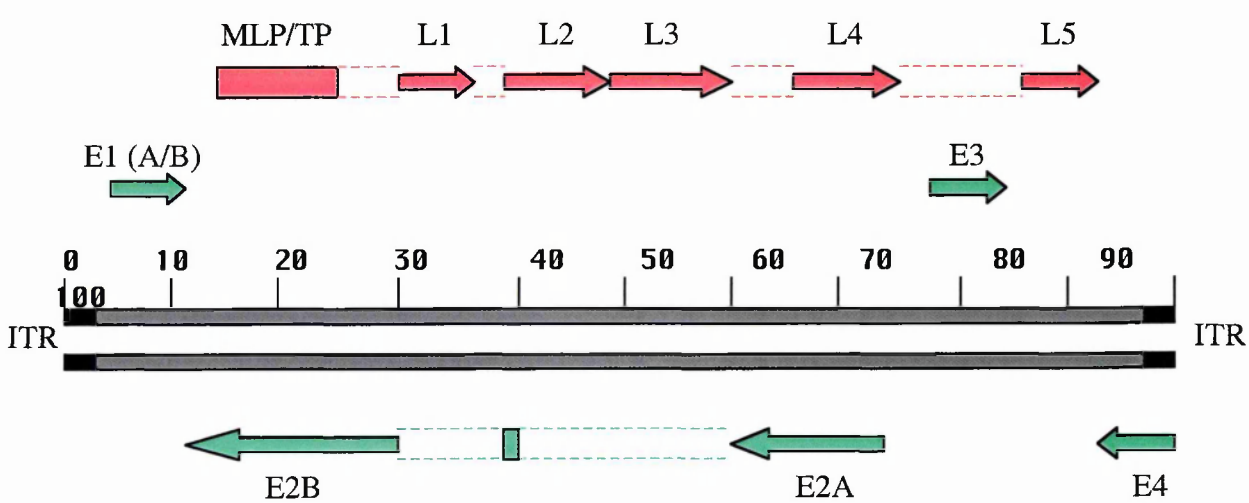

this vector will therefore be lacking enhancer/promoter sequences in the 5' LTR: resulting in an inability to transcribe RNA even in the presence of all viral proteins (Miyoshi et al., 1998; Zufferey et al., 1998).The major attraction to gene therapy of lentiviral vectors is their ability to transduce non-proliferating cells. This is due to the host nuclear import machinery actively transfering the HIV-1 pre-integration complexes through an intact nuclear membrane into the cell nucleus. Using lentiviral vectors various transgenes have been delivered into non-dividing tissues such as the central nervous system e.g. (Kordower et al., 2000). Another attractive target for these vectors are haematopoietic stem cells and pre clinical studies have been encouraging as to the utility of this vector system (Guenechea et al., 2000). As yet lentiviral vectors have not been approved for use in humans. This stems from the serious illnesses seen with wild type lentiviruses. The potential of lentiviral vectors is great but assessment of their true benefit to gene therapy will await their introduction in clinical trials.

1.6.4 Adenoviral vectors

1.6.4.1 Introduction

Viral vectors based on recombinant adenoviruses have found widespread use and applicability in a wide range of gene therapy protocols, and in particular cancer gene therapy (Vile et al., 2000). The reasons for this include the relative ease with which the adenoviral genome can be manipulated, the virus can be produced to high titre, has a broad host range including non-dividing cells and is non-integrating (Zhang, 1999). An important additional feature is that adenoviruses are immunogenic, which in the context of cancer gene therapy may be beneficial (Vile et al., 2000).

There are 47 different serotypes of human adenoviruses which are sub grouped from A-F according to genome size, organisation, and nucleotide composition etc (Shenk, T. 1996). The most studied and utilised adenoviruses are from subgroup C, specifically Ad2 and Ad5, which are considered endemic amongst the population causing sub-clinical infection or mild upper respiratory tract symptoms. The result is that the majority of people are positive for anti-adenoviral antibodies to these serotypes which is considered to be an important safety issue.

1.6.4.2 Virion structure

Adenoviruses are icosahedral structures 60-90nm in diameter. They are non-enveloped with a protein capsid surrounding a DNA-containing core. The capsid itself is made up of hexon, penton and fibre protein subunits. The hexon proteins form homotrimers and 240 of these hexomers form the basis of the icosahedral structure. The penton proteins form 12 pentomers and form the basis of the 12 vertices. The fibre proteins form trimers and associate with each of the 12 penton vertices, extending out from the capsid as the 'spike'. Stabilising the capsid and linking it to the core DNA binding proteins are a number of scaffolding proteins: polypeptides VI, VIII, IX and IIIa. The core DNA binding proteins include polypeptide VII which functions in a histone-like manner and allows coiling of the viral DNA. Another core DNA binding protein is the Terminal protein (TP), two copies per genome are covalently linked at each 5' end of the genome and are important in DNA replication (Shenk,T. 1996).

1.6.4.2 Genome

The genome consists of double stranded DNA approximately 36kb in length and conventionally this is divided up into 100 map units, see **Figure 1.12.** At each end of the genome are the inverted terminal repeat sequences (ITR) which contain the origin of replication and are essential for viral replication. Adjacent to the 5' ITR is the encapsidation signal which is essential for entry of cellular DNA into adenovirus empty virion capsids (Grable and Hearing, 1992). The genome is functionally divided into non-contiguous overlapping early and late regions, defined by the onset of transcription after infection. The early regions are E1A, E1B, E2, E3, E4 and there are 5 Late coding regions which predominantly encode the capsid, structural and core proteins. Each region encodes for a number proteins produced via alternate splicing and/or a number of open reading frames (ORF). The major protein products of individual regions will be discussed.

The E1A gene is the first viral transcript to be expressed following infection of the cell. The major function it exhibits is to drive cells in to S phase of the cell cycle (Querido et al., 1997b). It achieves this in part by activating E2F and thereby dissociating it from the negative regulators of S phase cell cycle progression; namely the retinoblastoma tumour-

suppressor family members (Zerfass et al., 1995). Protein products also interact with other cellular transcription factors to promote expression of the other adenoviral transcripts.

The E1B gene encodes two key proteins of 19kD and 55kD. E1B 55kD protein specifically binds to p53 and suppresses the functions of this key cellular protein (Querido et al., 1997a). E1B 19kD protein acts to prevent apoptosis which would arise as a result of the E1A actions (Rao et al., 1992) and also prevents the induction of apoptosis from external stimuli e.g. TNFα (Boyd et al., 1994).

The E2 gene encodes proteins essential for DNA replication including the adenoviral DNA polymerase (Ad pol), the DNA binding protein (DBP) and the preterminal protein (pTP). Additonal functions include activation of transcription from the major late promoter and repression of E4 transcription in order to delay viral particle assembly.

The E3 region is non-essential for viral replication in vitro as it functions mainly to prevent host immune responses developing against infected cells. It does this through a number of mechanisms including protein products binding MHC class 1 heavy chains in the ER and therefore preventiing viral epitopes being presented at the cell surface (Beier et al., 1994).

The E4 region encodes a number of ORFs which have protein products with broad involvement in late protein expression and inhibition of host cell synthesis. Additionally one of either ORF3 or ORF6 are essential for viral growth in vitro with E4 ORF6 encoding a 34kD protein which associates with E1B 55kD protein to prevent apoptosis.

Transcription of the late coding regions is controlled by the major late promoter which becomes increasingly active late in the infection. The large primary transcript (20kb) is processed by differential splicing and use of different poly(A) sites to yield the majority of capsid, scaffolding and core proteins (Shenk, T. 1996). The mRNAs produced from this promoter have a 5' tripartite leader sequence which allows their translation in preference to cellular mRNA (Zhang, 1999).

1.6.4.3 Entry

Adenoviruses enter cells via interaction with two cellular receptors. Initial binding is mediated via the fibre which attaches to the cocksacievirus and adenovirus receptor (CAR) (Bergelson et al., 1998). Subsequently the penton base via Arg-Gly-Asp (RGD) sequences

binds to cellular integrins, in particular $\alpha_v\beta_3$ and $\alpha_v\beta_5$ (Wickham et al., 1993). The virus is then trafficked into clathrin-coated pits and internalised by endocytosis. The penton base then undergoes conformational change within the acid environment of the endosome, disrupting the membrane and the virus gains entry to the cytoplasm. The virion is then thought to be targeted to the nucleus by signals in the capsid proteins (Greber et al., 1993).

1.6.4.4 Replication

Initiation of adenoviral DNA replication occurs at either terminal protein/ITR structure and involves both the adenoviral DNA polymerase and pTP. Replication can start at either end of the genome but it is uncommon to have active replication forks at both termini. Ad pol displaces one parental strand as it replicates the other. The DNA binding protein is essential to stabilise the displaced strand. Eventually the displaced parental strand is liberated and folds on itself forming a panhandle structure. This brings the terminal protein/ITRs at either end together, forming a structure identical to that recognised by the Ad pol/pTP machinery and replication complementary to this strand can commence. Late in infection the pTP is cleaved to form the TP which remains covalently bound to nucleotides at the 3' end of each ITR and so forming the TP/ITR structure.

1.6.4.5 Assembly and release

Initial oligomerization of the hexon, penton and fibre proteins occurs in the cytoplasm before they accumulate in the nucleus and form the empty capsids. The packaging of the adenoviral genome is dependant on the packaging sequence located at the left end of the viral genome (Hearing et al., 1987). Maturation of the virion then occurs involving proteolytic cleavage of some viral precursor proteins (Mangel et al., 1993; Webster et al., 1993). Escape from the cell is by cell lysis, brought about through disruption of the cytoskeleton caused in part by viral proteases produced from both early and late regions (Chen et al., 1993). Cell lysis occurs 32-36 hours after infection, the first 6-9 hours taken up with early gene expression, the remaining with late gene expression. At this time ~ 10,000 virions may be released per infected cell.

1.6.4.6 Vector production

Widespread use of adenoviral vectors for gene delivery came about when a helper cell line was produced which stably expressed the E1 gene products. These 293 human embryonic kidney cells contain fragments of the Ad5 genome (Graham et al., 1977): 5 copies per cell of the left most 12% of the viral genome and one copy of the right most 9% (Aiello et al., 1979). This allowed E1 deletion (ΔE1) of the recombinant vector, although the ITR, packaging signal and pIX sequences must be retained (Bett et al., 1994), with additional E3 deletion, the cloning capacity was then 7.5kb. The recombinant adenovirus is then able to be propogated in 293 cells allowing high titres after concentration and purification. These virions are then able to infect target cells but no further progressive viral infection is possible due to the lack of E1. Equally the lack of E1 means the toxic effects of adenoviral infection to the cell is markedly attenuated which is an important consideration in gene delivery.

The basic method for generating recombinant adenoviruses depends upon the insertion of the transgene expression cassette into a 'shuttle' vector: a plasmid which contains a small left-most end of the adenoviral genome, the insert sequences and then extended regions of the adenovirus genome subsequent to the E1 region. This shuttle vector is then co-transfected into 293 cells with the partial (i.e. Ad5 *Xba 1* large fragment) adenoviral genome and homologous recombination takes place forming the recombinant adenovirus (Chinnadurai et al., 1979). A problem with this technique is the presence of uncut adenoviral genome causing contamination. A variation on this method is therefore to incorporate the large adenoviral genome fragment in a plasmid containing additional sequences which results in a sequence too large to package. Only by undergoing recombination with the shuttle plasmid will a virus be produced, namely the desired recombinant (McGrory et al., 1988).

Additional methods have evolved to produce recombinant adenoviruses. These include selecting for postive recombinants in bacteria or yeast transformed with the shuttle and adenoviral genome vectors (Chartier et al., 1996; Ketner et al., 1994). Site specific recombination using the Cre/lox P system has also been developed to increase the formation of the recombinant adenovirus in helper cells (Hardy et al., 1997).

Another adenoviral vector strategy has been to develop vectors devoid of most viral information: the 'gutless' or mini-vectors (Kochanek et al., 1996). These vectors are capable of packaging upto 36 kb of insert but require the presence of a helper adenovirus to provide the essential viral proteins. Purification then becomes a particularly important issue with invariably some contamination of vector with helper, this is usually < 0.1%.

1.6.4.6 Utility of adenoviral vectors for gene therapy

The specific features that potentially make adenoviral vectors attractive for gene therapy are the ability to concentrate vector to high titre, routinely in the order of 10^{13} particles/ml. The distribution of CAR allows for a broad tropism and following entry the transgene will remain extrachromosomal, therefore minimising the risk of insertional mutagenesis. Vectors can transfect both dividing and non-dividing cells, and produce high levels of gene expression.

Countered against these features is the first fatal toxicity occurred in a protocol using an adenoviral vector being administered systemicaly (2000). This highlights the immune response which is generated to adenoviral infection, whether wild type virus or recombinant. Both humoral and cellular immune responses develop rapidly following infection (Yang et al., 1995). CTLs directed against viral antigens and/or the transgene product promote the clearance of infected cells. Humoral immune responses generated following primary infection result in a barrier to repeated administration of vector (Dong et al., 1996). However this humoral response can be bypassed if vector is delivered to particular compartments e.g. directly into a tumour (Bramson et al., 1997). In addition, in a cancer therapy context the immunogenicity of adenoviral vectors may be a favourable attribute as the vector itself has been shown to produce an adjuvant effect (Geutskens et al., 2000).

Widespread expression of CAR in normal tissues and the limited expression seen in some tumours could result in poor *in vivo* distribution of vector. Attempts to alter Ad tropism have focused on modifying the viral capsid (Krasnykh et al., 2000) or by introducing bi-specific antibodies e.g. to fibre and the epidermal growth factor receptor (Miller et al., 1998). Even following successful transduction of tumour cells *in vivo*, if there is rapid

division, due to non-integration of the vector genome, transgene expression will only be transient.

1.6.5 Discussion

There are important differences between each of the viral vector systems under development and some of these have been highlighted for retroviral, lentiviral and adenoviral vectors. Each system has positive and negative aspects with regard to their suitability for a particular gene therapy protocol. However the ideal vector for any given *in vivo* gene therapy protocol does not exist. *In vitro* gene delivery is much more straight forward and is an area that has already witnessed gene therapy benefitting patients (Bonini et al., 1997; Cavazzana-Calvo et al., 2000).

The problems encountered with *in vivo* delivery primarily rest with an inability to transduce sufficient numbers of target cells. This results in a deficiency of gene expression in the target cells and consequently a lack of therapeutic effect. Improvements primarily in targeting should lead to greater efficiency of gene delivery and improve the effective titre. Areas which may well play a role in targeting the gene expression may not just involve the vector envelope but also include transcriptional targeting and genetic engineering capable of producing selectively replicating viral vectors such as Onyx-015.

In the context of delivering a cytotoxic gene into cancer cells *in vivo* an adenoviral vector is the most attractive vehicle at the present time. This is due to the characteristics detailed previously: high titre, high level of gene expression in a wide variety of cell types and adjuvant effect of the adenoviral immunogenicity. Also prolonged gene expression is not required in this type of strategy.

1.7 Mechanisms of cell death

1.7.1 Introduction

Ultimately for any cancer therapy to be successful tumour cells must be eradicated. Apart from surgery this will mean that cancer cells will need to be killed within the host. The potential mechanisms of cell death are becoming increasingly defined. With that a better

understanding of the processes at play within normal 'physiological' cell death and those in disease states such as cancer are being realised. Three mechanisms of death are detailed below: two programmed, apoptosis and autophagy, and one pathological, necrosis. As indicated previously cytotoxic gene therapy strategies are highly unlikely to directly eradicate all tumour cells. A pre-requisite of successful gene therapy in this setting will likely be the induction of a tumour specific immune response (Melcher et al., 1999). The likelihood of inducing this immune response may well be related to the manner in which tumour cells die and will be discussed.

1.7.2 Apoptosis

Apoptosis has been extensively studied and now many aspects are relatively well defined. It is an energy dependent programmed cell death pathway which allows multicellular animals to control cell numbers and tissue size (Hengartner, 2000). Its identification came about by the observation of characteristic morphological changes seen in a wide variety of cell types (Kerr et al., 1972). It is a process highly conserved in animals and plays an integral part in tissue development and remodelling (Meier et al., 2000). It also plays a critical role in the deletion of damaged or rogue cells with defects in the apoptotic pathway thought to play an important role in tumourogenesis and resistance to cancer therapies (Jaattela, 1999). Equally, apoptosis occuring in excess is thought to play a significant role in a wide variety of diseases including neurodegenerative diseases.

1.7.2.1 Morphological changes

The specific morphological changes seen in cells undergoing apoptosis are quite characteristic (Wyllie, 1993). Affected cells shrink and lose contact with their neighbours. In the nucleus chromatin condenses into a few sharply delineated uniform masses under the nuclear membrane. Eventually the condensed chromatin breaks up (Saraste, 1999).The cytoplasm condenses with organelles including mitochondria remaining intact, only the endoplasmic reticulum dilates. The outline of the cell becomes convoluted and forms extensions. Membrane bound apoptotic bodies containing condensed chromatin and cytoplasm break off and are rapidly taken up by neighbouring cells by phagocytosis. The

plasma membrane has remained intact therefore there is no leakage of intracellular material and consequently very little inflammatory response seen in vivo.

1.7.2.2 Biochemical features of apoptosis and Caspases

The classically described hallmark of apoptosis is the degradation of genomic DNA into multiples of ~180 base pair fragments (the DNA ladder) (Wyllie, 1980). This effect is seen as the activated DNAse responsible cuts DNA between nucleosomes. The majority of the other characteristic morphological changes are also brought about by the same underlying biochemical process; namely the activation of effector caspases and their cleavage of specific substrates (Hengartner, 2000). Caspases (Cytosolic Aspartate-Specific Proteases) are a large family of proteases which cleave substrates at Aspartic acid-X residues. An individual caspase's specificity of target is dictated by the four amino acids amino terminal to the cleavage site (Thornberry and Lazebnik, 1998). The target protein is then cleaved, usually at a single site, resuting in a change in function.

Caspases are expressed as proenzymes which contain 3 domains: an amino terminal domain, a large subunit, p20(~20kD) and a small subunit p10 (~10kD) (Thornberry and Lazebnik, 1998). Activation sees association of the p20/p10 forming a heterodimer, two heterodimers combine to form the active heterotetramer mature enzyme. Activation of caspases can occur through a number of proposed mechanisms (Hengartner, 2000):

1.Processing by an upstream caspase: most caspases have Asp-X sites between their p20 and p10 subunits thus activated caspases can act in a cascade activating downstream members. This is the major activation route for the effector caspases: caspase-3,-6 and –7.

2.Induced proximity: binding of ligand to a death receptor e.g.CD95 (see below) causes aggregation of CD95 receptors. Through adaptor proteins e.g.Fas-associated death domain protein (FADD) numerous molecules of caspase-8 proenzyme are brought into close proximity. This is sufficient for the low intrinsic protease activity of procaspase-8 to trigger an activation cascade (Muzio et al., 1998).

3.Association with a regulatory subunit:pro caspase-9 does not undergo proteolysis for activation but a conformational change. For this to occur it requires association with Apaf-1, cytochrome *c* and ATP. Bcl-2 family memebers control cytochrome *c*

release from the mitochondria and are therefore a key component of the mitochondrial apoptotic pathway (see **Figure 1.13**).

It should be noted that initiator caspases contain in their prodomains specific regions which allow for interaction with upstream regulators. In the case of caspases 8 and 10 this domain is termed the death-effector domain (DED), caspases 2 and 9 contain a caspase activation and recruitment domain (CARD).

Although the majority of morphological changes seen in apoptosis can be attributable to effector caspase activation and action on defined substrates, apoptosis can occur in the absence of caspase activation (Borner and Monney, 1999).

1.7.2.3 Triggering events for apoptosis: Death-receptors and Mitochondria

The cell can undergo apoptosis following signals from both internal and external sensors. Internal signals initiate activation of apoptosis via mitochondrial cytochrome *c* release whereas external signals are relayed by death receptors (Ashkenazi and Dixit, 1998)(see **Figure 1.13**).

i. Death receptors. Receptors capable of transducing signals that activate apoptosis are a subset of the tumour necrosis factor receptor family (TNF-R) and termed death receptors. Specifically they contain a death domain in their cytoplasmic tail important for interaction with downstream proteins. A number of receptors have been described: CD95 (Fas), TNFR1, DR3 (Apo3), DR4 and DR5. Signalling occurs by the same pattern with each receptor:1) ligand binding, 2) receptor trimerization, 3) FADD binds by interaction with the death domain and in conjunction with the receptor forms the death-inducing signalling complex (DISC), 4) procaspase-8 associates with the DISC through the DED, 5) auto-catalytic cleavage of procaspase-8 occurs leading to activation of the cascade (Krammer, 2000). In some cells it seems DISC formation is not sufficiently plentiful to provide enough caspase-8 to proceed to cleave procaspase-3. In this situation caspase-8 cleaves the Bcl-2 family member Bid. Truncated Bid induces cytochrome *c* release from the mitochondria promoting caspase activation and apoptosis (Scaffidi et al., 1998). Associated with this simplified signalling process is a complex level of additional control mechanisms; an example of which is FLICE-inhibitory proteins (FLIPs). These proteins

Figure 1.13: Diagrammatic representation of the two major apoptotic pathways in mammalian cells. The death-receptor pathway is illustrated by CD95 and caspase-8 activation. The mitochondrial pathway illustrates the formation of the apoptosome following cytochrome *c* release. Each pathway activates effector caspase-3 (see text for full discussion, diagram modified from Hengartner).

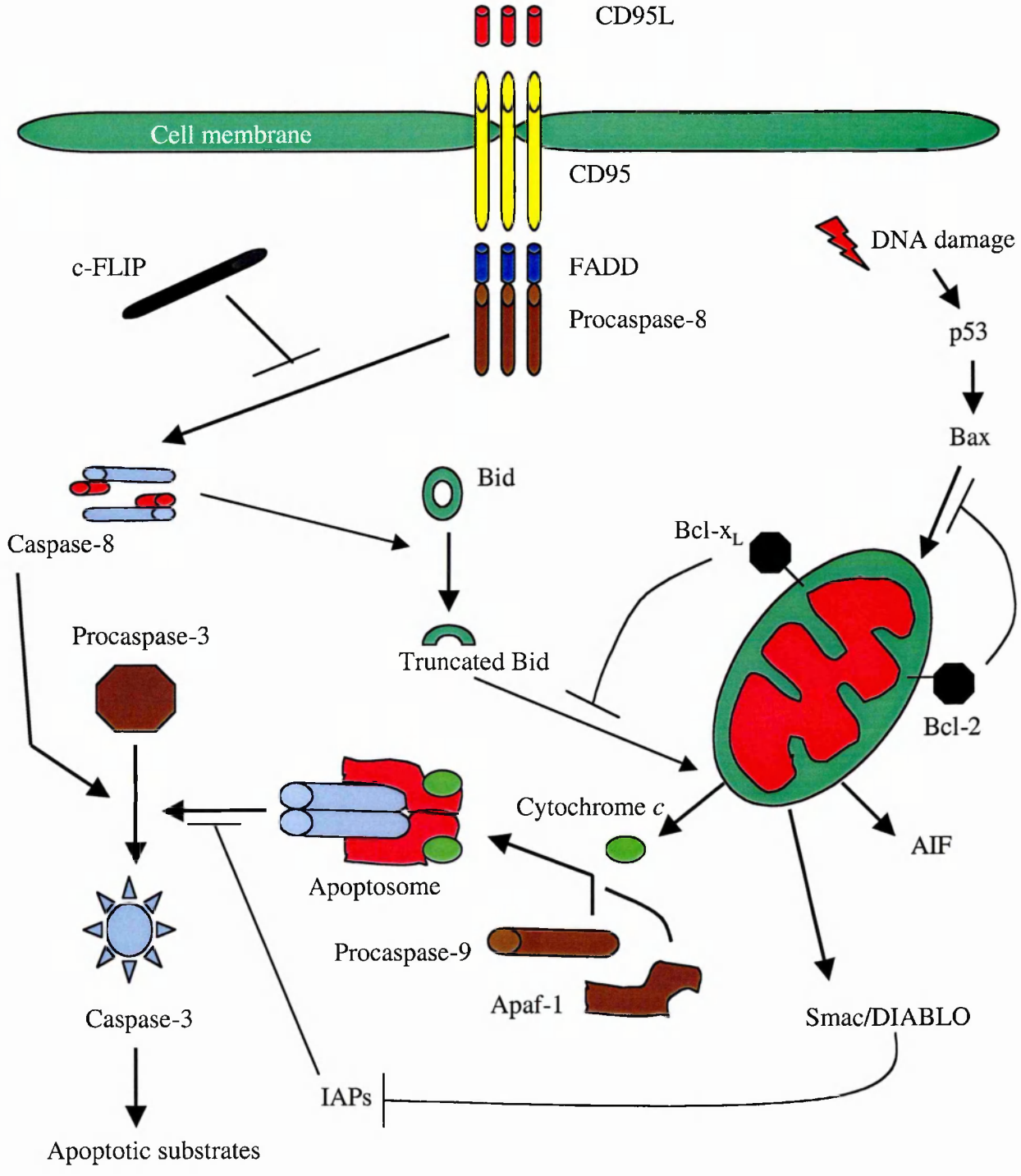

have DEDs and therefore compete with procaspase-8 for association with the DISC (Yeh et al., 2000).

ii. Mitochondria. Sensors within a cell, following their activation, are capable of inducing apoptosis by effecting cytochrome *c* release from the mitochondria. An example of this is the activation of p53 following DNA damage leading to apoptosis in certain cells (Vogelstein et al., 2000). Cytochrome *c* is a globular protein that resides in the intermembrane space where it plays a role in the mitochondrial oxidative phosphorylation pathway. Release of cytochrome *c* into the cytosol is dependent on a loss of integrity of the outer mitochondrial membrane. Control of this release is by the Bcl-2 family of proteins; a group of at least 15 proteins which contains both pro and anti-apoptotic members (Adams and Cory, 1998). Structural and functional criteria have been used to categorise the family into 3 groups. All proteins contain at least one of four conserved motifs termed Bcl-2 homology domains (BH1 to BH4): group 1 members contain at least BH1 and BH2 domains and all have anti-apoptotic activity. Within this group are Bcl-2 and Bcl-x_L. Group 2 members have BH1,2 and 3 domains. All have pro-apoptotic activity and includes Bax and Bak. Group 3 is a more diverse group structurally with members only possessing the BH3 domain. This group again is pro-apoptotic and includes Bid and Bik. The carboxy-terminal transmembrane tail of Bcl-2 proteins targets the proteins to intracellular membranes including the outer mitochondrial membrane.

Due to their structural arrangements Bcl-2 proteins can heterodimerize as well as homodimerize. This may allow pro and anti-apoptotic members to be balanced out in normal conditions but following upstream stimuli the balance moves to pro-apoptotic or pro-survival conditions. The exact mechanism of how Bcl-2 family members control cytochrome *c* exit is not entirely clear but 3 basic models have been proposed: a) Bcl-2 members form channels that facilitate protein transport, b) Bcl-2 members interact with other proteins to form channels, c)Bcl-2 members induce rupture of the outer mitochondrial membrane (Hengartner, 2000).

In addition to cytochrome *c* release loss of integrity of the outer mitochondrial membrane will cause the release of other pro-apoptotic stimuli. These include AIF (apoptosis inducing factor, a flavoprotein), procaspases-2, -3, -9 and Smac/DIABLO (an inhibitor of

caspase inhibitor proteins, IAPs (inhibitors-of-apoptosis). Therefore cell survival and mitochondrial function are firmly interlinked (Vander Heiden and Thompson, 1999).

1.7.2.4 Phagocytosis of apoptotic bodies

The end result of the apoptotic pathway is the production of apoptotic bodies. These apoptotic bodies are taken up by professional scavengers, such as macrophages, or by neighbouring cells. This allows for the whole process to remain immunologically silent and in fact the process may actively be anti-inflammatory (Voll et al., 1997). The factors associated with apoptotic body phagocytosis have been termed 'eat me' signals (Savill and Fadok, 2000). The best characterised is the exposure of phosphatidylserine (PS) on the outer surface of cells undergoing apoptosis; the normal position of PS is in the inner leaflet of the plasma membrane (Fadok et al., 1998). Changes in surface sugars also occur during apoptosis and are thought to promote phagocytosis via lectins on phagocytic cells. Less clear is how ICAM-3 and low-density lipoproteins mediate phagocytosis of apoptotic bodies. In addition further poorly defined 'eat me' signals promote binding of molecules present in the extracellular fluid such as components of the complement system C1q and iC3b, thrombospondin and β_2 glycoprotein 1 (Savill and Fadok, 2000).

1.7.3 Autophagy

Apoptosis is probably not the only programmed cell death. Detailed studies of developing mouse embryos lead researchers to identify three types of physiological cell death by their morphological characteristics (Kitanaka and Kuchino, 1999). Type 1 is compatible with apoptosis. Type 2 is compatible with autophagy or autophagic degeneration and will be detailed below. Type 3 described as non-lysosomal disintegration occurred in vacuolated cartilage and will not be detailed further.

Morphologically autophagy is characterised by the early appearance of large autophagic vacuoles in the cytoplasm. The nucleus undergoes very little change in the initial stages. Eventually the cell swells and fragments, with neighbouring cells phagocytosing the debris. Autophagy has been identified to occur in all nucleated cells analyzed (Klionsky and Emr, 2000). The function of the process is to sequester and degrade cytoplasmic components including organelles. Once broken down the constitutive parts can then be

recycled to the cell. In some situations, as indicated above, the process is progressive and leads to the death of the cell. Autophagy has been predominantly studied in yeast where conditions of starvation are sufficient to generate the morphological findings of vacuolation (Tsukada and Ohsumi, 1993). More recent studies of human cells have indicated the *beclin 1* gene as being involved in autophagy. Interestingly decreased levels of Beclin 1 protein were identified in breast cancer cells (Liang et al., 1999). Increasing Beclin 1 levels in those cancer cells was able to inhibit tumour cell proliferation and prevent tumourigenesis in nude mice.

The basic process of autophagy can be broken down into at least four steps (Klionsky and Emr, 2000): a) Induction, b) membrane formation sequestering cytosol and or organelles forming an autophagosome, c) docking and fusion with the lysosome, and d) finally breakdown within the lysosome. The lysosome is well suited to the role of degradation as it contains proteolytic enzymes and hydrolases capable of degrading any subcellular constituents.

As indicated above the molecular controls of autophagy have been primarily explored in yeast using mutants; starvation-sensitive or defective in the degradation of specific cytosolic proteins (Thumm et al., 1994; Tsukada and Ohsumi, 1993). These have shown overlap with the cytoplasm to vacuole targeting pathway. Initiation has been shown to be associated with down regulation of Tor kinase. This allows activation of phosphatases leading to autophagosome formation (Klionsky and Emr, 2000).As yet there is limited detail about the important initiators and mediators of autophagy in mammalian cells (Liang et al., 1999).

1.7.4 Necrosis

The term necrosis specifically describes cell death by any mechanism (Majno and Joris, 1995). It is now generally used to imply non-programmed or accidental (pathological) cell death which is an in vivo phenomenon (Melcher et al., 1999). Importantly this process is not passive and instantaneous but most commonly does involve active transcription of stress related and other genes occuring prior to death (Melcher et al., 1998). These stress response proteins attempt to protect the cell from potentially lethal insults e.g. ischaemia. The resulting necrosis indicates the cells protective mechanisms were not sufficient to

save the cell from death. This in vivo description of necrosis should be considered quite distinct from experimental ex vivo conditions such as repeated freeze thawing or bursting in distilled water.

The morphological features consistent with necrosis are quite different from those detailed for apoptosis and autophagy (see **Figure 1.14**). The first signs are of cellular swelling due to a failure of the ionic pumps of the plasma membrane. This leads to organelle swelling, vacuolation and membrane blebbing. The nucleus undergoes karyolysis, pyknosis and karryorhexis. Eventually the cell ruptures releasing intracellular contents into the surrounding environment, producing a pro-inflammatory stimulus.

1.7.5 Relevance of cell death to gene therapy

It is convenient to clearly delineate the process of cell death into the defined groups listed above with particular reference to apoptosis being immunologically silent and necrosis being pro-inflammatory. However in vivo the situation is undoubtedly not quite so straightforward (Melcher et al., 1999). One reason is that it would appear that classical apoptosis and necrosis are at different ends of a continuum (Kroemer et al., 1998). This is suggested following evidence that the same toxin can activate apoptosis if given in a lower dose or necrosis if higher. Further evidence includes the manipulation of intracellular ATP levels which can direct the death process to apoptosis or necrosis following the same stimuli: cells depleted of ATP die by necrosis, adequate ATP levels permit apoptosis to occur (Nicotera et al., 1998). Therefore it may be that in vivo, following a cytotoxic gene therapy strategy, both apoptosis and necrosis may occur in the target tumour. In addition therapy induced apoptosis as opposed to developmental/homeostatic apoptosis may result in sufficient death that the immediate mechanisms for apoptotic body clearance are overwhelmed. The resultant excess of apoptotic material will then proceed to secondary necrosis (Melcher et al., 1999).

The issues raised above may go some way to explaining why there is some apparent controversy in the literature either indicating that apoptosis is insufficient to induce an immune response (Gallucci et al., 1999; Matzinger, 1998; Melcher et al., 1998; Sauter et al., 2000) or that it is (Albert et al., 1998; Hoffmann et al., 2000; Restifo, 2000). Specific experimental conditions may give rise to these perceived differences in interpretation.

Figure 1.14: Morphological appearance of cell death pathways

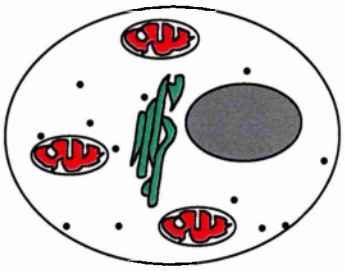

Normal cell

II. Apoptosis: characteristic features include shrinkage and pyknosis followed by budding and karyorhexis

III. Autophagy: characteristic features include formation of vacuoles (autophagasomes - yellow). Initially cell size and nucleus remain relatively unchanged.

I. Necrosis: characteristic features include cellular swelling, vacuolation, blebbing and increased permeability. Eventually karyolysis will occur.

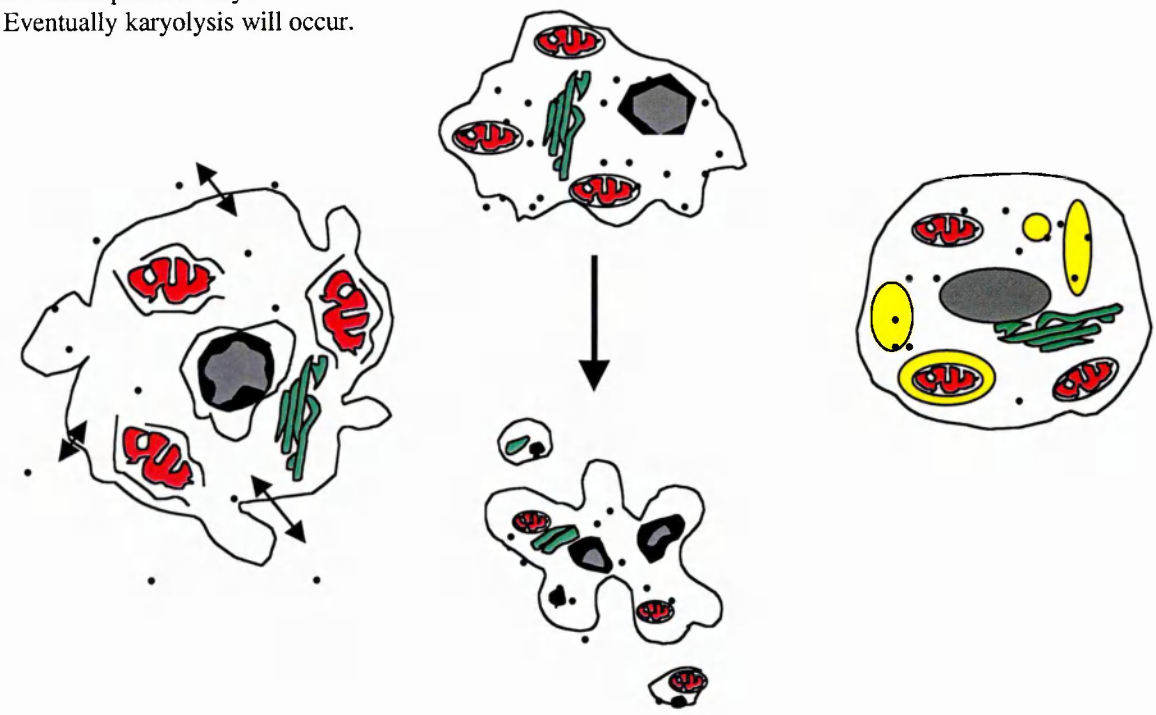

Careful assessment needs to be given to what constitutes necrosis and apoptosis in each model system.

As previously described the process of necrosis in vivo (including secondary necrosis of apoptotic bodies) generates a pro-inflammatory environment due to the release of intracellular material and stress signals such as heat shock proteins (see below). This environment influences the response of phagocytic/antigen presentation cells (macrophages, dendritic cells) which then promote the development of a cytotoxic T cell response (Gough et al., 2001). By engaging the immune system eradication of tumour cells is enhanced and the cancer therapy likely to be more successful. This is most likely to happen when tumour cells have undergone a stressful (necrotic) death whether induced by gene therapy or other anti-cancer therapies (Melcher et al., 1999).

1.8 Heat shock proteins and immunogenicity

1.8.1 Introduction

The previous section indicated the pro-inflammatory nature of necrotic cell death. A key component of this effect is likely to be the release of intracellular contents into the extracellular environment which occurs in necrosis. These released factors can then be sensed and act as a 'danger signal' (Matzinger, 1994); alerting the immune sysytem to potential pathological processes and an immune response initiated. It has become increasingly clear that members of the heat shock family play an important role in this mechanism (Srivastava et al., 1998).

1.8.2 Normal function of Heat shock proteins (HSP)

HSP are highly conserved across evolution and are found in almost all species from bacteria to man. The majority are essential to life with knock out mutations proving embryologically fatal. HSP are abundant in the cell and are found in the cytosol, mitochondria, nucleus, nucleolus, ER, lysosome and plasma membrane. HSP function is to assist with protein folding, translocation and dissolution of protein aggregates in the cell (Gething and Sambrook, 1992). In order to perform these functions HSP non-covalently

bind (poly)peptides and HSP-peptide complexes (HSP-PC) can be recovered from cells (Peng et al., 1997; Udono and Srivastava, 1993).

The identification of HSP came about following investigation of the heat shock response; many HSP are induced following exposure to increased temperature and thus they gained their name. HSP have been classified into six major families according to their molecular size: Hsp100, Hsp90, Hsp70, Hsp60, Hsp40, and small heat shock proteins. Within each gene family are members that are constitutively expressed, inducibly regulated, and/or targeted to different compartments.

1.8.3 The stress response

HSP as well as performing homeostatic functions play an integral role in protecting the cell from a variety of environmental insults (Welch et al., 1991), the best characterised of which is heat shock. Other stresses, including nutrient deprivation, oxygen radicals and metabolic disruption also result in changes in HSP expression. The pattern of expression does vary dependent on the stress and two major groups have been loosely defined: those referred to as heat shock proteins (e.g. hsp72) and those referred to as the glucose regulated proteins (e.g. gp96) (Welch et al., 1991). How the cell senses stress is not entirely clear but may be related to an increase in denatured or aggregated proteins. Following stress, transcriptional activation of the stress proteins is mediated by a transcription factor: heat shock factor (HSF) (Morimoto, 1993). This factor, present in an inactive monomeric form, is able to trimerise in response to stress. HSF trimer binds to specific DNA recognition sequences located 5' of heat shock responsive genes termed heat shock elements (HSE) and leads to transcription of the HSP.

The primary HSF associated with heat-induced HSP expression is HSF1 (a number of HSF have now been identified). Control of the oligomeric status of HSF1 is in part by HSP binding (Pirkkala et al., 2001). Under normal conditions HSP bind HSF1 and prevent trimerisation. If there is an increase in levels of denatured protein competing for binding to the HSP, HSF1 is released and free to oligomerise. This provides a feedback system for the regulation of HSF1.

1.8.4 HSP, cell death and immune activation

Should the protective mechanisms fail following stress the cell will die. If this is necrotically, intracellular contents including HSP will be released. The mechanisms which then lead to immune activation have come to light out of studies of tumour rejection antigens (Srivastava et al., 1998). One mechanism relates to HSP-PC, the second relates to the direct adjuvant effects of HSP themselves.

In mouse models, resistance to tumours could be generated by prior vaccination with the specific tumour cells (Srivastava and Old, 1988). Investigation into the tumour antigens responsible for this protection indicated a number of HSP as being important and more specifically HSP-PC (Udono and Srivastava, 1993). HSP-PC induce an immune response through receptor mediated uptake by antigen presenting cells (APC). The peptide chaperoned by the HSP is trafficked within the APC and presented in the context of MHC class 1 i.e. cross-priming (Srivastava et al., 1998). The antigenic peptide is therefore presented on a cell (APC) capable of activating naïve T cells.

A receptor mediating uptake on APC for HSP-PC has recently been defined as CD91 and acts for hsp70, calreticulin as well as hsp90 family members (Basu et al., 2001; Binder et al., 2000b). Additional receptors may be involved for some HSP (Lipsker et al., 2002; Ohashi et al., 2000). Receptor-mediated endocytosis results in HSP-PC being identified in clathrin-coated vesicles and not passing to the lysosomal degradation pathway (Arnold-Schild et al., 1999; Wassenberg et al., 1999). Once internalised the HSP-PC can then be identified in a secondary perinuclear endosome. The subsequent exact sequence of events leading to peptide presentation by MHC class 1 is not known and two models have been proposed (Berwin and Nicchitta, 2001). The first model proposes that the chaparoned peptides are then trafficked to the cytosol before being introduced into the ER by the TAP peptide transporter. Once in the ER the peptides bind nascent MHC class 1 molecules. The second model proposes that recycling class 1 molecules and dissassociated peptides from HSP-PC occur in the same endosome, bind and traffic to the cell surface. At present there is preliminary data supporting both models (Castellino et al., 2000; Gromme et al., 1999; Kleijmeer et al., 2001; Levitt et al., 2001).

HSP have also been shown to have direct adjuvant effects on APC. Hsp60 and Hsp70 induce the activation of monocytes and the secretion of the pro-inflammatory cytokines

TNF-α and IL-12 via interaction with CD14 (Asea et al., 2000; Chen et al., 1999; Kol et al., 2000). Hsp70 over expression and release during tumour cell killing induces a Th1 cytokine profile and promotes antigen uptake by immature APC (Todryk et al., 1999). gp96 immunization has been shown to induce maturation of APC and promote trafficking of these APC to draining lymph nodes (Binder et al., 2000a; Singh-Jasuja et al., 2000). This process is in part mediated by CD91 interaction and activation of the NF-κB pathway. Interestingly different HSP have been shown to have differential effects on APC with different DC activation markers being up regulated (Basu et al., 2000).

Release of HSP into the extracellular millieu which occurs in necrosis can be seen to fulfill the criteria for a 'danger signal' (Matzinger, 1998). Through their chaparone function and direct adjuvant effects HSP interact directly with APC, promoting activation of both the innate and adaptive immune systems (Srivastava et al., 1998). These processes go some way to explaining why the different death pathways may be sensed and have different immunological outcomes.

1.9 Cytokines in Gene Therapy

1.9.1 Introduction

As previously discussed the successful application of gene therapy to treat cancer will probably necessitate the generation of a tumour specific immune response. Engaging the immune system will hopefully bring specificity, potential for considerable expansion of response and durability (i.e. memory). Current views as how best to promote the generation of this tumour immune response include the manner in which tumour cells are killed, as previously discussed, and also the addition of adjuvants, including cytokines, to the gene therapy strategy (Cao et al., 1999).

Cytokines can be defined as hormone-like polypeptides that are crucial in the communication between normal cells and can promote activation of several important cellular functions (Parmiani et al., 2000). It is clear that cytokines are essential factors in the activation and development of an immune response. Many cytokines are now well characterised and have been examined in a gene therapy context. An example of an early

study was when a murine melanoma line was transfected with 10 different cytokines and used as an autologous vaccine. Granulocyte-macrophage colony-stimulating factor (GM-CSF) expressing tumour cells were the most effective at inducing a tumour specific immune response (Dranoff et al., 1993). This and other results suggest that GM-CSF can be a useful component of an anti-cancer gene therapy protocol.

1.9.2 GM-CSF

Human GM-CSF is encoded by the hGM-CSF gene on chromosome 5q. A variety of cell types can synthesise GM-CSF and include T cells, macrophages, mast cells, endothelial cells and fibroblasts. The GM-CSF produced has a paracrine effect acting locally and is not detectable in the circulation. The protein itself is 144 amino acids which includes a 17 amino acid leader sequence. It is a glycoprotein of 22kDa which can be heterogeneously glycosylated. GM-CSF has a wide range of biologic activity particularly effecting neutrophils, eosinophils and macrophages (Gasson, 1991). As its name implies the first identified function was as a potent stimulator to the proliferation and maturation of myeloid progenitors (Metcalf, 1985; Tomonaga et al., 1986). This lead to the first therapeutic role for GM-CSF: to augment the cytopaenic effects of chemotherapy.

With regard to gene therapy, additional effects of GM-CSF make it attractive. Pre-clinical models such as Dranoff et al., (1993) indicated that GM-CSF activates antigen presenting cells (APC), promotes APC class II MHC expression, enhances the antigen presentation capacity of APCs and enhances dendritic cell maturation and migration to regional lymph nodes (Inaba et al., 1992; Sallusto and Lanzavecchia, 1994). It also augments the primary antibody response (Warren and Weiner, 2000). Clinical studies have now been undertaken and the data complementary. Thirty three patients with metastatic melanoma were enrolled in a phase 1 study at the Dana Faber cancer Institute (Soiffer et al., 1998). Autologous melanoma cells were obtained from metastatic deposits, transduced with a retroviral vector expressing human GM-CSF and lethally irradiated. These cells were then used as a vaccine, given intradermally and subcutaneously at various intervals depending on the dose level. Examination of these vaccination sites indicated a marked infiltration with DC, macrophages, T lymphocytes and eosinophils. Indeed, a similar infiltrate was found in 11 of 16 patients from whom post vaccination metastatic tissue was obtained. Further analysis

of the immune cells infiltrating the metastases identified many CD8 and CD4 T lymphocytes, as well as large numbers of plasma cells. A cytokine profile of both a Th 1 and Th 2 response was identified as well as induction of IgG antibodies recognising surface melanoma cell antigens. The conclusions from this study are that this GM-CSF modified tumour cell vaccine protocol does stimulate antitumour immunity, although in this group of patients it does not translate into dramatic clinical benefit. A more likely group to benefit from a vaccination scheme are those patients with microscopic residual disease and studies are being developed. The applicability of this approach to other tumour sites has been encouraged by similar anti tumour immune responses seen in a prostate cancer vaccination protocol (Simons et al., 1999).

From a practical stand point allogeneic vaccines are more likely to be widely applicable to more patients due to the problems of obtaining and expanding primary tumour cell cultures from each individual patient. This allogeneic vaccine approach will clearly only be attractive if efficacy is maintained. Pre-clinical studies suggesting efficacy of allogeneic tumour cell vaccines have now been conducted. However once more expression of GM-CSF by the allogeneic tumour line was an integral component of the successful approach (Jaffee et al., 2001; Kayaga et al., 1999). Further vaccine strategies have been developed using DC transduced with tumour antigen (Klein et al., 2000) or DC-tumour cell fusion (Cao et al., 1999). In both models an enhanced therapeutic response was seen when DC were additionally transduced with vectors capable of expressing GM-CSF.

1.9.3 Discussion

GM-CSF, along with other cytokines such as IL-2, IL-12 etc, is undergoing extensive investigation as an immune adjuvant in a number of gene therapy settings. This is due to the observed promotion of both cellular and humoral immunity by GM-CSF. These effects are primarily due to the action of GM-CSF on APCs: promoting their expansion, maturation, antigen presentation capacity and migration to lymph nodes. This combined with a low toxicity profile make GM-CSF a likely component of future gene therapy approaches whether singly or in combination with other genes e.g. cytotoxic genes. I explored the co-expression of FMG with GM-CSF and this is detailed in Chapter 8.

CHAPTER 2: MATERIALS AND METHODS

CHAPTER 2: MATERIALS AND METHODS

2.1 MOLECULAR BIOLOGY

2.1.1 General Procedures

All solutions employed for the preparation and manipulation of nucleic acids were made up using distilled water. All solutions were autoclaved before use or, in the case of thermolabile substances, filter-sterilised using a 0.2μm filter and stored in a sterile container. Unless stated otherwise, all chemical reagents were supplied by Sigma (St. Louis, MO) and all enzymes used were purchased from New England BioLabs (Beverly, MA).

2.1.2 Determination of nucleic acid concentrations

The absorbance of an aqueous solution of the nucleic acid was measured at 260 nm (UV–1601, Spectrophotometer, Shimadzu Corporation, Kyoto, Japan). The convention was used that an absorbance of one unit is equivalent to a double stranded DNA concentration of 50μg/ml and an RNA concentration of 40μg/ml.

2.1.3 Amplification of DNA sequences by the polymerase chain reaction

Polymerase chain reaction (PCR) was performed by cycling samples containing template DNA mixed with sequence-specific oligonucleotide primers through three temperature incubations in the presence of *Thermus aquaticus* (*Taq*) DNA polymerase; either AmpliTaq (Perkin Elmer) for diagnostic procedures or AmpliTaq Gold (Applied Biosystems, Foster City, CA) for cloning procedures. These cycles were:

1. Denaturation of double stranded DNA.
2. Annealing of primers to DNA.
3. Extension of target sequences by *Taq* DNA polymerase.

The PCR was carried out in a Biometra TRIO-thermoblock (Biometra, Gottingen, FRG). The optimal cycle number and exact annealing and extension conditions were as described for each individual reaction (see Results). Primers were synthesised by the Molecular

biology Core Facility, Mayo Foundation, on an Applied Biosystems 380B Synthesiser. The reaction mixtures were prepared in a laminar flow hood isolated from normal areas of DNA handling. Each reaction sample consisted of: template DNA (1μg of genomic DNA or 0.1-0.5μg of plasmid DNA; for semi-quantitative rtPCR the cDNA equivalent of 0.1μg RNA was used), 8μl dNTPs (40mM), 5μl of 10x PCR buffer, 0.2μg 5' primer, 0.2μg 3' primer, 0.5μl *Taq* DNA polymerase (5 units/μl) and distilled water added to a total volume of 50μl. The reaction was then heated to 94°C for 10 minutes and then allowed to proceed through 20 to 30 cycles of denaturation, annealing and extension to produce the required degree of amplification. If the PCR product was required for cloning experiments a final 10 minute extension cycle at 72°C was added. The amplified PCR products were evaluated by mixing 12μl of the reaction mixture with 2μl of 6x loading buffer stock solution and run on an agarose gel.

2.1.4 Ligation of PCR products

PCR products were ligated into the pCR3.1 vector using a TA Cloning Kit (Invitrogen, Carlsbad, CA). This system takes advantage of the nontemplate-dependent activity of *Taq* polymerase which adds a single deoxyadenosine to the 3' termini of the double stranded molecules. The linearised vectors which are supplied possess single overhanging deoxythymidine residues at the 3' termini, thus allowing the PCR product to ligate efficiently with the vector. The ligation reactions were performed according to the manufacturer's instructions in 10μl volumes consisting of: 1μl of 10x ligation buffer, 1μl T4 DNA ligase, 2μl linearised vector (60ng pCR3.1), 1μl PCR reaction mixture and 5μl distilled water. The reaction mixture was incubated overnight at 14°C and was then transformed into competent *E.coli* (TOP10F' strain for pCR3.1) and plated onto L-agar containing kanamycin.

2.1.5 Agarose gel electropheresis of DNA

Gels were prepared by adding agarose (0.7 to 1.8% w/v) to 150ml 1 x TAE (Tris-acetate-EDTA) buffer (diluted from 50X TAE stock solution: 2M Tris base, 2M glacial acetic acid, 50 mM EDTA) and boiled in a microwave cooker for 5 minutes. On cooling to below 50°C, 2μl of ethidium bromide stock solution (10mg/ml) was added. Gels were

poured into a gel former with a well-comb in place. After setting, the gel was submerged in an electropheresis tank containing 1 x TAE buffer. Loading buffer (1/6 volume of 6X stock solution: 0.25% bromophenol blue, 40% w/v sucrose in water) was added to the DNA solutions which were then transferred into the wells, and electropheresis was performed using a voltage between 70 and 110 volts. The gel was transilluminated with short wave ultraviolet light and the DNA was visualised by 2uv transilluminator (UVP, Upland, CA) and Alpha Ease 5.04 Software (Alpha Innotech Corporation, San Leandro, CA). DNA fragments were sized by reference to a 'DNA ladder'.

2.1.6 Transformation of bacteria

The plasmid DNA was added to 100µl of competent *E.coli.* The suspension was cooled on ice for 45 minutes, warmed at 42°C for 1 minute and then returned to ice for 2 minutes. 400µl of L-broth was then added to the samples followed by incubation in a shaking incubator at 37°C for 1 h to permit expression of the antibiotic resistance gene on the plasmid. The bacteria were then plated out onto 90mm petri dishes (Becton Dickenson Labware, NJ) containing L-agar (L-broth with 1.5% w/v agar) with ampicillin (final concentration of 100µg/ml) or kanamycin (final concentration of 25µg/ml). The plates were incubated overnight at 37°C.

2.1.7 Small scale preparation of plasmid DNA ("miniprep")

Plasmid DNA was prepared from small cultures of bacteria using a QIAprep 8 plasmid minipreparation kit and QIAvac Manifold 6S (Qiagen, Valencia, CA), following the protocol supplied by the manufacturer. This procedure was based on the alkaline lysis method for rapid extraction of plasmid DNA from bacterial cells followed by the adsorption of DNA onto silica in the presence of high salt.

Single bacterial colonies were inoculated into 5ml of L-broth containing ampicillin and incubated overnight in a shaking incubator at 37°C. 1.4ml of the overnight cultures were centrifuged at 10,000*g* for 5 minutes and the bacteria were then resuspended in 250µl of resuspension buffer P1 (50mM Tris-HCl pH 8.0, 10mM EDTA, 100mg/ml RNAse). 250µl of lysis buffer P2 (200mM NaOH, 1% SDS) was then added and mixed, followed by adding 500µl of neutralisation buffer N3 which adjusts the sample to high salt binding

conditions and causes precipitation of denatured proteins, SDS, cellular debris and chromosomal DNA. The samples were then centrifuged at 10,000*g* for 10 minutes and the supernatants were then transferred to individual wells of a QIAprep 8 strip placed in a QIAvac Manifold 6S. Vacuum suction was applied to cause flow through the silica membrane which forms the floor of the wells. After washing with 2 ml of buffer PE to remove salts, the DNA was eluted by applying 100µl of distilled water to the silica membrane.

2.1.8 Large scale preparation of plasmid DNA ("maxiprep")

Qiagen Plasmid Maxi kit was used which is based on the modified alkaline procedure followed by binding of plasmid DNA to an anion-exchange resin. A single bacterial colony was used to inoculate a 2ml volume of L-broth containing ampicillin which was incubated for 8 h in a shaking incubator at 37°C. 1ml of this culture was used to inoculate 100ml of L-broth containing ampicillin which was then incubated overnight. The bacteria was pelleted by centrifugation at 6,000*g* for 20 minutes (J2-HS centrifuge, Beckman) and resuspended in 10ml of resuspension buffer P1. 10ml of lysis buffer P2 was then added and left at room temperature for 5 minutes. 10ml of neutralisation buffer P3 (3M potassium acetate pH 5.5) (pre-chilled to 4°C) was added and the lysate poured into a QIAfilter Maxi cartridge and incubated at room temperature for 10 minutes. The cell lysate was then filtered onto a QIAGEN-tip which had been pre-equilibrated with 10ml buffer QBT (750mM NaCl, 50mM MOPS pH7.0, 15% ethanol, 0.15% Triton X-100) and allowed to enter the anion-exchange resin by gravity flow. Under these conditions, the plasmid DNA binds to the anion-exchange resin. The resin was then washed with 60 ml of medium salt buffer QC (1M NaCl, 50mM MOPS, pH 7.0, 15% ethanol) to remove RNA, proteins and low molecular weight impurities. The DNA was eluted with 15ml of high salt buffer QF (1.25M NaCl, 50mM Tris-HCl pH 8.5, 15% ethanol), and was then desalted by precipitation with 10.5ml isopropanol. The DNA was pelleted by centrifugation at 15,000*g* for 30 minutes at 4°C, washed with 70% v/v ethanol, air dried and then dissolved in TE buffer.

2.1.9 Digestion of DNA with restriction enzymes

Plasmid DNA was digested in volumes of 30µl using 1-2 units of enzyme per µg of DNA, buffers supplied by the manufacturer and incubated for 60 minutes at the appropriate temperature; BSA was added when indicated.

2.1.10 Removal of 5' terminal phosphate groups

To reduce re-ligation of the vector DNA in cases where cohesive ends were present, treatment with calf intestinal alkaline phosphatase (CIAP) to remove the 5' phosphate groups of linear double stranded DNA was performed. At the end of a restriction enzyme digestion, 1unit of CIAP (Promega, Madison, WI) was added to the reaction sample with 5µl of 10x reaction buffer (50mM Tris-HCl pH 9.3, 1 mM $MgCl_2$, 0.1 mM $ZnCl_2$ and 1mM spermidine) and the reaction mixture made up to 50µl with dH_2O. This was then incubated for a further 60 minutes at 37°C. The sample was then run on an agarose gel and the appropriate fragment was purified as described above.

2.1.11 Purification of DNA restriction fragments

Agarose gels were visualised by UV transillumination and the bands of interest excised using a scalpel blade. The DNA was purified from the gel using the QIAquick gel extraction kit (Qiagen, Valencia, CA) following the instructions provided by the manufacturer. The method is based on the binding of DNA to silica under high salt conditions. The excised portion of gel was dissolved in 3 volumes of buffer QG and incubated at 50°C for 10 minutes. Once the gel had completely dissolved 1 volume of isopropanol was added if the DNA fragment being purified was between 500-4000 base pairs. The sample was then added to the QIAquick column and centrifuged at ≥10,000g for 1 minute. The column was then washed with 500µl of buffer QG and centrifuged as before. 750µl of buffer PE was then added and centrifuged as before. The DNA was eluted from the column by the addition of 30µl TE, waiting 1 minute before recentrifugation. 1µl of the eluate was run on an agarose gel to confirm successful purification of the DNA fragment.

2.1.12 Ligation of DNA fragments into vectors

Ligations were performed overnight at 14°C in volumes of 15µl using 1 unit of T4 DNA ligase and ligase buffer (50mM Tris-HCl pH 7.8, 10 mM $MgCl_2$ 10mM DTT, 1mM ATP, 25 µg/ml BSA). Reaction samples were such that the concentration of the 5' termini was 0.1-1.0µM. The molar ratio of vector to insert was in the range of 1:3 to 1:10.

2.1.13 Preparation of total RNA from cultured eukaryotic cells

RNA was obtained from adherent cell lines by employing an RNeasy Mini kit (Qiagen, Valencia,CA) which uses the selective binding properties of a silica-gel-based membrane. 1-5x10^5 cells were trypsinised and pelleted and then lysed in 350µl buffer RLT solution (containing guanidinium isothiocyanate). The lysate was then homogenized by passing it through a 20-G needle fitted to a syringe. One volume of 70% ethanol is then added and mixed well. The mixture is then added onto a RNeasy mini spin column and centrifuged for 15 seconds at ≥8000 x g. The RNeasy column is then washed with 700µl buffer RW1 and centrifuged as before. Next 500µl of buffer RPE is added to the column and centrifuged twice. After centrifugation the RNA is eluted by addition of 30µl Rnase-free water directly onto the RNeasy membrane and centrifuged as before.

2.1.14 Preparation of complementary DNA for analysis with PCR

The RNA sample was first incubated with 1µl DNAse (RNAse Free) (Boerhinger Mannheim) and incubated at 37°C for one hour. Next the RNA concentration was estimated by absorbance at 260 nm as previously described. A First strand cDNA was generated from an RNA template using a First Strand cDNA Synthesis Kit supplied by Boerhinger Mannheim Roche (Indianapolis, IN). For each RNA sample two aqueous solutions containing 1µg of total RNA were made up to 10µl with sterile water. To one sample 10µl of the 'Reaction Mixture' containing RNAase inhibitor, magnesium chloride, dNTPs, aqueous buffer and 2µl Oligo-p$(dT)_{15}$ primer was added; this was the rt negative control. To the other sample was added the same reaction mixture plus 1µl AMV reverse transcriptase; this was the rt positive sample. All samples were then incubated at 25°C for 10 minutes and then at 42°C for 60 minutes. For analysis with polymerase chain reaction (rtPCR) 2µl of the reaction mixture was used in each PCR sample. Both rt positive and rt

negative samples were first analysed for glyceraldehyde phosphate dehydrogenase (GAPDH) to confirm a lack of DNA contamination of the mRNA and identify equal quantities of input RNA to the rtPCR procedure. The GAPDH primers used were from the human GAPDH PCR primer pair (R&D systems, Minneapolis, MN) with the following sequence:

Forward: AAAGGGTCATCATCTCTGCC

Reverse: TGACAAAGTGGTCGTTGAGG

The PCR was performed as previously described using an annealing temperature of 55°C. A positive PCR is identified by a band at 576 base pairs. Subsequent analysis by PCR of the rt samples was performed using primers of interest with the appropriate PCR conditions.

2.1.15 Quantitative analysis of mRNA by Northern blot

The RNA samples obtained from the RNA extraction procedure were first incubated with 1µl DNAse (RNAse Free) (Boerhinger Mannheim) and incubated at 37°C for one hour. Next the RNA concentration was estimated by absorbance at 260 nm as previously described. 10µg of total RNA was made up to 20µl with diethyl pyrocarbonate (DEPC) treated distilled water for each sample. 2.5µl of 5x RNA loading buffer (64µl 5% bromophenol blue, 80µl 0.5M EDTA, 720µl 37% formaldehyde, 2ml glycerol, 3.084ml formamide, 4ml 10x MOPS, made up to 10ml with DEPC dH_2O)was added. (10x MOPS is 200mM 3-[N-morpholino] propanesulfonic acid (MOPS), 50mM sodium acetate, 10mM EDTA). The samples were then heated to 65°C for 4 minutes and kept on ice before loading on to a 1.2% agarose gel (1.6g agarose, 15ml 10x MOPS, made up to 150ml with DEPC dH_2O was heated to fully dissolve the agarose. After cooling to ~ 65°C 2.7ml formaldehyde and 5µl ethidium bromide was added and the gel poured). The gel was then equilibrated by running for 30 minutes at 80V in 1x running buffer (100ml 10x MOPS, 20ml 37% formaldehyde, 880ml DEPC dH_2O). After equilibration the samples were loaded on to the gel and run at ~80V for ~ 2 hours.

After running, the gel was imaged under ultraviolet light. It was then washed 4 times with DEPC dH_2O followed by 20x SSC (3M sodium chloride, 0.3M sodium citrate, at pH7.0). Transfer of the RNA to a nylon transfer membrane (Nytran supercharge, Schleicher and

Schuell, Keene, NH) was then performed by downwards transfer using the TurboBlotter apparatus and Turboblotter blotter pack (Schleicher and Schuell, Keene, NH) overnight with 20x SSC as the transfer buffer. After transfer the membrane was washed in 2x SSC, placed between 2 Whatmann 3mm papers and UV cross-linked using UVC UV Crosslinker (Hoefer Pharmacia Biotech Inc, San Francisco, CA). The membrane was then placed in a hybridization glass cylinder and 20ml of pre-warmed (65°C) hybridization buffer added (Rapid-hyb buffer, Amersham Pharmacia Biotech, Piscataway, NJ). The tube was then placed in a hybridization oven (Hybaid, Robbins Scientific, Sunnyvale, CA) and incubated at 65°C for 2 hours.

The DNA probe was produced using [α-^{32}P]dCTP. Previously the appropriate DNA fragment was obtained from a suitable plasmid by restriction enzyme digest, run on a gel and then 'gene cleaned' as previously described. This process yielded at least 250ng of DNA fragment. The probe was then made using the Prime-It II Primer Labeling kit (Stratagene, La Jolla, CA) according to manufacturer's instructions. Briefly 25ng of DNA template was mixed with dH_2O to a volume of 23µl in a microcentrifuge tube. 10µl of random oligonucleotide primers was added and the mixture incubated at 100°C for 5 minutes. The tube was then centrifuged briefly and kept at RT. Next 10µl of 5x dCTP primer buffer was added along with 5µl [α-^{32}P]dCTP and 1µl Exo (-) Klenow enzyme. This was then incubated at 37°C for 10 minutes before 2µl stop mix was added. The probe was purified by loading on to a NucTrap probe purification column (Stratagene, La Jolla, CA) and centrifuged for 10 minutes at 4,000 rpm. The recovered probe activity was confirmed by aliquoting 1µl into a scintillation vial containing 9ml of Opti-fluor (Packard Instrument company, Meriden, CT) and read on a β counter LS-6000 SC (Beckman Coulter, Fullerton, CA). 50µl of probe was denatured by a 5 minute incubation at 100°C and quenched on ice. This was added to 20ml of pre-warmed (65°C) hybridization buffer, mixed well and poured into the glass cylinder (the previous Rapid-hyb buffer having been discarded). Hybridization was allowed to proceed for 2 hours at 65°C.

After hybridization the membrane was washed for 20 minutes in 2xSSC (100ml) at RT, 15 minutes 0.2 xSCC, 0.1% SDS (100ml) at 65°C and 15 minutes 0.2 xSCC, 0.1% SDS (500ml) at 65°C. The membrane was then placed in a plastic protector and placed against Kodak film, stored at -70°C for an exposure of 1-24 hours prior to developing.

Stripping of the membrane was performed using stripping buffer (1% SDS, 0.1 xSSC, 40mM Tris-Cl pH7.5 made up to 1000ml with dH_2O) heated to ~ 95 °C and poured over the membrane followed by gentle shaking for 10 minutes. This was repeated 3 further times. If additional stripping was required this was performed using the previously mentioned stripping buffer at 50%, with 50% formamide, heated to 65°C and poured over the membrane followed by gentle shaking for 10 minutes. Again this was then repeated 3 further times. The membrane was then able to be reprobed with a different DNA probe e.g. GAPDH.

2.1.16 Automated sequencing of DNA

Automated DNA sequencing was performed using Perkin Elmer ABI Prism 377 DNA sequencer and read with Sequencher software (Gene Codes Corporation, Ann Arbor, MI).

2.2 CELL BIOLOGY

2.2.1 Eukaryotic cell culture - General procedures

All manipulations involving cell culture were carried out in a sterile environment provided by a laminar flow hood. All tissue culture reagents were filter sterilised by passage through a 0.22μm filter and stored in sterile autoclaved containers.

The cell lines used in this work were:

293 (Graham et al., 1977)

293A Quantum Biotechnologies, qbiogene

293 Cre4 (Chen et al., 1996a)

293T (Zufferey et al., 1997)

293Int (a kind gift from Dr F-L. Cosset, Lyon)

TEL.CeB.6 (Cosset et al., 1995) derived from the human rhabdomyosarcoma line TE671

HT1080 human osteosarcoma cell line

HT1080-F (a kind gift from Dr K-W. Peng, Molecular medicine program, Mayo Foundation)

HT1080 Cre (a kind gift from Dr K.J.Harrington, Molecular medicine program, Mayo Foundation)

AU-565 (ATCC CRL-2351 Metastatic AdenoCa Breast)

SCC-9 (ATCC CRL-1629 Squamous cell Ca Tongue)

Human melanoma cell lines, a kind gift from Professor I. Hart, London:

Mewo

Mel 17

HMB2

DX3

VUP

A378M

Adherent cell lines were grown as monolayers in plastic tissue culture flasks or dishes (Nunc, Nalge Nunc, Naperville, IL) in DMEM supplemented with 10% v/v heat-inactivated fetal calf serum (Gibco BRL, Life Technologies, Grand Island, NY) and incubated at 37°C in 5 or 10% CO_2. Cells were grown until just subconfluent (approximately 2 to 4 days) and were subcultured 1:10, using trypsin(0.05% w/v)/5mM EDTA to detach the cells. Cell counts were performed using an Improved Neubauer haemocytometer and an inverted microscope (Olympus 1X70).

2.2.2 Storage and recovery of cells stored in liquid nitrogen

Cells were trypsinised, pelleted and resuspended at approximately 10^6 cells/ml in medium containing 10% v/v dimethylsulphoxide (DMSO). 1ml aliquots were transferred to 1.5ml Nunc cryotubes which were then placed within a 1°C Freezing Container (Nalgene) and stored in a -70°C freezer. Using this apparatus, the cells cooled at approximately 1°C per minute. Frozen cells were then transferred to liquid nitrogen tanks (-196°C) the following day.

Recovery of cells from liquid nitrogen storage was performed by rapid thawing in a 37°C water bath. Thawed cells were washed in 10ml of medium, harvested by centrifugation (110*g* for 5 minutes) and were then transferred to 25cm^2 flasks containing fresh culture medium.

2.2.3 Gene transfer into eukaryotic cells

2.2.3.1 Growth selection systems

i) Geneticin (G418 sulphate)

Geneticin is an aminoglycoside antibiotic related to Gentamicin and is toxic to both prokaryotic and eukaryotic cells. Introduction of the neomycin phosphotransferase gene into eukaryotic cells can confer resistance to Geneticin added to normal medium (Southern and Berg, 1982). Geneticin (Gibco, Life Technologies, Scotland) was added to DMEM to a concentration of 5mg/ml for selective growth of B16 cells and to 1mg/ml for other cell lines, these being the concentrations previously determined to be optimal for selective growth of these cells.

ii) Puromycin

Puromycin inhibits protein synthesis in eukaryotic cells by acting as an analogue of aminoacyl-tRNA thus causing premature chain termination. The puromycin-*N*-acetyl-transferase gene from *Streptomyces alboniger* may be expressed in mammalian cells and used as a selectable marker for puromycin resistance (Vara et al., 1986). For selective growth of cells, puromycin was added to a concentration of 1.25μg/ml.

iii) Phleomycin

Phleomycin is a glycopeptide antibiotic of the bleomycin family isolated from a strain of *Streptomyces verticillus*. It is toxic to both prokaryotic and eukaryotic cells. The mechanism of cytotoxicity is due to intercalation of DNA. The ble gene, which confers resistance to phleomycin, may be expressed in mammalian cells and used as a selectable marker for phleomycin resistance (Mulsant et al., 1988). For selective growth of cells, phleomycin was added to a concentration of 50μg/ml.

2.2.3.2 Transfection protocols

Calcium phosphate/DNA co-precipitation (ProFection)

This method involves mixing DNA with $CaCl_2$ and a phosphate buffer to form a fine precipitate which is deposited onto the the cultured cells. Reagents provided in a ProFection kit (Promega) were used. Twenty-four hours prior to transfection, 5×10^5 cells were plated out in a $25cm^2$ flask. 10μg of the plasmid DNA to be transfected were made

up to 263µl using sterile distilled water followed by the addition of 37µl of 2M $CaCl_2$. 300µl of 2x HEPES (N-(2-hydroxyethyl)piperazine-N'-(2-ethanesulphonic acid)) buffered saline (supplied in the kit) was then added dropwise to the mixture, during which time a fine precipitate became visible. The sample was incubated at room temperature for 30 minutes and then added dropwise to the medium in the cell culture flask. On the following day the medium was removed and replaced with fresh medium.

Effectene Transfection

This method involves complexing DNA with a non-liposomal lipid and was performed as recommended by the manufacturer's guidelines (Qiagen). Briefly cells were prepared as for the calcium phosphate protocol. For transfection of a $25cm^2$ flask 1µg of DNA is first mixed with buffer EC to a total volume of 150µl. Next 8µl of Enhancer was added to condense the DNA before mixing with 10µl of Effectene. After standing for 5 minutes at room temperature 800µl of media was added and the mixture added to the cells.

If the aim was to obtain stable transfectants, the cells were split into selection medium after another 48 h. One method was to serially dilute the cells in selection medium and plate them in 96 well plates. After about 10-14 days wells containing a single colony were identified and transferred to a 24 well then $25cm^2$ flask. The other method used was to plate cells in selection medium into 6cm dishes. After about 10-14 days resistant colonies were either pooled or individually lifted using trypsin-soaked filter paper microsquares and transferred to individual wells of a 24-well plate, followed by expansion into larger cell culture flasks.

2.3 ASSAYS

2.3.1 Cell survival assay

293 cells were plated at a density of 5 $x10^4$ cells/well of a 96 well plate. After overnight incubation they were transiently transfected using the ProFection protocol detailed above. Four wells were transfected for each test plasmid or control. After 24 hours the cells were washed. Those wells containing cells transfected with suicide genes were then incubated

in media containing the appropriate prodrug: for HSVtk this was 5 μg/ml ganciclovir, for CD this was 3μM 5-fluorocytosine. All other cells were incubated in normal media. 5 days after transfection surviving cells were determined using trypan blue exclusion: cells were washed, trypsinised and collected in 1ml of medium. 15μl was then mixed with ~1μl of trypan blue and the number of viable cells counted using an Improved Neubauer haemocytometer and an inverted microscope (Olympus 1X70). Counts were performed 3 times for each well, averaged and the value for all 4 wells per condition combined to give a single value as to the total surviving .

With Aphidicolin

An identical procedure as described for the cell survival assay was performed. The only variation was that select wells contained 293 cells incubated in 5 μg/ml aphidicolin for the 24 hour period prior to transfection.

2.3.2 GM-CSF ELISA

ELISA plates (Rainin) were first prepared with the addition of 100μl capture antibody/well (R&D Systems anti-human GM-CSF antibody MAB615) at 2μg/ml in PBS. The plate was then sealed and incubated overnight at RT. The plate was then aspirated and washed three times with wash buffer (0.05% Tween 20 in PBS) using a MultiWash Plus microplate washer. The plate was then blocked with 300μl of PBS containing 1% BSA, 5% sucrose and incubated at RT for 60 mins. The aspiration / wash procedure was repeated as described above and 100μl/well of test samples and standards were added in triplicate and incubated for 2 hours at RT. Standards were made up from a stock of 118ng/ml recombinant human GM-CSF (R&D Systems): 20μl of stock was added to 2.36mls of diluent (0.1% BSA, 0.05% Tween 20 in PBS) giving an upper standard value of 1ng/ml. Serial dilutions of 1:2 were then performed down to 15.625pg/ml.

The aspiration / wash procedure was repeated as described. The 'detection' Biotinylated anti-human GM-CSF antibody (R&D Systems antibody BAM215) was then added as 100μl to each well from a working stock of 1μg/ml in diluent (0.1% BSA, 0.05% Tween 20 in PBS). This was sealed and incubated for 2 hours at RT.

The aspiration / wash procedure was repeated as described. Streptavidin-Horseradish peroxidase (Zymed laboratories Inc., San Francisco, CA) was then added as 100µl to each well: 1:5000 in diluent (0.05% Tween 20 in PBS) of a 1.25mg/ml stock. This was sealed and incubated for 20 minutes at RT.

The aspiration / wash procedure was repeated as described. 100µl of 'substrate' solution (1:1 mixture of H_2O_2 and Tetramethylbenzidine (BD Pharmingen, San Diego, CA)) was then added to each well and incubated in the dark for 30 minutes. 50µl of 1M H_2SO_4 was added as a 'stop' solution and the optical density determined at 450nm with wavelength correction of 570nm using the SPECTRAmax 190 (Molecular Devices, CA).

2.3.3 Matrix metalloproteinase-2 (MMP-2) activity assay

This assay was performed using the Biotrak cellular communication assay system (amersham pharmacia biotech, Piscataway, NJ) according to manufacturer's instructions. Both active and total MMP-2 can be measured by this system. Pro (inactive) or active MMP-2 are captured by an anti–MMP-2 antibody coating the 96 well plate provided. If only active MMP-2 is to be measured in those samples then the assay proceeds to the next step. If total MMP-2 is to be measured then the pro form of the enzyme needs to be activated, and this is achieved by incubating with p-aminophenylmercuric acetate (APMA). The assay then relies on the cleavage by active MMP of a pro form of a detection enzyme, converting the detection enzyme from inactive to active. The activated detection enzyme then cleaves a chromogenic peptide substrate producing a colour change which can be read at 405nm.

Cells from a number of cell lines were plated in 25cm^2 culture flasks and incubated in 5ml of media for 48 hours. After that period the supernatant was collected for analysis. The cells were trypsinised off the plate and the number of cells counted for each cell line in the standard manner. 100µl of test sample (undiluted supernatant and 1:10 dilution with assay buffer), pro MMP-2 standards, or assay buffer was added to the appropriate wells of the assay plate, and incubated overnight at 4 °C. The plate was then washed 4 times with wash buffer using the MultiWash Plus microplate washer. 50µl of APMA was then added to those wells containing standards and sample wells where total MMP-2 was to be measured. 50µl of detection reagent (containing equal volume of detection enzyme and

substrate) was added to all wells and incubated at 37 °C for 1.5 hours. The plate was then read at 405nm using the SPECTRAmax 190 (Molecular Devices, CA).

2.3.4 Lactate dehydrogenase (LDH) release assay

This colorimetric assay was performed using the Cytotoxicity detection kit (LDH) (Boehringer Mannheim) and performed according to the manufacturer's guidelines. The principle of the test is the measurement of the amount of cytoplasmic enzyme (LDH) released into the supernatant following cell membrane damage. The initial step is the conversion of lactate to pyruvate, reducing NAD^+ to NADH and H^+, catalysed by LDH in the supernatant. In the second step diaphorase catalyses the conversion of tetrazolium salt, a pale yellow colour, to formazan salt (red colour) by the transfer of H/H^+ from $NADH/H^+$, producing NAD^+. The amount of LDH correlates to the amount of formazan formed: the absorption of which can be measured at 500nm. For the assay, supernatant was collected from adherent cells grown in 6 well plates. The supernatant was centrifuged at 3,000rpm for 5 minutes and the supernatant collected.100µl supernatant was then pipetted into a well of a microtitre plate (in triplicate/sample). 100µl reaction mixture (250µl of diaphorase solution: 11.25mls tetrazolium salt solution) was added to each well and incubated for 30 minutes at RT in the dark. The optical density was determined at 492nm with wavelength correction of 620nm using the SPECTRAmax 190 (Molecular Devices, CA).

2.3.5 Digital Image Analysis Assay

Cells were cultured on Labtek chamber slides (Nalge Nunc International, Nutting Lake, MA). At 80% confluency the cells were transfected with control or test plasmids using the standard Effectene transfection methodology. At various timepoints the cells were washed in PBS and then fixed in 4% Formaldehyde in PBS (10% Formaldehyde solution, Tousimis, Rockville, Maryland) for 15 minutes at RT. The slides were then Feulgen stained by the Digital Image Analysis Laboratory, Mayo Foundation according to their standard protocol. They then captured and analyzed 200 nuclei per slide using a CAS 200 image analyzer (Bacus Laboratories, Lombard, Illinois). The nuclear morphometry features of area, DNA index and average optical density were obtained for each nucleus using Cell SheetTM software. These features were summarized with means and standard

deviations. Differences in the nuclear morphometry features among the slides were assessed using two-way analysis of variance (ANOVA) models with terms for transfection, time period, and the interaction between the two. The nuclear morphometry features were analyzed on a natural logarithmic scale in order to meet model-fitting assumptions required by ANOVA. All tests were two-sided and p-values less than 0.05 were considered statistically significant. Statistical analysis was performed by Dr Christine Lohse, Section of Biostatistics, Mayo Foundation.

2.3.6 Electron microscopy (EM)

Samples for EM were prepared by trypsinising and pelleting cells previously cultured as a monolayer. The cell pellets were then fixed in Trump's fixative (1% glutaraldehyde and 4% formaldehyde in 0.1M phosphate buffer, pH 7.2). Tissue was then rinsed for 30 minutes in 3 changes of 0.1M phosphate buffer, pH 7.2, followed by a one hour postfix in phosphate-buffered 1% OsO_4. After rinsing in 3 changes of distilled water for 30 minutes the cell pellet was en bloc stained with 2% uranyl acetate for 30 minutes at 60°C. After en bloc staining, the pellet was rinsed in 3 changes of distilled water, dehydrated in progressive concentrations of ethanol and 100% propylene oxide and embedded in Spurr's resin. Thin (90 nm) sections were cut on a Reichert Ultracut E ultramicrotome, placed on 100-200 mesh copper grids and stained with lead citrate. Micrographs were taken on a JEOL 1200 EXII operating at 60KV.

2.3.7 Immunofluorescence

Experiments were conducted with cells previously plated in chamber slides. At the commencement of the staining protocol the media was aspirated from the chamber and the adherent cells washed with PBS. The cells were then fixed with 4% Formaldehyde in PBS (10% Formaldehyde solution, Tousimis, Rockville, Maryland) for 15 minutes at RT. The cells were then washed 3 times with PBS. If intracellular staining was then required cells were incubated for 5minutes with 0.1% Triton in PBS at RT followed by wash 3 times with PBS. The cells were then incubated with Blocking buffer (5% Goat Serum, 5% Glycerol, in PBS) for 60 minutes at RT. The cells were then incubated with the primary antibody diluted in blocking buffer. Subsequently the slides were washed 3 times with

PBS before incubation with the appropriate secondary antibody diluted in blocking buffer and incubated at RT for 60 minutes. The slides were then washed a final 3 times in PBS, allowed to air dry before mounting with Prolong antifade (Molecular probes, Eugene,OR) containing 2μl 4',6-diamidine-2'-phenylindole dihydrochloride (DAPI)/ml (Boehringer Mannheim) and covered with a coverslip.

Examination of the slides was conducted the following day by confocal fluorescence microscopy using the LSM 510 confocal laser scanning microscope system (Carl Zeiss, Germany) comprising a Zeiss Axiovert inverted microscope, helium neon laser (excitation 633nm), argon/krypton ion laser (excitation 488nm, 568nm, 647nm) and Coherent enterprise laser (UV excitation 351nm, 364nm).

Primary antibodies used in this thesis are:

Mouse monoclonal anti-heat shock protein 70 clone BRM-22 (H5147, Sigma)

Mouse monoclonal anti-Cytochrome *c* antibody (65971A, Pharmingen)

Human anti-mitochondrial antibody (kind gift of Dr McNiven, Department of Tumor Biology, Mayo Foundation)

Mouse monoclonal anti-human HSP-60 antibody (SPA-806, Stressgen biotechnologies Corp.)

Mouse monoclonal anti-α-Tubulin antibody (T9026, Sigma)

Fluorescein isothiocyanate-conjugated rat anti-human GM-CSF monoclonal antibody (BVD2-21C11, Pharmingen)

Secondary antibodies used in this thesis are:

Donkey anti-mouse IgG FITC labelled (Jackson ImmunoResearch Laboratories Inc)

Donkey anti-mouse IgG TRITC labelled (Jackson ImmunoResearch Laboratories Inc)

Donkey anti-human IgG TRITC labelled (Jackson ImmunoResearch Laboratories Inc)

Miscellaneous immunofluorescent stains:

Phalloidin-TRITC labelled (P1951, Sigma)

DiI – 1,1'-dioctadecyl-3,3,3',3'-tetramethylindocarbocyanine perchlorate ($DiIC_{18}(3)$)

PI – Propidium Iodide (Boehringher Mannheim)

2.3.8 Lysotracker Red/ Propidium iodide assay

Cells were plated in 25cm^2 culture flasks and incubated in 5ml of media until 80% confluent. They were then transfected with control or test plasmid using the Effectene transfection method previously described. After 48 hours the adherent cells were washed and re-incubated with media containing 50nM Lysotracker Red (L-7528, Molecular Probes) or 2µl of 0.5mg/ml solution propidium iodide (Boehringher Mannheim) per 1ml of media. After 30 minute incubation at 37°C the cells were washed 3 times in PBS and then viewed using an inverted microscope with light and red filter (Olympus 1X70). Images were captured using the camera Olympus SC35 Type 12.

2.3.9 Apoptosis, terminal deoxynucleotidyl transferase-mediated deoxyuradine triphosphate nick end labeling (Tunel), detection Assay

This assay was performed using the Fluorescein In situ cell death detection kit (Roche, Mannheim, Germany) and carried out according to the manufacturer's protocol with minor modification. The assay is based on the production of double and single strand DNA breaks in genomic DNA during the process of apoptosis. Fluorescein labelled deoxyuridine (fluorescein-dUTP) is added to the free 3'-OH termini at the DNA breaks by the enzyme terminal deoxynucleotidyl transferase (TdT) thus fluorescently labelling the strand breaks.

This assay was performed on adherent cells. Cells grown in chamber slides were washed with PBS and then fixed with 4% paraformaldehyde in PBS for 15 minutes at RT. Slides were then washed with PBS and permeabilised with 0.1% Triton X-100 in PBS for 5 minutes at RT. Once washed twice with PBS the slides were incubated with Tunel reaction mixture (TdT and fluorescein-dUTP) and incubated for 60 minutes at 37°C in a humidified chamber. Negative controls were performed in all experiments using a Tunel reaction mixture without the TdT. The slides were then washed 3 times with PBS, air dried and mounted with Prolong antifade (Molecular probes) containing 2µl DAPI/ml (Boehringer Mannheim) and covered with a coverslip. Examination of the slides was conducted the following day on a confocal fluorescence microscope.

2.3.10 Flow cytometry

Adherent cells were first trypsinised and washed once in growth medium. Cells were then washed twice in ice-cold wash buffer (PBS with 0.1% w/v BSA and 0.1% sodium azide) and seperated into 1 x 10^6 cells/sample. The cells were then suspended in 100µl wash buffer containing primary mouse monoclonal IgG anti-F antibody (Y503, a kind gift of Dr Fabian Wild, Lyon, France) (dilution 1:100) and incubated at 4°C for 60 minutes. As a negative control, wash buffer alone was added. After washing and spinning down the cells three times with wash buffer, 100µl of TRITC-conjugated donkey anti-mouse IgG (Jackson ImmunoResearch Laboratories Inc) secondary antibody (diluted 1 in 50) was added to the cells and incubated at 4°C for 60 minutes. After three washes with wash buffer, the cell pellet was resuspended in 500µl of fresh formaldehyde solution (4% in PBS) and stored overnight at 4°C. The cells were then analysed using a Becton Dickinson FACScan and Cellquest software (Becton Dickinson Immunocytometry systems, San Jose, CA).

2.3.11 Cell staining for β-gal expression

Adherent cells transduced with β-gal were washed twice in PBS and fixed in 1ml fresh formaldehyde solution (4% in PBS) for 10 minutes at 4°C. After 2 further washes in PBS cells were overlaid with 1ml filtered (0.45µm) X-gal stain (100mM sodium phosphate pH 7.3, 1.3mM $MgCl_2$, 3mM $K_3Fe(CN)_6$, 3mM $K_4Fe(CN)_6$, 1mg/ml X-gal). After incubation overnight at 37°C cells were examined for blue staining by light microscopy.

2.3.12 Western blots

General preparation of cell lysates

Cells were grown in 75cm^3 flasks, washed in cold PBS and 2ml lysis buffer added (50mM Tris-HCL pH 8.0, 62.5 mM EDTA, 1% Igepal CA-630, 0.4% deoxycholic acid sodium salt) for 5-10 minutes with rocking. The supernatant was then collected and centrifuged at 7000 rpm for 10 minutes at 4°C. The supernatant was then collected and the protein concentration determined using a colorimetric assay: DC protein assay (Bio-Rad, Hercules,CA). This assay was conducted as per the manufacturer's instructions in a microplate and is based on the reaction of protein with an alkaline copper tartrate solution

followed by the reduction of a Folin reagent; producing a blue colour, measurable at an absorbance of 750nm using the SPECTRAmax 190 (Molecular Devices) spectrophotometer. Briefly a protein standard was prepared using 1:2 dilutions of BSA; range 1.4mg/ml-0.088mg/ml.'Working reagent A' was produced by adding 20µl of reagent S (SDS) to 1ml of reagent A (1-5% sodium hydroxide, <1% sodium tartrate, <0.1% copper sulfate). Next 5µl of standards and samples were pipetted into wells of a microtitre plate and 25µl of working reagent A added. This was followed by the addition of 200µl of reagent B (Folin reagent), the plate agitated and incubated for 15 minutes at RT. The absorbance was then read at 750nm and sample values obtained from the standard curve. 2µg of total protein was then added to protein loading buffer (312.5 mM Tris/HCl pH 6.8, 10% SDS, 33% glycerol, 0.06% bromophenol blue, 1.95ml β-mercaptoethanol) to produce a total volume of 20µl. This was then heated at 95°C for 5 minutes, cooled on ice for 2 minutes, and loaded onto a Tris-HCl precast gel (Bio-rad).

Protocol for pro-caspase-3 activation and PARP cleavage Westerns

The protocol used for these Westerns was developed in the laboratory of Dr Kaufmann, Department of Molecular Pharmacology and Experimental Therapeutics, Mayo Foundation and has been previously described (Kaufmann et al., 1986). HT1080 or TEL.CeB.6 cells were plated in 25cm^2 flasks and incubated overnight. The following day they were transfected with pCG-F1 and pCG-H5 plasmids or pCG-H5 alone using standard transfection protocols. Jurkat cells treated with etoposide (VP16) or Fas ligand were used as positive controls. After incubation for 18 or 40 hours post transfection both adherent and non-adherent cells were harvested for protein preparation. Media was removed from the cells and placed in a 15ml Falcon tube. Adherent cells were removed by trypsin and added to the respective Falcon tube, which was then centrifuged at 1,000 rpm for 3 minutes at 4°C. The supernatant was then aspirated and the cell pellet washed in cold PBS, and the PBS aspirated. The pellet was then incubated for 10 minutes in a solution of 30µl phenylmethylsulphonyl fluoride (PMSF) and 30µl β-mercaptoethanol in 3ml of alkylation buffer (6M guanidine HCL, 250mM Tris HCL (pH 8.5), 10mM EDTA). Samples were then sonicated and allowed to reduce overnight. Thereafter 300µl of

iodoacetamide (278mg/ml) and PMSF (10µl/ml) in alkylation buffer was added, mixed and incubated for one hour in the dark. At this time 30µl β-mercaptoethanol was added and the samples were dialysed against 4M urea and 50mM Tris (pH 7.4) for 90 minutes, then against 4M urea for 90 minutes (x4), and finally against 0.1% SDS for 90 minutes (x3). At this stage an aliquot of 100µl was removed for quantification (Bio-Rad) (as indicated previously). The remainder of the sample was frozen on dry ice and lyophilized to dryness. Subsequently the protein sample was resuspended in SDS sample buffer (4M deionized urea, 2% (w/v) SDS, 62.6 mM Tris HCl (pH 6.8), 1mM EDTA) at a concentration of 5µg/µl. This was then heated to 65°C for 20 minutes and then run on a 10% SDS-PAGE gradient gel. Wet transfer was performed to a nitrocellulose membrane at 60 V at 4°C. The membrane was then blocked and exposed to antibody as detailed below.

Preparation of secreted protein in the supernatant

Cells were grown in 25cm^2 flask and 24 hours prior to supernatant collection were incubated in 1.5ml of serum free media. 1.2mls of supernatant was collected and centrifuged at 3,000rpm for 5 minutes at 4°C. The supernatant was collected and 300µl trichloro acetic acid (TCA 110% in dH_2O) added to precipitate protein in the supernatant. This mixture was vortexed and mixed for 10 minutes at 4°C before being centrifuged at 14,000rpm for 10 minutes at 4°C. The supernatant was then removed and a repeat spin performed for 1 minute followed by further supernatant removal to leave a dry protein pellet. The pellet was then dissolved in 20µl protein loading buffer (2µl of 2M Tris added if the buffer colour changed from blue to yellow) and shaken at 55°C for 25 minutes. 15µl of sample was then loaded onto a Tris-HCl precast gel (Bio-rad).

Gels were run using a Mini-PROTEAN II cell and PowerPac 200 power supply (Bio-Rad, Hercules, CA). 10µl of kaleidoscope standards (Bio-Rad, Hercules, CA) was run on each gel.

The gel was run in 1x running buffer (3.02g Tris base, 14.4g glycine, 1g SDS made to 1 litre with dH_2O) at 80V for approximately 1 hour.

Transfer was performed either as semi-dry or wet.

For semi-dry transfer the gel was placed on top of three sheets of Whatmann 3mm paper pre-soaked in 1x transfer buffer (2.32g Tris Base, 1.17g glycine, 0.15g SDS, in 400 ml of dH_2O) on the positive electrode of a semi-dry blotting aparatus (Trans-blot SD, Bio-Rad). A sheet of Hybond-C+ nitrocellulose membrane (amersham pharmacia biotech, Buckinghamshire, UK), pre-soaked in dH_2O followed by 1x transfer buffer, was placed in direct contact with the gel, followed by 3 more sheets of 3MM paper pre-soaked in 1x transfer buffer and the negative electrode plate. Transfer was allowed to take place for 50min at a constant current of 20V.

For wet transfer PVDF membrane was presoaked in methanol for 1 minute followed by 10 minutes in transfer buffer (2.4g Tris, 14.4g glycine, 200ml methanol,1ml 10% SDS, made up to 1 litre with dH_2O). This was then placed on the positive electrode side of the gel, with pre-soaked fibre pads and 2 Whatmann 3mm filter papers on either side, in the locking gel cassette of the mini trans-blot cell (Bio-Rad). Transfer was allowed to take place for 60 minutes at 80V.

The membrane (blot) was then blocked in 30ml of 5% milk in PBS containing 0.05%Tween-20(PBS-T) for 1 h at RT with gentle shaking and then washed briefly three times with PBS-T. The blot was then incubated for 1 hour with primary antibody in 1-5% milk PBS-T at RT. It was then washed 2 times with PBS-T and one further time overnight at 4°C. The following morning it was incubated for 60 minutes with the appropriate secondary in 1% milk PBS-T. If the secondary antibody was HRP conjugated the blot was washed a further 3 times.If the secondary antibody was biotin conjugated the blot was then washed 3 times as before and incubated for 60 minutes with streptavidin-HRP 1:10000 (Zymed laboratories Inc., San Francisco, CA). The blot was then washed as before. The filter was finally washed thoroughly with PBS-T, and bands were revealed using the enhanced chemiluminescence (ECL) system (SuperSignal West Pico Chemiluminescent substrate, Pierce, Rockford, IL). This system requires the mixing of equal volumes of a stable peroxide solution and luminol/enhancer solution prior to covering the blot and incubating for 5 minutes. The blot was then removed, placed in a plastic protector and placed against Kodak film for an exposure of 30 seconds to 5 minutes prior to developing.

Primary antibodies used in western analysis:

Rabbit anti-Procaspase 3 antibody (a kind gift from Dr S. Kauffmann, Department of Molecular Pharmacology and Experimental Therapeutics, Mayo Foundation)

Rabbit anti-PARP antibody (a kind gift from Dr S. Kauffmann, Department of Molecular Pharmacology and Experimental Therapeutics, Mayo Foundation)

POC Rabbit anti-H antibody (a kind gift from Dr R.Cattaneo, Molecular medicine program, Mayo Foundation)

POC Rabbit anti-F antibody (a kind gift from Dr R.Cattaneo, Molecular medicine program, Mayo Foundation)

Mouse monoclonal anti-human GM-CSF antibody (AF-215-NA, R&D Systems, Minneapolis, MN)

Secondary antibodies used in western analysis were obtained from Dako Corporation, Carpinteria, CA.

2.3.13 Immunohistochemistry Assay

Tumours excised from mice were fixed in formalin. Sections were taken and mounted on slides by the Histopathology department, Mayo Foundation and the unstained slides returned. The first step involved removing paraffin from the section by washing in xylene for 30 minutes. Rehydration followed by 5 minute incubations in 96%, 70%, 50% ethanol and then dH_20. Slides were then steamed for 30 minutes in 10mM citrate buffer pH 6.0. The slides were then cooled slowly to RT before being incubated with 3% H_20_2 for 10 minutes. The slides were then washed in dH_20 and then blocked with 5% mouse serum in PBS/0.5% Tween-20 for 10 minutes. Next they were incubated with mouse anti-measles Haemagglutinin monoclonal antibody (Chemicon) 1:100 dilution or control antibody (anti-mouse IgG1) for 45 minutes. Slides were washed 3 times with dH_20 followed by blocking with 5% normal goat serum in PBS/0.5% Tween-20 for 10 minutes. They were then incubated with biotinylated goat anti-mouse immunoglobulin (Dako) at a dilution of 1:400 for 30 minutes. Slides were washed 3 times with dH_20 and incubated with HRP sreptavidin 1:500 (Zymed laboratories) for 30 minutes. Once more the slides were washed 3 times with dH_20 and then incubated with AEC (Dako) for 5 minutes. A further series of washes

was followed by counterstain with Gill's hematoxylin for 30 seconds. After a final wash a coverslip was applied with Immu-mount (Shandon) and the slides examined under an inverted microscope.

2.4 ANIMAL STUDIES

All animal studies presented in this thesis were approved by the Institutional Animal Care and Use Committee at the Mayo Foundation. Specific details regarding each experiment will be presented with the data.

2.5 PRODUCTION OF RECOMBINANT ADENOVIRUSES

The production of adenoviruses contained in this thesis was based on the Adeno-Quest system(Quantum Biotechnologies, qbiogene, Carlsbad, CA).

2.5.1 Co-transfection of recombinant transfer vector and QBI-viral DNA

cDNA was cloned into the pQBI-AdCMV5-IRES-GFP using standard cloning techniques described above. 10μg of this plasmid was linearised following digestion with Fse 1: 10μg of DNA, 10μl Fse 1 enzyme, 10μl 10x buffer 4, 1μl BSA, made up to 100μl with dH_2O. This was incubated at 37°C for 60 minutes. The linearised DNA was extracted with phenol:chloroform:isoamyl alcohol (25:24:1, v/v) (Gibco BRL, Rockville, MD) and precipitated with $1/10^{th}$ volume of 3M sodium acetate pH5.2, mixed well and 2 volumes of ice cold ethanol added. This was incubated overnight at -20 °C then centrifuged at 14,000rpm at 4 °C for 30 minutes. The DNA pellet was then washed with 70% ethanol, air dried in a sterile lamina flow hood and resuspended in 80μl of sterile 0.1x TE. 5μl was then run on an agarose gel to confirm linearisation and approximate concentration. 40μl (5μg) of the linearised cDNA was then mixed with 10μl (5μg) of QBI-viral DNA. This was then used in a standard calcium phosphte transfection protocol to transfect 293A cells,

plated the previous day at 1 x 10^6 in a 60mm dish, resulting in 80-90% confluency at the time of transfection.

The following day the cells were washed and split into 3 60mm dishes and observed for the development of plaques: normally appearing 7-9 days from the day of transfection.

2.5.2 Collection of plaques

Once plaques appeared they were picked using sterile cloning rings. Briefly cloning rings were produced by cutting off the upper portion of 600µl microcentrifuge tubes with scissors and then sterilised. The media was aspirated from the dish and the cloning ring was then placed over a viral plaque, being used in conjunction with sterile vacuum grease to allow a seal to the cell monolayer/dish around the periphery of the region of the plaque. 100µl of PBS was then pipetted up and down in the cloning ring, resulting in the cells being dislodged from the plaque, and the sample stored in a 1.5ml microcentrifuge tube in the -70°C freezer.

2.5.3 Screening and purification of plaques

Approximately 14-25 plaques were collected per transfection. In those recombinant viruses expressing GFP only green plaques were picked. The collected samples were freeze/thawed 3 times and then 40µl transferred onto 293A cells growing in a 24 well plate in 1ml of media/well. The 293A cells had been plated the day before at a density of 5 x 10^4/well. The wells were allowed to proceed to complete cytopathic effect (CPE) and the well contents collected and stored at -70°C. The collected samples were then freeze/thawed 3 times, centrifuged (5,000rpm for 5 minutes) and the resulting supernatant is then referred to as the primary stock. 50µl of this sample was then added to HT1080 target cells in a 6 well plate:

For AD F and AD H confirmation of GFP expression was assessed as was syncitia formation on co-administration.

For AD Stop GALV HT1080–Cre expressing cells were used as targets. Positive clones were identifed by formation of syncitia and GFP expression.

2 positive clones per virus were then plaque purified. $8x10^5$ 293A cells were plated per well of a 6well plate. Effective dilutions of 0.01µl, 0.001µl, 0.0001µl of the primary stock were added in 1ml of media per well. After overnight incubation the media was aspirated and the cells overlayed with agarose. The agarose overlay was prepared as follows: sterile 2% Noble agar was melted in a microwave and equilibrated to 45 °C in a water bath. Media containing 5ml 2xDMEM (Gibco), 1ml new born calf serum, 0.75ml dH_2O was also equilibrated to 45 °C in the water bath. Media was aspirated from the 293A cells and 6.75mls of media was mixed with 3.25mls Noble agar; 3mls/well was then immediately overlayed.

The plates were then observed until the development of plaques, usually 4-6 days. Approximately 10 plaques/virus were then picked as agar plugs using sterile clipped 200µl pipette tips and dispensed into PBS. Again in those recombinant viruses expressing GFP only green plaques were picked. These clones were treated as before: stored at -70°C, freeze/thawed 3 times, centrifuged and the supernatant collected represented the secondary stock. This stock was then screened as before. 1 positive clone /virus was then repeat plaque purified, producing the tertiary stock, screened and the optimum clone selected for amplification.

2.5.4 Amplification

Following the plaque purification and screening process one clone per recombinant adenovirus was selected for amplification:

First round of amplification:$1x10^5$ 293A cells were plated in a well of a 24 well plate the previous day. 200µl of tertiary stock was added and the volume of media was made up to 1ml. The plate was incubated until full CPE, the contents of the well collected, freeze/thawed x3, centrifuged as before and the supernatant collected (as per protocol this should represent approximately $5x10^7$ viral particles).

Second round of amplification:$7.5x10^6$ 293A cells were plated in a $75cm^2$ the previous day. The media was aspirated. 0.5ml of amplified stock was made up to 2mls with media and added to the flask and evenly spread over the cell monolayer by gently rocking. The media covering the cells was made up to 10mls and the flask incubated until full CPE. The 10mls of media was recovered and stored in a 15ml falcon tube, freeze/thawed x3, centrifuged at

3,000rpm and the supernatant collected (as per protocol this should represent approximately $2.5x10^9$ viral particles).

Third round of amplification: $1.5x10^7$ 293A cells were plated per $175cm^2$ flask; three flasks were plated the previous day. The media was aspirated. 3mls of the previous supernatant was mixed with 12ml media; 5ml was added to each flask, rocked as before, and a further 25ml of media added. The flasks were incubated to full CPE and the contents stored in a 50ml Falcon tube. This was then freeze/thawed x3, centrifuged at 3,000rpm and the supernatant collected (as per protocol this should represent approximately $1.5x10^{10}$ viral particles).

Final round of amplification:$1.5x10^7$ 293A cells were plated per $175cm^2$ flask and twenty were plated the previous day. The media was aspirated. 60ml of supernatant was mixed with 40ml media; 5ml added to each flask, rocked as before, and a further 25ml of media added. The flasks were incubated to full CPE and the contents collected in 20 50ml Falcon tubes. These tubes were then centrifuged at 800rpm for 10 minutes. The supernatant was discarded and the cell pellet collected in 1.5ml ice cold 0.1M Tris (pH 8.0)/falcon, products from 10 flasks being pooled together. This suspension was then freeze/thawed x3, centrifuged at 6000rpm for 10 minutes using the SLA-600TC rotor in a Sorvall RC5C-Plus. The supernatant was then collected and made up to two 19ml viral lysates with 0.1M Tris.

2.5.5 Caesium chloride (CsCl) purification

For this process a number of CsCl solutions were required and were made up as follows:

Solution	Grams CsCl	Volume TD
1.25g/ml	36.16g	100ml
1.35g/ml	51.2g	100ml
1.40g/ml	62g	100ml

(TD = 8g NaCl, 0.38g KCl, 0.1g Na_2HPO_4, 3g Tris pH 7.5 made up to 1l with dH_2O)

The initial CsCl gradients were prepared by layering 7.6ml 1.4g/ml CsCl solution below 11.4ml 1.25g/ml CsCl solution in ultra-clear centrifuge tubes (25mm x 89mm, Beckman). 19ml of viral lysate was then overlayed per tube and centrifuged at 28,000rpm for 2 hours at 15°C using a Surespin rotor in the Sorvall Discovery 100S ultracentrifuge.

The packaged adenoviral band formed at the interface between the 1.25g/ml and 1.4g/ml CsCl solutions, with a less dense empty capsid band above this and cellular debris accumulated at the upper level of the tube. The packaged adenoviral band was therefore collected using side puncture of the tube with a 19-gauge needle and syringe; approximately 1.5-2.5ml volume was collected per tube. This was loaded into 13mm x 51mm ultra-clear centrifuge tubes (Beckman) and if required topped up with 1.35g/ml CsCl solution to within 2-3mm of the top of the tube. The tube was balanced with a corresponding tube filled with 1.35g/ml CsCl solution. The 2 tubes were centrifuged at 40,000rpm for 15 hours at 15°C using a TH-660 rotor in the Sorvall Discovery 100S ultracentrifuge. Again two viral bands were seen; one in the centre of the tube representing the packaged adenovirus and one at the top representing empty capsids. The central band was collected in the same manner described above in a volume ≤ 2.5ml and kept on ice.

2.5.6 Desalting the purified viral stock

A PD-10 column (amersham pharmacia) was equilibrated with 25ml PBS. The purified viral sample was then added to the column in a total volume of 2.5ml (if less sample was obtained from the purification it was made up to 2.5ml with PBS). The virus was eluted by the addition of 6ml PBS to the column and collected in 0.5ml fractions. The virus was collected in 1.5ml microcentrifuge tubes containing 50µl glycerol. Fractions 2-7 contained purified, desalted, high titre stock, were stored at -70°C and were used for all future experiments. Prior to storage 50µl of fraction 3 was aliquoted to enable titre assessment experiments to be undertaken.

2.5.7 Assessment of Titre

Two procedures were routinely used to estimate viral titre: optical absorbance at 260nm and plaque assay.

For the optical absorbance procedure 25µl recombinant adenovirus was mixed with 475µl viral lysis buffer(0.1% SDS, 10mM Tris-Cl, 1mM EDTA) in a 1.5ml microcentrifuge tube, heated to 55 °C for 10 minutes and vortexed throughout. 200µl of sample was then placed in a cuvette and the OD_{260} determined using viral lysis buffer alone as control. The concentration of adenovirus virions was determined by multiplying the absorbance by the dilution factor (1:20), divided by the extinction coefficient for wild type adenovirus (ε_{260}= 9.09 x 10^{-13} OD ml cm virion^{-1}) (Mittereder et al., 1996). The OD_{260} was determined twice for each sample.

The plaque assay was conducted in duplicate for each recombinant adenovirus. 8x 10^5 293A cells were plated per well of a 6well plate. Effective log dilutions of 0.1µl-0.000001µl of the adenovirus were added to wells in 1ml of medium per well (this dilution corresponds to an adenoviral titre range of 10^6-10^{11}). After overnight incubation the medium was aspirated and the cells overlayed with agarose. The agarose overlay was prepared as follows: sterile 2% Noble agar was melted in a microwave and equilibrated to 45 °C in a water bath. Media containing 5ml 2xDMEM (Gibco), 1ml new born calf serum, 0.75ml dH_2O was also equilibrated to 45 °C in the water bath. Media was aspirated from the 293A cells and 6.75mls of media was mixed with 3.25mls Noble agar; 3mls/well was then immediately overlayed. The plates were incubated for a further 14 days, requiring repeat agarose overlays on days 5 and 10. On day 14 plaques were counted from the two wells with the greatest dilution of adenovirus, from both plates, the mean value corresponded to the titre by plaque assay and represented the pfu (plaque forming units).

2.5.8 Hirt extraction of adenoviral DNA

This procedure was conducted to confirm the identity of the recombinant adenovirus. 7.5x10^6 293A cells were plated in 75cm^2 flasks the previous day. Recombinant adenovirus was added to the 10ml of media at an approximate m.o.i of 10 and the flask incubated until full CPE. The flask contents were collected in a 15ml falcon tube and centrifuged at 800rpm for 5 minutes. The supernatant was removed and 750µl Hirt buffer (2ml 2M Tris, 16ml 0.25M EDTA, 24ml 10% SDS, pH 7.5, to 400ml with dH_2O) added. This was incubated at RT for 10 minutes before the contents were transferred to a 1.5ml microcentrifuge tube. 188µl of 5M NaCl was added, mixed and the sample stored at -20°C

for 60 minutes. After thawing, the sample was then centrifuged at 14,000rpm for 90 minutes at 4°C. The clear supernatant was then transferred to a new tube. 6.5µl of 20mg/ml stock of pronase was added and the sample incubated at 37 °C for 60 minutes. The samples were then extracted twice with phenol:chloroform:isoamyl alcohol (25:24:1, v/v) (Gibco BRL, Rockville, MD) and once with chloroform; this involved mixing well and centrifuging the sample at 14,000rpm for 3minutes with each extraction. The DNA was then precipitated with $1/10^{th}$ volume of 3M sodium acetate pH5.2, mixed well and 2 volumes of ice cold ethanol added. This was incubated overnight at -20 °C then centrifuged at 14,000rpm at 4 °C for 30 minutes. The DNA pellet was then washed with 70% ethanol, air dried in a sterile lamina flow hood and resuspended in 40µl TE containing 50µg/ml RNase (Boehringer Mannheim).

Additional adenoviruses used in this thesis:

Ad-GFP	Genzyme, Framingham
Ad Cre	Merck

CHAPTER 3: INTRODUCTION TO FMG AND COMPARISON TO SUICIDE GENES

Chapter 3: Introduction to FMG and comparison to suicide genes

3.1 Introduction

Gene therapy remains an attractive concept to treat cancer. However, as indicated in Chapter 1, both better delivery systems and more effective genes are required before gene therapy enters routine clinical use in the treatment of cancer. With this in mind I set out to explore the utility of using FMG to kill tumour cells. The concept to use FMG in this way arose out of the observation that a retroviral envelope, when expressed in a retroviral packaging cell line, caused extensive cytotoxicity through cell-cell fusion. This meant it was unattractive in a vector production capacity but warranted further study as a potential cytotoxic agent. The envelope in question was GALV and, as discussed in Chapter 1, this particular sequence was terminally truncated rendering it hyperfusogenic (see **Figure 1.4**). Reference to GALV (envelope) in this thesis refers to this truncated, hyperfusogenic form. Once established as a concept it seemed appropriate to include other FMG for study. For reasons discussed in Chapter 1 Measles virus F and H FMG were also studied in depth. In the preliminary experiments described in this Chapter vesicular stomatitis virus envelope glycoprotein (VSV-G) was also included to assess the therapeutic potential of FMG.

3.1.1 VSV-G

Vesicular stomatitis virus is a member of the rhabdovirus family, genus vesiculovirus. It has a single negative strand RNA genome encoding 5 viral proteins. The virus has a single transmembrane protein, glycoprotein G. VSV-G, like the majority of FMG, forms trimers. VSV-G binds phosphatidylserine in cell membranes (Schlegel et al., 1983) and this explains the broad tropism of VSV. Following binding, virions enter the cell by the endocytic pathway; requiring acidification of the endosome to trigger the conformational change in VSV-G to permit fusion. Fusion is optimal around pH 6 (Gaudin, 2000) as opposed to fusion mediated by GALV and F and H which occurs at neutral pH. Other differences between VSV-G (or rhabdoviral FMG) and the majority of other viral FMG are: I) the low pH-induced conformational change is reversible, II) no coiled-coil structure is predicted for VSV-G, III) the fusion domain for VSV-G is not located at the N-terminal of the molecule but the centre of the protein (Zhang and Ghosh, 1994).

VSV-G is used in a number of strategies to pseudotype retroviral vectors due to its broad tropism and stability; it is therefore a familiar reagent in gene therapy laboratories. Transfection into a number of cell lines had indicated the development of syncitia even without changing the pH of the media, a phenomenon previously reported (Roberts et al., 1999). However more extensive syncitia formation was known to occur if the pH was lowered (Florkiewicz and Rose, 1984).

3.2 Results

3.2.1 FMG expression constructs

Three FMG were obtained and tested in the initial experiments. The truncated GALV cDNA was a kind gift of Dr S. Russell, Molecular medicine program, Mayo Foundation; Measles F and H cDNA were a kind gift of Dr R. Cattaneo, Molecular medicine program, Mayo Foundation; VSV-G was a kind gift of Dr Y. Takeuchi, London.

The GALV gene, received from Dr S. Russell, was encoded within the plasmid MoVGaLVSEATOenv, a retroviral packaging construct (Delassus et al., 1989). The GALV FMG was subcloned into the pCR3.1 vector (Invitrogen) so as to be expressed from a CMV promoter and be removed from other retroviral sequences.
pCR3.1 GALV was generated by PCR using MoVGaLVSEATOenv plasmid as template and the following primers, both containing *Mlu 1* restriction enzyme sites:

Forward primer: GALV 1: acgcgtacgcgttaagcctggtaccgtaacaa
Mlu 1 Mlu 1

Reverse primer: GALV 2: acgcgtacgcgtggtggccctcctatagtgag
Mlu 1 Mlu 1

The PCR conditions used using AmpliTaq Gold were 94°C 10 minutes to activate the polymerase, followed by 20 cycles of denaturing at 94°C for 1 minute, annealing at 60°C for 1.5 minutes, extension at 72°C for 3 minutes, and completed with a 10 minute extension at 72°C. The 2.2kb PCR product was cloned into the pCR3.1 vector. Restriction

enzyme digest with *BamH 1* identified correctly orientated clones and one was selected; forming pCR3.1 GALV. Functional activity of pCR3.1 GALV after PCR was confirmed by transfection of a number of cell lines and syncitia formation identified. The plasmid was also sequenced and found to be identical to the published sequence.

Measles F and H genes were encoded by the expression plasmids pCG-F1 and pCG-H5 which also contained a CMV promoter of identical sequence to that contained in pCR3.1.

VSV-G gene was encoded by the expression plasmid pCMV-VSV-G, again expression being generated by a CMV promoter.

3.2.2 Effect of FMG expression in suitable cell lines

Preliminary experiments were performed by transfecting a wide range of cell lines with each of the FMG. Tumour cells were plated in 6 well plates at a density so that after overnight incubation they were 80% confluent. At this time the cells were transiently transfected with the FMG plasmid using the ProFection method or the Effectene lipid reagent. The cells were then observed under the light microscope for morphological changes and cytotoxicity. An example of the morphological changes seen following FMG expression in susceptible cell lines is seen in **Figure 3.1**. For clarity immunofluorescent dyes were used. TEL.CeB.6 cells were transiently transfected with pCR3.1 GALV. At 48 hours post transfection the cells were fixed and stained with DiI (a red lipophyllic dye) and DAPI (blue staining nuclei). Approximately 120 nuclei can be seen within a single syncitium, the membrane outlined with the red DiI membrane dye. Under light microscopy these morphological changes were also easily identified following FMG expression in susceptible cell lines.

These initial observations gave general features of FMG mediatiated cytotoxicity and are listed:

1. Multinucleate syncitia developed approximately 18-24 hours after transfection.
2. Cytotoxicity as evidenced by syncitia rounding up and loss of trypan blue exclusion developed shortly after this time point but was progressive over days.
3. Some syncitia having formed remained viable for days.

Figure 3.1: Syncitia formation occurring in TEL.CeB.6 cells transiently transfected with FMG. TEL.CeB.6 cells were transfected with pCR3.1 GALV. After 48 hours the cells were fixed and stained with DiI (red) which is lipophyllic and outlines cell membranes, and Dapi (blue) which binds DNA and identifies nuclei. A syncitium can be seen containing ~120 nuclei.

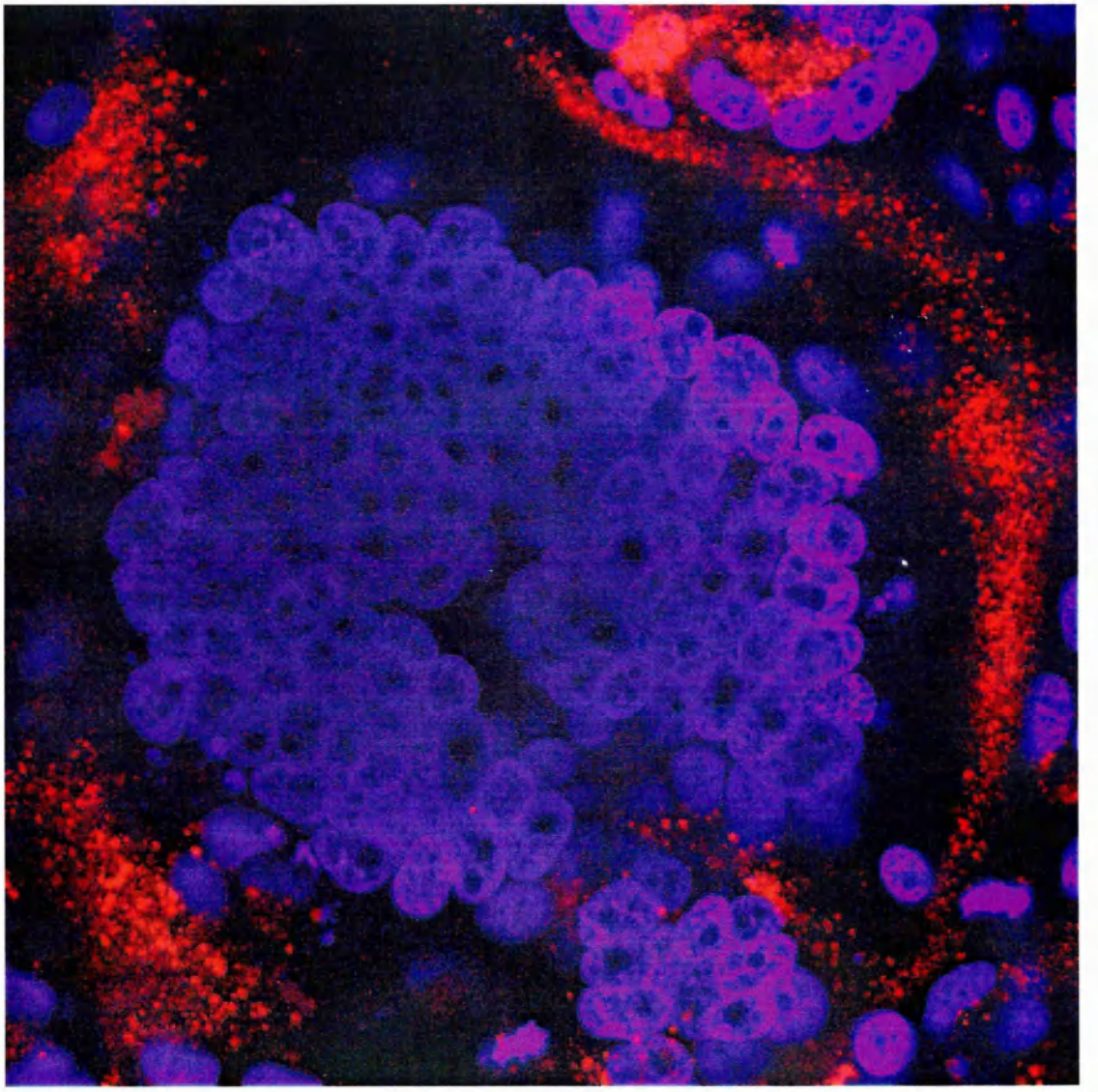

4. GALV and F and H caused fusion in human cell lines and not murine, whereas VSV-G was able to induce fusion in murine cell lines – this was an expected finding due to receptor usage.
5. VSV-G at normal pH induced significantly less syncitia in human cell lines than GALV or F and H.
6. Extent of syncitia formation was related to tumour cell confluency and efficiency of transfection.

It became clear from these initial experiments that for useful comparisons to be made between FMG and/or cell lines it would be helpful to have a standardised scoring system for syncitia formation; which was termed a fusion index. An exact measure of fusion would have required counting individual nuclei incorporated into syncitia. Counting syncitia alone would not have been accurate; due to the wide variation in size of these syncitia i.e. an extreme example would be with more and more extensive fusion occurring in a population, the number of syncitia would actually decrease until all the syncitia having fused, formed a single giant syncitium. Counting individual nuclei within syncitia was not practical for the majority of preliminary experiments and therefore the following fusion index was used:

Percentage of cells incorporated into syncitia	Fusion Index
0	0
>0 - 20	+
>20 - 40	++
>40 – 60	+++
>60 - 80	++++
>80	+++++

This fusion index was tested between investigators and proved sufficiently accurate, reproduceable and easy to use. An example of the preliminary data generated can be seen when a number of melanoma cell lines were transfected with FMG.

Human Melanoma cell lines

Cell line	Fusion Index	Transfection efficiency
Mel 17	+++++	5-10%
HMB2	++	5-10%
DX3	+++	5-10%
VUP	+++++	5-10%
Mewo	++++	5-10%
A378M	++	1%

Table 3.1: Susceptibility of fusion induced by FMG in Melanoma cell lines

A number of melanoma cell lines were plated in 6 well plates. After overnight incubation they were transiently transfected with pCR3.1 GALV. 48 hours later the degree of syncitia formation was recorded using the fusion index (detailed above). As a control, cells were also transfected with β-gal plasmid. At 48 hours cells were stained with x-gal and an assessment made of the efficiency of transfection.

These results indicated that there was variation in the degree of fusion seen in cell lines. This could not be explained by differences in FMG receptor expression: RNA was extracted from each of the melanoma cell lines and semi-quantitative rtPCR was performed for GAPDH and PiT 1. All cell lines expressed PiT 1 and there was no significant difference in the intensity of the bands detected.

These preliminary experiments did indicate that FMG were cytotoxic: demonstrated by observation of cells in culture following transfection with FMG, trypan blue exclusion, PI staining and LDH release assay. The next step was to compare the efficacy of FMG mediated killing to suicide genes.

3.2.3 FMG cytotoxicity compared to suicide genes

Suicide genes have been developed and used in a number of cancer gene therapy studies (detailed in Chapter 1). To perform their cytotoxic function they require both expression

within the cell and delivery of the appropriate prodrug. To assess the utility of FMG it seemed appropriate to test their cytotoxicity against commonly used suicide genes in vitro. A cell survival assay was performed according to the protocol outlined in Chapter 2. 293 cells were transfected with 5 μg of plasmid DNA (HSVtk, CD, pCG-F1 alone or pCG-H5 alone) or 2.5 μg pCG-F1 with pCG-H5 2.5 μg. 5 days post transfection and incubation in the appropriate media, surviving cells were counted. The experiment was performed three times and a representative result can be seen in **Figure 3.2**.

A similar experiment was performed comparing HSVtk/ganciclovir killing to all three FMG tested. The experimental conditions were identical to those detailed above with 293 cells being transfected with 5 μg of plasmid DNA (HSVtk, GALV, VSV-G) or 2.5 μg pCG-F1 with pCG-H5 2.5 μg. Again 5 days after transfection and incubation in the appropriate media surviving cells were counted. The experiment was performed three times and a representative result can be seen in **Figure 3.3**.

The combined results from these two experiments indicated that the cytotoxicity of FMG was superior to that of either of the two suicide genes tested. In addition GALV and F and H were significantly more potent than VSV-G under these experimental conditions.

The likely explanation for the enhanced cytotoxicity of FMG over the suicide genes tested was that FMG have a greater bystander effect. To test this an additional experiment was performed. 293 cells were set up as previously described and after 24 hours transfected with HSVtk, GALV or β-gal. At this time 293 cells stably expressing β-gal were plated at a density of 10^5 cells/well. After 24 hours the transfected 293 cells were trypsinised and collected. These cells transfected with HSVtk or GALV were then added to the 293 β-gal cells at varying concentration: the number of transfected cells was estimated by assessing the transfection efficiency of the parental 293 cells with CMV β-gal, which was about 7%. 0, 1, 10, 100, 10^3, 10^4 and 10^5 transfected 293 cells were added per well to the 293 β-gal cells. Five days later wells were washed and stained for β-gal as a measure of surviving cells. The result can be seen in **Figure 3.4** and is representative of three experiments.

Using these experimental conditions it appeared that in excess of 10^4 HSVtk transfected cells had to be added to come close to eradicating the target population. In contrast at least 1 log fewer GALV transfected 293 cells were sufficient to eradicate completely the target population. The approximate numbers of cells killed by a bystander effect in these

Figure 3.2: Enhanced cytotoxicity was seen with FMG mediated cell killing compared to suicide genes. 293 cells were transfected with no DNA (None), non-cytotoxic DNA (F), suicide genes (HSVtk, CD) or FMG (F+H). 24 hours later cells were washed and media applied: for HSVtk transfected cells this contained 5μg/ml ganciclovir, for CD transfected cells this contained 3μM 5-fluorocytosine. 5 days post transfection the number of viable cells were recorded (Bars represent SD).

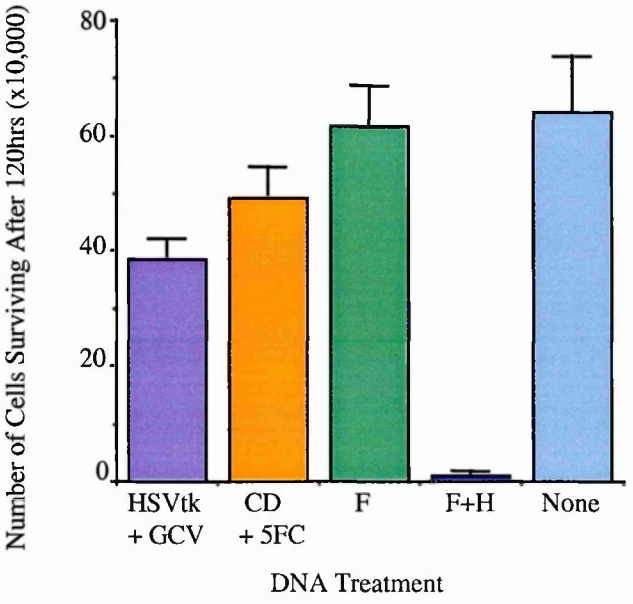

Figure 3.3: All three FMG show enhanced cytotoxic effect compared to HSVtk/ganciclovir. The same experimental procedure was performed as for Figure 3.2. In this experiment 293 cells were transfected by suicide gene (HSVtk) or FMG (F+H, GALV or VSV-G) or control (None). 5 days post transfection and incubation in appropriate media surviving cells were counted (Bars represent SD).

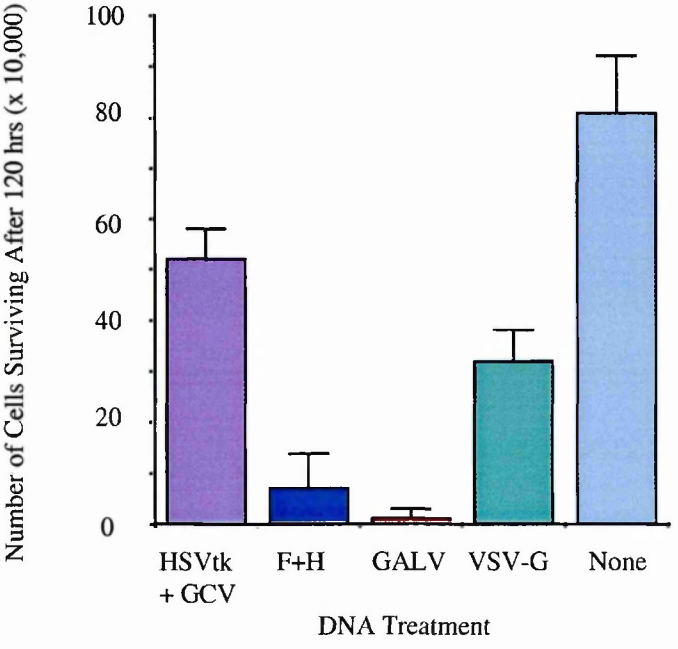

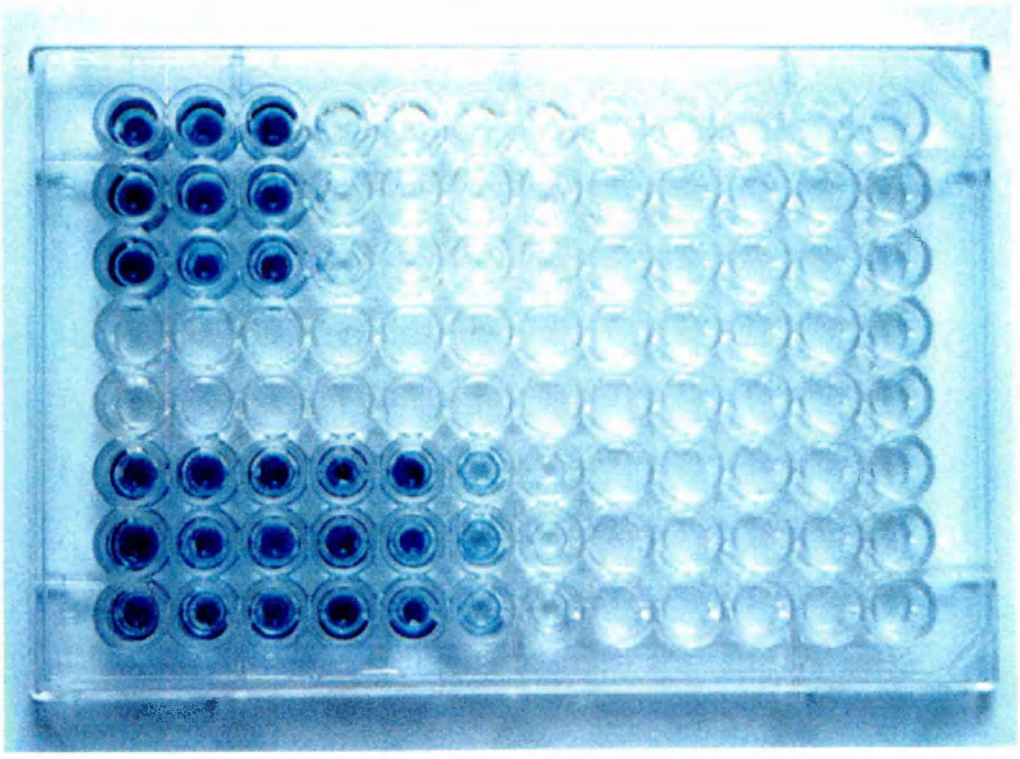

Figure 3.4: The bystander effect of FMG was one log greater than suicide genes. 293-β-Gal cells were plated in triplicates in 96-well plates at a density of 10^5 cells/well. Twenty-four hours later, increasing numbers of GALV-transfected (upper row of triplicates) or HSVtk-transfected (lower row) 293 cells were added to the wells. The number of transfected cells was estimated using transfection of parental 293 cells with CMV- β-Gal 24h previously. From left to right, the number of cells added per triplicate set of wells was 0, 1, 10, 100, 10^3, 10^4, and 10^5. Both FMG- and HSVtk-transfected wells were treated with GCV. Five days later, wells were washed and stained for β-galactosidase as a measure of surviving cells.

experiments was estimated at approximately 10 for HSVtk and 100 for GALV; which is in keeping with the findings of the previous experiments.

3.2.4 FMG mediated cytotoxicity is independent of the stage of the cell cycle

Many cytotoxic agents including a number of suicide genes require cells to be in S phase of the cell cycle to be effective. With highly variable tumour doubling times, especially in vivo, this requirement can limit the efficiency of tumour cell killing. It seemed unlikely that the stage of the cell cycle would play a role in FMG mediated cytotoxicity. However it seemed appropriate to formally examine this and an experiment was designed incorporating aphidicolin to block DNA synthesis. 293 cells were pre-incubated with 5 μg/ml aphidicolin for 24 hours or in normal media. The cells were then transfected with pCR3.1 GALV, GALV-EGF or nothing. GALV-EGF contains the EGF ligand NH_2-terminally displayed on GALV and results in a >90% inhibition of its fusogenic capacity, a kind gift from Dr A. Fielding, Molecular medicine program, Mayo Foundation. GALV-EGF was used as a transfection control in the experiment. 48 hours after transfection viable cells were counted. A representative result of three experiments can be seen in **Figure 3.5**.

The result indicated that FMG mediated cytotoxicity occurred independently of the cell cycle; with approximately 10% of cells surviving in the GALV group relative to mock transfected, whether pre-incubated with aphidicolin or not.

3.2.5 FMG expression in tumour cells can prevent tumour development in vivo

The in vitro experiments detailed above indicated the potential utility of FMG as cytotoxic gene therapy agents. However it was clearly necessary to assess whether FMG remained cytotoxic in an in vivo setting. A number of experiments were designed; the initial experiments conducted were with plasmid and will be detailed. As indicated the primary aim was to establish whether FMG were as effective in vivo as they had been in vitro. In addition these initial experiments also attempted to address the issue as to whether specificity of effect could be added in. For this a FMG was placed under the control of a tissue-specific promoter. Specifically GALV cDNA was expressed from the human tyrosinase promoter, which confers tissue-specific expression to melanocyte derived cells

Figure 3.5: FMG mediated cytotoxicity was independent of the cell cycle. 293 cells were incubated with aphidicolin (arrests cells in S phase)(/Aphid) or normal media. After 24 hours cells were transfected with no DNA (MOCK), non-fusogenic GALV (GALV-EGF) or FMG (GALV). After a further 48 hours the number of viable cells were recorded (Bars represent SD).

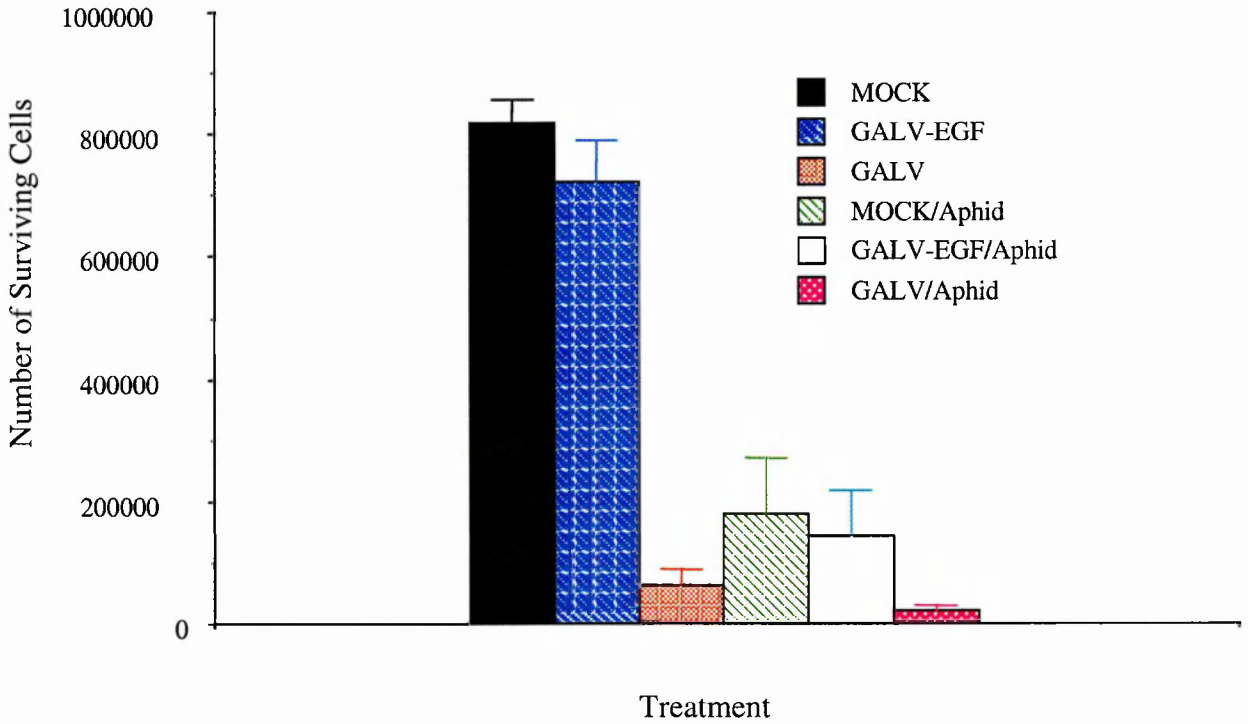

	Killing Relative to Mock Transfected Control
No Aphidicolin	
MOCK	0%
GALV-EGF	12%
GALV	92.5%
With Aphidicolin	
MOCK	0%
GALV-EGF	11%
GALV	88.2%

(Bentley et al., 1994; Diaz et al., 1998). The tissue-specific component was contained within the plasmid 3xTDE-Su prom-pGL3, a kind gift of Dr R. Diaz, Molecular medicine program, Mayo Foundation. The luciferase gene (expressed from this plasmid) was able to be excised using restriction enzymes *Xba1* and *Hind III*. GALV was able to be excised from pCR3.1 GALV by the same enzymes; therefore tyrosinase GALV (TYR-GALV) was able to be produced by standard restriction enzyme digest and ligation.

Human tumour xenografts of HT1080 or Mel624 were injected s.c. into nude athymic mice. Prior to tumour cell innoculation the cells had been transfected with plasmid in vitro. Tumour cells had been plated in 25 cm^2 flasks 24 hours previously; so as to be 80% confluent prior to transfection. They were then transfected with pCR3.1 GALV, CMV β-gal or TYR-GALV. Transfection was performed using Effectene lipid and 10 μg of DNA/10^6 tumour cells. Three hours post transfection, cells were washed three times in PBS and then injected into the mice. The results of the experiment are seen in **Figures 3.6 and 3.7**.

At a dose of 10^6 tumour cells/mouse 90-100% of mice in the control CMV β-gal develop small, palpable tumours by 72 hours. These progressed over 12-14 days to become >1cm in diameter and the animals were sacrificed. This was seen with both HT1080 or Mel624 test groups. With regard to the HT1080 TYR-GALV group, this behaved in a similar manner. Both HT1080 and Mel624 cells transfected with pCR3.1 GALV showed a significant difference. 100% of HT1080 and 90% of Mel624 tumour-bearing mice saw their tumours eradicated and were long term survivors. Mel624 tumours transfected with TYR-GALV also regressed in 100% of the mice.

The prevention of tumour outgrowth by pCR3.1 GALV indicated that FMG did remain cytotoxic in vivo. The result from the TYR-GALV group indicated that in this model transcriptional control of expression was an effective means of targeting FMG-mediated gene therapy to specific tumour types.

3.2.6 FMG gene expression is associated with increased expression of immunostimulatory signals

The manner in which tumour cells die is thought to influence the potential for developing a tumour specific immune response and has been discussed in Chapter 1. A 'stressful',

Figure 3.6: FMG expression can prevent primary tumour outgrowth in vivo. HT1080 cells were transfected in vitro with control plasmid (CMV-β-Gal), GALV (CMV-GALV) or GALV expressed from a melanoma tissue specific promoter (TYR-GALV). Three hours post transfection cells were seeded s.c. in nude mice (10^6 cells/mouse) and tumour development monitored. 7 days post innoculation (I) those tumours containing cells transfected with CMV-GALV began to regress, so that at 90 days (II) all 10 mice were tumour free. In the remaining groups mice were sacrificed once the tumour reached 1.2cm in the longest diameter.

I. HT1080 7 days

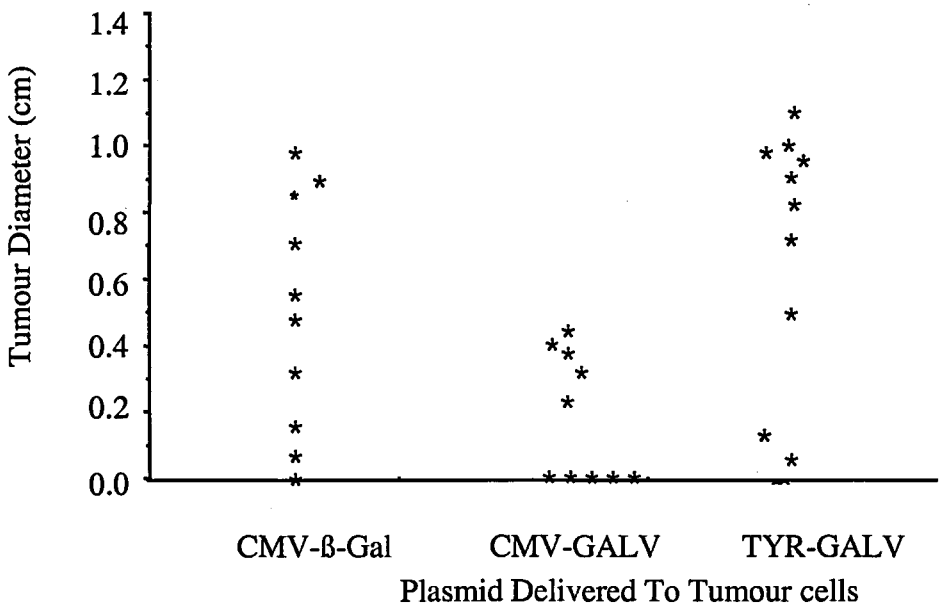

II. HT1080 90 Days

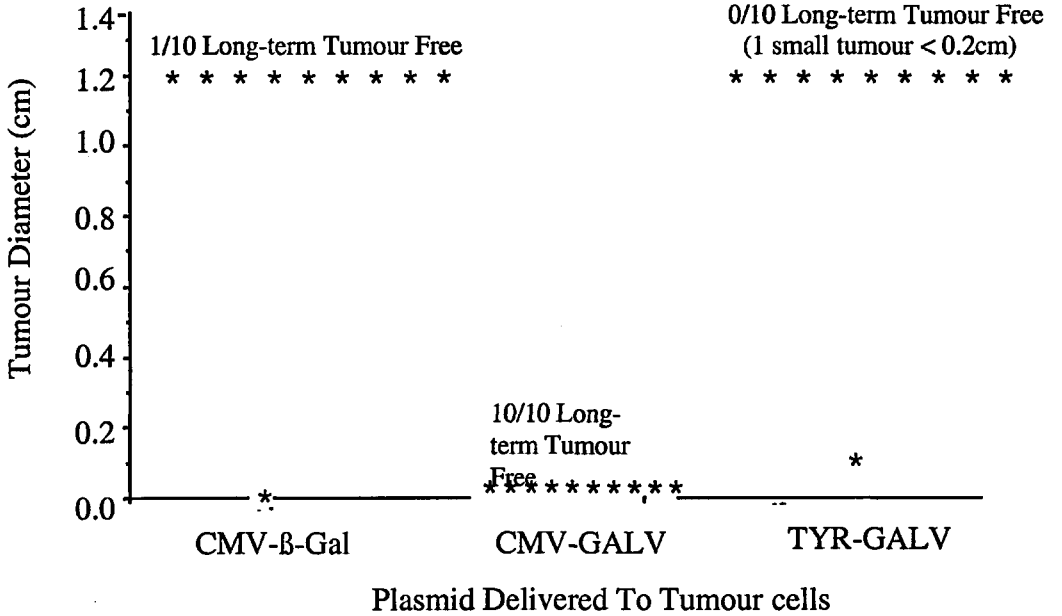

Figure 3.7: FMG expression can be controlled in vivo by a tissue specific promoter. Cells of the human melanoma cell line Mel624 were transfected in vitro with control plasmid (CMV-β-Gal), GALV (CMV-GALV) or GALV expressed from a melanoma tissue specific promoter (TYR-GALV). Three hours post transfection cells were seeded s.c. in nude mice (10^6 cells/mouse) and tumour development monitored. Tumour growth and development was prevented in those mice injected with cells previously transfected with CMV-GALV or TYR-GALV.

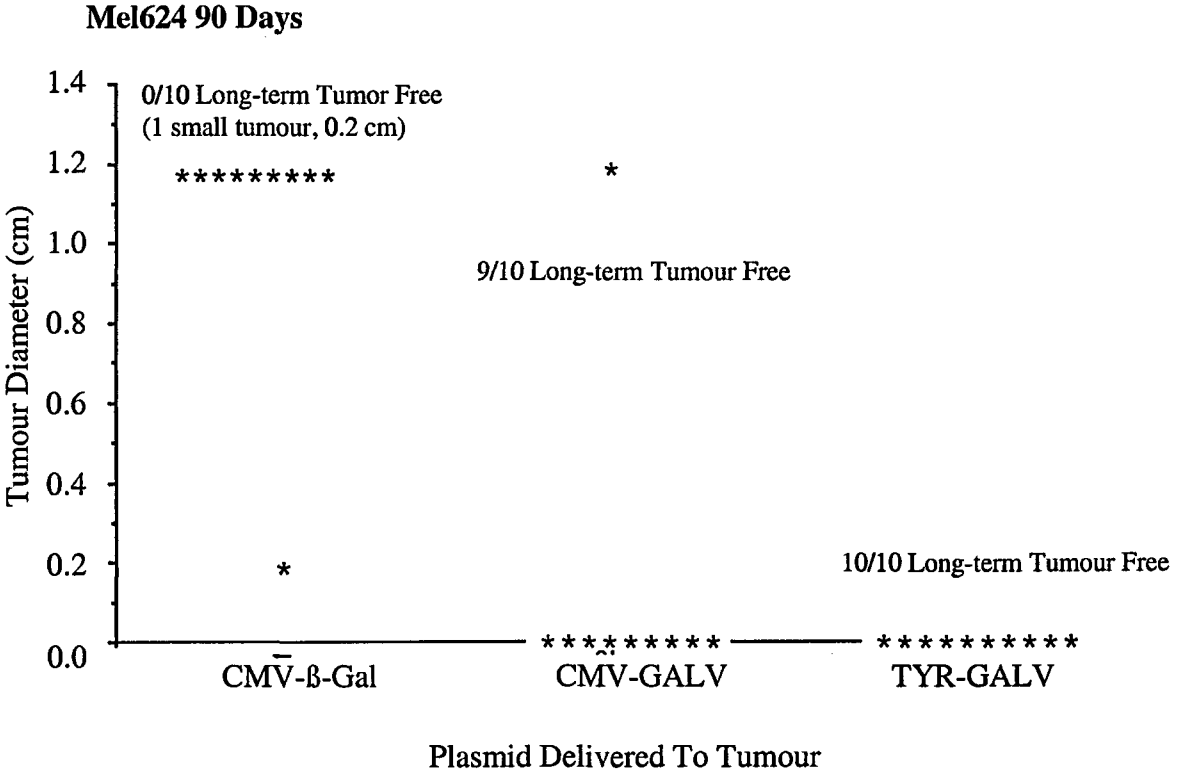

necrotic death is more likely to induce an immune response due to the release of 'danger signals' into the tumour environment. A component of these danger signals are Heat shock proteins (HSPs). I wished to identify whether FMG mediated cytotoxicity caused changes to cellular HSPs.

TEL.CeB.6 cells were plated in 6 well plates. After overnight incubation they were transfected with 5μg DNA; either pCR3.1 GALV or the non-fusogenic GALV-EGF, according to the ProFection protocol. After a further 24 hours the cells were washed and RNA harvested and rtPCR performed. Primers for inducible Hsp70, gp96 and GAPDH were used; the result can be seen in **Figure 3.8.**

Non-fusogenic GALV (GALV-EGF) did not produce induction of Hsp70 and levels of gp96 match parental cells. Fusogenic GALV expression did cause induction of mRNA for both inducible Hsp70 and gp96. GAPDH indicated equal RNA loading.

Hsp70 protein could also be identified by immunofluorescence. TEL.CeB.6 cells were plated in chamber slides. After overnight incubation they were transfected with pCR3.1 GALV or mock transfected. After 24 hours cells were washed and fresh media replaced. At various timepoints post transfection cells were fixed, permeabilised and stained. Mouse monoclonal anti-heat shock protein 70 antibody was used as the primary at a concentration of 1:100, with Donkey anti-mouse IgG FITC labelled as secondary. Some mock transfected cells were heat shocked at 42°C for 30 minutes prior to fixing and acted as a positive control. Representative images can be seen in **Figure 3.9.**

The results indicated a low level background of Hsp70 in control cells (mock transfected). Heat shocked cells acted as positive control. At early timepoints syncitia exhibit Hsp70 protein primarily in the cytoplasm. At later timepoints Hsp70 can also be seen to be localising within the nuclei: this is an indicator of an active stress response above basal Hsp70 levels.

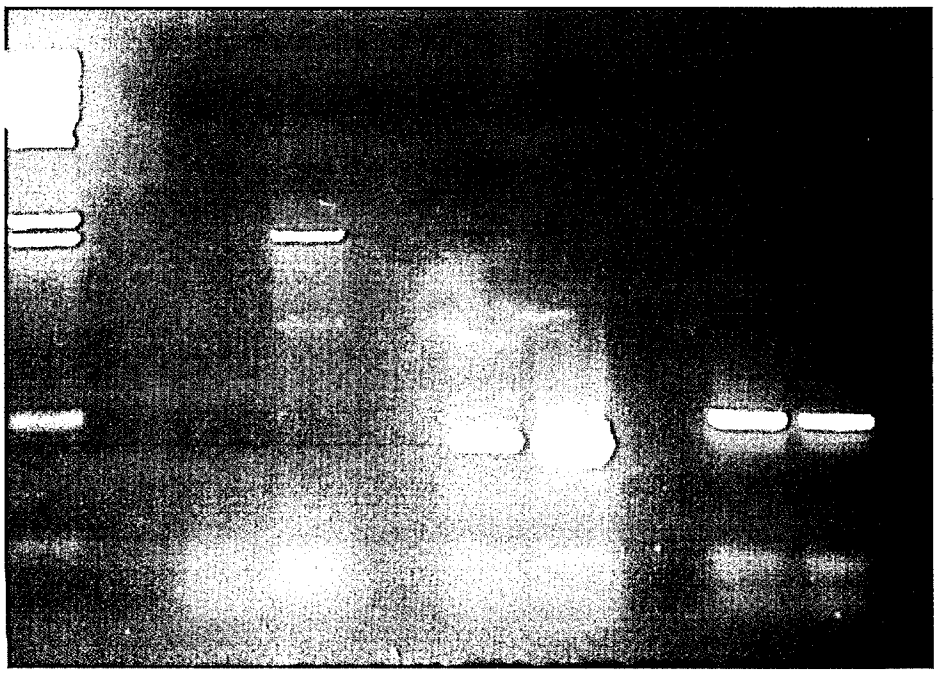

Figure 3.8: Expression of GALV, mediating syncitia formation, induces heat shock protein expression. An RT-PCR was performed 24h after transfection of TEL.CeB.6 cells. Cells were transfected with GALV plasmid: lanes 3,5 and 7, or control non-fusogenic GALV plasmid: lanes 2,4, and 6. Primers for HSP: inducible Hsp70; lanes 2 and 3, gp96; lanes 4 and 5, or control GAPDH primers; lanes 6 and 7, were used. Lanes 6 and 7 confirm equal loading of cDNA. Inducible Hsp70 is only detected with fusogenic GALV and the level of gp96 expression is increased with fusion.

Lane 1:	*Hind*III molecular weight markers	
Lane 2:	cDNA from cells transfected with Non-fusogenic GALV	} Primers for inducible Hsp70
Lane 3:	cDNA from cells transfected with GALV	
Lane 4:	cDNA from cells transfected with Non-fusogenic GALV	} Primers for gp96
Lane 5:	cDNA from cells transfected with GALV	
Lane 6:	cDNA from cells transfected with Non-fusogenic GALV	} Primers for GAPDH
Lane 7:	cDNA from cells transfected with GALV	

Figure 3.9: Identification of an active stress response induced by FMG expression. TEL.CeB.6 cells were transfected with control plasmid (I and II) or pCR3.1 GALV (III and IV). A sample of control transfected cells were heat shocked and acted as a positive control (II). At various timepoints cells were fixed, permeabilised and stained for Hsp70 expression (green) and nuclei (blue). At the later timepoints of syncitia formation positive staining for Hsp70 can be seen to have migrated from the cytoplasm to the nuclei, indicating an active stress response.

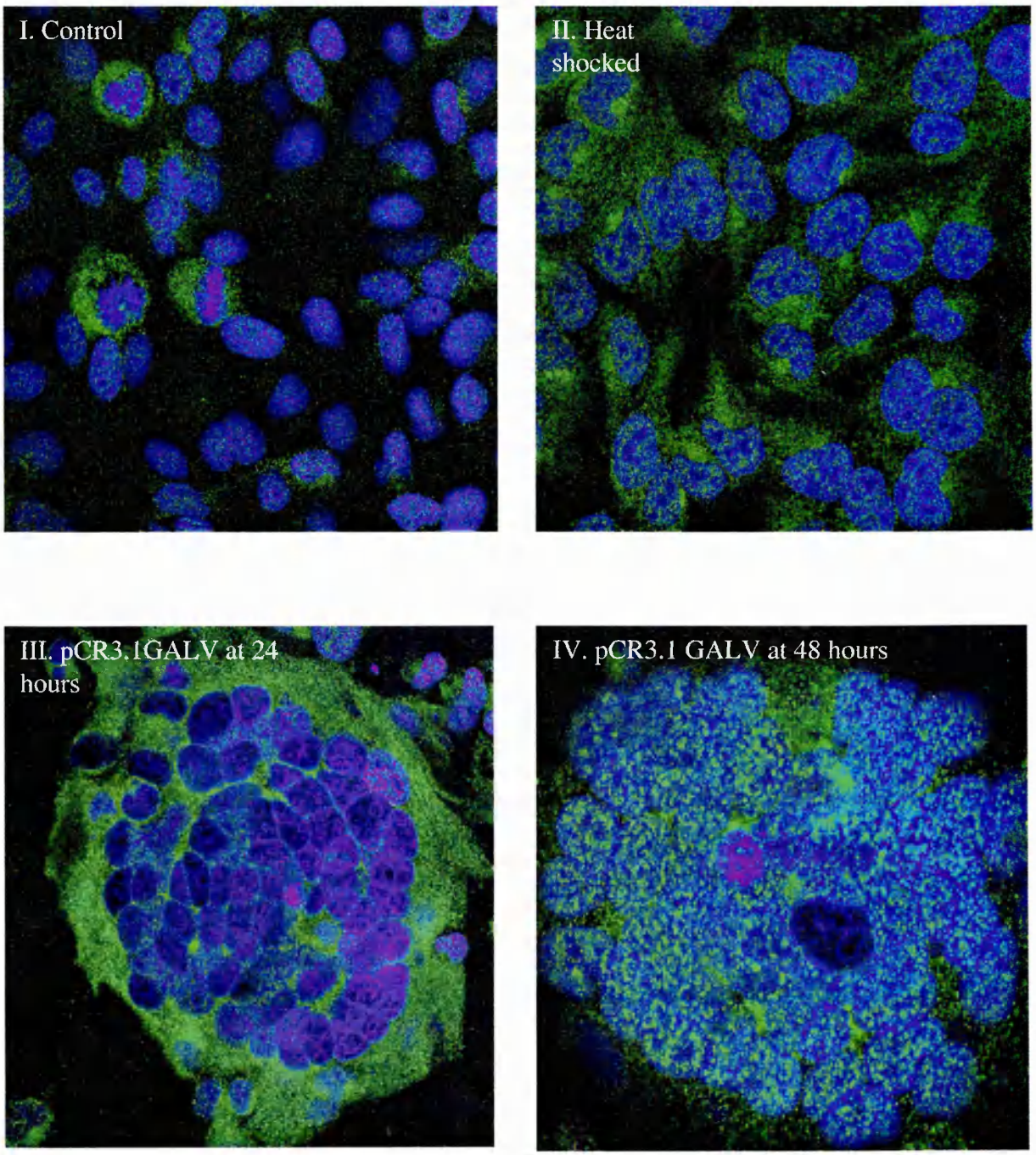

3.3 Discussion

These preliminary experiments sought to address whether FMG gene expression had potential as a cytotoxic gene therapy. Plasmid transfection in vitro of a wide range of human tumour cell lines showed the broad applicability of this approach; in keeping with the ubiquitous expression of the receptors for GALV and F and H. Extent of fusion and therefore cytotoxic effect was dependent on the cell density and transfection efficiency, but was independent of the cell cycle and did not require additional factors e.g. prodrug. Direct comparison with suicide genes indicated an enhanced therapeutic effect for FMG in vitro. This was due to a superior bystander effect. Transfection of tumour cells with FMG prior to innoculation in vivo showed the cytotoxic effect is not confined to the in vitro setting. In addition FMG mediated syncitia formation in vitro was found to be associated with a stress response.

These findings suggested that FMG did have potential as cytotoxic gene therapy agents. Subsequent aims were to identify the mechanism of cell death induced by FMG: detailed in Chapter 4, and develop vectors capable of delivering FMG in vivo: detailed in Chapters 5-7.

The data presented in this chapter formed part of the following paper:

Fusogenic Membrane Glycoproteins As Novel Class of Genes for the Local and Immune-mediated Control of Tumor Growth

Andrew Bateman, Francis Bullough, Stephen Murphy, Lisa Emiliusen, Dimitri Lavillette, Francois-Loic Cosset, Roberto Cattaneo, Stephen J. Russell, and Richard G. Vile

Cancer Research 60, 1492-1497, March 15, 2000

CHAPTER 4: MECHANISM OF CYTOTOXICITY

Chapter 4: Mechanism of Cytotoxicity

4.1 Introduction

This chapter details the experiments conducted to ascertain the general mechanism of cytotoxicity produced following FMG mediated syncitia formation. The initial experiments in Chapter 3 indicated that FMG expression in permissive cell lines could produce extensive cell death with a significant bystander effect. An understanding of the death process in syncitia was felt to be important as it might lead to an ability to enhance the cytotoxic effect, indicate the likely utility of FMG gene therapy (see Chapter 1.7 Mechanisms of cell death) and suggest future applications.

4.2 Results

4.2.1 Syncitia Morphology

From Chapter 1.7 Mechanisms of cell death it can be seen that the various defined forms of cell death have quite distinct morphological appearances associated with each process. The initial experiments to identify the particular process occurring in syncitia were planned to detail the morphological appearance of syncitia development and death. These experiments included light microscope studies to assess the syncitia as a whole, detailed assessment of nuclear morphology using DAPI staining and ultrastructural information from electron microscopy.

For each of these procedures cells were plated in Labtek chamber slides or T25cm^2 flasks. After overnight culture they were transfected with FMG plasmid using the calcium phosphate/DNA co-precipitation or Effectene protocols depending on cell line. The following day the cells were washed with PBS and new media applied. Cells were collected for analysis from 24hours to 96 hours post transfection. For light microscope assessment cells were merely washed with PBS and then viewed using an inverted microscope with light and phase contrast, and images captured by camera. For DAPI staining the cells were prepared as per the immunofluorescence protocol: the chamber slides were washed three times with PBS and then the cells fixed with 4% Formaldehyde in PBS for 15 minutes. The slides were then washed a final 3 times in PBS, allowed to air

dry before mounting with Prolong antifade containing 2µl/ml of DAPI and covered with a coverslip. The protocol used for electron microscopy studies is as described in Chapter 2. For each technique multiple cell lines were tested on a number of occasions. Representative results will be detailed below.

Light microscope

Figure 4.1 details some of the characteristic findings seen in TEL.CeB.6 cells following transfection of FMG and subsequent syncitia formation. At 24 hours post transfection large multinucleate syncitia have developed with evidence of some cell death as indicated by some non-adherent syncitia, LDH release assay data (see below), and trypan blue or PI staining (data not shown). Remaining adherent syncitia were identified ranging from those with normal appearing nuclei and no identifiable abnormalities of the membrane or cytoplasm, to those exhibiting cytoplasmic blebbing and less distinct nuclear outline (**Figure 4.1.A**). Adherent syncitia were also identified with apparently normal appearing cell membrane and cytoplasm but brightly appearing nuclei; these were shown to be dead by positive staining with PI or trypan blue. Over time the number of adherent syncitia would decline due to increased cell death occuring again as evidenced by a greater amount of non-adherent material, LDH release assay, trypan blue or PI staining. The majority of syncitia remaining exhibited greater morphological changes with increased cytoplasmic blebbing and disruption of the nuclei (**Figure 4.1.B**). Greater numbers of syncitia were identified rounding up and becoming non-adherent. During this process continued evidence of cytoplasmic blebbing could clearly be identified (**Figure 4.1.C**). By 96 hours very few syncitia (< 1%) were left adherent and viable as identified by dye exclusion.

DAPI staining

For more detailed studies of nuclear changes within syncitia the DNA stain DAPI was used and representative results can be seen in **Figure 4.2**. At early stages of syncitia development (24-48 hours) the majority of nuclei within syncitia appeared normal **Figure 4.2.i**. However the occasional hyperchromatic, pyknotic nucleus could be identified: in a wide field of view these nuclei would make up 1-2% of nuclei identified. At later time points (48 hours and beyond) a common finding was of large areas of interphase DNA breaking away within areas of syncitia formation, **Figure 4.2.ii**. However two other patterns of morphological changes were identified at these later timepoints under the same

experimental conditions and are illustrated in **Figures 4.2.iii and iv**. Specifically in less than 5% of syncitia multiple nuclei within a particular syncitium could be seen to be condensing their chromatin into prometaphase appearing chromosomes, **Figure 4.2.iii.A**. This phenomenon could also be identified effecting all the nuclei of a syncitia, with the whole structure becoming dispersed spreading chromosomes across the field of view, **Figure 4.2.iii.B**. The other finding was of nuclear fusion occuring between adjacent nuclei within a single syncitium, **Figure 4.2.iv.A**. This nuclear fusion process could also be identified effecting all the nuclear material within a syncitium particularly at later timepoints (72-96 hours) and was more prevalent than the chromosome appearance, approximately effecting 20-30% of syncitia examined at these timepoints, **Figure 4.2.iv.B**. Rarely a combination of nuclear fusion and chromosome condensation was identified in the same syncitium, **Figure 4.2.iv.C**.

Electron microscopy (EM)

A representative finding of electron microscope examination of a syncitium can be seen in **Figure 4.3**. The most striking feature of the EM images was the large areas of nuclear material identified which would be in keeping with fusion of multiple nuclei in a syncitium. It was also noteworthy that the nuclear material appeared similar to that seen in control cells; specifically the DNA was not condensed. Of equal importance was the finding that the organelles within these syncitia appeared normal.

Conclusions

Taken together the studies of morphology suggested that syncitia die by necrosis. The light microscope images indicated a blebbing process occuring in some syncitia which had appearances quite different from apoptotic bodies and is in keeping with the descriptive features of necrosis (see **Figure 1.14**). Other syncitia could be identified which had normal size nuclei but gave a 'bright light' appearance. These syncitia stained with PI or trypan blue indicating their loss of viability due to plasma membrane permeability: as this occured before any significant nuclear changes it would be in keeping with necrosis. The DAPI staining clarified the morphological changes seen in the nuclei. The classical changes described for cells undergoing apoptosis were only seen rarely within syncitia with the vast majority of nuclei undergoing karryorhexis compatible with necrosis. The feature of nuclear fusion was unexpected and is as yet unexplained. The finding of

Figure 4.1: Light microscope images showing blebbing of TEL.CeB.6 cells following pCR3.1 GALV transfection and syncitia formation.

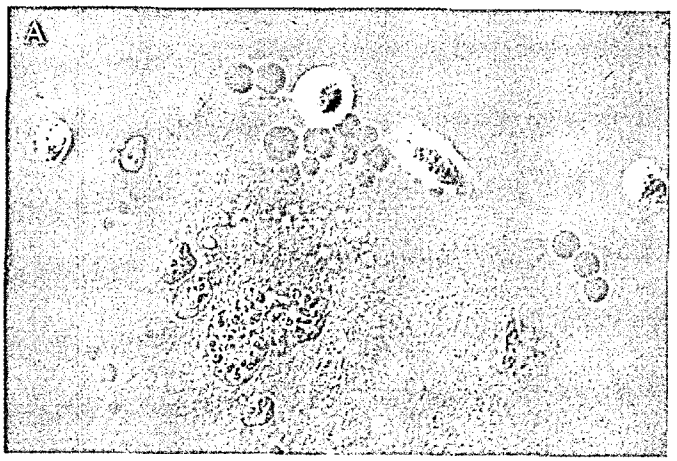

A.24-48 hours

Post transfection

B+C >48 hours

Post transfection

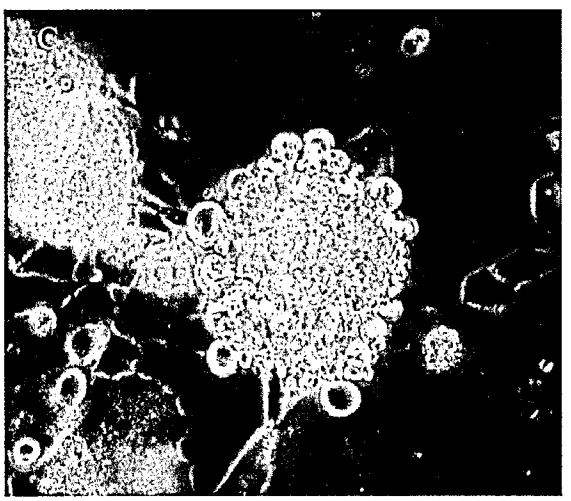

Figure 4.2.i + ii: pCR3.1 GALV transfected TEL.CeB.6 cells stained with Dapi

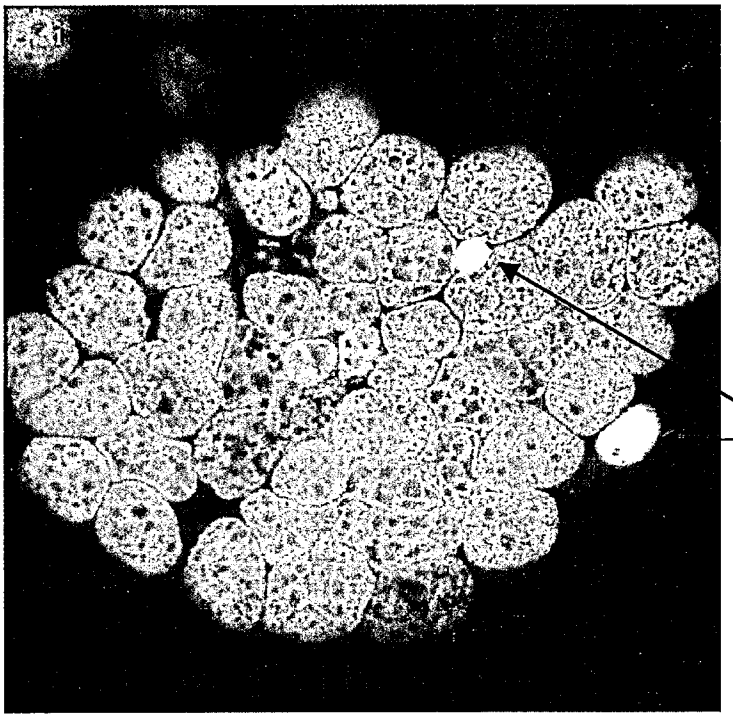

i. Early timepoints 24-48 hours

Occasional Hyperchromatic, pyknotic nuclei can be identified. But the majority of nuclei appear normal.

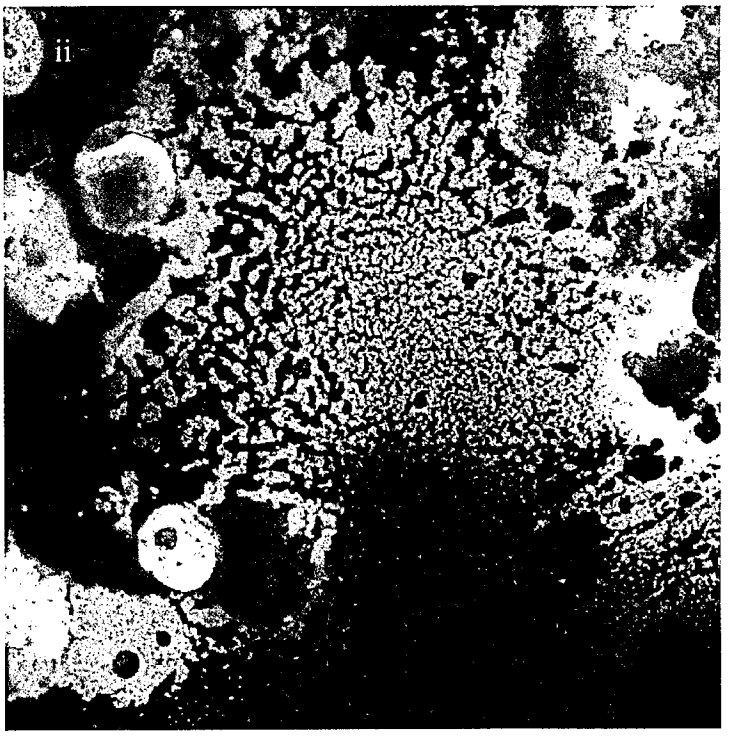

ii. Later timepoints > 48 hours

Figure 4.2.iii: Chromosome condensation can be seen to occur in nuclei within syncitia. TEL.CeB.6 cells were transfected with pCR3.1 GALV and followed for nuclear changes by Dapi staining (A + B).

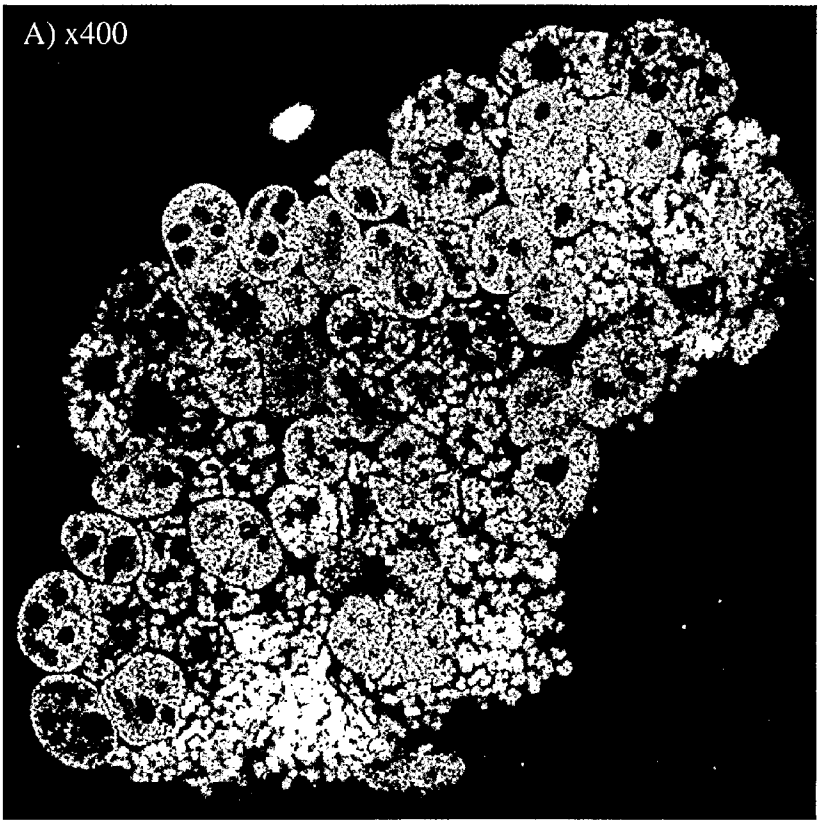

A). Chromosome condensation can be seen in some nuclei within a syncitium with a normal appearance of the remaining nuclei

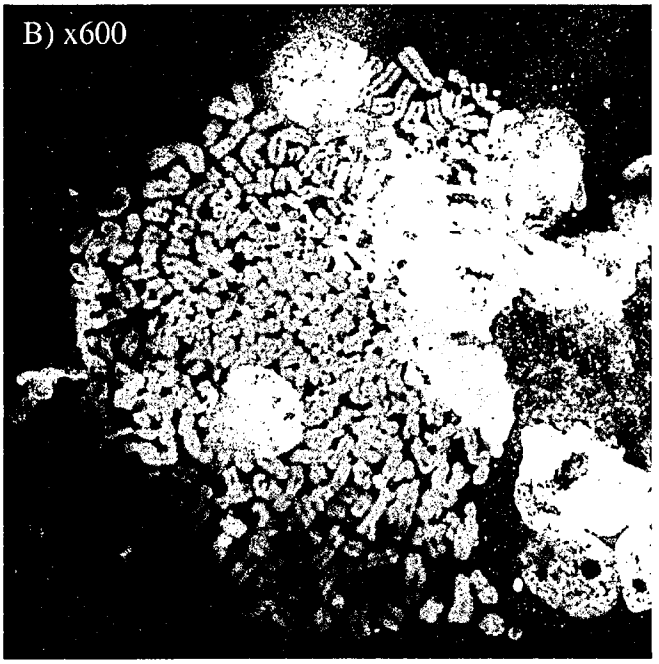

B). Prometaphase chromosomes are seen falling out from nuclei within a syncitium

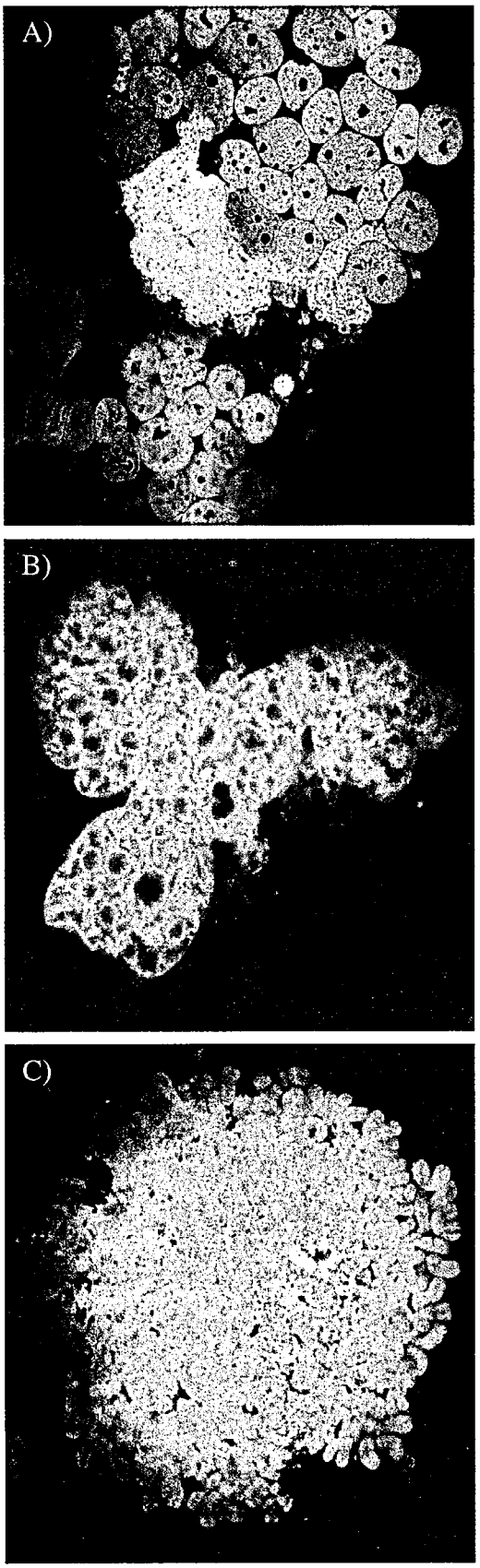

Figure 4.2.iv : Nuclear fusion is seen in TEL.CeB.6 cells transfected with pCR3.1 GALV. TEL.CeB.6 cells were transfected at Day 0 and followed for nuclear changes by Dapi staining. Nuclear fusion is seen to appear by Day 3 (A-C): involving a portion of the nuclei within a syncitium (A), the whole syncitium (B), or once formed breaking down through chromosome condensation (C).

Figure 4.3: Electron micrograph of TEL.CeB.6 cells after transient transfection with pCR3.1 GALV.

A) Normal TEL.CeB.6 cells: x2500

B) Multiple nuclei and nuclear fusion seen in a syncitium at 3 days post pCR3.1 GALV transfection: x2500

The white bar in each image represents 2μm

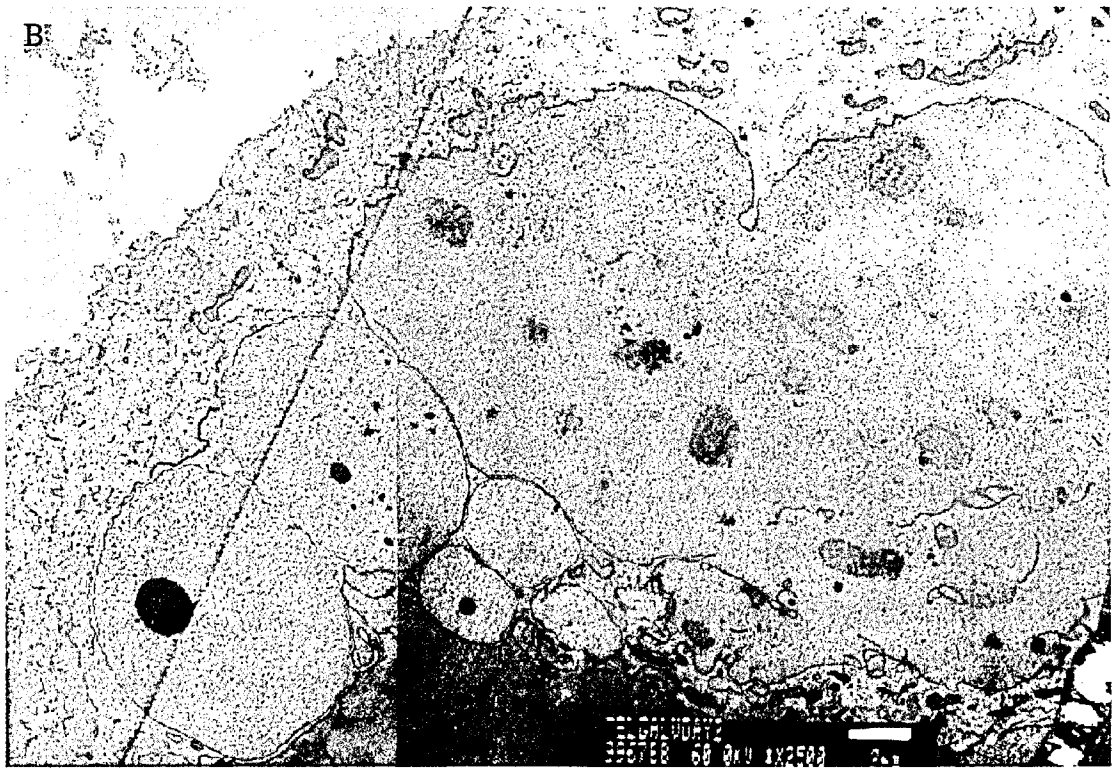

prometaphase appearing chromosomes raised questions about the cell cycle status of nuclei within syncitia and will be addressed below. The EM studies again did not indicate features compatible with apoptosis and were in keeping with the other findings.

4.2.2 Assessment of apoptosis

In Chapter 1 the biochemical features of apoptosis are detailed. Assays have been developed to detect these specific features and a number were used to help indicate whether apoptosis played a significant role in the cytotoxicity associated with FMG mediated syncitia formation; these will be detailed below.

Tunel assay

TEL.CeB.6 and HT1080 cell lines were transiently transfected with pCR3.1 GALV and the Tunel assay performed as described in Chapter 2. The experiments were repeated on three occasions. Data from TEL.CeB.6 cells is seen in **Figure 4.4** and is representative of findings from all Tunel assays performed. The results indicated that at early timepoints (24-48 hours) there was very little positive staining identified. Occasional positive staining was seen at the periphery of nuclei aggregated in a syncitia from 48 hours onwards in approximately 10% of fields of view, as seen in **Figure 4.4.II-IV**. These images are incorporated here as they indicate the positive functioning of the assay. The finding of occasional positive staining of individual nuclei is in keeping with the morphological studies showing the occasional hyperchromatic, pyknotic nucleus seen in association with syncitia, **Figure 4.2.i**. At later timepoints again the majority of nuclei and areas of nuclear fusion show no positive staining. As the nuclear material from syncitia breaks up (the karryorhexis previously described) scattered positive staining can be seen, **Figure 4.4.IV**. This is to be expected as the Tunel assay detects DNA breaks and is not specific for caspase mediated (apoptotic) DNA cleavage. The conclusions drawn from this assay were that dying syncitia do not demonstrate positive staining compatible with significant apoptosis. The occasional individual nucleus at the periphery of a syncitium or cells in the vicinity of syncitia appeared to demonstrate positive staining compatible with apoptosis.

Figure 4.4: Tunel assay of TEL.Ceb.6 cells forming syncitia following transient transfection with pCR3.1 GALV. TEL.Ceb.6 cells were transfected at Day 0 with pCR3.1 GALV or control. Samples were then analysed at 24 hour periods by Tunel assay (FITC) and Dapi nuclear stain (blue): representative images are presented for GALV transfected samples. Positve staining is represented by light blue staining (FITC and Dapi overlayed). Only a small proportion of nuclei associated with syncitia show evidence of apoptosis by Tunel at any time point.

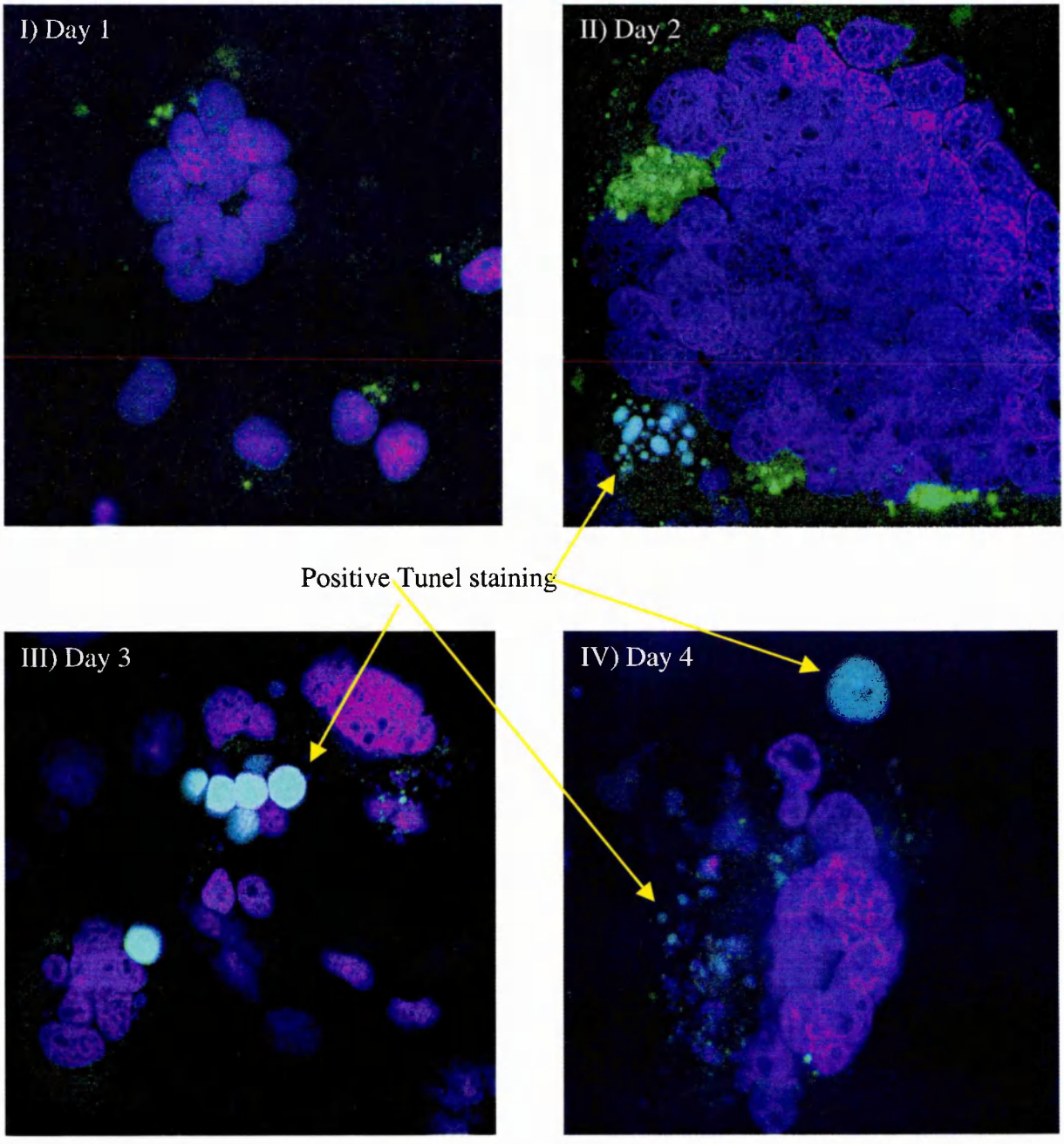

Caspase inhibition

Caspases can be irreversibly inhibited by incubation of cells with low molecular weight peptides containing a carboxy-terminal aspartate derivatized to a halomethylketone (Kauffmann '99). An example of such an inhibitor is Z-Val-Ala-Asp(Ome)-Fluoromethyl Ketone (Z-VAD-FMK)(Enzyme Systems Products, Livermore, CA). If caspase activation played a major role in syncitia death following FMG mediated fusion it was expected that changes would be detectable in experiments conducted in the presence or absence of Z-VAD-FMK. The read out of cytotoxicity induced by FMG used in these experiments was the LDH release assay (see Chapter 2). An additional read out available for GALV FMG was GM-CSF due to development of a vector co-expressing GALV and GM-CSF (GM-F-GALV, detailed in Chapter 8). If significant changes in biology occurred due to the presence of Z-VAD-FMK it was expected there would be differences in GM-CSF levels detectable in the media.

HT1080 cells were plated in 6 well plates at $2x10^5$ per well. The following day they were transiently transfected with control (pCR3.1 GM-CSF) or FMG (pCG-F1 and pCG-H5, or pCR3.1 GM-F-GALV) plasmids. After overnight incubation the cells were washed and fresh media applied or fresh media containing 50mM/ml Z-VAD-FMK. Every 24 hours media from individual wells was collected, spun down and stored at –70 °C. Similar media to before was then reapplied to the cells. This pattern was repeated over 4 consecutive days. At completion the stored supernatant was subjected to a LDH release assay or GM-CSF ELISA (protocols as described in Chapter 2).

The experiment was conducted on 3 separate occasions and representative results of the LDH release assay can be seen in **Figuire 4.5**. The result indicates that the profile of cytotoxicity for each FMG (GALV or F and H) was the same in the absence or presence of Z-VAD-FMK. The GM-CSF ELISA data also indicated no difference for GALV mediated cytotoxicity with or withour Z-VAD-FMK.

Western analysis for caspase activation and substrate cleavage

A large number of antibodies have been developed to allow the detection of integral components, activation states and effects of molecules within the apoptotic pathway. Procaspase-3 and PARP status were chosen in an attempt to detect whether apoptosis was occuring in FMG mediated syncitia formation and subsequent cell death. Procaspase-3

was chosen due to the role of caspase-3 as a major effector caspase (see Chapter 1.7). If the effector caspase pathway was active then the Western would give a low to unrecordable level of the inactive procaspase form relative to controls. Poly(ADP-ribose) Polymerase (PARP) was chosen as it is a well defined substrate of effector caspases (Soldatenkov and Smulson, 2000). Again if apoptosis was occuring in response to FMG mediated fusion then the inactive cleaved form of PARP would be detected by Western. The primary antibodies used to detect procaspase-3 or PARP (including its inactive cleaved form) in these experiments were kindly provided by Dr Kaufmann, Department of Molecular Pharmacology and Experimental Therapeutics, Mayo Foundation.

The experiments were conducted according to the protocol detailed in Chapter 2. HT1080 or TEL.CeB.6 cells were untransfected, transfected with FMG (F and H plasmids) or control (H alone). Cells were then harvested at 18 and 40 hours post transfection and protein extracted. This was then utilised according to the protocol described. Jurkat cells exposed to etoposide (VP16) or Fas ligand were used as positive controls for the assays, normal HT1080 and TEL.CeB.6 cells as negative controls. The results can be seen in **Figure 4.6**. As can be seen procaspase-3 levels are markedly decreased in Jurkat cells exposed to Fas ligand compared to control Jurkat cells. Between control samples (H plasmid transfection alone) and test samples (F+H plasmid transfections) at specific timepoints and in both cell lines, very little appreciable difference in procaspase-3 level is detected. Similarly exposure of Jurkat cells to etoposide or Fas ligand was associated with significant PARP cleavage as indicated by the detection of both the full size 116 kDa band and the large cleaved fragment at 85 kDa. This effect was absent from cultures of tumour cells transfected with FMG except for a faint band seen in TEL.CeB.6 cells transfected with F+H after 40 hours. This would be in keeping with the morphology and Tunel findings of a low level (1-2% of cells) of apoptosis in TEL.CeB.6 cells at later timepoints following FMG transfection.

The conclusions drawn from Western analysis data of procaspase-3 and PARP were that caspase-3 activation and PARP cleavage play a minimal role in FMG-mediated cytotoxicity.

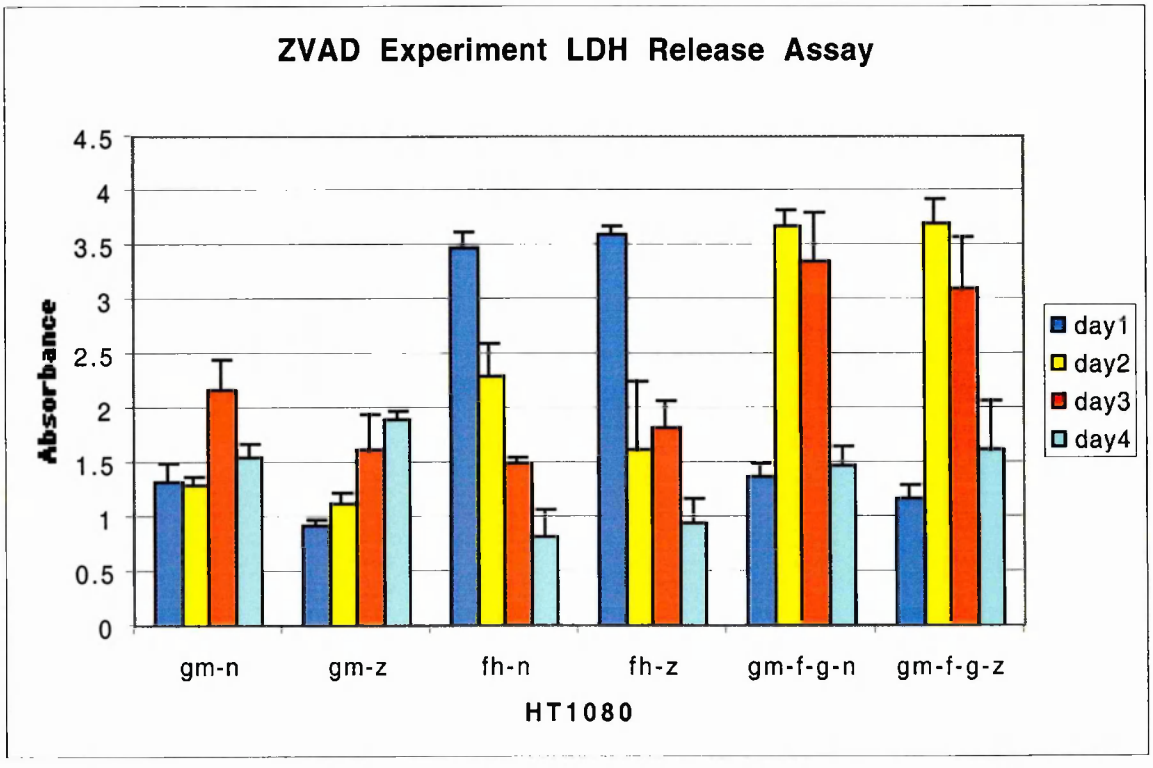

Figure 4.5: Caspase inhibition did not effect FMG mediated cytotoxicity

HT1080 cells were transiently transfected with control plasmid (pCR3.1 GM-CSF) or FMG containing plasmids (pCG-F1 + pCG-H5 or pCR3.1 GM-F-GALV) and incubated in the presence -z, or absence -n of Z-VAD-FMK. Supernatant was collected at 24 hour time points and analysed for lactate dehydrogenase. Caspase inhibition did not alter the cytotoxicity profile obtained.

Figure 4.6: Immunoblots indicating a lack of activation of procaspase-3 or PARP cleavage in cells undergoing FMG mediated syncitia formation. HT1080 or TEL.CeB.6 cells were transiently transfected with no DNA, pCG-H5 or pCG-H5 and pCG-F1. Protein samples were collected at 18 and 40 hours. Jurkat cells were used as positive controls. Procaspase-3 activation produces a decreased signal as seen in Jurkat cells exposed to Fas ligand. PARP cleavage is indicated by positive signal at 116 kDa and 85 kDa: this can be identified in Jurkat cells exposed to VP16, Fas and at a low level in Tel.CeB.6 cells transfected with FH at 40 hours.

Procaspase-3

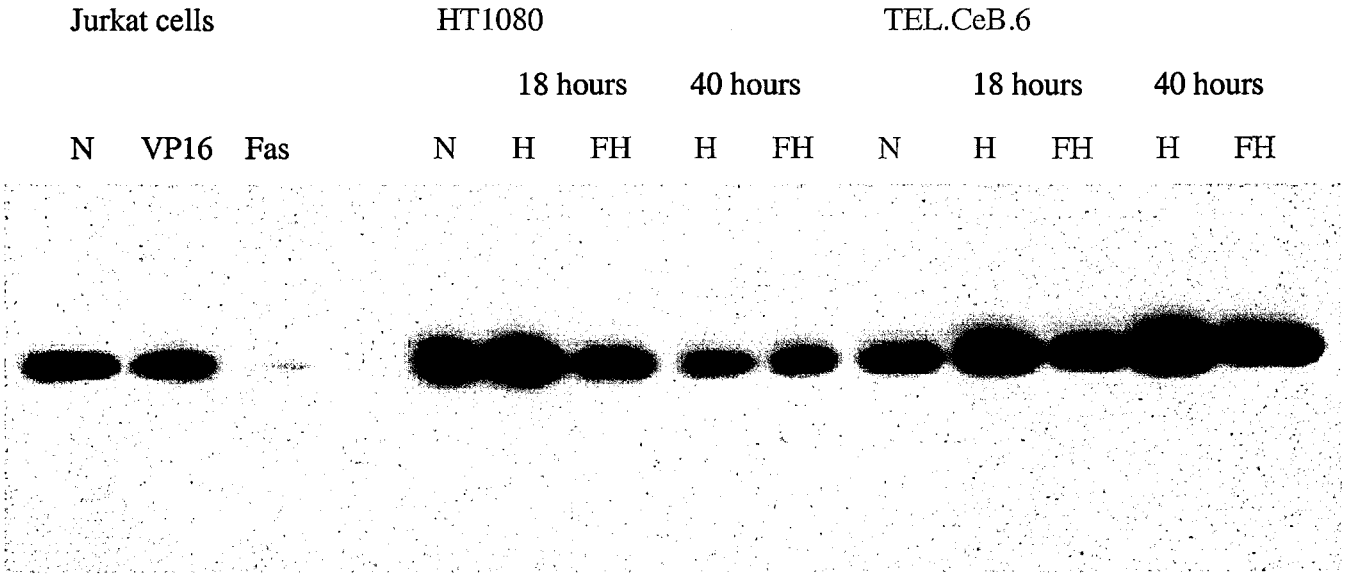

PARP

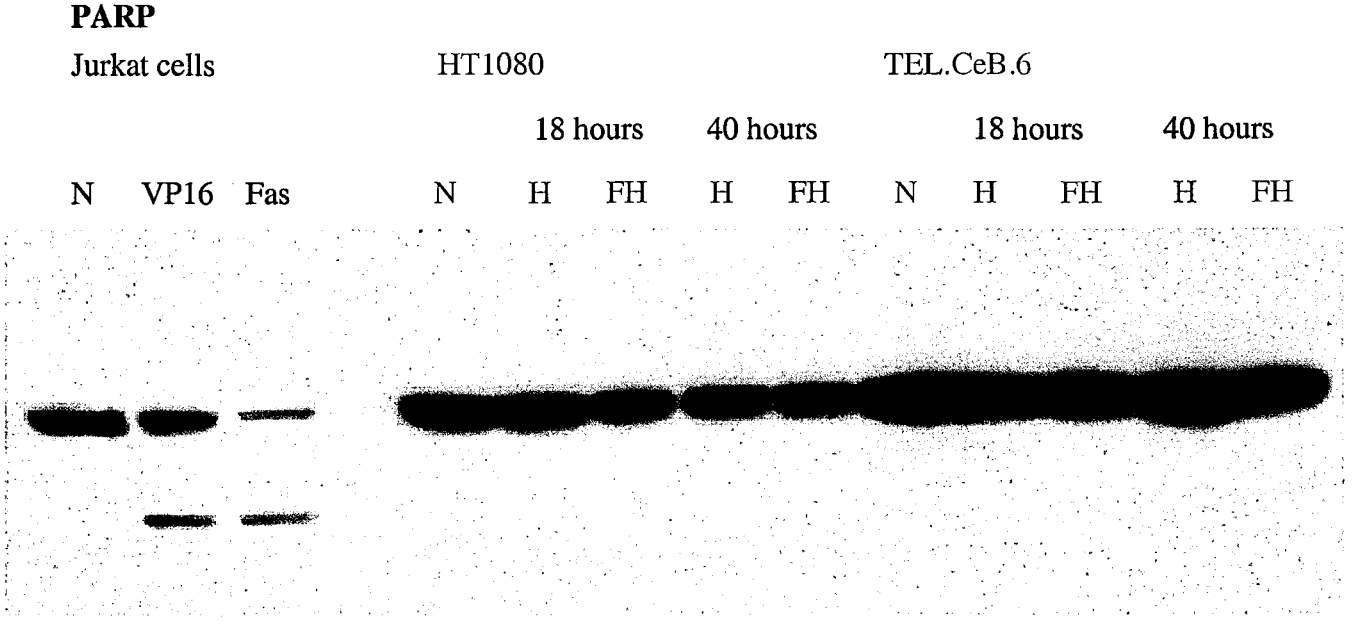

Figure 4.7: Cytochrome *c* remains within mitochondria in FMG mediated syncitia formation. AU565 cells were transfected with control plasmid (I) or pCG-F1 + pCG-H5 (II). Cells were stained at 48 hours for cytochrome *c* (FITC)(b+c), mitochondria (PE)(a+c) and Dapi (Blue)(a-c).

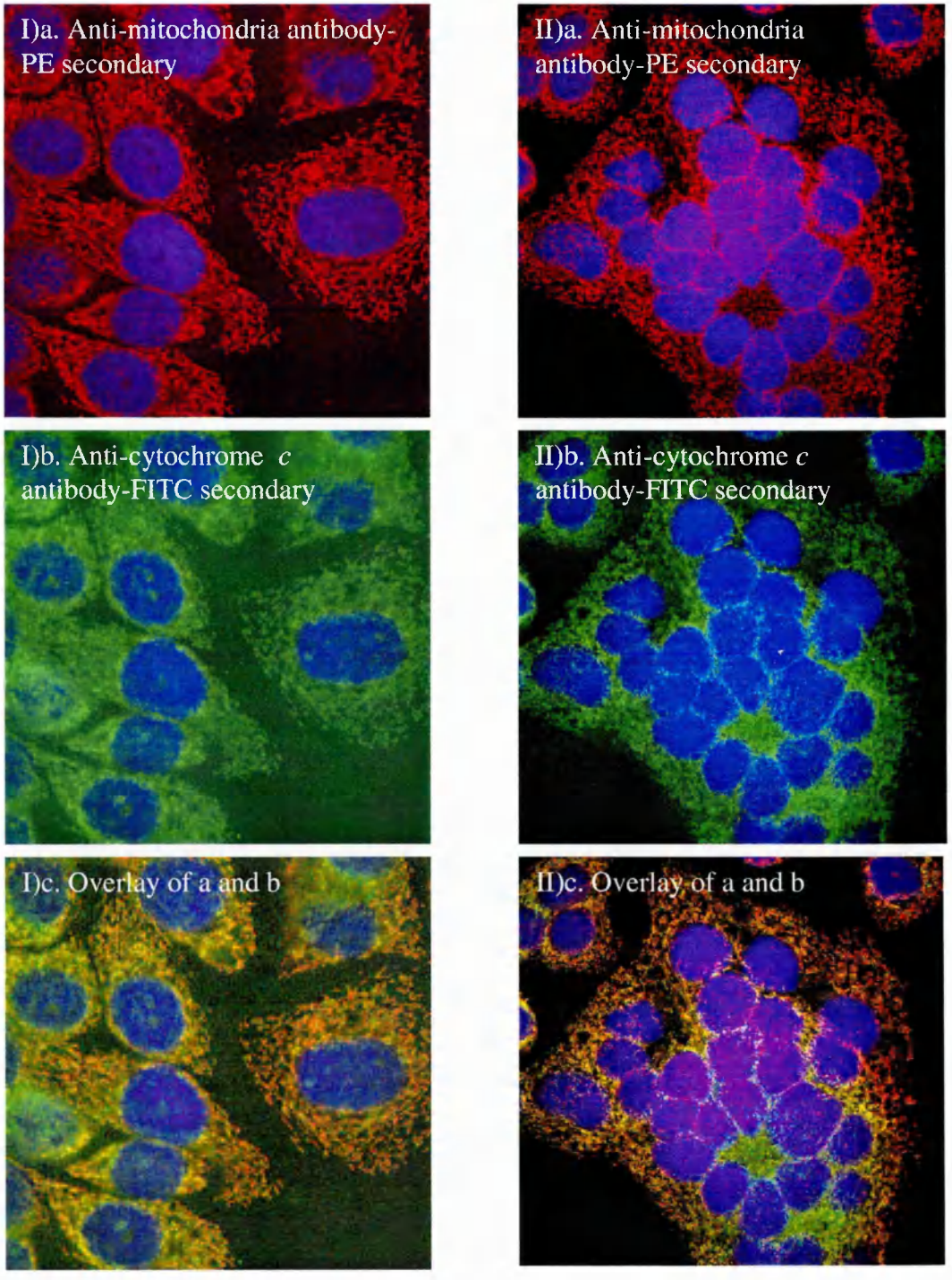

Cytochrome *c* staining

Cytochrome *c* release from mitochondria can serve as an important signal for the initiation of the apoptotic cascade (see Chapter 1.7). Experiments were therefore designed to investigate whether this process occurred in FMG induced syncitia. A number of cell lines were studied including TEL.CeB.6, HT1080 and AU565. Cells were plated in chamber slides, transfected with control or FMG plasmid. 48 hours post transfection cells were fixed and stained with ant-cytochrome *c* antibody, anti-mitochondrial antibody and DAPI as per the immunofluorescence protocol described in Chapter 2. A representative result is seen in **Figure 4.7**. As can be seen cytochrome *c* (green) co-localises with the mitochondrial stain (red) in both control and FMG transfected cells. There was no evidence in the cell lines tested that cytochrome *c* was being released from mitochondria.

Conclusions

The studies detailed above would have been expected to detect apoptosis if it was a significant feature of FMG-mediated cytotoxicity. An additional experiment was conducted to attempt to identify the classical DNA ladder effect seen with apoptosis. No DNA laddering was seen in cells transfected with FMG. The data from all these studies support those of the observational morphology studies. Indicating the major pathway of cell death following FMG expression and syncitia formation is non-apoptotic, and has appearances compatible with necrosis. Occasional cells in some cell lines tested when exposed to FMG can undergo apoptosis but this makes up only a very small component (approximately 1-2%) of the cytotoxicity identified.

4.2.3 Morphology of syncitia seen in SCC 9 cells following FMG expression

Some syncitia forming in some cell lines following FMG expression exhibited remarkable vacuolation and prompted an investigation of this effect. SCC 9 cells demonstrated this effect most readily but it was also observed in a range of other lines including 293 cells, AU565 and HCT116. Equally it was never identified in HT1080 cells following FMG transfection.

Light microscope

Initial interest and study was by light microscope examination. Following transient transfection of SCC 9 cells with FMG after 24 hours syncitia could be identified

containing numerous vacuoles. Aproximately 20-30% of syncitia would demonstrate this phenomenon. Over time the vacuolation would become more marked with fewer but larger vacuoles appearing in these syncitia. Extensive areas of the syncitia would be taken up by the vacuoles and yet the syncitia remained adherent for long periods (>72 hours post transfection) suggesting they were still viable. An example of the light microscope findings can be seen in **Figure 4.8.**

Propidium iodide staining

In order to assess the viability of these vacuolated syncitia trypan blue and propidium iodide staining was used. A representative example of the propidium iodide staining can be seen in **Figure 4.9.I.** The protocol used for this staining is detailed in Chapter 2. Propidium iodide (PI) will stain nuclei and can be visualised as a red stain using the appropriate filter. However PI is unable to cross the cell membrane of viable cells. It requires a loss of cell membrane integrity, associated with cell death, to enter the cell and stain the nucleus. As can be seen in **Figure 4.9.I** the nuclei within the syncitia exhibiting marked vacuolation do not stain with PI. However surrounding syncitia not demonstrating vacuolation can be seen to be necrotic by way of positive PI staining.

Lysotracker red staining

Autophagy is a recognised form of programmed cell death, detailed in Chapter 1.7. Formation of vacuoles and enhanced activity of the lysosome are features of this process. Due to the morphological features it was felt that autophagy may well be the process accounting for the vacuolation seen in these syncitia. Therefore an experiment was conducted to identify whether these vacuoles were lysosomal using Lysotracker red (Molecular Probes) and following the protocol listed in Chapter 2. Lysotracker red is composed of a fluorophore linked to a weakly basic amine. It accumulates in cellular compartments with low internal pH and therefore can be used to investigate lysosome biology (Molecular Probes handbook). A representative result of the lysotracker red staining is seen in **Figure 4.9.II.** From this data it appeared to show that the vacuoles were indeed staining positively: suggesting they were lysosomal in origin and in keeping with the process of autophagy. It therefore did appear that a programmed cell death pathway could be activated in some syncitia. The promotion of the autophagacytic pathway in these syncitia also fitted with data outlining a process of metabolic exhaustion leading to

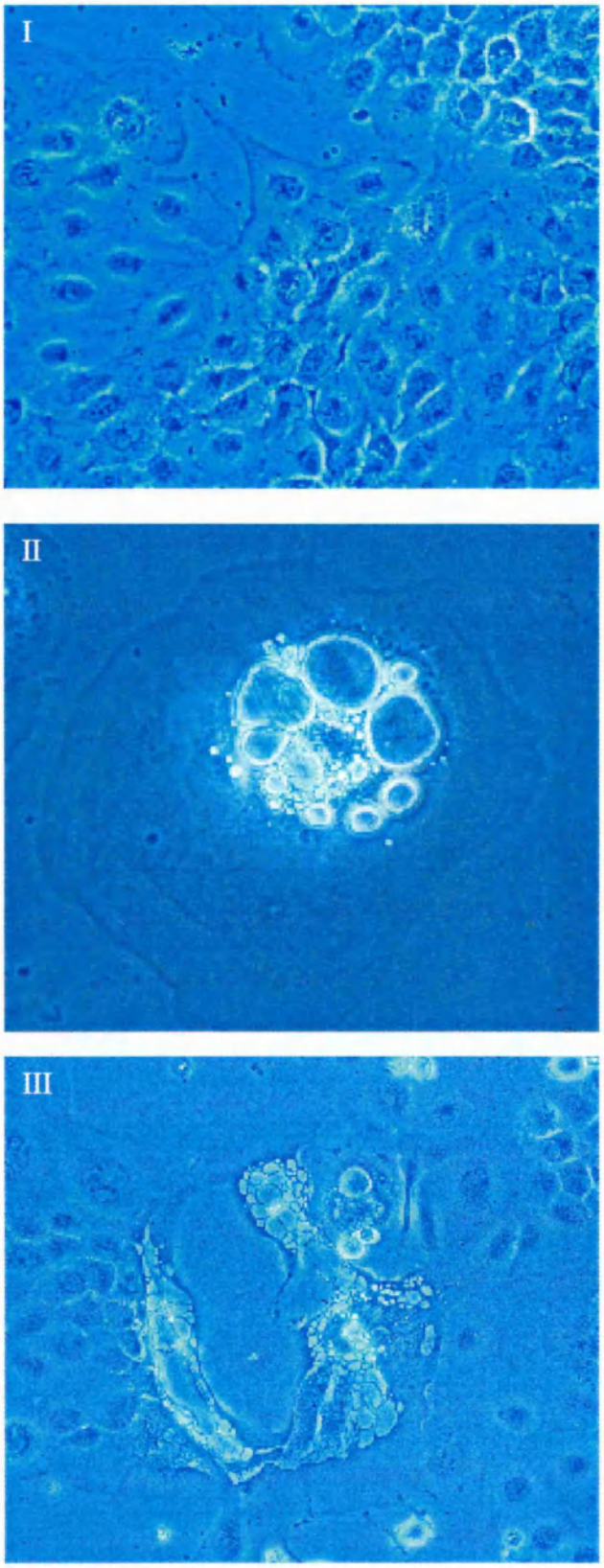

Figure 4.8: Syncitia forming in SCC9 cells can exhibit marked vacuolation. SCC9 cells were transfected with control plasmid (I) or pCG-F1 and pCG-H5 (II-III). Light microscope assessment identified marked vacuolation occurring in a proportion of FMG induced syncitia.

Figure 4.9: SCC9 cells demonstrate marked vacuolation on FMG mediated syncitia formation: nuclei within these syncitia are negative for propidium iodide staining and the syncitia show enhanced staining for lysosomes. SCC9 cells were transfected with pCG-F1 and pCG-H5. 48 hours later they were incubated with propidium iodide (I) or lysoTracker red (II). Propidium iodide can be seen to stain non viable syncitia surrounding a viable syncitium with extensive vacuoles (I). LysoTracker red concentrates in acidic organelles of viable cells and shows enhanced staining in syncitia with vacuolation (II). These features are in keeping with autophagy occurring in these syncitia.

I. Propidium Iodide staining

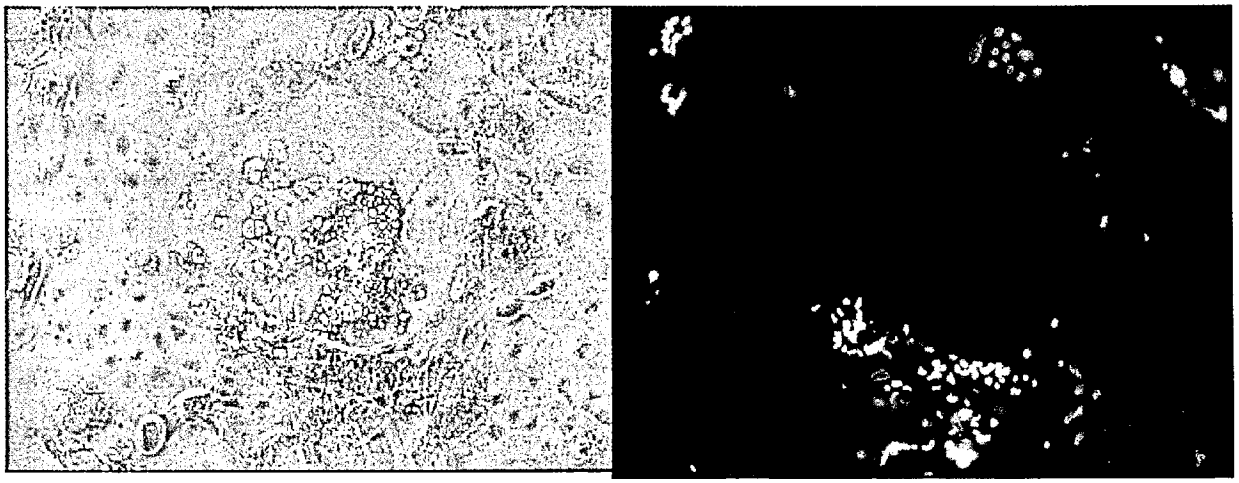

II. LysoTracker red staining

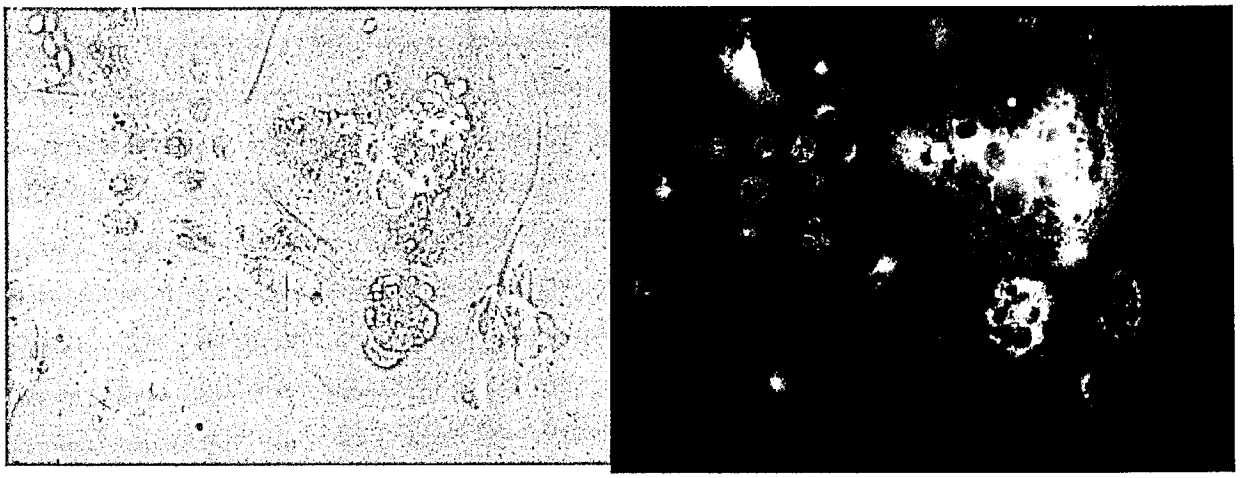

necrotic death following FMG expression in Hep3 cells produced by a collaborating laboratory (Higuchi et al., 2000), and will be detailed below in the discussion.

4.2.4 Assessment of cell cycle status of nuclei within syncitia

From the morphology studies the majority of nuclei within syncitia did not appear to be progressing through the cell cycle as the control population of cells were. The cell lines used in these studies had doubling times of approimately 24-48 hours and mitotic figures were commonly identified with DAPI staining. No mitotic figures were seen within syncitia but as indicated there were some syncitia where chromosome condensation could be seen. Chromosome condensation was then thought to be a terminal event as it appeared the chromosomes were not ordered along a mitotic spindle and it was difficult to see how further progression through mitosis was going to occur. The hypothesis proposed was that nuclei within syncitia would be blocked at some point within the cell cycle. In occasional syncitia this block could be overcome and nuclei progress to prometaphase but this was a relatively rare event. To address this hypothesis appropriate assays were sought. Due to the nature of the syncitia (e.g. too large to conduct FACS studies) digital imaging analysis was chosen as the favoured investigation of choice. This assay is based on the Feulgen stain. This stain developed in the 1920s will stain DNA (Feulgen R, 1924). The optical density of the stain directly correlates with the amount of DNA in the nucleus (Gurley et al., 1990) thereby giving the cell cycle status.

The protocol used is as described in Chapter 2. HT1080 and HCT-116 cell lines were plated on chamber slides. After overnight incubation they were transiently transfected with control plasmid (CMV β-Gal), pCR3.1 GALV or pCG-F1 and pCG-H5 (F and H). Slides were fixed and stained at 24, 48 and 72 hours post transfection for HT1080 cells, with the same timepoints for HCT-116 but with an additional collection at 96 hours. An example of Feulgen stained slides can be seen in **Figure 4.10**. Digital images were obtained of approximately 200 hundred representative nuclei per slide i.e. from FMG slides only nuclei from within syncitia were captured. DNA mass and nuclear morphometry features of area, DNA index and average optical density were obtained for each nucleus. The DNA mass data will be presented.

Figure 4.11 illustrates the DNA mass data for HCT-116 cells transfected with control plasmid overtime (IA-IC) and the same cells transfected with FMG (F and H) overtime (IIA-IIC). The result showed this cell line to be tetraploid (mean DNA mass 8pg). At 24 hours control transfected cells can be seen to have been arranged through the cell cycle with cells in G1, S and G2/M (**Figure 4.11.1A**). At 72 and 96 hours most of the cells were in G1 with evidence of a progressive reduction in the proportion of cells in S and G2/M (**Figure 4.11.1B-C**). The assumption was made that this result was due to less favourable growth conditions arising in vitro over time due to cell crowding and a decrease availability of nutrients. In contrast cells transfected with an FMG showed a significant and progressive right shift in their distribution within the cell cycle (**Figures 4.11.IIA-C**). As a consequence, by 96 hours after transfection, the majority of the cells were in the G2/M phase of the cell cycle. Very few cells were seen in G1 or S suggesting the transfected cells were accumulating or blocking in G2/M. An identical pattern of changes was seen with the GALV transfected HCT-116 cells. The same pattern was also seen for the HT1080 cells.

Conclusions

This data confirmed the hypothesis that nuclei were blocked in the cell cycle.It confirmed that the block occurred at the G2/M boundary. The shift through S phase of the cell cycle also indicated that following syncitia formation these multinucleate structures were still capable of synthesising DNA. This finding is in keeping with a previous report which studied the effects of fusing murine and human cells using a para-influenza 1 virus (Harris and Watkins, 1965). This study indicated that syncitia were capable of not only synthesising DNA but also RNA and protein. An additional feature of the DNA mass data collected was that there was no evidence of accumulation of nuclei within syncitia at a sub-G1 peak: further evidence that apoptosis was not occuring in these cells.

Figure 4.10: Feulgen staining of HT1080 cells transfected 48 hours previously with control plasmid (I) or pCG-F1 and pCG-H5 (II).

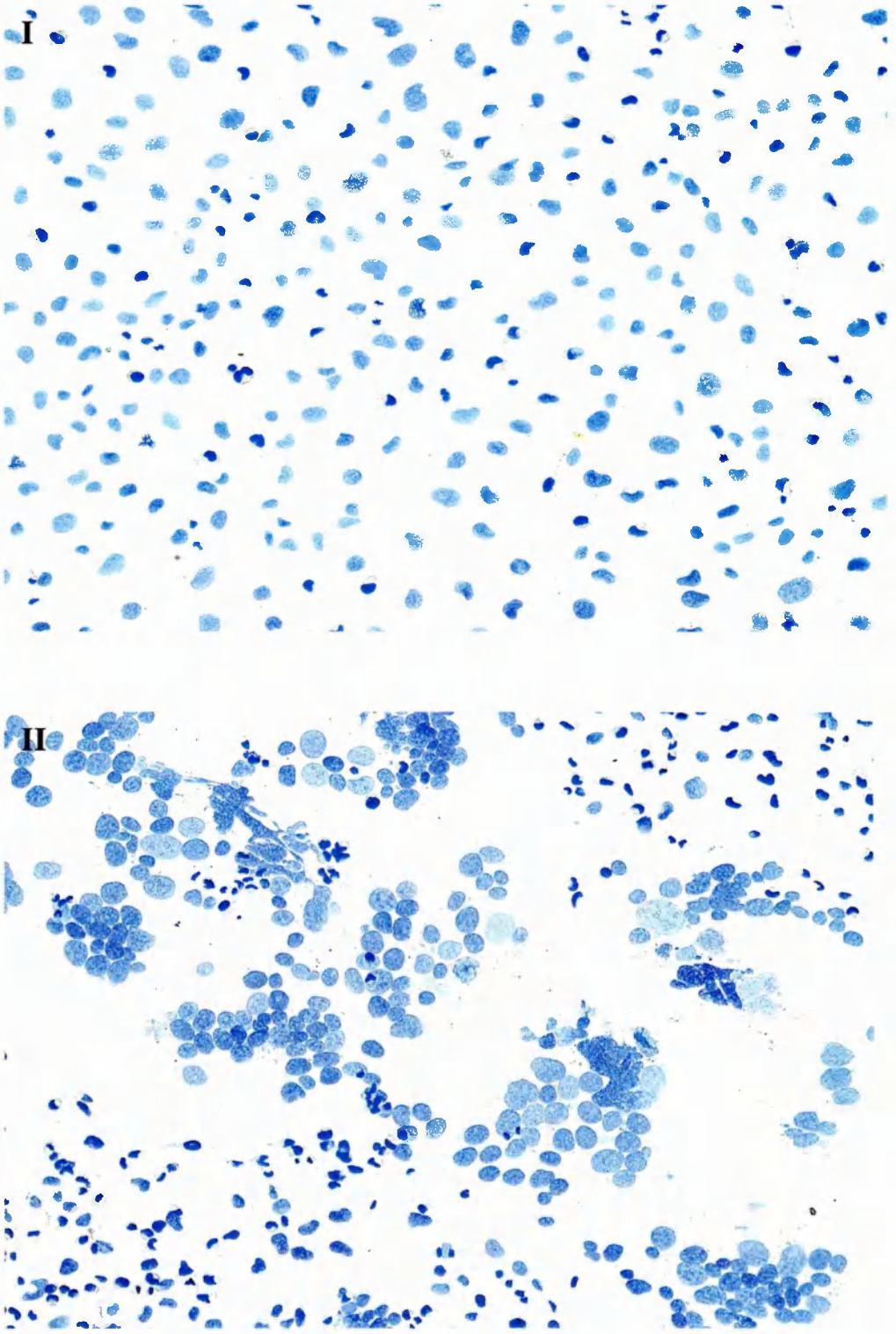

Figure 4.11: Feulgen staining data indicates nuclei within syncitia accumulate at the G2/M boundary of the cell cycle. HCT-116 cells were transfected with control plasmid (I) or pCG-F1 and pCG-H5 (II). Samples were collected at 24 (A), 72 (B) and 96 hours (C).

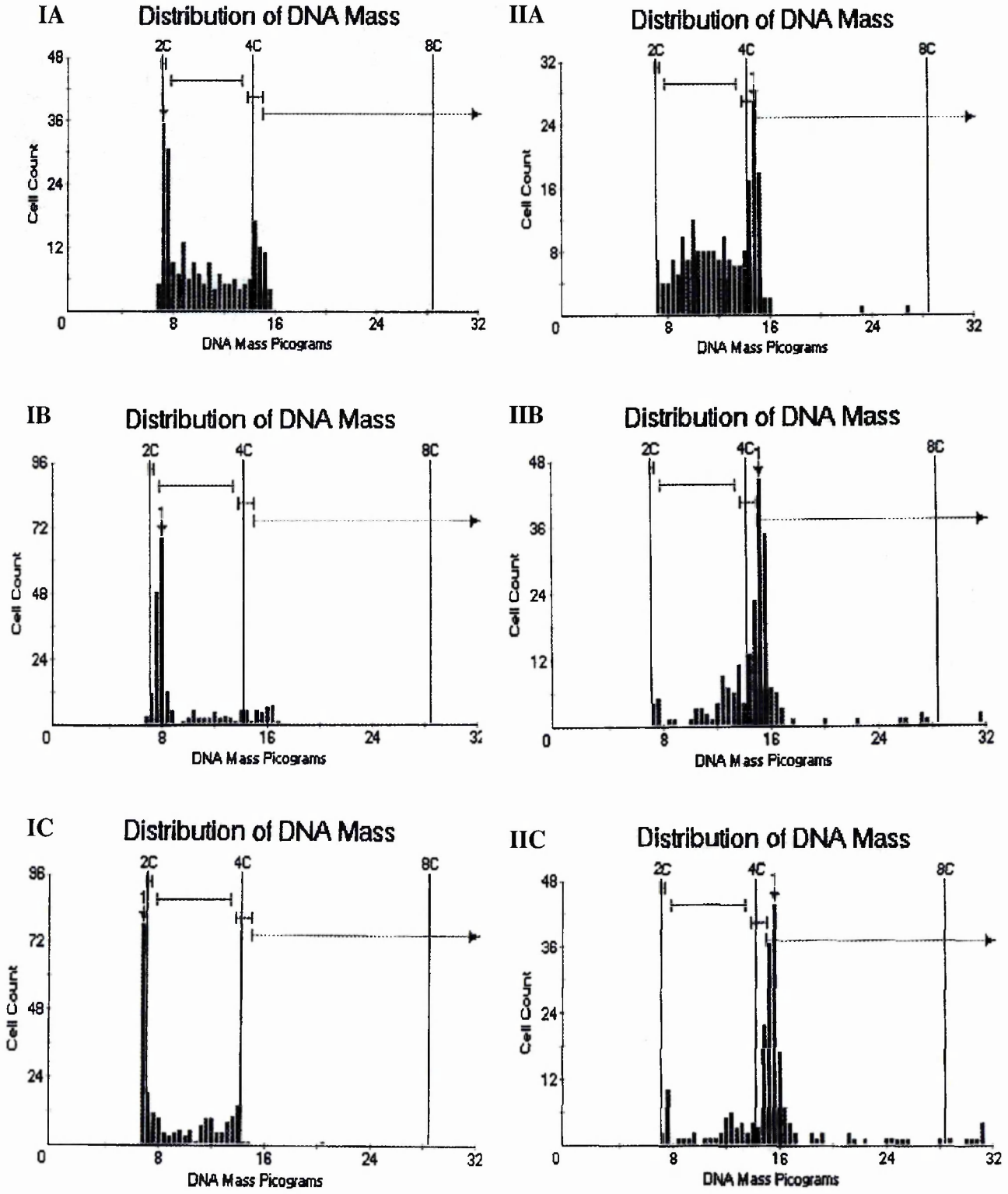

4.2.5 Cytoskeleton and organelle arrangement within syncitia

Although FMG mediated syncitia formation did ultimately lead to cell death it was clear that syncitia could remain viable for prolonged periods of time. This, combined with the evidence that syncitia remain metabolically active and the particular feature that nuclei within syncitia were clustered together, suggested a specific organisation in the formation and organisation of these structures. A critical component of that organisation would be the arrangement of the cytoskeleton. Experiments were performed to identify the tubulin and actin filament arrangement within syncitia. HT1080 cells were plated in chamber slides. The following day they were transiently transfected with control plasmid (CMV β-Gal) or pCG-F1 and pCG-H5 (F and H). 48 hours post transfection the slides were stained according to the immunofluorescence protocol detailed in Chapter 2. Following fixation and permeabilisation slides were probed with mouse monoclonal anti-α-Tubulin antibody. In one series donkey anti-mouse IgG TRITC labelled secondary antibody was used. A representative result is seen in **Figure 4.12.IA** and **IIA**. In a second series donkey anti-mouse IgG FITC labelled secondary antibody was used in combination with Phalloidin-TRITC labelled (a fluorescently labelled actin binding protein). A representative result can be seen in **Figure 4.12.1B** and **IIB**.

These images indicated that the tubulin and actin networks were highly ordered within syncitia. They identified large tubulin bundles had formed within syncitia, seen especially in **Figure 4.12.IIA**. It appeared these bundles facilitated the movement of incoming nuclei from the site of fusion to the site of nuclear aggregation. This correlated with a previous report of microtubules and 10-nm filaments being responsible for positioning nuclei in syncitia of baby hamster kidney cells, syncitia forming following simian virus 5 infection (Wang et al., 1979). Positioning of other organelles within the cell is also dependent on the cytoskeleton. Immunofluorescent staining was performed to see the effect on mitochondria positioning. HSP-60 localises to the mitochondria and therefore can serve as a surrogate marker of mitochondria location. HT1080 cells were prepared in exactly the same manner as indicated for the studies of the cytoskeleton. 48 hours post transient transfection slides were fixed, permeabilised and probed with mouse monoclonal anti-human HSP-60 antibody followed by donkey anti-mouse IgG TRITC labelled secondary antibody. Representative results can be seen in **Figure 4.13.I-IV**.

Figure 4.12: Cytoskeleton staining identifies structural organisation of syncitia. HT1080 cells were transiently transfected with control plasmid (IA+IB) or pCG-F1 and pCG-H5 (IIA+IIB). Cells were stained in one series with anti-tubulin antibody and TRITC secondary (red) (IA+IIA); or cells were stained with anti-tubulin antibody and FITC secondary (green) with rhodamine phalloidin (red)(IB+IIB). In all samples nuclei were stained with Dapi (blue). Images were obtained using different magnification.

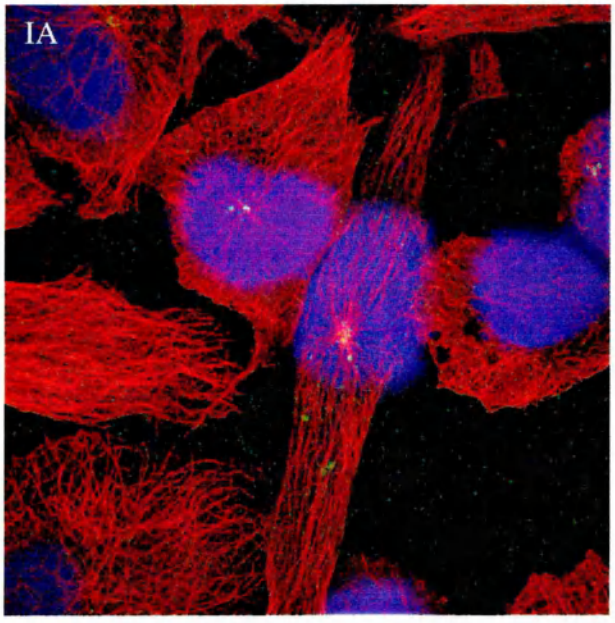

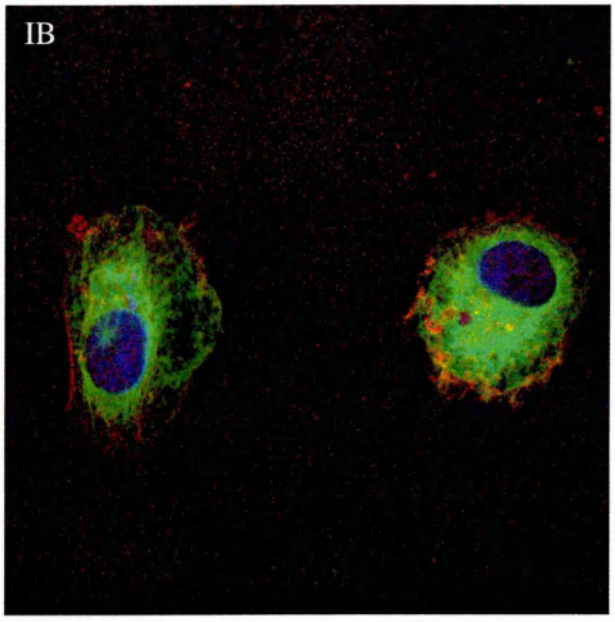

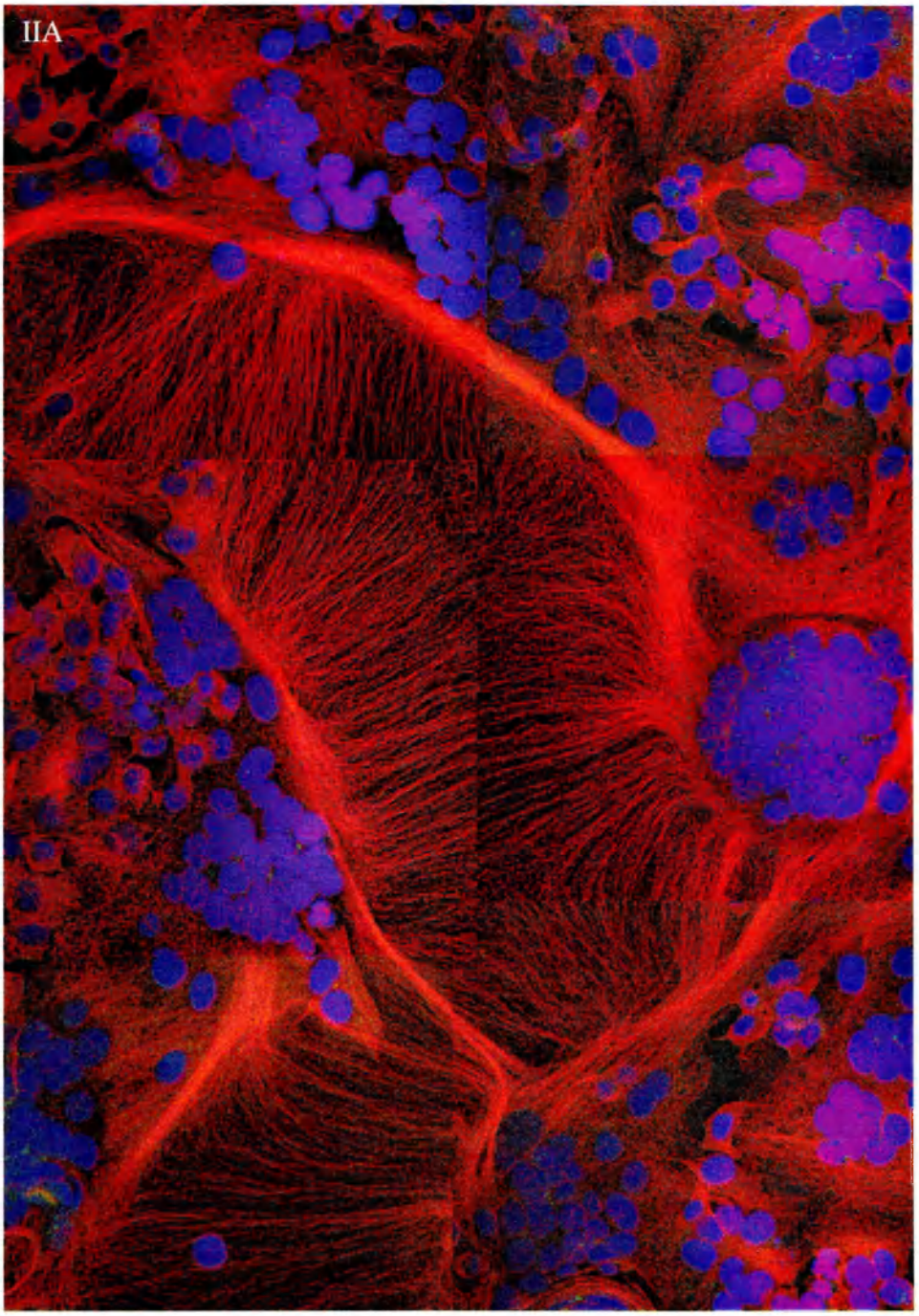
IIA

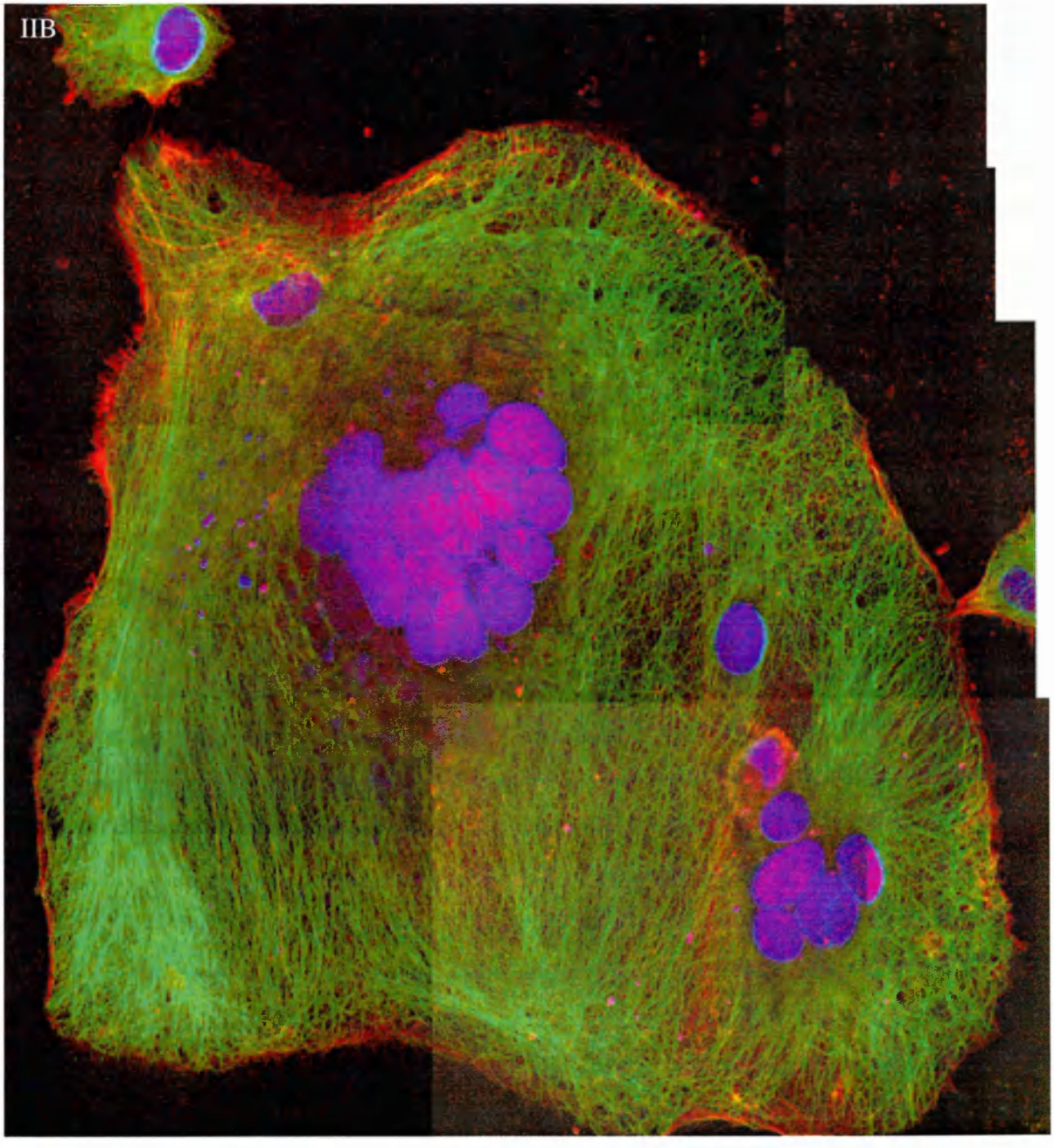
IIB

Figure 4.13: HSP 60 staining identifies mitochondria within syncitia situated away from the perinuclear location. HT1080 cells were transiently transfected with pCG-F1 and pCG-H5 (II-IV) or control plasmid (I). After 48 hours samples were stained with anti-HSP 60 antibody (I, II + IV) and TRITC secondary (red) or TRITC secondary alone (III). Nuclei were stained with Dapi (blue).

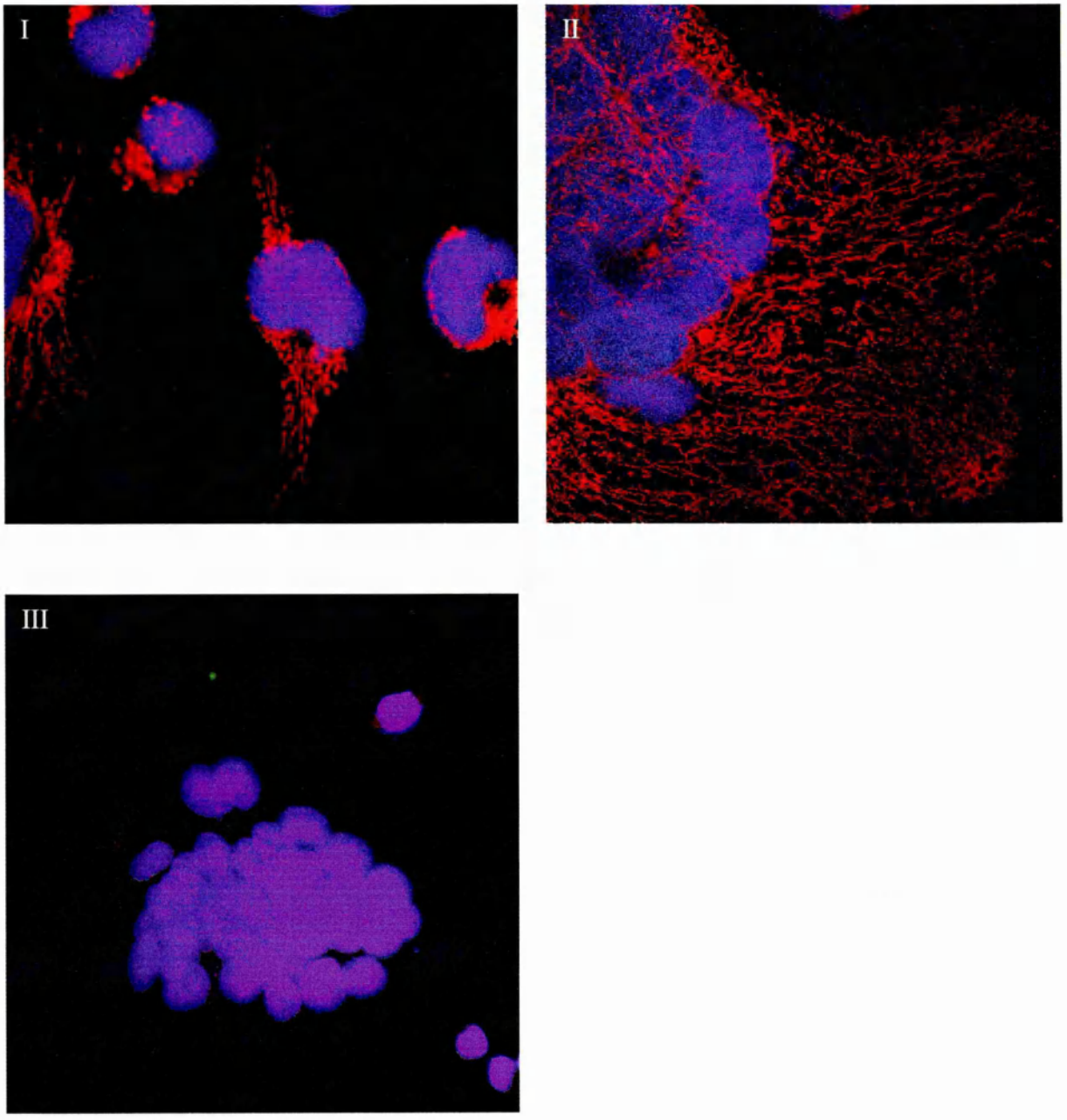

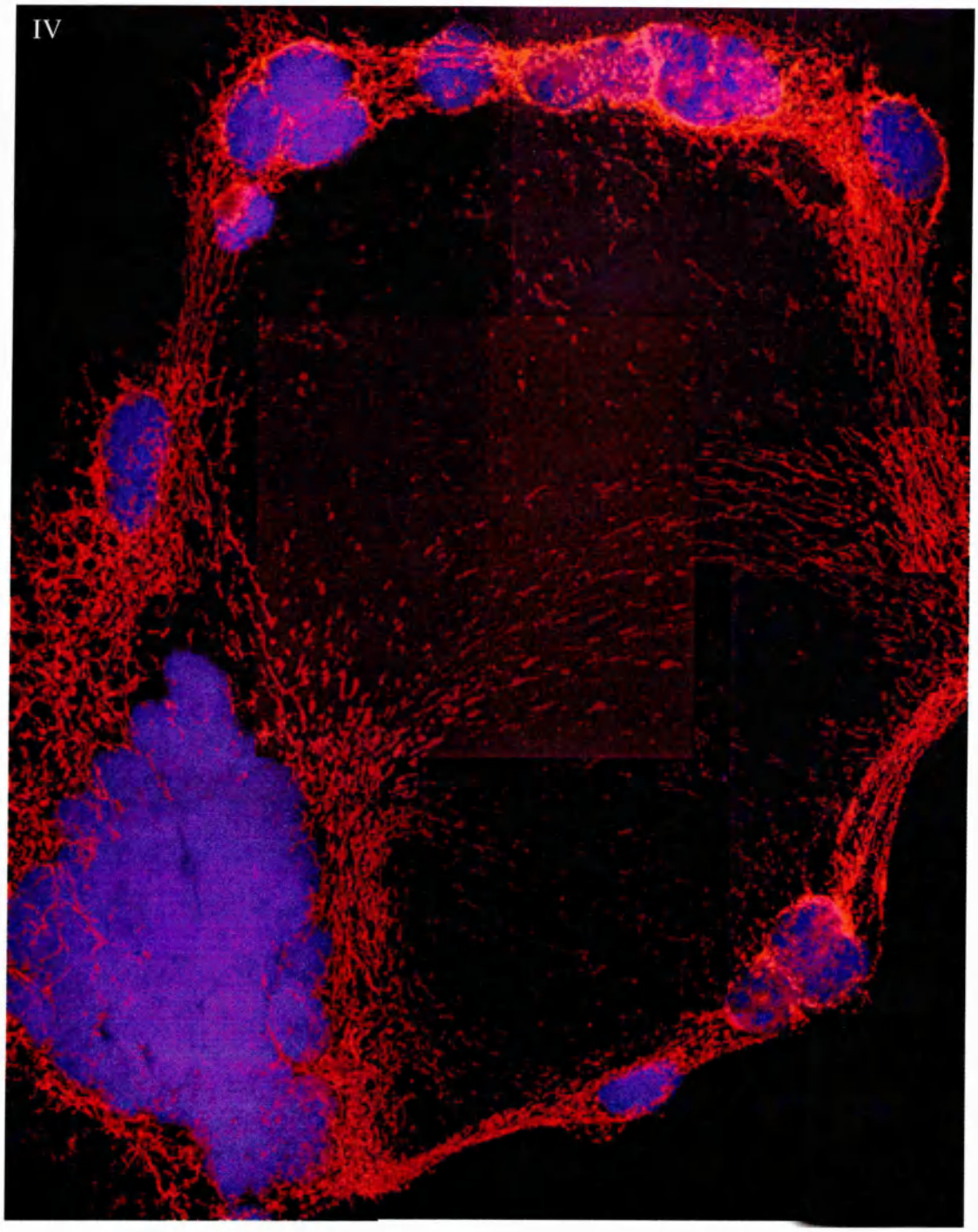
IV

These images indicated that mitochondria were distributed widely through the syncitium. Specifically mitochondria in control cells had a perinuclear orientation, **Figure 4.13.I**. Within syncitia, mitochondria appeared to be spread widely, which largely correlated with the cytoskeleton organisation **Figure 4.13.II** and **IV**. Whether this altered location had an effect on mitochondrial function was unclear and may have relevance to syncitia death, this will be discussed below.

4.3 Discussion

The data presented in this Chapter aimed to indicate some of the biology and particularly the mechanism of death seen in cells compelled to form syncitia following FMG expression. From simple observation it was clear that large mulinucleate syncitia could form within approximately 18 hours of FMG transfection. These syncitia would become non-viable at varying time over the following 6 to 96 hours or even longer. The rapidity of onset of cytotoxicity appeared in part due to the cell line transfected but also the FMG involved (for example see the different LDH release profiles for F and H compared to GALV in the Z-VAD-FMK assay, **Figure 4.5**). The viability of syncitia was not unexpected as multinucleate cells exist in nature e.g.syncitiotrophoblast of the placenta. Examination of cytoskeletal elements indicated the ordered process involved in maintaining the integrity of the structure. Digital imaging analysis confirmed that DNA synthesis was maintained and nuclei accumulated at the G2/M boundary. The occasional syncitium exhibiting chromosome condensation indicated that given sufficient pro-mitotic stimuli this boundary could be crossed. This state however would then be predicted to be a terminal event due to failure of all the nuclei to proceed further through mitosis.

The actual manner in which the majority of syncitia died appeared to be necrotic. This conclusion can be reached due to the morphology of death and the exclusion of apoptosis. Extensive investigation was conducted to detect apoptosis by the studies detailed. No assay identified apoptosis as a major component of FMG induced syncitia formation and death. Collaborators conducted additional assays including RNA protection assays designed to examine RNA levels of important members of the apoptotic pathway (Dr K.J.Harrington in (Bateman A, 2002)) or similar assays in hepatoma cells (Higuchi et al., 2000) and again did not identify apoptosis in this setting. Autophagy was identified in

some FMG induced syncitia in some cell lines. This fits with the conclusions we (Bateman A, 2002) and our collaborators (Higuchi et al., 2000) reached as to the likely mechanism of death. Higuchi et al. were able to show that following FMG expression in Hep3B cells and syncitia formation mitochondrial dysfunction and ATP depletion occurred. This led to a bioenergetic form of cell death with necrosis.

To summarise, FMG induced syncitia formation is not sustainable. The exact reason for this is unknown but mitochondrial dysfunction is a significant feature. Maintaining such a huge cellular structure as these syncitia may itself be bioenergetically too demanding. Whether the positional changes noted with regard to mitochondria plays any role is unknown. The end result is ATP depletion and as described in Chapter 1.7, in energy depleted states cells are unable to activate apoptosis and necrosis is the resultant death process. In some syncitia the bioenergetic stress described appears to be sensed and an autophagic response initiated. However this again is not sufficient to overcome the imbalances and death results.

Data from Chapter 3 indicated that FMG were potent cytotoxic genes (Bateman, A. et al., 2000). The identification that the cytotoxicity occurred through necrosis enhanced their potential application for therapy. As discussed in Chapter 1 an integral part of any successful cytotoxic gene therapy strategy will involve the promotion of an anti-tumour immune response. This is most likely to occur if tumour cells are killed in a pro-inflammatory manner. FMG induced cell death appeared to fulfill this criteria. The further development of FMG gene therapy was therefore warranted. To that end the priority was to develop vectors capable of delivering FMG genes in vivo and this will be the focus of the following three chapters.

The data presented in this chapter formed part of the following paper:

Viral Fusogenic Membrane Glycoproteins kill solid tumour cells by non-apoptotic mechanisms which promote cross presentation of tumour antigens by Dendritic cells.

A. Bateman, K. J. Harrington, A. Ahmed, A. Melcher, M. Gough, D. Riddle, A. Dietz, M. Crittenden and R. Vile

Submitted to Cancer Research, July 2002.

CHAPTER 5: FMG RETROVIRAL VECTOR DEVELOPMENT

Chapter 5: FMG retroviral vector development

5.1 Introduction

As described in the previous chapters FMG expression in tumour cells in vitro results in extensive cell death via non-apoptotic mechanisms and has a bystander effect significantly greater than that seen with suicide genes. In order to assess the utility of FMG as a potential gene therapy further it was necessary to develop suitable vectors for in vivo delivery. Due to the detailed knowledge and experience with retroviral vectors we chose to explore the value of delivering GALV FMG by these vectors; while at the same time developing FMG adenoviral vectors.

A description of retroviral vectors has been given in Chapter 1. C-type based retroviral vectors are the most widely used vector system in gene therapy clinical trials (Rosenberg et al., 2000). This is due in part to their ease of manipulation and production, lack of immunogenicity, ability to integrate and potential to influence infectivity by choice of envelope and/or envelope modification (Cosset and Russell, 1996). C-type retroviruses expressing GALV were constructed and will be detailed below. Lentiviral vectors can infect both dividing and nondividing cells and therefore may be more advantageous than C-type retroviruses in some gene therapy settings. Lentiviral GALV vectors were also constructed.

5.2 Results

5.2.1 Retroviral vectors expressing GALV

The C-type retroviruses expressing GALV were derived using a third generation Mo MuLV based vector system: the pBabe vector (Morgenstern and Land, 1990). PCR3.1 GALV was digested with *EcoR1* and the 2.2 kb fragment purified according to the QIAquick gel extraction kit protocol described in Chapter 2. pBabe puromycin was digested with *EcoR1* and the linearised plasmid incubated with CIAP to remove the 5' phosphate groups, then purified. Ligation of GALV into the pBabe puromycin plasmid was then performed using standard methods. Confirmation of ligation was performed by restriction enzyme digest: *EcoR1* confirmed the presence of the insert, digestion with

Kpn1 confirmed the correct orientation with fragments of 1, 2.5 and 3.7 kb. One correctly orientated clone was selected and formed pBabe GALV.

A lentiviral vector expressing GALV was constructed based on a self-inactivating HIV-1 vector (Zufferey et al., 1998). PCR3.1 GALV was digested with *BamH1* and *Xho1*, and the 2.2 kb fragment purified. pHR'CMV-LacZ SIN was digested with *BamH1* and *Xho1*, removing the β-Gal gene. The plasmid backbone was purified and ligated with GALV using the standard protocol. Positive clones were selected by restriction enzyme digest and one was selected forming pHR'CMV-GALV SIN (Lenti-GALV). This construct was made by RM Diaz.

5.2.2 Comparison of pBabe GALV to Lenti-GALV in vitro

In these two retroviral vectors GALV is expressed from different promoters: in the pBabe vectors the transgene is expressed from the MoMLV LTR, in the lentiviral construct GALV is expressed from the CMV promoter. To ensure that the strengths of the different promoters would not affect subsequent evaluation of the two vectors an experiment was conducted in vitro to assess their relative activities. $1x10^6$ HT1080 cells were plated in 25 cm^2 flasks. The next day they were transfected with 1μg of pBabe GALV, Lenti-GALV or CMV β-Gal using the Effectene transfection protocol. After overnight incubation the cells were washed and incubated for a further four days. At completion of this time the number of surviving cells was recorded; the result is illustrated in **Figure 5.1**. As can be seen there are two logs less surviving cells following pBabe GALV and Lenti-GALV transfection relative to control (CMV β-Gal), and their relative values are equivalent. Observation of the cell cultures during the experiment indicated extensive syncitia formation following pBabe GALV and Lenti-GALV transfection but not CMV β-Gal. The conclusion from this experiment was that the two GALV expressing vectors could be compared on a similar level in subsequent infection assays.

Figure 5.1: Comparison of retroviral vectors.
HT1080 cells were transfected with pBabe GALV, Lenti-GALV or control (CMV-ß-Gal) and incubated for 5 days. Surviving cell numbers were counted.

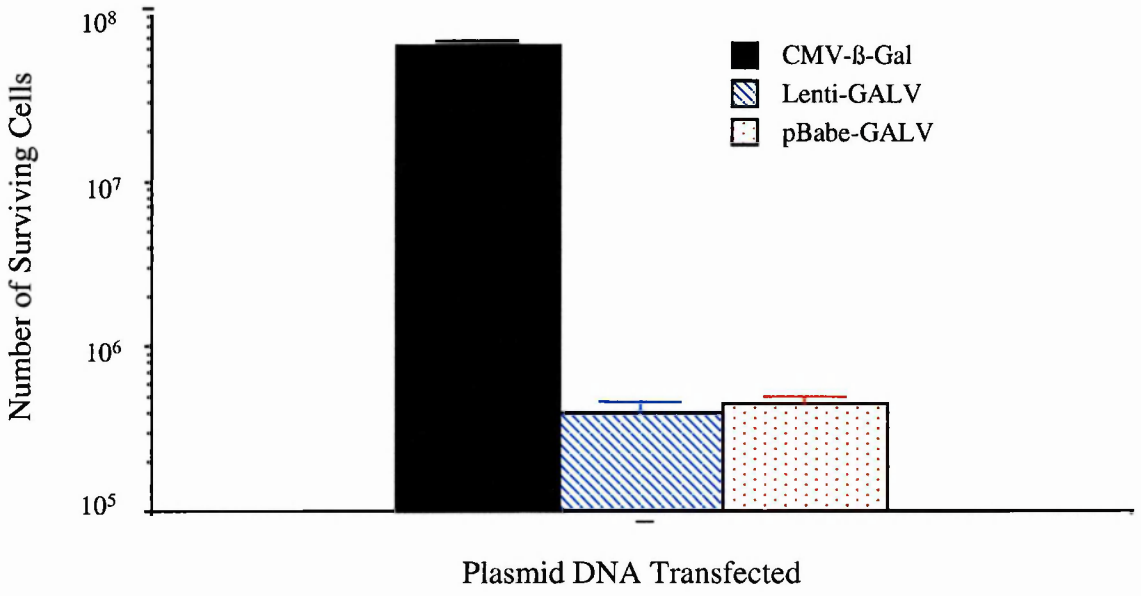

Figure 5.2: Lenti-GALV infected both dividing and quiescent tumour cells.
HT1080 cells were incubated in the presence (+ A) or absence (-A) of Aphidicolin. They were then infected with retrovirus. After 48 hours a relative titre was determined by counting the number of syncitia.

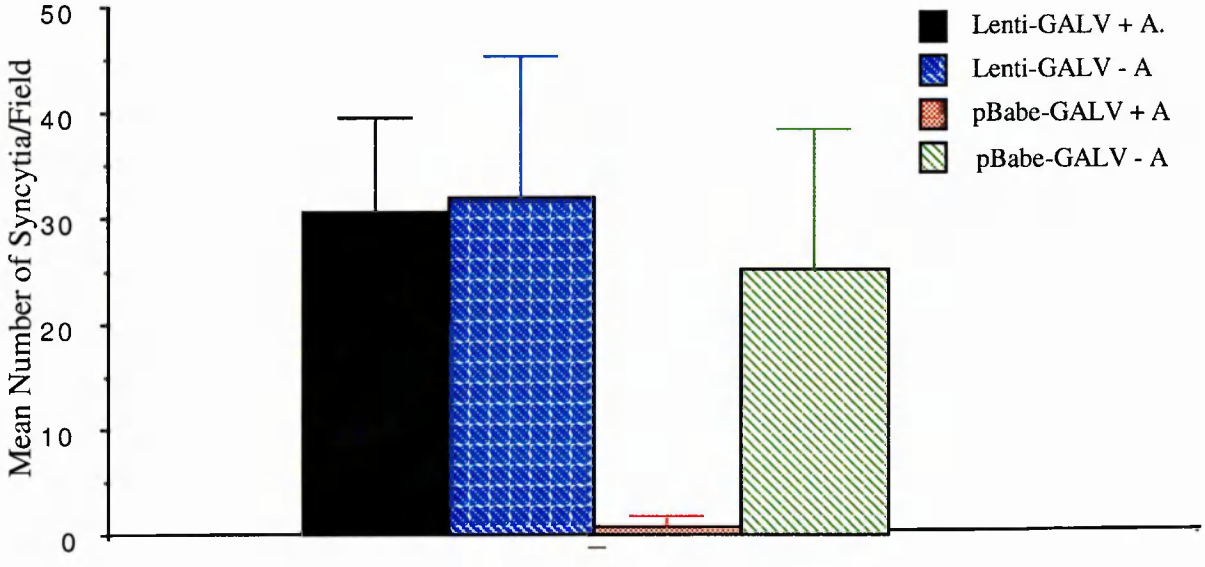

5.2.3 Packaging of C-type and lentiviral vectors expressing GALV

To generate infectious viral stocks of retroviruses expressing GALV a variety of different packaging cell lines and protocols were used. A summary can be seen in **Table 5.1**. Initially the murine packaging cell line AM12 was transfected with pBabe GALV. AM12 is a clone of NIH 3T3 cells stably transfected with the Mo MLV *gag* and *pol* genes on one construct and the 4070A amphotropic *env* gene on another construct (Markowitz et al., 1988). 5 μg pBabe GALV was transfected, using the Profection method, into 1 x 10^6 AM12 cells cultured in a 25cm^2 flask. After overnight incubation cells were washed and media replaced. After a further 48 hours the media was removed and the cells serially diluted, incubated in 96 well plates with media containing 1.25μg/ml puromycin. After 10-14 days 35 resistant colonies were transferred to 24 well plates, then 25cm^2 flasks. The clones were then incubated in 1ml of medium for a further 48 hours before supernatant was removed from the cells and filtered through a 0.45 μm filter. The titre of retrovirus recovered was estimated by exposing HT1080 cells in the absence of polybrene to different dilutions of viral supernatant in serum-free media for 4 hours in 24 well plates. 48 hours later the number of syncitia per well were used as a read out and recorded as syncitia forming units (s.f.u.) per ml. The titres were consistently < 10^2 from all clones. Transient transfection of pBabe GALV into AM12 using the same protocol as described above but without selection was then performed. After overnight incubation cells were washed and 1ml media replaced. 48 hours later supernatant was removed from the cells, filtered through a 0.45 μm filter and the titre estimated. Again the titre was low at < 10^3 s.f.u./ml. The reason for the low titre was assumed to be due to the formation of mixed heterotrimeric envelope complexes between GALV and 4070A which were not competent for infection of target cells.

Production of a GALV expressing C-type retrovirus which would not be sensitive to inactivation to human complement inactivation was attempted. The human FLY-13 packaging cell line was transiently transfected with pBabe GALV and the protocol described above was followed to recover viral particles. Due to the human origin of the FLY cell line (Cosset et al., 1995) extensive syncitia formation was seen following transfection. This cytotoxicity and the probable heterotrimeric envelope complexes again

formed between GALV and the 4070A expressed by FLY-13, resulted in a low titre of < 10^3 s.f.u./ml.

To avoid envelope mixing a packaging cell line was chosen that did not express an envelope: 293Int. This strategy relied upon the GALV protein expressed acting as an envelope to pseudotype the pBabe GALV core particles. Transfection of pBabe GALV was performed and viral particles harvested according to the protocol previously described. As this cell line was derived from human 293 cells extensive syncitia formation was seen following transfection. The titres were consistently < 10^2 s.f.u./ml indicating hyperfusogenic GALV was not a satisfactory envelope; a result consistent with the evidence that modifications to the R peptide region of the TM can significantly reduce the ability of the envelope to be incorporated into infectious viral particles (Januszeski et al., 1997). In an attempt to overcome this limitation and bypass the heterotrimer formation VSV-G was introduced as a suitable envelope: VSV-G has previously be shown to pseudotype C-type core particles to high titre (Burns et al., 1993). Transfection and recovery of virus was performed as described with the modification of co-transfecting 5 μg pCMV VSV-G in addition to 5 μg pBabe GALV into 293Int cells. Extensive cytotoxicity was seen with syncitia formation once more. Titre of the virus recovered was 3 x 10^4 s.f.u./ml.

Lenti-GALV virus was produced by transient transfection as no packaging cell line is currently available. Two lentiviruses were produced: one was pseudotyped with VSV-G envelope and the other relied upon the GALV expressed to act as the viral envelope. 293T cells were plated in 10 cms plates. After overnight incubation the cells were transfected using the Profection method with 10 μg Lenti-GALV, 10 μg pCMV R8.91 encoding the HIV gag, pol, tat and rev genes (Zufferey et al., 1997). For the VSV-G pseudotyped virus 5 μg pMD.G encoding VSV-G was also transfected. After overnight incubation the cells were washed and minimal fresh media applied. After a further 48 hours cell supernatants were recovered and filtered through a 0.45 μm filter. The titres recovered for the Lenti-GALV viruses can be seen in **Table 5.1**: again hyperfusogenic GALV appeared to serve poorly as an envelope with a titre of < 10^2. In contrast the VSV-G pseudotyped Lenti-GALV virus achieved a titre of 4 x 10^6; significantly higher than that seen with the C-type vector.

Table 5.1: Packaging of GALV-containing retroviral vectors

Vector	Packaging cell line	Pseudotyping envelope	Complement resistant	Stable cell line possible	Stable titre	Transient titre
C-type pBABE GA	AM12	407A + GA	No	Yes	$<10^2$	$<10^3$
C-type pBABE GA	FLY 13	407A + GA	Yes	No	-	$<10^3$
C-type pBABE GA	293INT	GALV	Yes	No	-	$<10^2$
C-type pBABE GA	293INT	VSV-G + GA	Yes	No	-	3×10^4
Lenti-GALV	293T	GALV	Yes	No	-	$<10^2$
Lenti-GALV	293T	VSV-G + GA	Yes	No	-	4×10^6

GALV is represented by GA or GALV in this table

Table 5.1 illustrates the GALV expressing retroviral vectors developed and the titres achieved. A variety of envelopes were used to pseudotype the viral particles. Only AM12, due to its murine origin, was not fused following GALV transfection and therefore permitted the generation of a stable cell line.

5.2.4 Lenti-GALV infected both dividing and quiescent human tumour cells

A potential benefit of lentiviral vectors for gene therapy applications is their ability to infect non-dividing cells (Kay et al., 2001). The effect of Lenti-GALV/VSV-G was compared to pBabe-GALV/VSV-G on human tumour cells in the presence or absence of aphidicolin, which blocks cells in the G1-S phase of the cell cycle. HT1080 cells were plated in 6 well plates and incubated with normal medium or medium containing 5 μg/ml aphidicolin. 24 hours later cells were infected with the lenti or C-type viral stocks. After a further 48 hours the cells were fixed in 4% paraformaldehyde and the number of syncitia per random field were counted; 10 fields examined per plate. The result can be seen in **Figure 5.2**. It demonstrates that the titre of the Lenti-GALV vector was largely unaltered by the effects of cell cycle arrest whereas the effective titre of the C-type pBabe-GALV vector was substantially reduced in the non-cycling population.

5.25 GALV-expressing retroviral vectors killed cells with a large bystander effect

Experiments were conducted to assess the cytotoxic effects of GALV expression from these retroviral vectors. 10^5 HT1080 cells were plated per well in 6 well plates. Following overnight incubation cells were infected with increasing amounts of Lenti-GALV/VSV-G or pBabe-GALV/VSV-G. 24 hours later the cells were washed and fresh media applied. The cells were then incubated for a further 6 days, being washed and having fresh media applied every 48 hours. Seven days from infection the cells were fixed, stained with crystal violet and surviving cell number/well counted. The result for Lenti-GALV/VSV-G can be seen in **Figure 5.3**. Similar results were obtained for pBabe-GALV/VSV-G. The result indicated that as few as 10^3 s.f.u. of retrovirus could kill in excess of 10^5 HT1080 cells through syncitia formation and subsequent cell death. This gave a bystander killing effect of 1 (transduced): 100 (non-transduced) cells. This was in keeping with the data obtained from plasmid transfection in vitro (as described in Chapter 3).

5.2.6 Lentivirus vector expressing GALV eradicated growth of established tumours in nude mice

Although the absolute titre of Lenti-GALV/VSV-G was only in the order of 4 x 10^6 two factors suggested it would be appropriate to test this vector in vivo. First was the large bystander effect seen with GALV expression. Second was the relative increased effective titre in vivo of Lenti-GALV/VSV-G compared to C-type retroviral vectors as productive infections could occur even in nondividing cells. Therefore the following in vivo experiment was conducted. Athymic nude mice were injected s.c. with 2 x 10^6 HT1080 tumour cells. When the mean tumour diameter in each group of mice (10 mice per group) reached 0.2cm, tumours were injected with 100µl of PBS, control vector (Lenti-β-Gal/VSV-G) or Lenti-GALV/VSV-G (4 x 10^5 s.f.u.) per day for 3 consecutive days. Tumour size was then followed and mice sacrificed when tumours reached 1cm x 1cm. The result can be seen in **Figure 5.4**. It indicates that Lenti-GALV/VSV-G vector eradicated tumour growth in the whole cohort of 10 mice compared to one mouse in the PBS group and two of 10 in the Lenti-β-Gal/VSV-G group.

Figure 5.3: GALV expressing retroviral vectors killed cells with a large bystander effect

10^5 HT1080 cells were plated per well of a 6 well plate. 24 hours later they were infected with increasing amounts of retroviral vector; A: 0 s.f.u. --> F: 10^5 s.f.u. performed in duplicate. After 7 days the cells were fixed, stained with crystal violet and surviving cells recorded. The plates for Lenti-GALV are illustrated below. pBabe-GALV/VSV-G gave similar results.

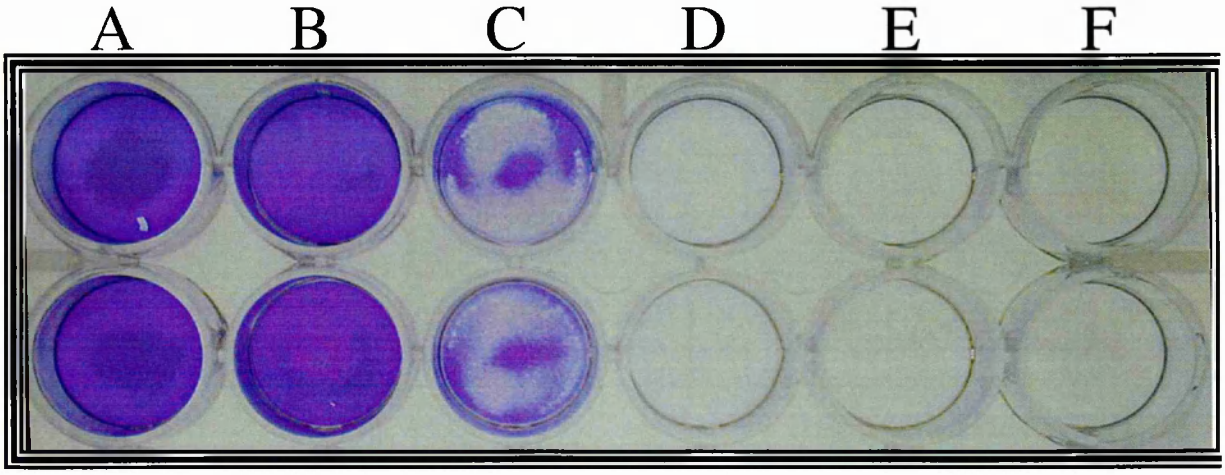

	A	B	C	D	E	F
virus added (sfu)	0	10	10^2	10^3	10^4	10^5
Number of surviving cells	∞	∞	$>10^4$	$>10^2$	0	0

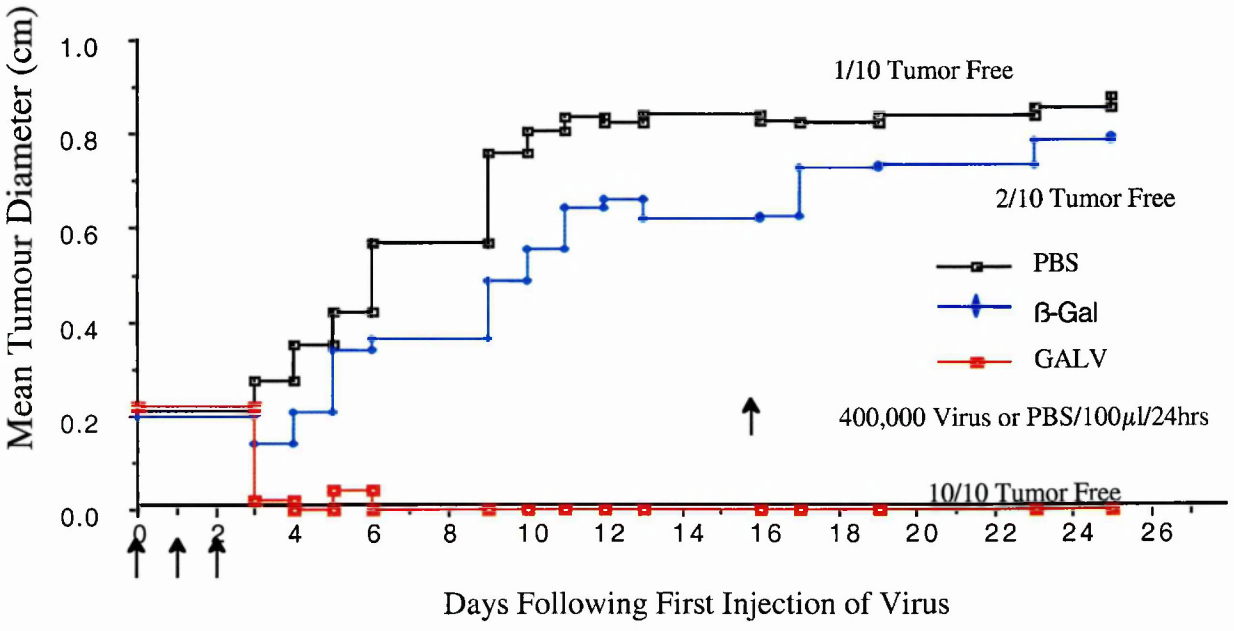

Figure 5.4: Lenti-GALV vector eradicated established human tumour xenografts. HT1080 tumours were seeded s.c. in athymic nude mice. When tumours reached 0.2cm x 0.2cm they were injected with PBS, Lenti-ß-Gal or Lenti-GALV for 3 consecutive days. Tumour size was monitored and animals sacrificed when the largest tumour diameter reached 1.0cm.

This experiment was performed in conjunction with Dr RM Diaz. Specifically she prepared the HT1080 cells for tumour formation and we were equally responsible for the production of the viral vectors used in the experiment. She went on to develop additional aspects of this study: HT1080 tumours seeded in vivo were injected once with Lenti-β-Gal/VSV-G, Lenti-GALV/VSV-G or PBS. Tumours were recovered from injected mice and were re-established in culture. Extensive syncitia were observed following 24 hours of growth in vitro in cultures from Lenti-GALV/VSV-G injected tumours but not from PBS or Lenti-β-Gal/VSV-G groups; providing indirect evidence that the mechanism of tumour cell killing was through syncitia formation. She also went on to analyse gene expression from explanted tumour cells by rtPCR. GALV mRNA was readily detected following a single injection of Lenti-GALV/VSV-G 48 hours after injection. Human heat shock proteins hhsc70 and hsp70A and also human MICB mRNA was detected in tumours injected with GALV vector and not PBS or β-Gal vector. These findings were in keeping with the in vitro data recorded previously in Chapter 3 which indicated FMG mediated cell killing induces a stress response. Murine IFN-γ mRNA was also detected from tumours injected with Lenti-GALV/VSV-G consistent with an immune-mediated response, this was not seen in Lenti-β-Gal/VSV-G injected tumours.

5.3 Discussion

The generation of retroviral vectors expressing GALV proved problematic for a number of reasons. First was the cytotoxicity seen in packaging/producer cell lines of human origin which developed rapidly after introduction of the FMG gene. Secondly was that as GALV is a truncated form of the wild-type GALV envelope, due to the truncation it either incorporates poorly into viral particles or is functionally impaired to direct productive binding and fusion when required to pseudotype core particles. As an envelope it also appeared to interfere with the ability of 4070A to pseudotype core particles through probable heterotrimer formation. Consequently titres of functional vector for both C-type and lentiviral were low. Further studies have also provided an explanation as to the low titres of Lenti GALV seen in the above experiments when GALV was pseudotyping the lenti cores. Christodoulopoulos et al., (2001) showed that wild-type GALV envelope is unable to pseudotype lentiviral particles. This is due to incompatible features in the

cytoplasmic tail of the wild-type GALV envelope. This incompatibility can in part be overcome by a number of strategies including: replacing the wild-type GALV cytoplasmic tail with the corresponding MuLV sequence, mutation of two residues just upstream of the R peptide cleavage site, or by removing the R peptide (GALVΔR). With regard to removing the R peptide in these studies, the titre of lentiviral vector produced pseudotyped with GALVΔR was still significantly less than lentiviral vector pseudotyped with MuLV. This situation is comparable to the experiments with the truncated, hyperfusogenic GALV used in this thesis

Despite the low titre Lenti-GALV/VSV-G was able to eradicate established human xenografts in nude mice. This was due to the low titre of the lenti-GALV vector being in some way compensated by a number of factors. First is the potency of GALV with the significant bystander effect seen with FMG. Secondly is the ability of lentiviral vectors to infect non-dividing cells. With C-type vectors a large component of vector injected in vivo is likely to encounter non-dividing tumour cells resulting in nonproductive infections. This reduces the effective titre. For lentiviral vectors this is not the case and was demonstrated for Lenti-GALV/VSV-G. Thirdly the stress and necrotic death induced by FMG mediated syncitia formation even in nude mice may have induced an immune mediated antitumour effect, through natural killer (NK) cells for example, which may have contributed to the therapeutic effect seen.

In summary, retroviral vectors expressing a FMG have been produced. A lentiviral vector expressing GALV has been tested in vivo and was capable of eradicating small established human xenograft tumours in nude mice.

The data presented in this chapter formed part of the following paper:

A Lentiviral Vector expressing a Fusogenic Glycoprotein for Cancer Gene Therapy

Rosa Maria Diaz, Andrew Bateman, Lisa Emiliusen, Adele Fielding, Didier Trono, Stephen J. Russell and Richard G. Vile

Gene Therapy (2000) 7, 1656-1663

CHAPTER 6: DEVELOPMENT OF ADENOVIRAL VECTORS EXPRESSING MEASLES VIRUS F AND H GENES

Chapter 6: Development of adenoviral vectors expressing Measles virus F and H genes

6.1 Introduction

This chapter describes the construction of adenoviral vectors expressing Measles F and H genes, their subsequent characterisation and use in in vivo experiments. .

Following the previous findings of enhanced cytotoxic effect of FMG over suicide genes in vitro, a next logical step was to investigate aspects of in vivo efficacy. For this investigation a key component, as indicated in Chapter 5, is the vector of gene delivery. Adenoviral vectors due to their high titre, transient gene expression to high levels and ease of manipulation appeared the most favourable to explore FMG effects in vivo. I therefore set out to generate adenoviral vectors expressing Measles F and H genes using the method from Quantum Biotechnologies.

Measles F and H genes were the initial FMG of choice as individually these genes are non-fusogenic and could be incorporated in adenoviral vectors in a straightforward manner (as apposed to GALV which due to its inherent fusogenicity reguired additional control elements to allow adenoviral vector production, see Chapter 7). The specific Quantum system used to construct adenoviral vectors expressing Measles F and H genes contained the green fluorescent protein (GFP) reporter gene downstream of an internal ribosome entry site (IRES or I) see **Figure 6.1**. The adenoviral vectors expressing the Measles genes thus produced were labelled AD F-I-GFP and AD H-I-GFP. After obtaining suitable clones they were characterised in vitro before use in in vivo experiments.

6.2 Results

6.2.1 Construction of recombinant adenoviral shuttle vectors expressing Measles F and H genes

Measles F and H genes were encoded by the plasmids pCG-F1 and pCG-H5 and were a kind gift from Dr R. Cattaneo. The cDNA sequence coding for F, including the 5' intron sequence immediately upstream of the gene contained within pCG-F1, was PCR amplified

using oligonucleotide primers AQF1 and AQF2. These primers had restriction sites added at their 5' ends to allow future cloning into the pQBI-AdCMV5-IRES-GFP adenoviral shuttle vector (see **Figure 6.1**). For both the F gene and subsequently the H gene the cloning site into the pQBI-AdCMV5-IRES-GFP shuttle vector was *Bgl II. Bgl II* was also contained twice within the H gene. A strategy was therefore required which enabled H to be cloned into the shuttle vector without using *Bgl II* . The strategy devised cloned the F gene using the *Bgl II* site and incorporated novel restriction sites *Mlu 1* in the forward primer, *Xba 1* and *Pme 1* in the reverse primer. This allowed for the H gene to be PCR amplified using oligonucleotide primers AQH1 and AQH2. These incorporated the H gene and the 5' intron sequence as well as added a *Mlu 1* restriction site to the forward primer and *Pme 1* to the reverse (see **Figure 6.2**). The sequence of the primers are shown below with restriction sites underlined:

AQF1 agatctacgcgtatcccccgatcctgagaacttca

Bgl II Mlu 1

AQF2 agatcttctagagtttaaactcaggtgggcttgatgctgggtgcggtggt

Bgl II Xba 1 Pme 1

AQH1 attacgcgtatcccccgatcctgagaacttca

Mlu 1

AQH2 gtttaaacggttcactagcagccctatctgcg

Pme 1

The PCR conditions used for both F and H genes using AmpliTaq Gold were 94°C 10 minutes to activate the polymerase, followed by 20 cycles of denaturing at 94°C for 1 minute, annealing at 60°C for 1.5 minutes, extension at 72°C for 4 minutes, and completed with a 10 minute extension at 72°C. The PCR products were cloned into the pCR3.1 vector as an intermediate step. Functional activity of both F and H genes after PCR was confirmed by co-transfection of HT1080 cells with the pCG vectors and the pCR3.1

Figure 6.1: Recombinant adenoviral shuttle vector

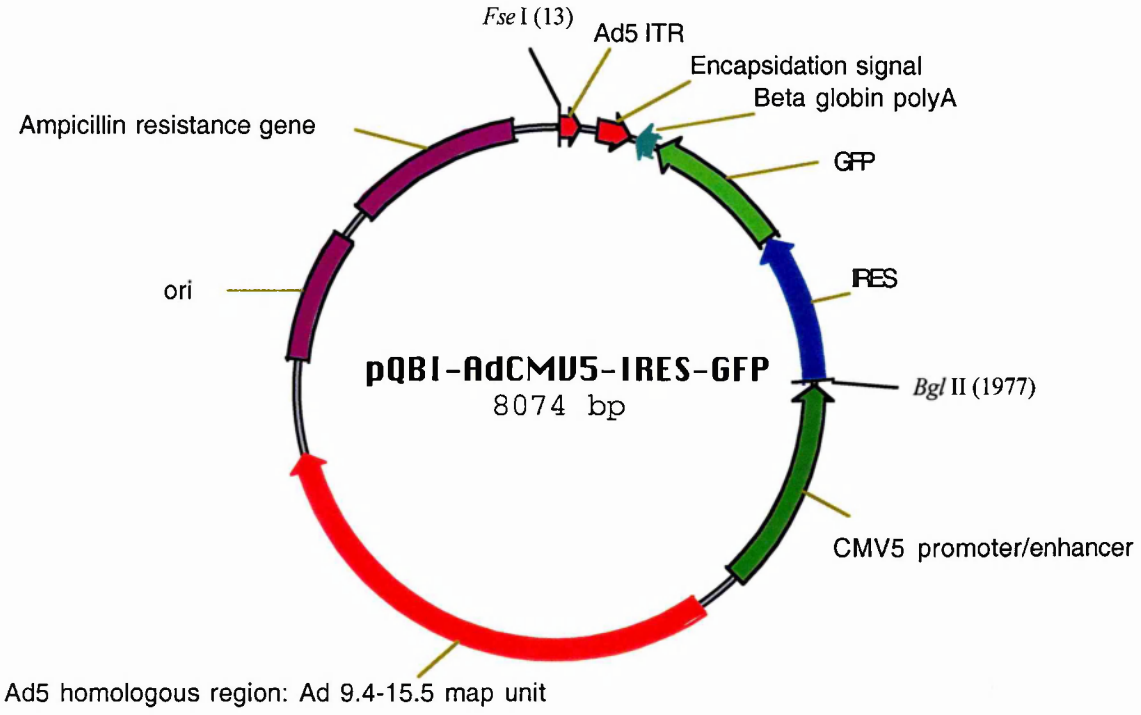

Figure 6.2: F and H PCR products cloned into pCR3.1 prior to restriction enzyme digest and ligation into pQBI-AdCMV5-IRES-GFP

(enzyme sites screened: *Bgl II, Fse 1, Mlu 1, Pme 1, Xba 1*)

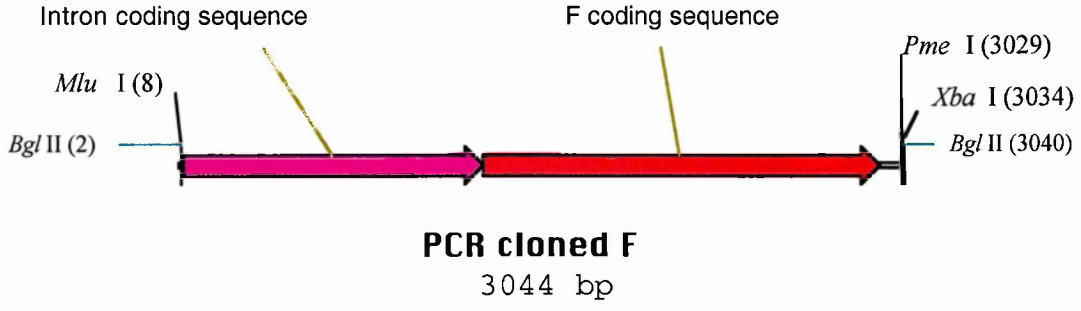

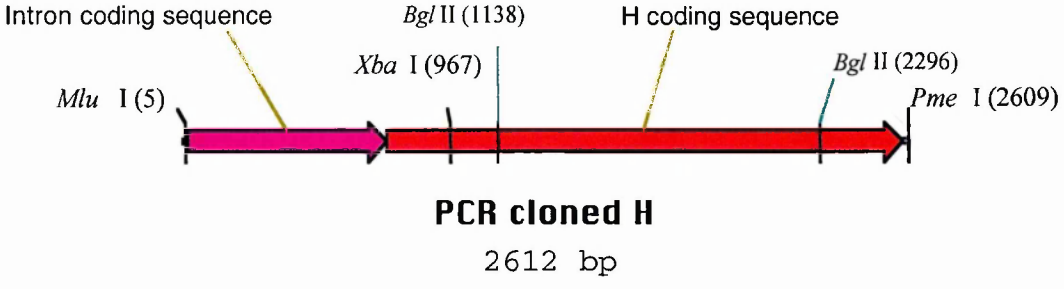

vectors. Syncitia formation readily occurred after overnight transfection with pCG-F1 + pCR3.1 H and pCG-H5 + pCR3.1 F.

pQBI-AdCMV5-IRES-GFP and pCR3.1 F were digested with *Bgl II* and F ligated into the adenoviral shuttle vector: forming pAd F-I-GFP.

pAd F-I-GFP and pCR3.1 H were digested with *Mlu 1* and *Pme 1*, and H ligated into the adenoviral shuttle vector: forming pAd H-I-GFP.

6.2.2 Production of Adenoviruses expressing Measles F and H genes

pAd F-I-GFP and pAd H-I-GFP were prepared concurrently for co-transfection with QBI-viral DNA as described in Chapter 2. Plaques were collected 7-10 days post transfection. The presence of GFP allowed for the direct selection of plaques containing positive recombinants and therefore 5 F (F_1-F_5) clones and 7 H (H_1-H_7) clones were collected. These were prepared as previously described and clones F_1, F_2, H_1, H_4 showed good GFP expression and syncitia formation. These were selected for plaque purification and further selection. After plaque purification 5 clones were collected from each sample: $F_1^{1\text{-}5}$, $F_2^{1\text{-}5}$, $H_1^{1\text{-}5}$, $H_4^{1\text{-}5}$ and were screened as before. Clones F_1^2, F_2^5, H_1^2, H_4^2, were selected for a further round of plaque purification. 5 clones were collected per sample (labelled V-Z) and screened as before. The plaques from clones F_1^2Z and H_4^2X when examined showed all 293A cells reaching CPE expressed GFP. Extensive syncitia formation was also seen with co-infection of HT1080 cells. These were selected for amplification and subsequently were termed Ad F-I-GFP and Ad H-I-GFP.

6.2.3 Titre of amplified, purified Ad F-I-GFP, Ad H-I-GFP and Ad GFP

Once amplified and double CsCl purified the viruses were titred using standard optical absorbance and plaque assay methods. This included Ad GFP (Genzyme) which was used as a control in future experiments and was prepared from an intial 5µl stock (purified Ad GFP in 10% glycerol/PBS).

Adenovirus	Absorbance at 260nm	Viral particles/ml x10^{12}
Ad GFP	0.0919	2
	0.0884	1.9
Ad F-I-GFP	0.1980	4.4
	0.2042	4.5
Ad H-I-GFP	0.2036	4.5
	0.02023	4.45

Table 6.1: Optical absorbance, OD_{260}, of purified recombinant adenoviruses

Adenovirus	Plaques in well at 10^{-9} dilution	Mean PFU/ml x10^{10}
Ad GFP	29	3.3
	35	
Ad F-I-GFP	1	0.35
	6	
Ad H-I-GFP	32	3.6
	40	

Table 6.2: Plaque assay result of recombinant adenoviruses

The titres shown here are from the first amplification, purification and are consistent with all further rounds of production of these viruses used in this thesis.
The Ad F-I-GFP titre was consistently one log lower than the Ad H-I-GFP titre.

6.2.4 Confirmation of recombinant adenovirus by Hirt extraction

Incorporation of the F or H genes within the recombinant adenoviruses was confirmed by Hirt extraction. The recovered DNA was analysed in a PCR: 2µl of sample DNA was added per PCR mix. Primers AQF1and AQF2 were used to test for incorporation of the F gene, primers AQH1 and AQH2 for H. Both PCRs were performed using AmpliTaq with the following conditions: 94°C for 10 minutes, then 30 cycles of 94°C for 1 minute, 60°C

for 1.5 minutes, 72°C for 4 minutes. Samples from both PCRs were run on the same gel (see **Figure 6.3**).

The PCR detects the incorporation of the 3044 bp fragment corresponding to the F gene and the 2612 bp fragment corresponding to the H gene in their designated adenoviruses.

6.2.5 Microscope Examination to assess Ad F-I-GFP and Ad H-I-GFP function

293A cells were infected with recombinant adenovirus at 10 p.f.u. 24 hours later cells were visualised using light microscopy to assess morphological changes and green filter to detect the expression of GFP (see **Figure 6.4**).

Individually Ad F-I-GFP and Ad H-I-GFP did not produce any morphological changes relative to the Ad GFP control and both express GFP as visualised under a green filter. When co-infection occurred, syncitia formation became readily apparent by 12 hours and proceeded rapidly over the next 24 hours to incorporate >95% of cells within syncitia; at which point the cell monolayer became non-adherent.

6.2.6 Western analysis of Ad F-I-GFP and Ad H-I-GFP

Production of F and H protein by Ad F-I-GFP and Ad H-I-GFP was analysed by western. HT1080 cells, or HT1080-F cells (see below), were infected with recombinant adenovirus at a m.o.i. of 10. Infected cells were incubated for 72 hours prior to protein extraction bar cells co-infected with Ad F-I-GFP and Ad H-I-GFP, which were collected after 48 hours due to extensive syncitia formation. Samples were processed in a standard manner as described in Chapter 2. The specific conditions for the F western were: 10% Tris-HCL Precast gel, POC rabbit anti-F antibody diluted 1:5,000 in 1% milk PBS-T and HRP conjugated goat anti-rabbit secondary antibody diluted 1:10,000 in 1% milk PBS-T. The specific conditions for the H western were: 7.5% Tris-HCL Precast gel, POC rabbit anti-H antibody diluted 1:5,000 in 5% milk PBS-T and HRP conjugated goat anti-rabbit secondary antibody diluted 1:10,000 in 1% milk PBS-T. The result is shown in **Figure 6.5**.

The anti-F antibody binds an epitope found in F_0 and F_1. Consequently a positive sample is recognised by 60Kd and 40Kd staining corresponding to F_0 and F_1 protein respectively.

The anti-H antibody detects the 80Kd H protein.

Figure 6.3: Diagnostic PCR performed on Hirt extracted DNA from 293A cells infected with recombinant adenoviruses.

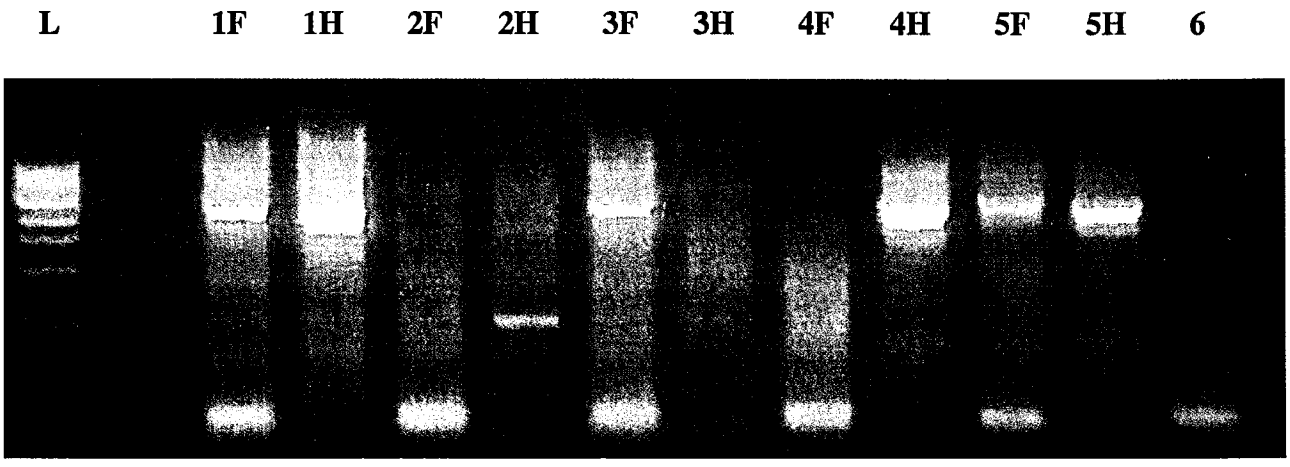

L	1Kb Ladder
1	Positive controls
2	Ad GFP
3	Ad F-I-GFP
4	Ad H-I-GFP
5	Ad F-I-GFP + Ad H-I-GFP
6	Negative control

Figure 6.4: Adenovirus infection of 293A cells:

Examination by light microscopy and green filter at 24 hours

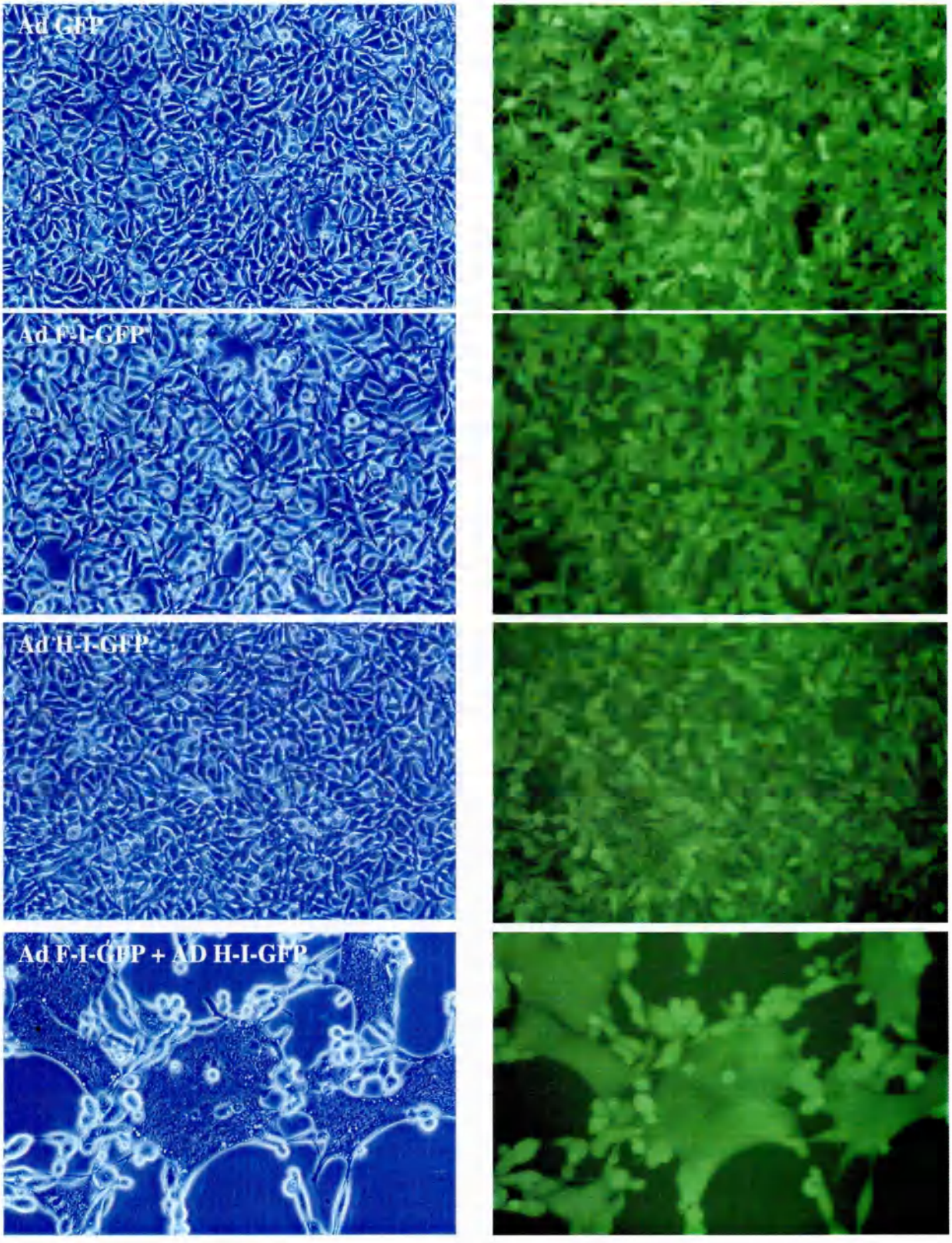

Figure 6.5: Immunoblots showing protein expression following Adenoviral infection

F antibody detects F_0 and F_1 forms

HT1080-F stably expresses F protein

Identical samples run in both blots

F Immunoblot

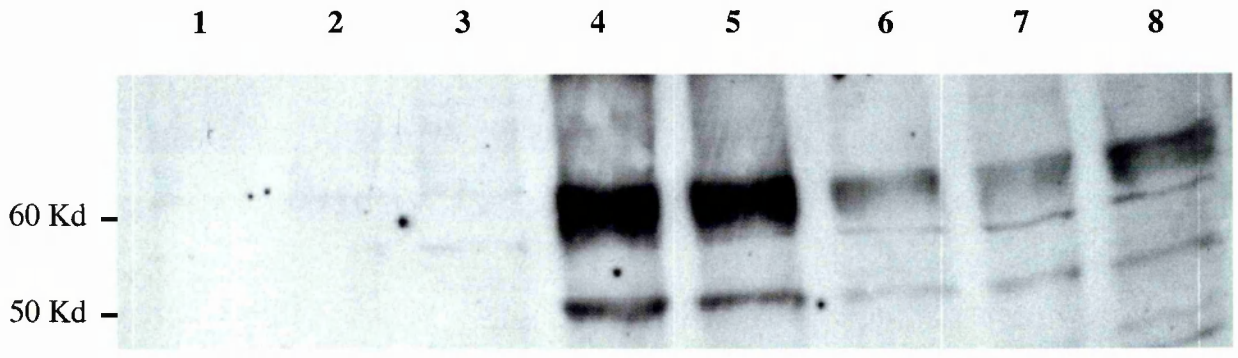

H Immunoblot

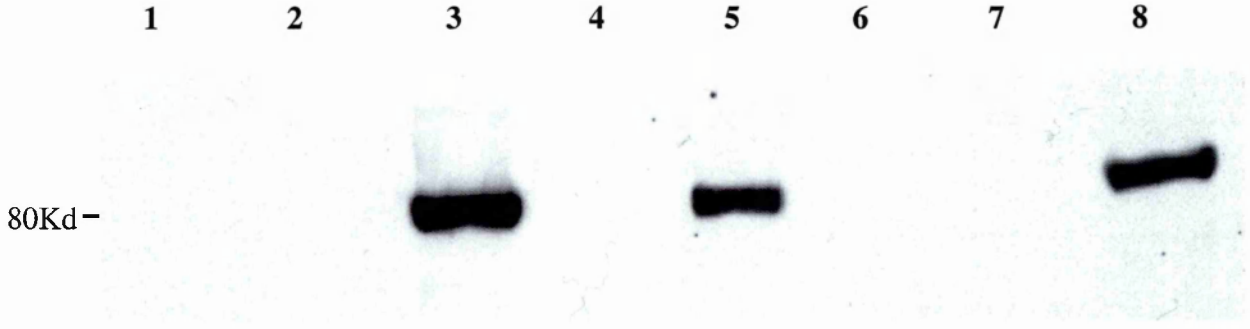

HT1080 cells: **1** parental

2 Ad GFP

3 Ad H-I-GFP

4 Ad F-I-GFP

5 Ad F-I-GFP + Ad H-I-GFP

HT1080-F cells: **6** parental

7 Ad GFP

8 Ad H-I-GFP

Figure 6.6: Facs analysis of HT1080 cells infected with Ad GFP or Ad F-I-GFP

A) Dot plot of i) parental HT1080 cells alone, ii) with Ad GFP infection, or iii) Ad F-I-GFP infection. Indicates high percentage of cells infected by adenoviruses and GFP expression. Also shows overlap into FL 2 detection range at upper FL 1 values.

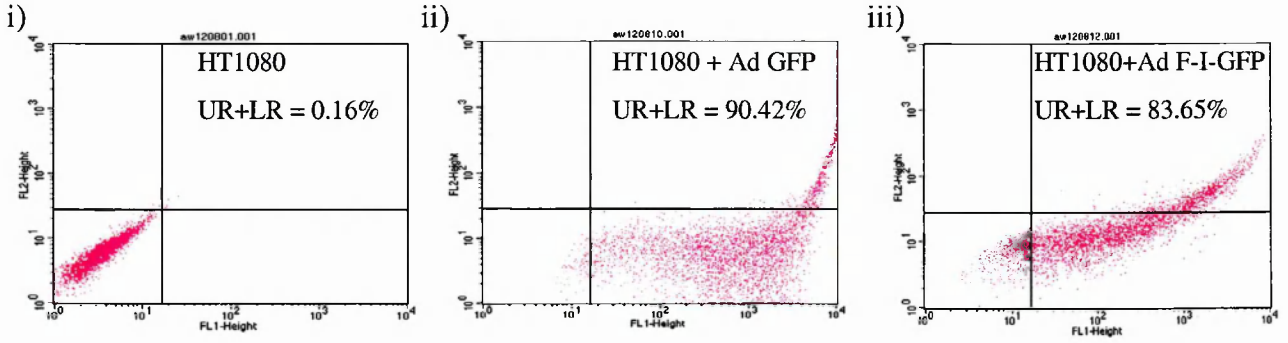

B) Histogram plot of A) showing extensive GFP expression from i. Ad GFP and ii. Ad F-I-GFP infection.
Blue - HT1080 alone
Green - infected HT1080

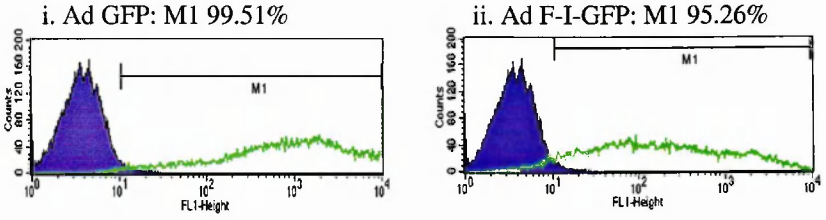

C) Dot plot of HT1080 cells infected with Ad F-I-GFP.
i) PE secondary alone
ii) Anti-F antibody and PE secondary

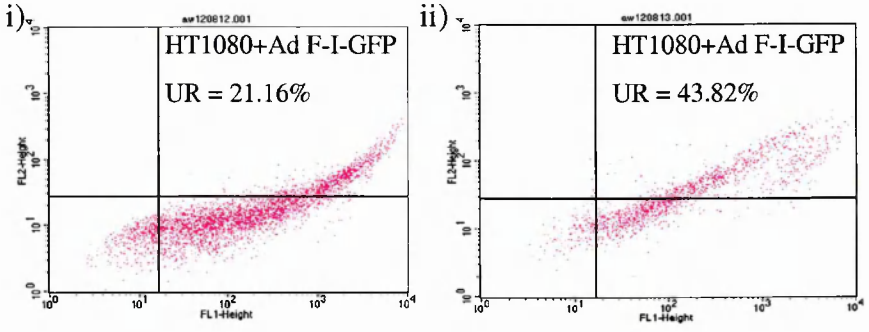

D) Histogram plot of C)
i. Ad GFP control
ii. Ad F-I-GFP
Blue-PE secondary alone
Green - Anti-F antibody and PE secondary
M1 values in ii) 48.73%-blue 71.77%-green

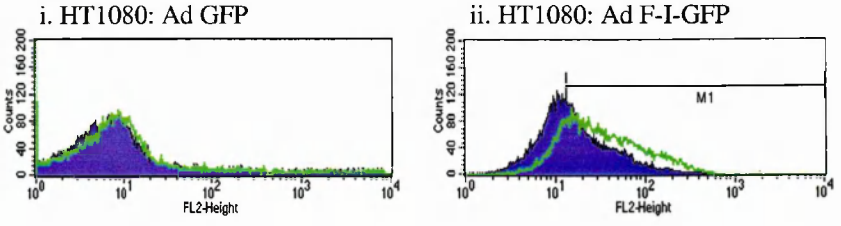

6.2.7 FACS analysis of Ad F-I-GFP

Surface expression of F protein on cells infected with Ad F-I-GFP was confirmed by FACS (see **Figure 6.6**). HT1080 cells were infected with adenovirus at an m.o.i of 10 and collected after 48 hours. The Facs was performed using the Y503 anti-F antibody diluted 1:50 and PE secondary diluted 1:100. The FL 1 detection confirmed extensive GFP expresion and high rate of infectivity of HT1080 cells in vitro: both with Ad GFP and Ad F-I-GFP. Infectivity could be estimated at >80% for both viruses. F protein expression was detected primarily in cells expressing high levels of GFP (as identified by high FL 1 value) in those cells infected by Ad F-I-GFP.

6.2.8 Effect of ratios of Ad F-I-GFP : Ad H-I-GFP in inducing syncitia

The effect of ratios of Ad F-I-GFP titre to AdH-I-GFP titre in inducing syncitia was explored. HT1080 cells were plated in 6 well plates at 2 x 10^5/well the day previously. The following day various m.o.i of viruses were added and morphological changes using the fusion index recorded at 24 hours and 48 hours:

24 Hours

H

F **m.o.i**	**1000**	**100**	**10**
100	Massive cell death	Massive cell death	+++++
10	+ and cell death	Massive cell death And +++++	+++++
1	No syncitia And cell death	++++	+++

48 Hours

H

F	**m.o.i**	**1000**	**100**	**10**
	100	Massive cell death	Massive cell death	Massive cell death due to syncitia
	10	Massive cell death	Massive cell death And syncitia	Massive cell death due to syncitia
	1	No syncitia And cell death	+++++	+++++

Table 6.3: Effect of varying Ad F-I-GFP : AD H-I-GFP titres on syncitia formation
HT1080 cells were plated in 6 well plates. The following day virus was added at variable m.o.i. and morphological changes followed for 48 hours and recorded according to the fusion index. Control wells of Ad GFP, Ad F-I-GFP or Ad H-I-GFP alone showed no syncitia formation, minimal CPE and grew to confluency.

The result indicated a toxic effect on HT1080 cells in vitro with high concentration of virus but also that syncitia formation occurred with wide ranges of Ad F-I-GFP to Ad H-I-GFP ratios.

6.2.9 In vivo experiment assessing efficacy of Ad F-I-GFP and Ad H-I-GFP

A pilot study was conducted in nude mice to test the in vivo efficacy of Ad F-I-GFP and Ad H-I-GFP. HT1080 tumours were seeded by innoculation of $5x10^5$ cells at day 1 in 6 mice. Tumours became palpable by day 14 and received intra-tumoural injections of PBS, Ad GFP or Ad F-I-GFP and Ad H-I-GFP. There were two mice per treatment group and each received three consecutive days of injections. The PBS dose was 100µl/day, Ad GFP $2x10^9$ pfu in 100µl/day, Ad F-I-GFP $2x10^8$ pfu and Ad H-I-GFP $2x10^9$ pfu in 100µl/day. Tumours were harvested two days after the last injection and underwent H+E staining (Mayo Foundation Histopathology research department). **Figure 6.7** indicates the finding of some areas of syncitia formation within those tumours treated with Ad F-I-GFP and Ad H-I-GFP, this was not seen in the PBS or Ad GFP groups.

Figure 6.7: Syncitia formation in vivo following injection of Ad F-I-GFP + Ad H-I-GFP

HT1080 tumours grown in nude mice injected with recombinant adenoviruses:

I. Ad GFP II. Ad F-I-GFP + Ad H-I-GFP A. x250 magnification B. x500 magnification

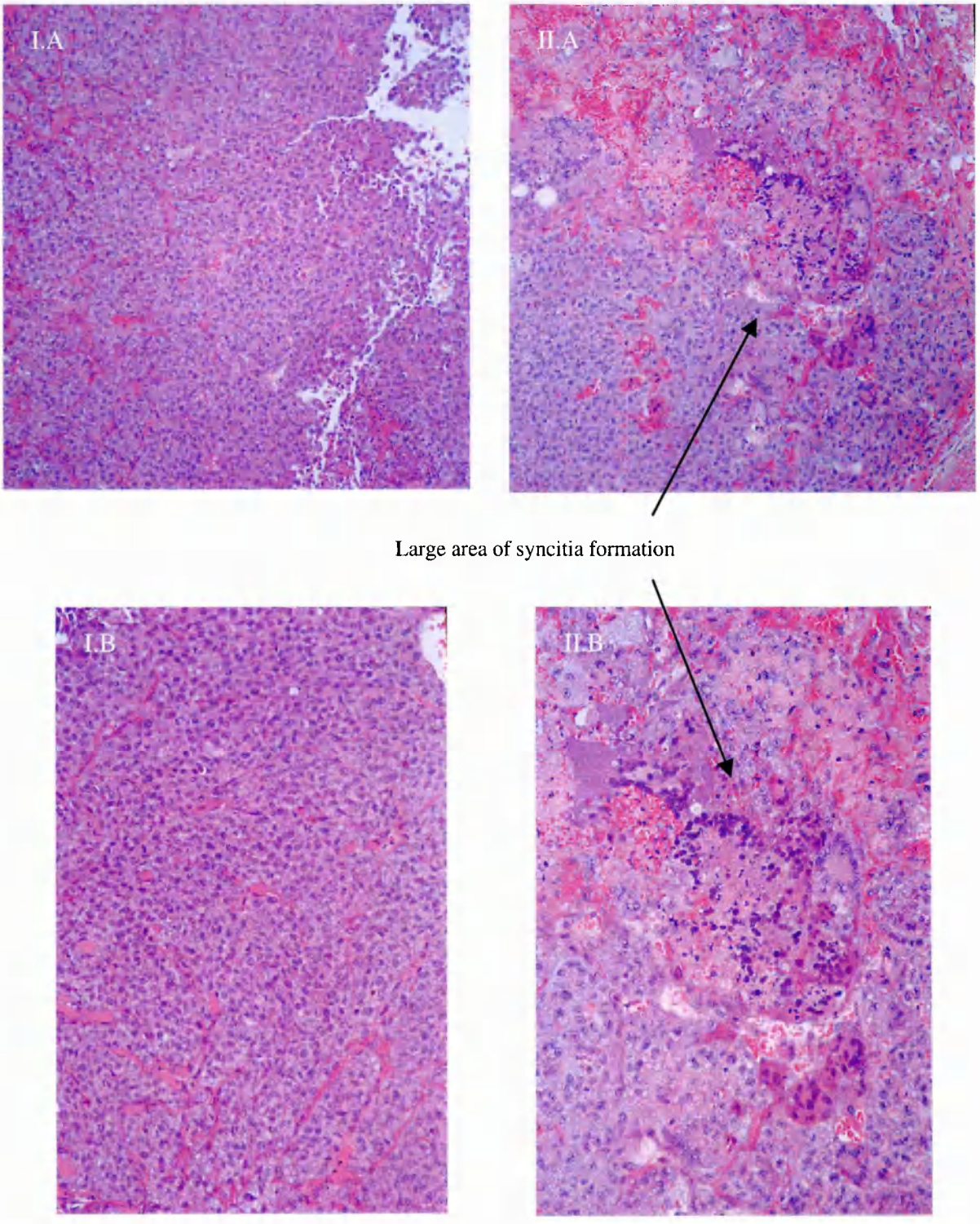

Despite identifying areas of syncitia formation within test tumours there were two outstanding concerns following the pilot study. Firstly there remained the discrepancy in viral titre between Ad F-I-GFP and Ad H-I-GFP. Secondly the extent of syncitia formation was patchy and not widespread within the tumours. I therefore opted to explore the possibility of proceeding using an HT1080 cell line stably expressing Measles F. This would allow injection of tumours with only one test adenovirus.

6.2.10 Assessment of HT1080-F cells and infection with Ad H-I-GFP

A clonal population of HT1080 cells expressing the measles F protein (HT1080-F) were produced by Dr K-W. Peng and Dr S.J. Russell (Molecular medicine program, Mayo Foundation) and were a kind gift. The HT1080-F cell line was produced by transfection of HT1080 cells with pBaBe F plasmid, selecting with phleomycin for stable transfectants. Expression of the F protein was confirmed by immunoblot **Figure 6.5**, lanes 6-8, Facs analysis **Figure 6.8** and were conducted as described previously. In vitro activity upon infection with Ad H-I-GFP was confirmed: 2 x 10^5/well HT1080-F cells were plated in a 6 well plate. The following day the cells were infected with nothing or Ad GFP or Ad H-I-GFP at an m.o.i. of 10. Morphological changes were observed over the subsequent 4 days (see **Figure 6.9**). Widespread syncitia formation occurred rapidly in the Ad H-I-GFP group only (Figure 6.9ii), progressed (Figure 6.9iv) and resulted in extensive cell death and clearing of the plate.

In view of these data it was decided to progress to the initial in vivo experiments formally assessing the efficacy of measles F and H proteins at inducing syncitia and cytotoxicity. These experiments were proposed using the HT1080-F cells and infection with Ad H-I-GFP.

6.2.11 In vivo experiment assessing efficacy of Ad H-I-GFP and HT1080-F cells

Mice were arbitrarily grouped into 3 by planned 'treatment': PBS alone, Ad GFP or Ad H-I-GFP. Tumours were seeded in nude mice by innoculating 5x10^5 cells at day 1. Tumours were injected when they became palpable at Day 14: 100μl/mouse/day of PBS, Ad GFP titre of 1x10^9 in 100μl/mouse/day, or Ad H-I-GFP titre of 1x10^9 in

Figure 6.8: FACS analysis of HT1080-F cells

Blue - Parental HT1080

Red - HT1080-F with PE secondary alone

Green - HT1080-F with anti-F primary antibody and PE secondary

M1	Blue	11.3%
	Red	49.9%
	Green	77.36

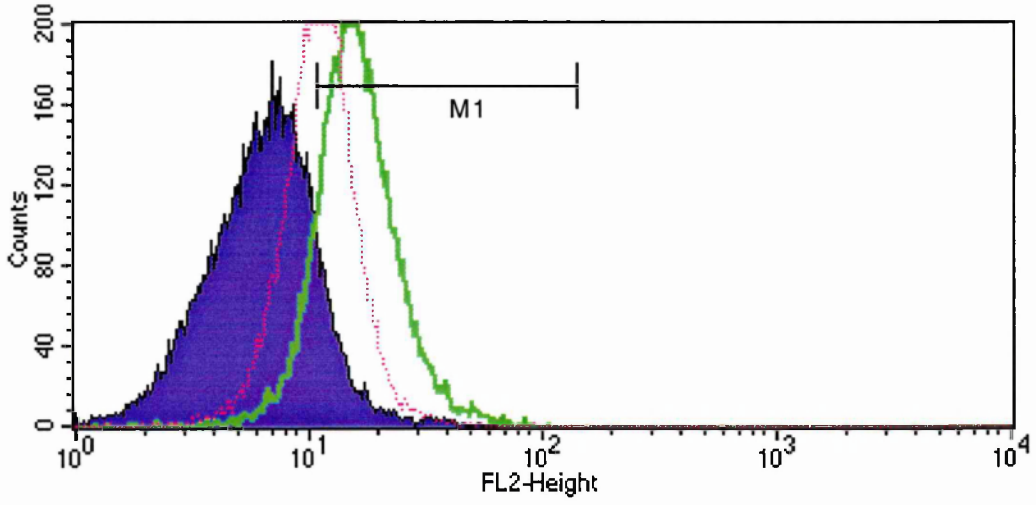

Figure 6.9: HT1080-F cells infected with Ad H-I-GFP Light microscope images at 48 hours (i + ii) and 72 hours (iii + iv). Extensive and progressive syncitia formation seen with HT1080-F infected with Ad H-I-GFP. Ad GFP acted as control.

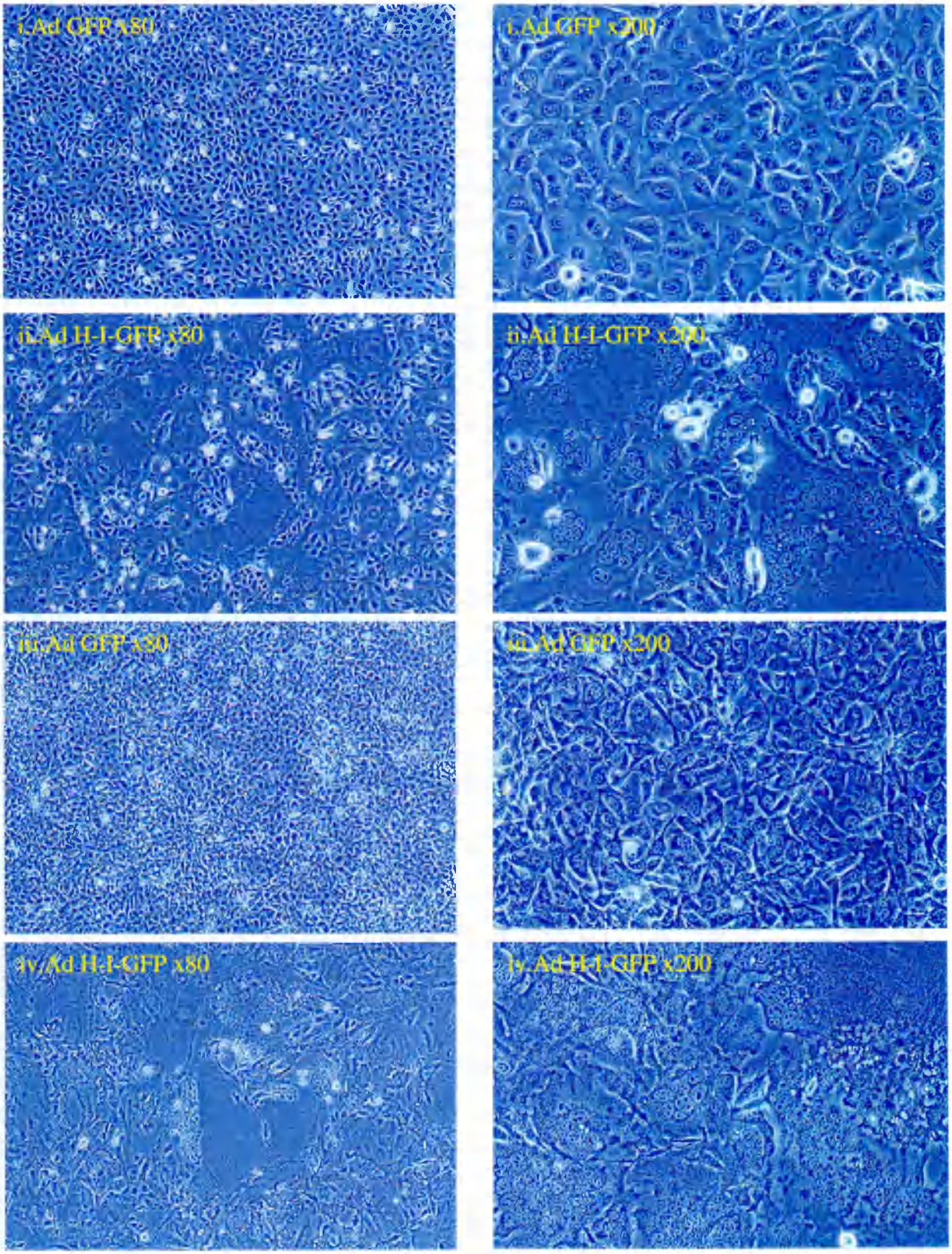

100µl/mouse/day was injected intratumourally for 5 days. Tumours were followed until a single tumour dimension exceeded 1cm or for 60 days, which ever occurred earliest.
Survival curves were plotted for each group: death was determined when any single tumour dimension exceeded 1cm.
The data from this experiment show HT1080-F cells, when innoculated in nude mice, form rapidly progressive tumours which are uniformally fatal at 21 to 33 days. Injection of control adenovirus, Ad GFP, does not significantly alter this outcome. However administration of Ad H-I-GFP leads to tumour eradication and longterm survival in a third of animals. The data is presented in **Figure 6.10** and represents the sum of two experiments.

6.2.12 Assessment of gene expression in vivo

Two tumours from each group were excised three days after the last injection in the second in vivo experiment. Tissue was investigated for evidence of morphological changes consistent with gene expression. Tumours were fixed in formalin and sent to the Histopathology department, Mayo Foundation. Sections were taken and mounted on slides. Unstained and H+E stained slides were prepared for each tumour.
GFP expression was assessed from unstained slides viewed on an inverted microscope with light and green filter, **Figure 6.11**.
Ad GFP did not induce significant morphological changes as seen in H+E stained slides. Green fluorescence was identified in unstained sections. However despite injection of $1x10^9$ Ad GFP pfu/ day for 5 days a detectable level of green fluorescence was confined to less than 10% of the tumour area examined.
H expression was assessed by observation of morphological changes seen in H+E stained slides, **Figure 6.12**. The H+E staining did identify areas of syncitia formation. However, similar to the low level of detection of green fluorescence with the Ad GFP samples, the areas of syncitia formation were not widespread or extensive.
Immunohistochemistry was also performed on unstained slides using mouse anti-measles haemagglutinin monoclonal antibody or control, according to the protocol described in Chapter 2. Despite repeated attempts no positive staining was identified.

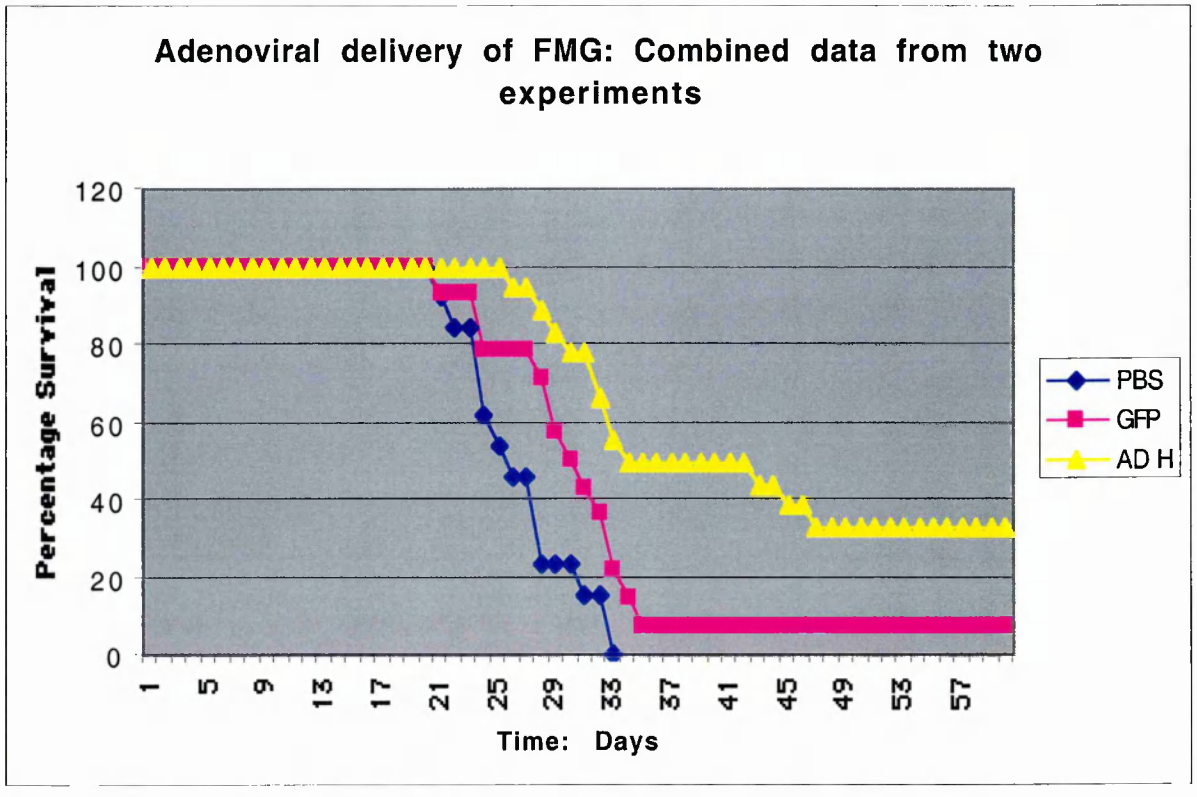

Figure 6.10: Intratumoural injection of Ad H-I-GFP results in improved survival over Ad GFP or PBS controls in nude mice developing HT1080-F tumours.
Nude mice were innoculated with $5x10^5$ HT1080-F cells at day 0. Once palpable at Day 14 tumours were directly injected on 5 consecutive days with PBS, Ad GFP or Ad H-I-GFP. Data from two experiments were combined: n = 13 PBS, 14 Ad GFP and 17 Ad H-I-GFP.

Figure 6.11: HT1080-F tumour sections show a relatively low transduction efficiency by AD-GFP. HT1080 tumours were seeded in nude mice. Once palpable tumours were directly injected with adenovirus or control, daily for 5 days. 2 days after the last injection tumours were harvested and stained with H+E (I) or unstained and observed under light microscope with green filter (II).

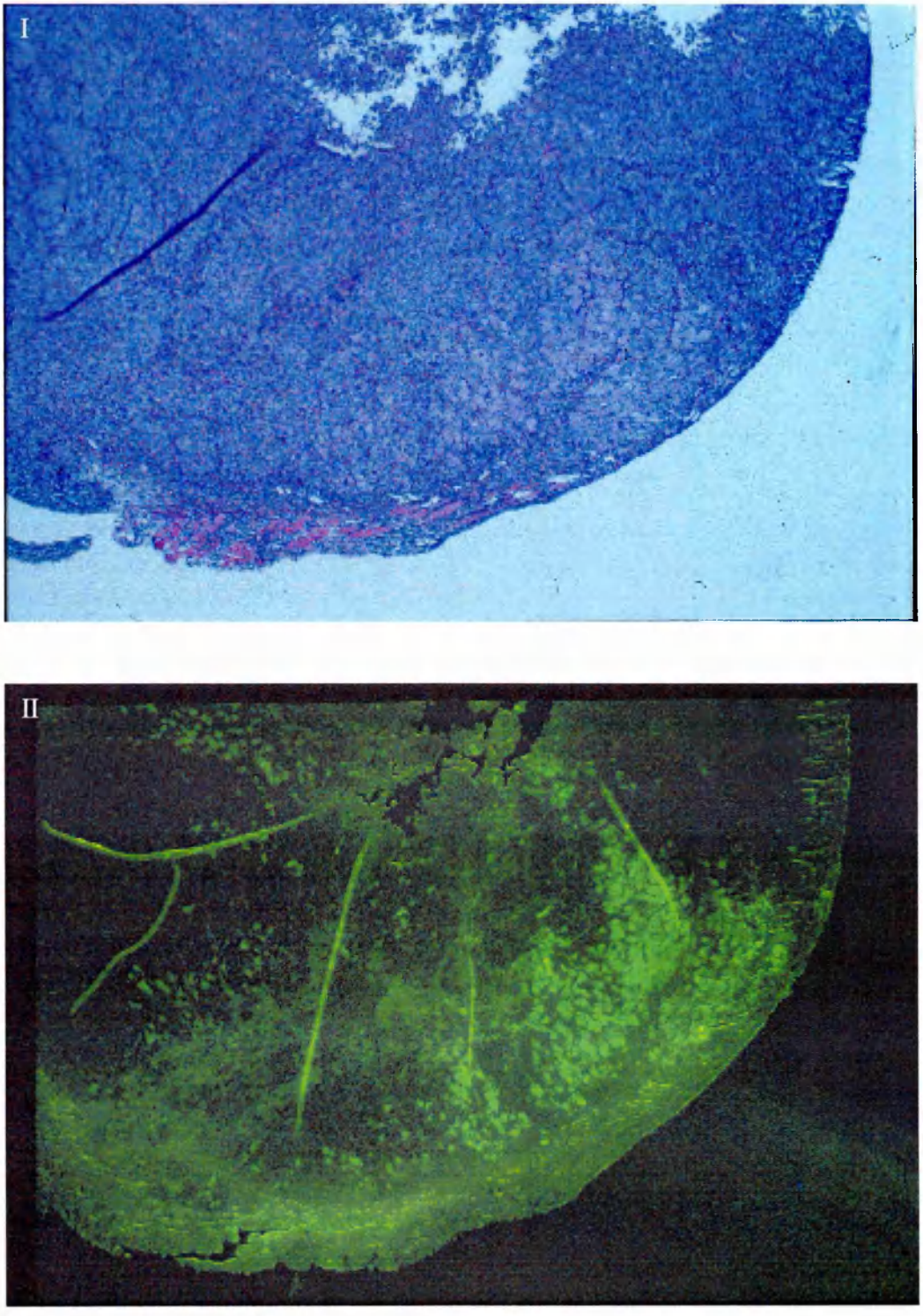

Figure 6.12 : Syncitia formation is identifiable in H+E sections from HT1080-F tumours injected with Ad H-I-GFP. HT1080-F tumours were seeded in nude mice. Once palpable these tumours were injected for 5 days with PBS (I) or Ad H-I-GFP and harvested 2 days later. Light microscope images were obtained at x200 magnification from H+E sections.

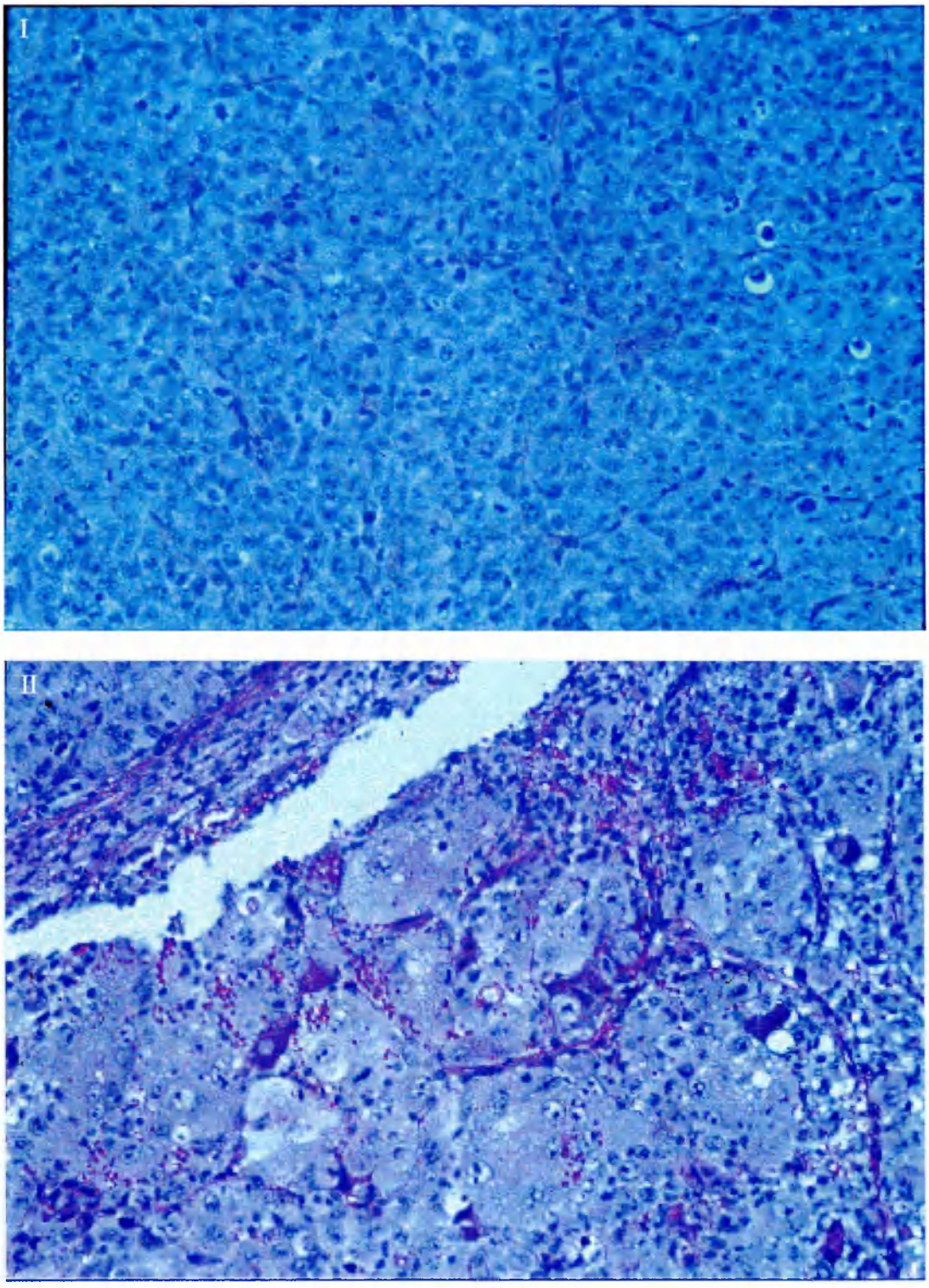

6.3 Discussion

Adenoviral vectors expressing Measles F and H genes were produced in the standard manner using the system from Quantum Biotechnologies. Incorporation of the GFP marker gene facilitated the identification of positive recombinants and aided their subsequent analysis. Ad H-I-GFP could be concentrated to a reasonable titre but Ad F-I-GFP was consistently one log less. This may be due to the direct low level of cytotoxicity seen with F expression in 293 cells (personal observation) but was not formally investigated. In vitro infection of human tumour cells with the recombinant adenoviruses expressing F and H was capable of inducing extensive syncitia formation. Examination of the relative ratio of F to H capable of inducing syncitia and cell death in tumour cells in vitro indicated a wide range of ratios could produce a functional effect. This was studied because of concerns that when the adenoviruses were to be injected in vivo, it was likely that any one cell would be infected by a variable level of each virus. Despite the identification that the ratio of F to H was not critical, a preliminary in vivo experiment indicated syncitia formation within tumours injected with FMG was not widespread. It was decided therefore to assess the in vivo efficacy of FMG mediated cytotoxicity using tumour cells stably expressing F: allowing just one virus to be administered to produce an effect. In a third of mice injected with H expressing adenovirus small tumours were eradicated. Again in tumours excised two days after adenoviral injection the level of gene expression was low; whether it was green fluorescence in the Ad GFP group or syncitia formation in the Ad H-I-GFP group. Specifically less than 10% green fluorescence in the Ad GFP group indicated a significantly reduced level of infection or gene expression than would be expected under the experimental conditions used. This suggested that either the tumour cell line used in these experiments was relatively resistant to adenoviral infection in vivo, or components of the experimental conditions used were sub-optimal. Factors that limited the level of gene expression are being examined in further experiments.

One additional factor that may have led to less than 100% of the mice in the FMG group surviving was that HT1080 or HT1080-F were 'aggressive' when grown in vivo, reaching a volume requiring animal sacrifice after only 20-30 days. A tumour model with a less rapid phenotype was explored in conjunction with a collaborator, Dr E. Galanis, Mayo Foundation. The human glioma U87 tumour cell line was seeded in the flanks of nude

mice and injected with control virus (Ad GFP) or Ad H-I-GFP and Ad F-I-GFP. In the control group 80% of mice had to be sacrificed due to tumour progression between 30-50 days post inoculation whereas 100% of the mice injected with the FMG expressing adenoviruses survived beyond 70 days (Galanis et al., 2001).

These experiments confirmed that the process of syncitia formation and cell death could be induced by adenoviral expression of FMG in vivo. Expression of FMG was associated with a therapeutic effect. This data was obtained in nude mice so that no assessment could be made of the immunostimulatory effects of FMG mediated cell killing which would be predicted to enhance this therapeutic effect.

The data presented in this chapter formed part of the following paper:

Use of viral fusogenic membrane glycoproteins as novel therapeutic transgenes in gliomas

Galanis E, Bateman A, Johnson K, Diaz RM, James CD, Vile R, Russell SJ

Human Gene Therapy 2001 May 1: 12 (7): 811-821

CHAPTER 7: PRODUCTION OF AN ADENOVIRAL VECTOR EXPRESSING GALV

Chapter 7: Production of an adenoviral vector expressing GALV

7.1 Introduction

Despite the relative ease of producing adenoviral vectors expressing Measles F and H genes, GALV was considered the preferred FMG for primary investigation and incorporation into an adenoviral vector for two reasons. Firstly because GALV fusogenicity is contained within one gene product allowing one 'hit' to induce fusion. Second because expression of the GALV protein would be immunostimulatory, potentially promoting a tumour specific immune response and therefore enhanced therapeutic effect in appropriate hosts. This is in direct contrast to the well documented immune suppression seen with Measles infection which is attributable in part to F and H gene expression (see Chapter 1).

However the construction of an adenovirus expressing the fusogenic GALV envelope posed a challenge due to the very nature of direct fusogenicity and therefore cytotoxicity of the individual GALV protein. A number of strategies have previously been implemented for the production of recombinant adenoviruses expressing toxic genes. These strategies can be classified as follows:

1. Development of a resistant adenovirus producer cell line
2. Cytotoxic gene expression under the control of an inducible promoter system
3. Production of an initial recombinant adenovirus with the cytotoxic transgene downstream of a transcriptional silencer. This transcriptional silencer is later excised by a DNA recombinase leading to transgene expression.

I chose to develop a strategy based on the transcriptional silencer approach incorporating the requirement for Cre recombinase.

7.1.1 Cre Recombinase

The Cre/*lox* system originates from the bacteriophage P1 (Sauer, 1987; Sauer, 1993). Cre is a DNA recombinase which performs efficient recombination at *loxP* sites. The *loxP* site consists of two 13 base pair inverted repeats flanking an 8 base pair asymmetric core region. The repeats represent the Cre binding sites, with the central core being the site where recombination occurs and indicates directionality of the site (Hoess and Abremski,

1984). The incorporation of *loxP* sites flanking a DNA sequence, followed by the addition of Cre, results in one *loxP* site and the intervening DNA sequence being excised as a circularised entity. Manipulation of this system allows vectors to be produced with a transcriptional silencer flanked by *loxP* sites introduced upstream of a gene of interest. In the absence of Cre the gene is not expressed. With the addition of Cre the transcriptional silencer is excised and the gene expressed.

In the studies I performed, Cre was either introduced by infection with an adenoviral vector expressing Cre (Ad Cre – Merck Pharmaceuticals) or was stably expressed in those cell lines (293Cre4 cells – Merck Pharmaceuticals, HT1080-Cre a kind gift from Dr K.J.Harrington, Molecular medicine program, Mayo Foundation).

The cloning strategy to produce an adenoviral vector expressing GALV is outlined in **Figure 7.1** and will be detailed below.

7.2 Results

7.2.1 Construction of a recombinant adenoviral shuttle vector expressing transcriptionally silent GALV

An adenoviral shuttle vector incorporating the transcriptional stop sequence (STOP), flanked by lox P sites, 5' of the GALV sequence was produced in two stages: first was insertion of the GALV sequence into the pQBI-AdCMV5-IRES-GFP adenoviral shuttle with a mutated restriction enzyme site to facilitate step two: which was the insertion of the STOP sequence.

The GALV gene was PCR amplified from pCR3.1 GALV using oligonucleotide primers QstopGALV 1 and QstopGALV 2. These primers had the following restriction enzyme sites mutated at their 5' ends:

QstopGALV 1 aaacgcgtgcggccgccgtacgtaaaagacgatggtattgct

Mlu 1 Not 1 BsiW 1

QstopGALV 2 ggggtttaaactctagaggtggccctcctatagtgag

Pme 1 Xba 1

Figure 7.1: Diagramatic representation of the adenoviral shuttle vector produced to contain the transcriptionally silent GALV gene. Green and blue components represent the elements contained within the pQBI-AdCMV5-IRES-GFP vector immediately adjacent to the cloning site.

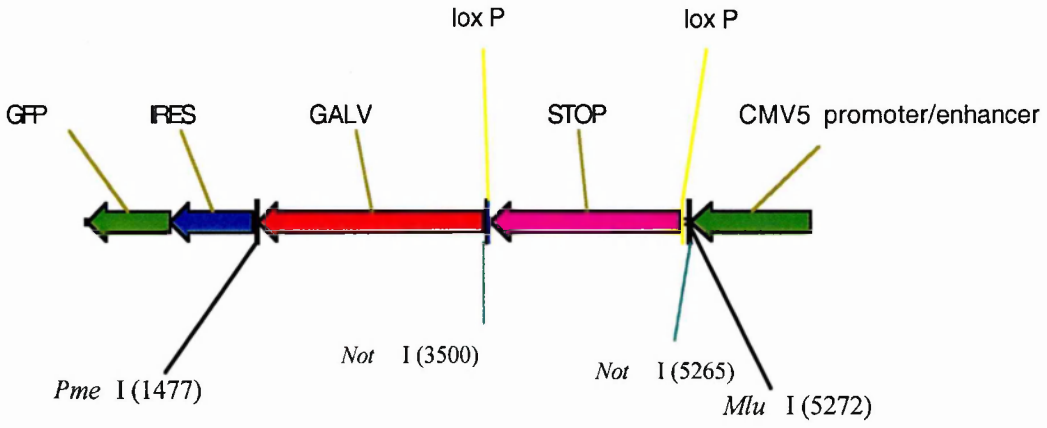

pAd STOP-GALV-I-GFP

In the presence of Cre recombinase the transcriptional STOP sequence is excised and the GALV gene expressed. Excision produces a circularised form containing the STOP and a single lox P site. The same molecular mechanisms occurred in the plasmid or the recombinant adenovirus developed.

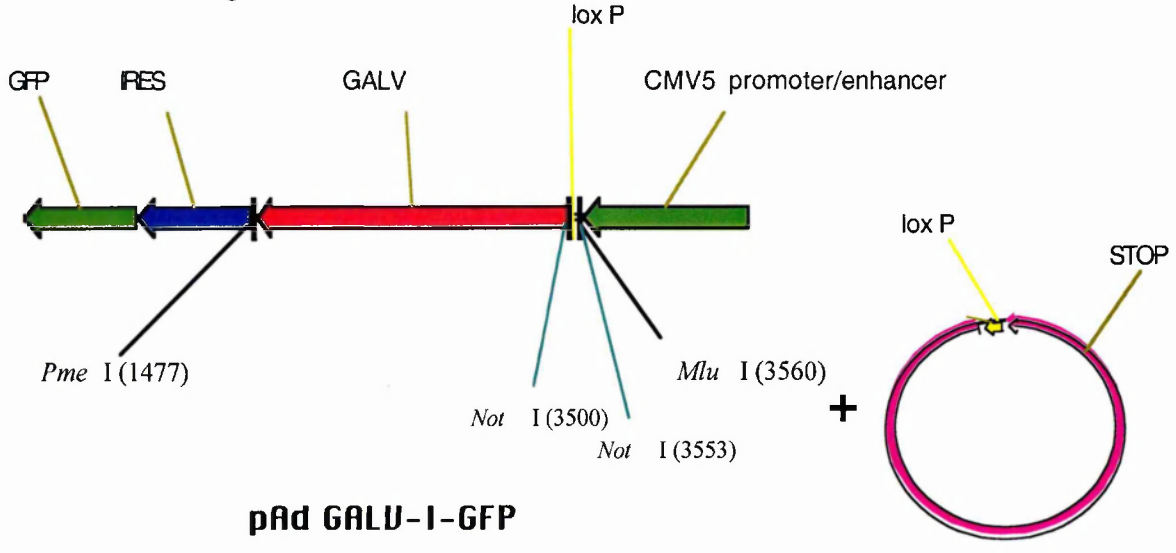

pAd GALV-I-GFP

Circularised Stop and single lox P site

The PCR conditions using AmpliTaq Gold were: 94°C 10 minutes to activate the polymerase, followed by 20 cycles of denaturing at 94°C for 1 minute, annealing at 60°C for 1.5 minutes, extension at 72°C for 4 minutes, and completed with a 10 minute extension at 72°C. The PCR products were cloned into the pCR2.1 vector as an intermediate step using the 'TOPO ligation kit', forming pCR2.1 AdQ GALV.

This vector, pCR2.1 AdQ GALV and pAd F-I-GFP were then digested with *Mlu 1* and *Pme 1*, and GALV ligated into the adenoviral shuttle vector: forming pAd GALV-I-GFP.

This construct was tested for function by transfection onto HT1080 cells; syncitia formation and GFP expression were detected by light and green filter microscopy 48hours post transfection.

7.2.2 Transcription termination (STOP) cassette

The transcription silencer used in the construction of the GALV adenovirus was derived from the RAGE (recombination activated gene expression) vector pBS302 (Gibco BRL). The STOP sequence is flanked by directly repeated *lox* P sequences. At the 5' end of the STOP is a splice donor site followed by a false translation initiation signal (ATG). This is followed by an 825 bp fragment from SV40 containing the polyadenylation signal. The final component is then a 550 bp spacer DNA from the yeast *his3-ded1* region (Lakso et al., 1992). In this vector the whole STOP cassette and flanking *lox* P sequences was isolated as a *Not* 1 fragment.

7.2.3 Construction of pAd STOP-GALV-I-GFP

pBS302 and pAd GALV-I-GFP were digested with Not 1 and the 1.6 kb fragment from pBS302 ligated with the linearised pAd GALV-I-GFP forming pAd STOP-GALV-I-GFP. Orientation of the STOP sequence was confirmed by *Bgl II* restriction enzyme digest: positive orientation confirmed by generating 1.4 kb, 2.2 kb and 8.9 kb fragments.

A correctly orientated pAd STOP-GALV-I-GFP clone was selected and function tested on 293A cells and 293Cre cells. Syncitia formation was clearly identifiable in the Cre expressing cells but was not detected in the parental 293A cells.

7.2.4 Production of an adenovirus containing a transcriptionally silent GALV gene

The production of an adenoviral vector containing a transcriptionally silent GALV was produced following the protocol described in Chapter 2. pAd STOP-GALV-I-GFP was linearised by digestion with Fse 1 and following phenol:chloroform:isoamyl alcohol extraction the DNA was co-transfected with 5μg of QBI-viral DNA onto 293A cells. Plaques appeared at day 5 and 22 were collected (labelled 1^1-22^1). 50μl of the primary stock from these plaques was put onto either HT1080 or HT1080-Cre expressing cells and the development of syncitia with GFP expression looked for. Only plaque 10^1 showed syncitia formation in HT1080-Cre cells and no syncitia formation in HT1080 cells. Plaque purification of plaque 10^1 followed methods previously described. 40 plaques collected after several attempts were unable to produce a purified clone capable of inducing syncitia formation. Consequently plaque 10^1 was carefully assessed for 'purity' by serial dilution and infection onto both 293A and 293Cre cells. The day following infection the cells were overlayed with agarose and the development of plaques observed. The 293A cells developed plaques as normal where as the 293Cre cells developed significantly abnormal plaques with syncitia formation and GFP expression, see **Figure 7.2.** Importantly there was no 'normal' plaque formation in the 293Cre cells to suggest another 'contaminating' adenovirus. Therefore clone 10^1 primary stock was used to progress to the amplification and purification stages of Ad STOP GALV-I-GFP.

7.2.5 Titre of purified Ad STOP GALV-I-GFP

The purified Ad STOP GALV-I-GFP was titred using the standard methods described in Chapter 2. The optical absorbance reading was:

OD_{260}= 0.2714 Corrected value with dilution factor 1:25 = $6x10^{12}$ total viral particles (average of two assays)

The plaque assay gave a reading of:

Pfu = $3 x10^{10}$ (average of two plaque assays)

The purified Ad STOP GALV-I-GFP was tested for activity by infection of HT1080 and HT1080-Cre expressing cells. Virus was put onto cells in 6 well plates at an m.o.i. of 10. There were no morphological changes or GFP expression seen in the HT1080 cells;

Figure 7.2: Syncitia formation and abnormal CPE seen with Ad STOP GALV-I-GFP infecting 293 Cre cells:

A) 293 Cre cells. B) infected with Ad STOP GALV-I-GFP at 18 hours. C) at 24 hours

A

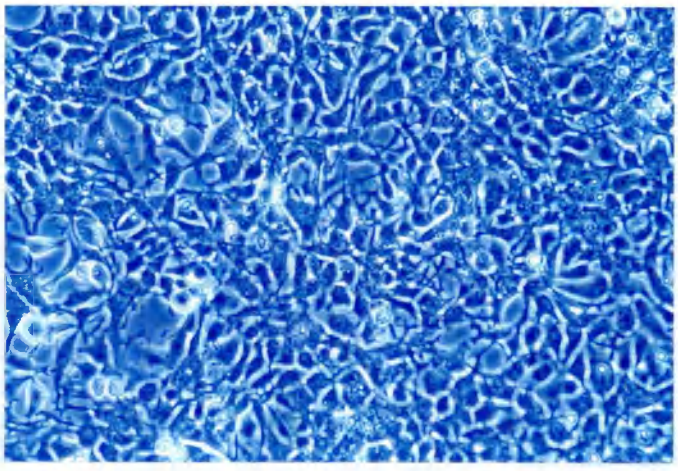

B

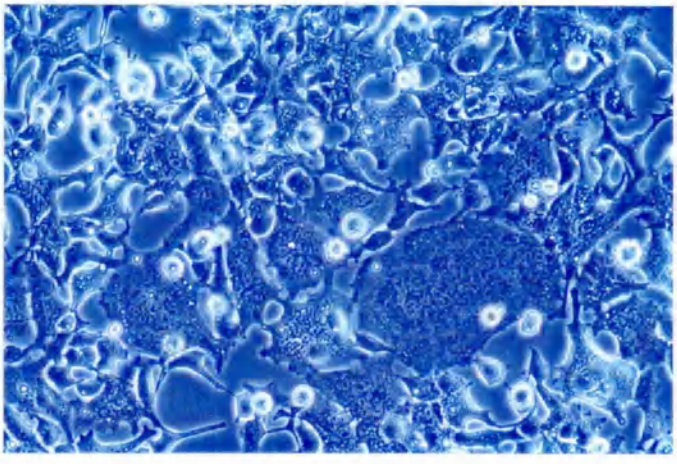

C

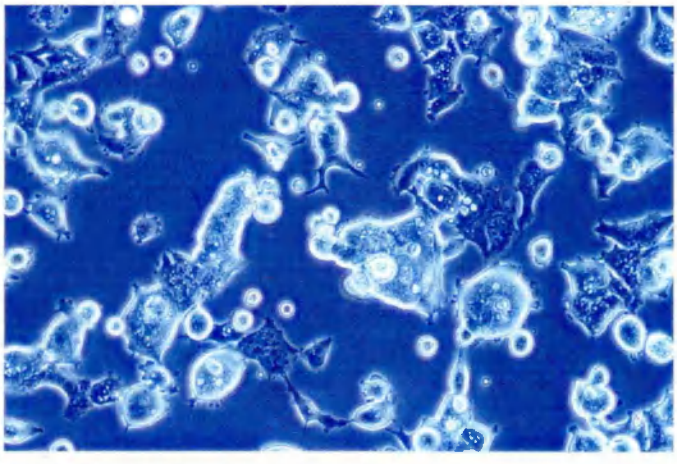

widespread syncitia formation with GFP expression was seen in the Cre expressing cell line.

7.2.6 Production of an adenovirus containing a transcriptionally active GALV gene

Ad GALV-I-GFP virus was produced by infecting 293Cre cells at a m.o.i. of 10 with Ad STOP GALV-I-GFP. 16 175cm^2 flasks of 293Cre cells were infected. Abnormal CPE developed rapidly and rounded up cells and syncitia were collected at 36 hours and recombinant adenovirus purified.

The titre of purified Ad GALV-I-GFP was then assessed by optical absorbance:
OD_{260}= 0.387 Corrected value with dilution factor 1:25 = $8.5x10^{12}$ total viral particles (average of two assays).

It was impossible to perform a plaque assay in the conventional manner due to the cytotoxicity of Ad GALV-I-GFP on 293 cells. In view of the OD_{260} value a provisional approximation of pfu was made of $4x10^{10}$.

The activity of Ad GALV-I-GFP (and the accuracy of the titre estimation) was confirmed by infecting HT1080 cells at a m.o.i. of 10. Widespread syncitia formation and GFP expression was seen, see **Figure 7.3**.

7.2.7 Confirmation of recombinant adenovirus by Hirt extraction

Incorporation of the GALV gene or STOP sequence within the recombinant adenoviruses was confirmed by Hirt extraction. The recovered DNA was analysed by PCR: 2µl of sample DNA was added per PCR mix.
Primers QstopGALV 1 and QstopGALV 2 were used to test for incorporation of the GALV gene. The PCR was performed using AmpliTaq with the following conditions: 94°C for 10 minutes, then 30 cycles of 94°C for 1 minute, 60°C for 1.5 minutes, 72°C for 4 minutes. The result is shown in **Figure 7.4A:** all samples contain the GALV gene as evidence by a 2 kb band except sample 4 which represents the Ad GFP control.

Figure 7.3: Adenovirus infection of HT1080 cells: Light microscope and green filter

Syncitia formation and GFP expression seen with STOP sequence excised by Cre; either when present in adenoviral producer cells resulting in Ad GALV-I-GFP (iv), or present in cells at time of Ad STOP GALV-I-GFP infection (iii).

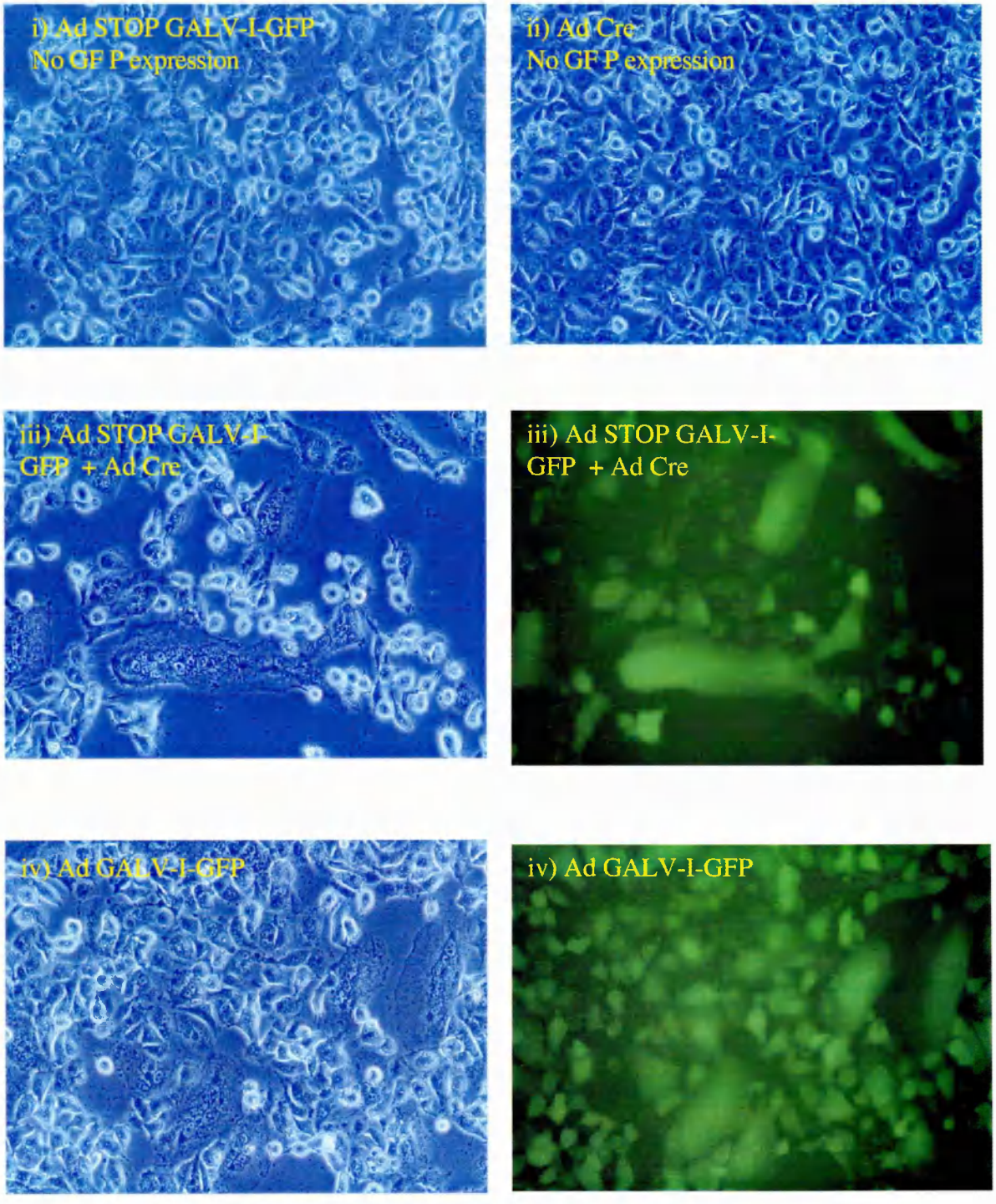

Figure 7.4: Diagnostic PCRs performed on Hirt extracted DNA from 293A cells infected with recombinant adenoviruses

A) PCR performed using primers designed to detect the presence of the GALV gene

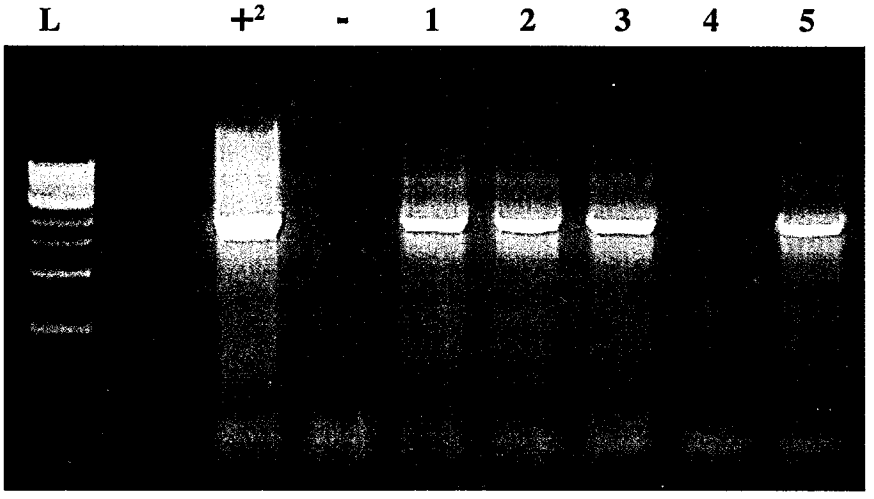

B) PCR performed using a forward primer complimentary to the 3' end of the CMV promoter and a reverse primer complimentary to the 3' end of the GALV gene: If the STOP GALV sequence is present a positive band at 3.6 kb results, if the STOP sequence is absent a 2.1 kb band is produced.

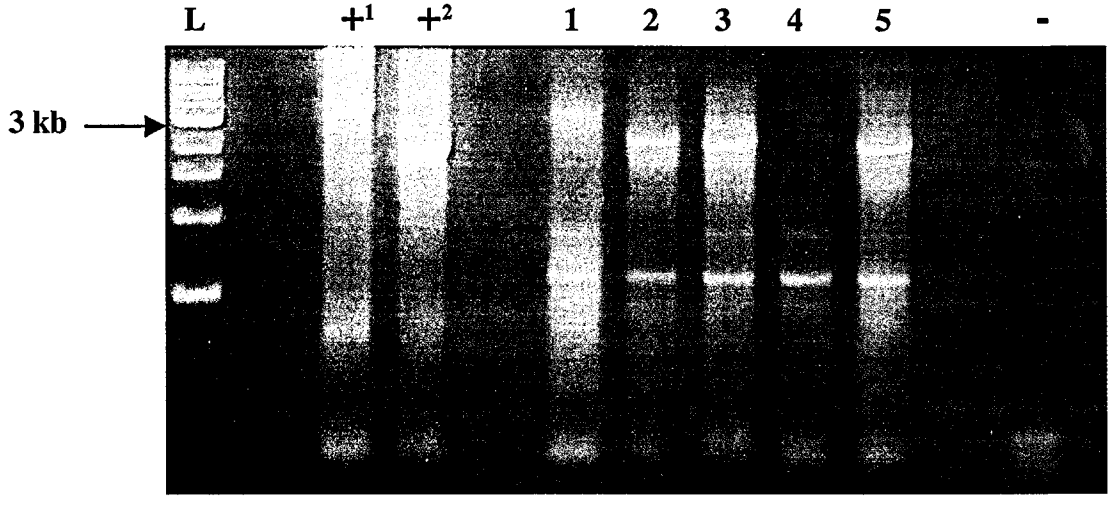

L	1 kb ladder	1	Ad STOP GALV-I-GFP
		2	Ad STOP GALV-I-GFP + Ad CRE
+1	pAd STOP-GALV-I-GFP	3	Ad GALV
		4	Ad GFP
+2	pAd GALV-I-GFP	5	Ad STOP GALV-I-GFP infecting
-	No input DNA		293 Cre cells

To test by PCR for the incorporation of the STOP sequence a forward primer was used, which was complimentary to the 3' end of the CMV5 promoter: AdQ CMV 1999 (sequence commenced at bp1999 in the pQBI-AdCMV5-IRES-GFP plasmid). The reverse primer was QstopGALV 2. A diagramatic representation of the PCR is shown below:

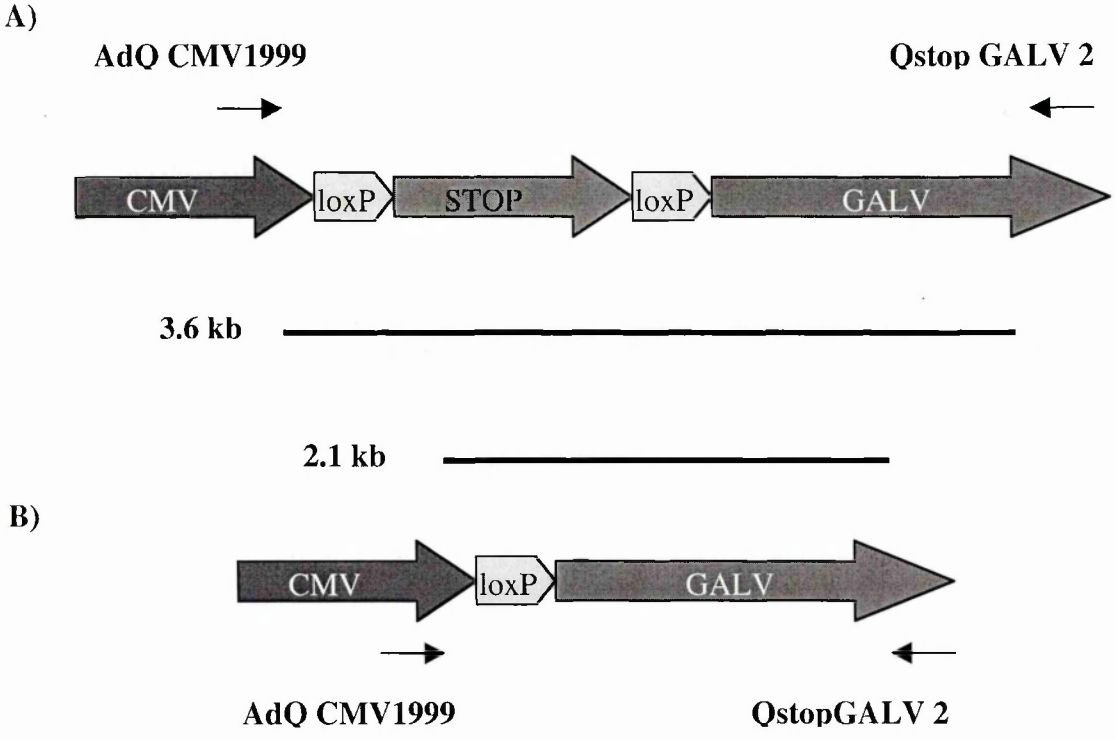

In samples where the STOP sequence was present a 3.6kb band would be produced, if excised by Cre recombinase a 2.1kb band would be produced. The result can be seen in **Figure 7.4B**. Sample 1 represents Ad STOP GALV-I-GFP and a 3.6kb band can be identified matching the band seen in lane $+^{1}$, the positive control pAd STOP GALV-I-GFP. The remaining samples from cells infected with Ad STOP GALV-I-GFP occurred in the presence of Cre; either stably expressed as in the 293Cre cells (sample 5) or transiently following co-infection with Ad Cre (sample 2). Sample 3, from cells infected with Ad GALV-I-GFP, again shows no evidence of STOP sequence incorporation. The 2.1kb bands seen in lanes 2, 3 and 5 are larger than the band seen in lane **+2.** This is because pAd GALV-I-GFP lacks the short sequence downstream from the 5' *Not 1* site to the lox P site and the single lox P site, both of which remain following Cre excision of the STOP sequence.

7.2.8 Assessment of the efficiency of Cre excision in Ad GALV production

Additional evidence was obtained to indicate the very efficient excision of the STOP sequence. This was by serial dilution of Ad GALV-I-GFP infection on HT1080 or HT1080-Cre expressing cells. If Ad GALV-I-GFP contained significant amounts of 'unprocessed' Ad STOP GALV-I-GFP then it was expected that there would have been a differential in syncitia formation between HT1080 and HT1080-Cre. Cells were plated in 6 well plates as previously. The following day Ad GALV-I-GFP at m.o.i. of 100-0.01 serial log dilutions were used to infect both cell lines. Development of syncitia was observed and quantified. At 48 hours there was no difference between HT1080 or HT1080-Cre infected with Ad GALV-I-GFP: there was massive cell death at m.o.i. of 100, +++++ syncitia formation at an m.o.i. of 10 and no morphological changes seen at lower m.o.i.'s. The experiment was performed in duplicate and the results are representative of both of these.

7.2.9 Assessment of expression of GALV recombinant adenoviruses

Identification of both GALV and GFP expression was assessed by rtPCR. HT1080 cells were plated in 25cm^2 flasks and then infected with adenovirus the following day. A m.o.i. of 10 was used for each virus and the infection allowed to proceed for 72 hours. Total RNA was then prepared followed by cDNA. The cDNA was then tested in a number of PCRs, see **Figure 7.5**. The constitutively expressed GAPDH gene was identified in samples 1-5 indicating succesful RNA extraction and cDNA synthesis. The reverse transcriptase negative controls for each sample (samples 6-10) showed no band indicating no DNA contamination. This negative control was also repeated for the GALV PCR to indicate no contamination with extrachromosomal DNA. GALV gene expression was identified strongly for samples 2 and 5; corresponding to cells infected with Ad GALV-I-GFP and co-infected with Ad STOP GALV-I-GFP and Ad Cre respectively. A low level of GALV expression was identified in cells infected with Ad STOP GALV-I-GFP suggesting incomplete transcriptional inactivation by the STOP sequence. This was also evident in the PCR to detect GFP expression: a strong signal was detected in the cells infected with Ad GALV-I-GFP or co-infected with Ad STOP GALV-I-GFP and Ad Cre, with a smaller signal in cells infected with Ad STOP GALV-I-GFP. These findings were

Figure 7.5: rtPCRs of RNA extracted from HT1080 cells infected with GALV recombinant adenoviruses

A) GAPDH

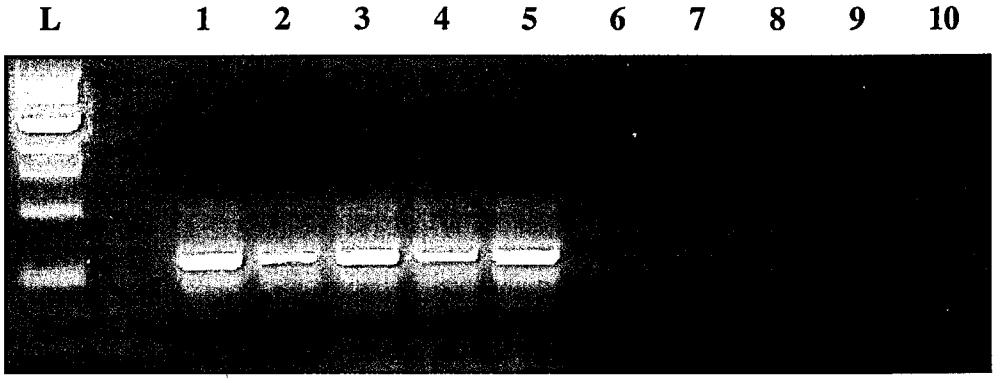

B) GALV

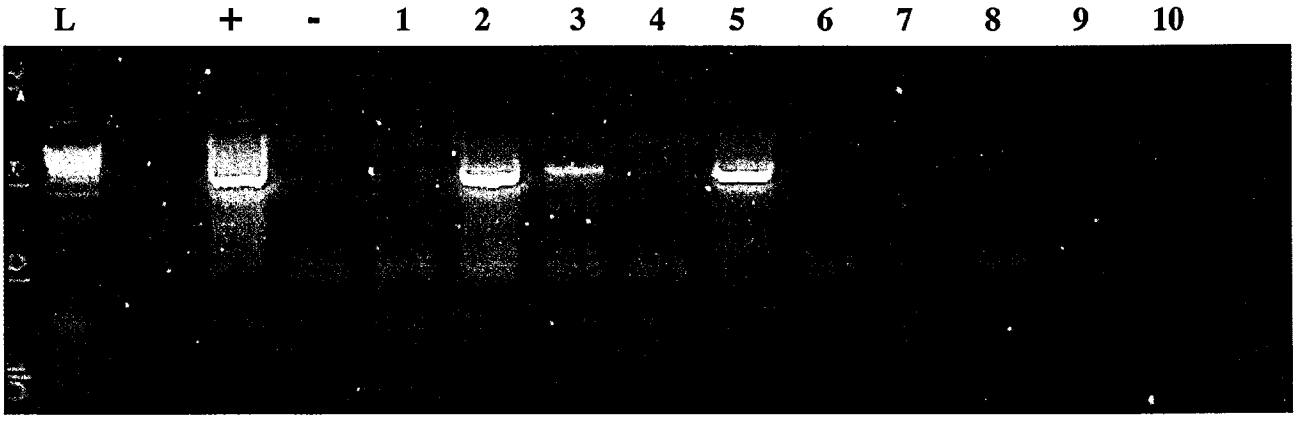

C) GFP

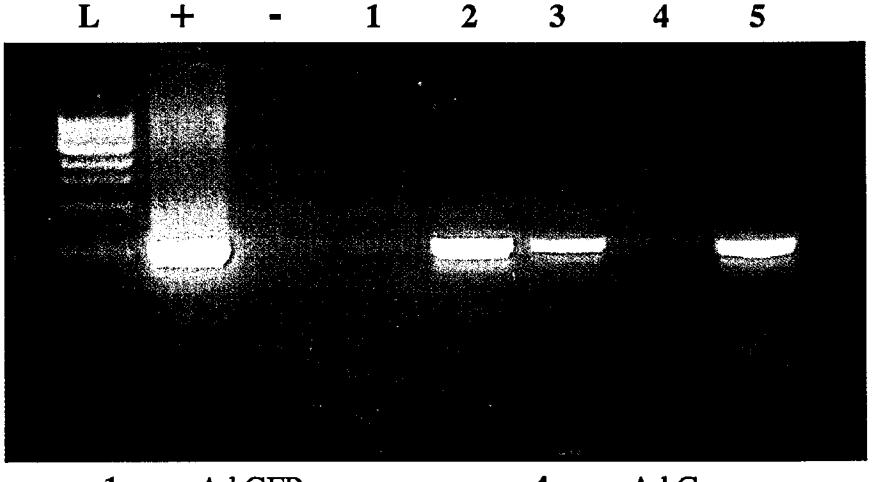

L	Ladder	1	Ad GFP	4	Ad Cre
+	Positive control	2	Ad GALV-I-GFP	5	Ad STOP GALV-I-GFP + Ad Cre
-	Negative control	3	Ad STOP GALV-I-GFP		

6 - 10 rt negative controls corresponding to samples1-5

consistent with the morphological changes previously described in **Figure 7.3**. Most notable was the lack of syncitia formation or visualisation of GFP expression from cells infected with Ad STOP GALV-I-GFP.

The GAPDH PCR was performed using the primers and conditions outlined in Chapter 2. The GALV PCR was performed using the QstopGALV1 and 2 primer pair, with the conditions previously listed.

The GFP PCR was performed using primers complementary to a 500bp sequence identified within the GFP gene contained within pQBI-CMV5-IRES-GFP:

Forward: gataatggtctgctagttgaacgcttccat

Reverse: atggctagcaaaggagaagaactcttcact

The conditions used were with AmpliTaq polymerase: 94°C for 10, then 30 cycles of 94 °C for 1min, 60 °C for 1.5min, 72 °C for 2min.

7.3 Discussion

A functional adenovirus expressing GALV was produced using a transcriptional silencer/DNA recombinase approach. This strategy was able to bypass the FMG cytotoxicity to the human adenoviral producer cells (293A). Without silencing, the initial transfection of adenoviral shuttle vector with adenoviral backbone would have induced extensive syncitia formation and cell death, preventing recombination and production of recombinant adenovirus. Even with the silencer the number of positive recombinants was low; one recovered from 22 plaques collected. This was presumably due to the incomplete silencing of the GALV gene in the STOP containing vectors, as seen by detectable GALV mRNA expression from Ad STOP GALV-I-GFP (**Figure 7.5**), leading to cell death and failure to produce virus.

The efficiency of the Cre/*lox* system was highlighted by the inability to detect residual Ad STOP GALV-I-GFP following infection and purification from 293Cre cells. The titre of Ad GALV-I-GFP recovered indicated syncitia formation per se was not an inhibitor to viral production. Sufficient titre of GALV expressing adenovirus has been produced and the virus been shown to be active in vitro. The next step of testing Ad GALV-I-GFP in appropriate in vivo models will be embarked upon.

CHAPTER 8: CO-EXPRESSION OF FMG AND CYTOKINE

Chapter 8: Co-expression of FMG and Cytokine

8.1 Introduction

Achieving the optimum therapeutic approach is the aim of all cancer therapies. As discussed previously an integral part of a successful gene therapy strategy will likely be the generation of a tumour specific immune response. Optimising the conditions of the gene therapy strategy to generate this immune response is an important concern. FMG gene therapy, as previously discussed, would appear to have suitable components for generating a pro-inflammatory environment as it includes proteins of viral origin, induction of HSPs and a necrotic cell death process. Combining these aspects with agents likely to enhance an immune response was an attractive proposal. Due to the biologic activity discussed in Chapter 1, GM-CSF was considered an appropriate cytokine to combine with FMG in a co-expression strategy. The scenario envisaged was that FMG would induce tumour cell death and release tumour antigens in a pro-inflammatory environment. APCs attracted to the site would encounter high local levels of GM-CSF. This would promote APC antigen uptake, maturation and trafficking to lymph nodes. There by facilitating the generation of a tumour specific cellular and humoral immune response.

Expression of two genes in the same cell at the same time is best achieved by combining both genes in the same construct rather than attempting to get two vectors into the same cell. Expression of these two genes, in this case FMG and GM-CSF, can be engineered by a number of mechanisms. Probably the most experience has been gained using internal ribosome entry site (IRES) elements. Bicistronic expression vectors are designed to have the first gene translated in a cap-dependent manner and the second gene in an IRES-dependent manner. IRES elements were first identified in picornavirus RNAs such as encephalomyocarditis virus. They have now been identified in a range of viral and cellular eukaryotic mRNAs (Martinez-Salas, 1999). Although having widely differing neucleotide sequence and length the majority share a Y shaped secondary structure. This structure allows the IRES containing mRNA to remain preferentially associated with polysomes (Martinez-Salas, 1999). The IRES driven expression can be lower than the cap-dependent expression but this can be a variable phenomenon.

Additional studies designed to promote the production of two or more gene products from a single vector have included use of a single cistron encoding multiple products as a single fusion protein. This fusion protein contains cleavage sites for proteases; so that on encountering the specific protease the fusion protein is cleaved into its constitutive components. An example of this approach are 'Fusagene' vectors which aim to recruit the ubiquitous endoprotease Furin (Gaken et al., 2000). The approach mirrors what is occuring in normal physiology. Namely that many polypeptides are initially synthesised as large inactive precursors. Processing then occurs in the endocytic pathway at the level of the *trans*-Golgi network. Proteolytic cleavage is brought about by furin acting at the consensus sequence Arg-Xaa-(Lys/Arg)-Arg releasing the active peptide (Denault and Leduc, 1996; Nakayama, 1997). In Fusagene vectors the chimeric fusion protein can contain a number of active proteins separated by furin sensitive consensus sequences which, following processing, release the individual biologically active proteins (Gaken et al., 2000).

Another family of proteases can be recruited to activate a chimeric fusion protein in a similar manner. Matrix metalloproteinases (MMP) recognise a consensus sequence Pro-Leu-Gly-Leu-Trp-Ala and this can be incorporated into the fusion protein sequence. Here it is expected cleavage will occur extracellularly and only in conditions where MMPs are activated, most notably in tumours. This approach was shown to be effective for a strategy aiming to target retroviral vectors (Peng et al., 1999). A polypeptide fused to the SU of the viral envelope glycoprotein inhibited viral entry. However on encountering MMP the polypeptide was cleaved and viral entry possible. This strategy appeared particularly attractive to co-expression as it appeared to offer a mechanism of producing both biologically active and targeted FMG and GM-CSF. In the absence of MMP GM-CSF would be bound to FMG and inhibit its fusogenicity. This would occur in the normal tissue environment, see **Figure 8.1**. However expression of the fusion construct in a tumour environment where MMP are active; fusion, syncitia formation and death would occur in association with high local concentration of GM-CSF, see **Figure 8.1**.

This chapter therefore details the production of vectors capable of expressing both GM-CSF and GALV: vectors containing an IRES, furin sensitive and MMP sensitive sites as well as a control vector linking GM-CSF to GALV via a non-cleaveable linker. The non-

Figure 8.1: Diagrammatic representation of rationale for co-expression strategy utilising an MMP sensitive linker

I. Normal cellular environment - no matrix metalloproteinases (MMP), no fusion.

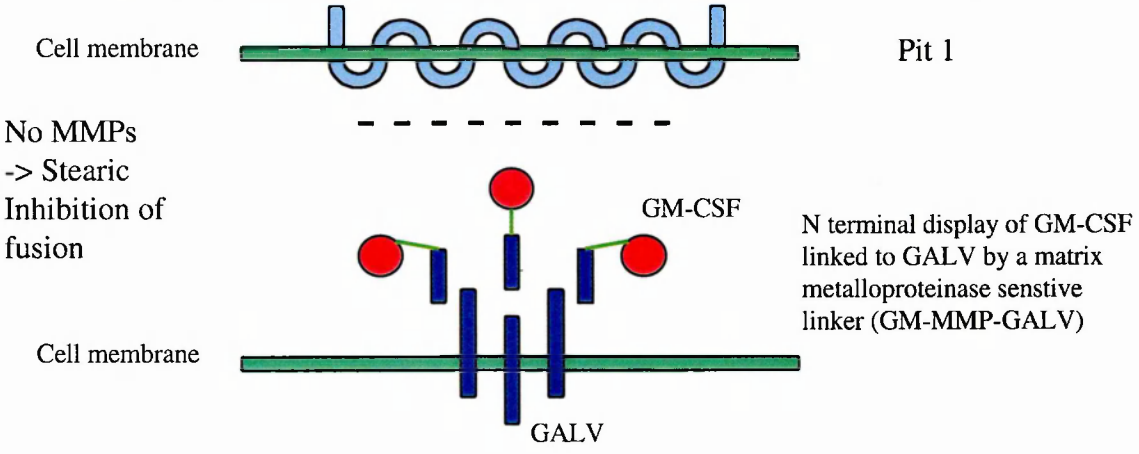

II. Tumour environment: Transfected cells expressing GM-MMP-GALV in the presence of tumour associated MMP are capable of fusing neighbouring cells after cleavage of GM-CSF (**1**). Syncitia form then die necrotically; releasing HSPs, tumour antigens and intracellular contents (**2**). The pro-inflammatory environment attracts professional antigen presenting cells (**3**). These engulf antigen (**4**). High local concentration of GM-CSF promotes APC maturation and trafficking to local lymph nodes (**5**).

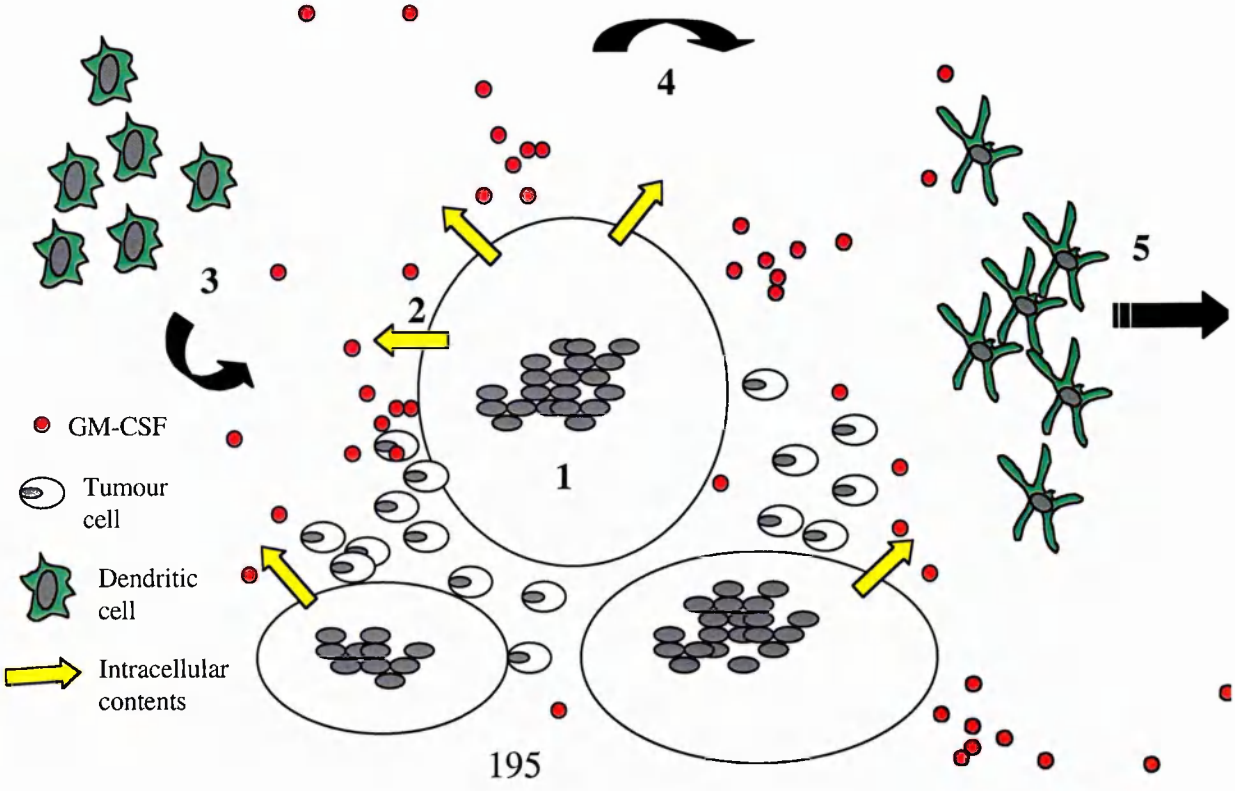

cleaveable linker had the consensus sequence Gly-Gly-Gly-Gly-Ser. This had previously been shown to fulfill the desired role of being non-cleaveable (Peng '99). Once produced these vectors were then investigated to assess their properties.

8.2 Results

8.2.1 Production of pCR3.1 co-expression constructs

A diagrammatic representation of the constructs used in this chapter is seen in **Figure 8.2** The human granulocyte-macrophage colony-stimulating factor gene (GM-CSF) was contained within a non-expression vector pRgM-3 (kind gift of Dr Jackson, ICRF, Leeds). This was used as a DNA template in a PCR using primers:

GM3 cgtacgcgtacggctggaggatgtggctgcag
BsiW1BsiW1

GM4 cgtacgcgtacgatgcctgtatcagggtcagt
BsiW1BsiW1

PCR was performed using AmpliTaq with the following conditions: 94°C for 10 minutes, followed by 30 cycles of denaturing at 94°C for 1 minute, annealing at 60°C for 1.5 minutes and extension at 72°C for 2 minutes. The PCR product was TA cloned into pCR3.1 forming pCR3.1 GM-CSF.

Three 'linker' constructs were produced in the same manner: first GM-CSF was TA cloned into pCR3.1. Primers were written which removed the STOP codon and added *BsiW 1* restriction enzyme sites at the 3' end of the gene:

Forward actagttggaggatgtggctgcagacgctgctg
Spe 1

Reverse cgtacgcgtacgctcctggactggctcccagca
BsiW1BsiW1

Figure 8.2: Co-Expression constructs: All inserts are in the pCR3.1 vector. GM-CSF (1) and GALV (4) expression vectors contain the complete cDNA of the respective genes. Linker constructs (2): Furin sensitive, matrix metalloproteinase sensitive and non-cleaveable constructs contain GM-CSF cDNA with the Stop sequence removed, then the linker sequence followed by the GALV cDNA with its leader sequence removed. The IRES construct (3) contains the full GALV cDNA, the IRES sequence from the encephalomyocarditis virus followed by the GM-CSF cDNA in frame.

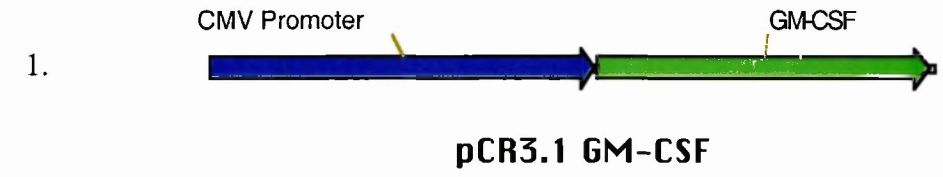

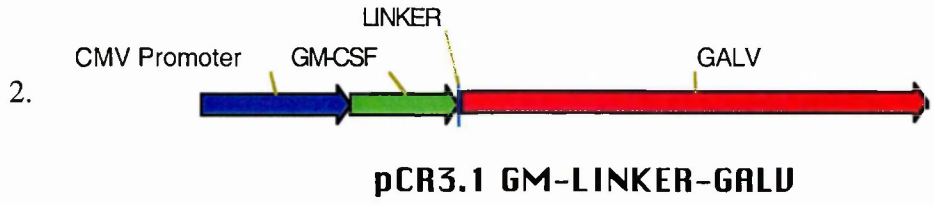

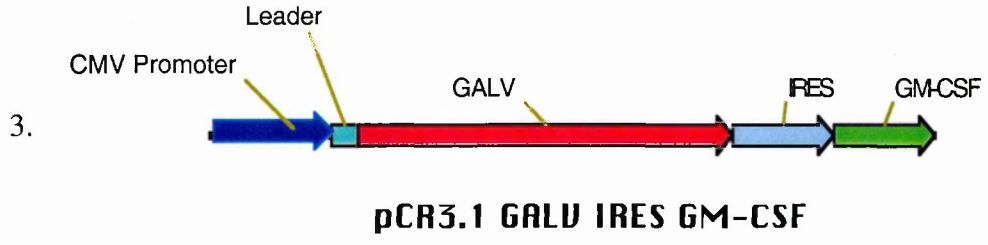

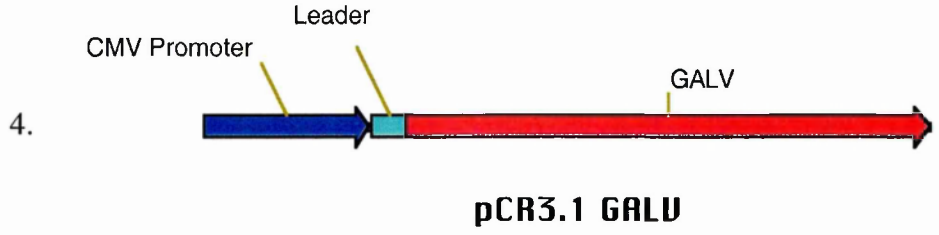

This PCR product was then TA cloned into pCR3.1, producing pCR3.1 GM L. This formed the 5' sequence of all the 'linker' constructs. The downstream component was again produced by PCR cloning: forward primers were written which were complementary to the GALV sequence just 3' to the leader sequence, with BsiW 1 sites and the linker sequence added. Forward primers:

Furin sensitive linker: cgtacgcgtacg**cgattaaggaga**agtctgcaaaataagaacccccaccag
BsiW1BsiW1 **R L R R** 'leaderless' GALV sequence

MMP sensitive linker: cgtacgcgtacg**cctttgggactttgggca**agtctgcaaaataagaacccccaccag
BsiW1BsiW1 **P L G L W A** 'leaderless' GALV sequence

Non cleaveable linker: aaacgtacg**ggaggaggaggaagt**agtctgcaaaataagaacccccaccag
BsiW1 **G G G G S** 'leaderless' GALV sequence

The same reverse primer was used for each PCR which also included a BsiW 1 site:

GALV 2: acgcgtacgcgtggtggccctcctatagtgag
BsiW1

All three 'linker' GALV components were produced by PCR using pCR3.1 GALV as the DNA template. The conditions for the PCR were the same using AmpliTaq gold: 94°C for 10 minutes followed by 20 cycles of denaturing at 94°C for 1minute, annealing at 60°C for 1.5 minutes and extension at 72°C, followed by a final extension at 72°C for 10 minutes. The PCR products were TA cloned into pCR3.1 in the standard manner forming pCR3.1 Furin GALV, pCR3.1 MMP GALV, pCR3.1 G_4S GALV.

To form the co-expression constructs pCR3.1 GM L and pCR3.1 'linker' GALV were cut with *BsiW 1*; linearising pCR3.1 GM L and dropping out the 'linker' GALV sequence. These were then ligated. Correct orientation of the 'linker' GALV fragment was confirmed by diagnostic restriction enzyme digest with *EcoR V*: a positive orientation producing 5.5kb and 2kb bands, a negative 7.5kb and 165bp bands. Correctly orientated

clones were selected and formed pCR3.1 GM-F-GALV, pCR3.1 GM-MMP-GALV and pCR3.1 GM-G_4S-GALV.

An IRES containing construct was also produced to co-express GALV and GM-CSF genes. This again involved a number of cloning steps. The first was to insert GM-CSF in frame immediately downstream of the IRES sequence in the pCITE-2a vector (Novagen). This was produced by PCR cloning using primers to form appropriate restriction enzyme sites in the GM-CSF gene. The forward primer introduced an *Nco 1* site at the start codon (atg) allowing future insertion into the pCITE-2a vector and by doing so mutated the second amino acid in the GM-CSF leader sequence from a tryptophan to glycine (mutated base t → g shown in bold):

Forward primer: acgcgtccatg**g**ggctgcagagcctgctgctc

Nco 1

Reverse primer: cccgggtctagatcactcctggactggctccca

Xma 1 Xba 1

PCR was performed with pCR3.1 GM-CSF as template DNA using AmpliTaq gold and the following conditons: 94°C for 10 minutes followed by 20 cycles of denaturing at 94°C for 1minute, annealing at 60°C for 1.5 minutes and extension at 72°C, followed by a final extension at 72°C for 10 minutes. The PCR product was TA cloned into pCR3.1 in the standard manner forming pCR3.1 GM-I. This construct was confirmed to be functional by transient transfection into HT1080 cells, collection of the supernatant after 48 hours and analysis by ELISA.

Restriction enzyme digest with *Nco 1* and *Xba 1* of pCR3.1 GM-I and the pCITE-2a vector was performed with ligation of GM-CSF downstream of the IRES sequence producing pCITE GM-CSF.

The pCITE GM-CSF vector was then used as template DNA in a further PCR to allow cloning into pCR3.1 GALV. This next step used the following primers:

Forward: accctcgaggggcgaattaattccggttat

Xho 1

Reverse: aaatctagatcactcctggactggctccca

Xba 1

The PCR was performed as before using AmpliTaq gold and the following conditons: 94°C for 10 minutes followed by 20 cycles of denaturing at 94°C for 1minute, annealing at 60°C for 1.5 minutes and extension at 72°C. The PCR product was run on an agarose gel, the 900bp band representing IRES-GM-CSF excised and purified. The eluted DNA and pCR3.1 GALV were then digested with *Xho 1* and *Xba 1* and ligated. Insertion of the IRES-GM-CSF fragment downstream of the GALV gene in pCR3.1 GALV was confirmed by *Pme 1* restriction enzyme digest which dropped out a 3.2kb fragment. A suitable clone was selected and formed pCR3.1 GALV IRES GM.

All constructs were sequenced by automated sequencing, performed by the DNA sequencing Core facility, Mayo Foundation, and found to exactly match the predicted data.

8.2.2 Initial analysis of co-expression constructs: assessment by light microscopy

The co-expression constructs were then compared in transient transfection of HT1080 cells using the Effectene protocol and syncitia formation observed over the subsequent 3 days. pCR3.1 GM-CSF and pCR3.1 GALV were used as controls. The fusion index was used to score syncitia formation. The results from a number of experiments are summarised in **Table 8.1** and representative images seen in **Figure 8.3**.

Plasmid	Day 1	Day 2
pCR3.1 GM-CSF	-	-
PCR3.1 GM-F-GALV	+++	++++
PCR3.1 GM-MMP-GALV	+/++	++/+++
pCR3.1 GM-G_4S-GALV	-	-
PCR3.1 GALV-IRES-GM	+++	++++
PCR3.1 GALV	+++	++++

Table 8.1: Transient transfection of co-expression constructs and assessment of syncitia formation. HT1080 cells were transiently transfected with the plasmids listed and syncitia formation recorded according to the fusion index. The data represent results from greater than three experiments. Syncitia formation equivalent to pCR3.1 GALV is seen with the furin and IRES constructs, somewhat reduced fusion is seen with the MMP construct and no fusion seen with the non-cleaveable linker G_4S (see also **Figure 8.3**).

8.2.3 Initial analysis of co-expression constructs: assessment by ELISA

ELISA data from the same experiments is presented in **Figure 8.4**. After overnight transient transfection supernatant was removed from the cells, the cells washed and 2ml fresh media added/well of a 6 well plate. After each subsequent 24 hour period the supernatant was collected, spun down and the supernatant collected for future analysis. Fresh media was added as before.

These initial results indicated that all co-expression constructs secreted GM-CSF but at varying levels relative to pCR3.1 GM-CSF: the IRES construct less, MMP and G_4S constructs equivalent amounts and the furin construct significantly more. They also demonstrated that the GALV expression from these constructs could induce cell-cell fusion except in the case of the non-cleaveable G_4S linker, but also that the fusion process seemed somewhat impaired in the MMP construct relative to GALV. The specific questions that arose from these preliminary data are addressed for each individual linker construct below.

Figure 8.3: Light microscopic examination of HT1080 cells transfected with co-expression constructs. Images collected at 24 hours post transfection. No fusion seen with pCR3.1 GM-CSF (i) and pCR3.1 GM-G_4S-GALV (iv), moderate fusion seen with pCR3.1 GM-MMP-GALV(iii), extensive fusion seen with pCR3.1 GALV (vi), pCR3.1 GM-F-GALV (ii) and pCR3.1 GALV IRES GM (v).

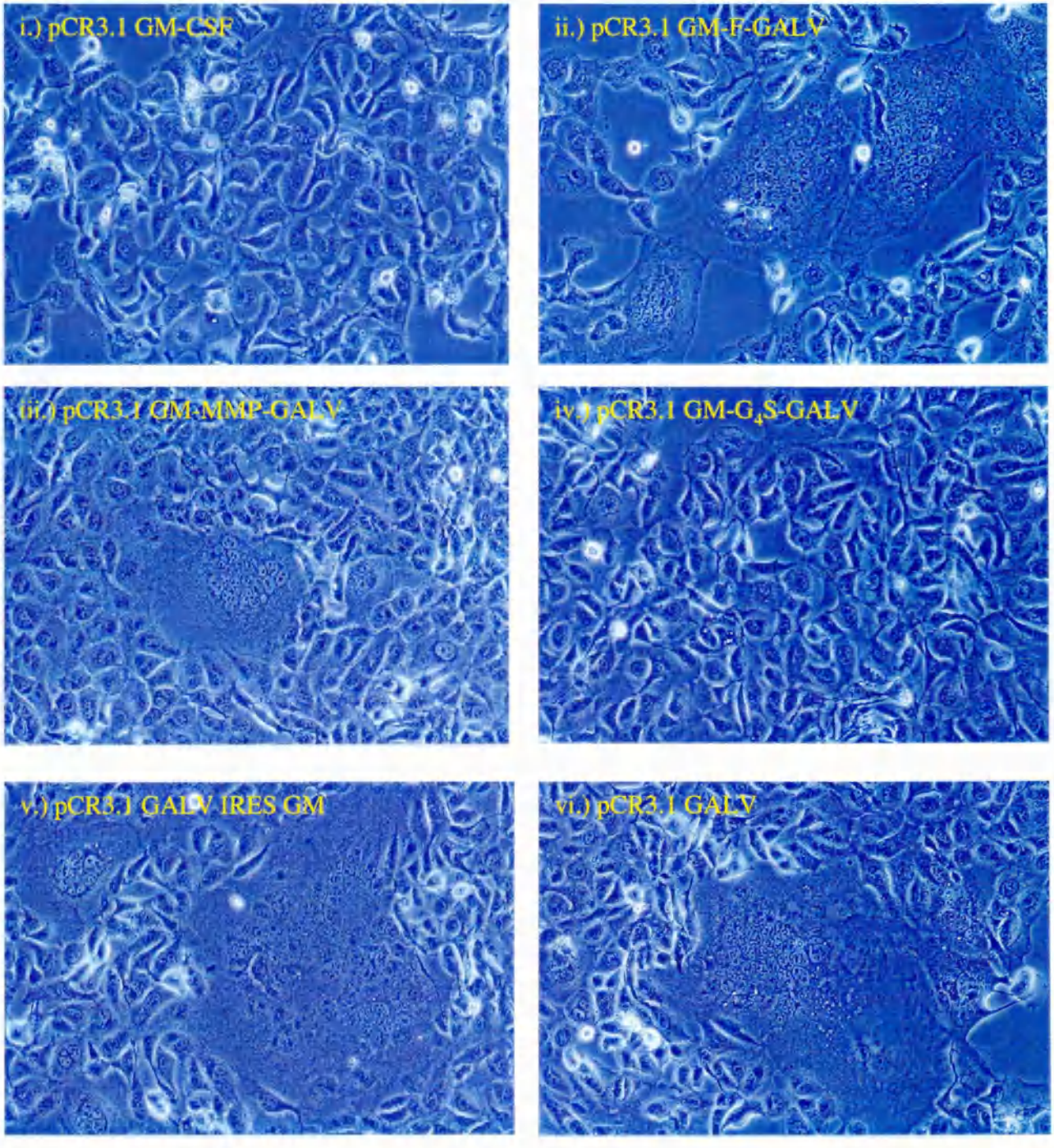

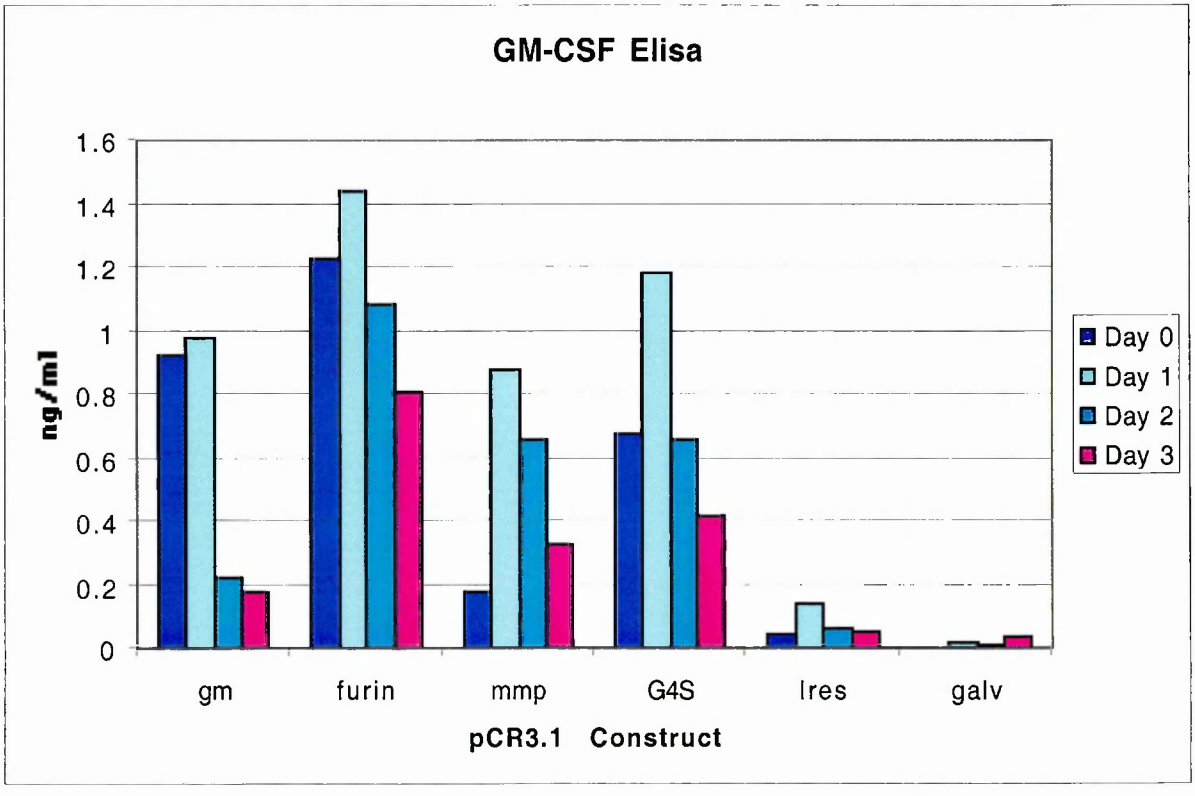

Figure 8.4: HT1080 cells transfected with co-expression constructs show variable amounts of GM-CSF secreted into the supernatant. HT1080 cells were transiently transfected with pCR3.1 plasmids containing GM-CSF (gm), GALV (galv), or constructs co-expressing GM-CSF and GALV containing furin or MMP sensitive linkers, a non-cleaveable linker (G4S), or by way of an internal ribosome entry site (Ires). After overnight incubation the supernatant was collected for assessment (Day 0). The cells were washed and fresh supernatant added. After 24 hours the supernatant was collected for assessment (Day 1). This process was repeated for a further 48 hours.

The furin construct consistently gave the highest value which is sustained over the test period. The gm, mmp, G4S values are intermediate with the Ires construct giving low levels. GALV acts as a negative control.

8.2.4 Analysis of the non-cleaveable linker construct

As indicated above pCR3.1 GM-G_4S-GALV did not induce fusion in transiently transfected cells. This confirmed that N-terminal display of GM-CSF blocked the fusogenicity of GALV. However it was not initially clearly apparent why GM-CSF secretion was detected by ELISA and experiments were conducted to address this issue. Confirmation that GM-CSF was anchored to the transmembrane GALV protein was seen by immunofluorescence, **Figure 8.5**. HT1080 cells were plated on chamber slides and were transiently transfected. 48 hours after transfection slides were prepared as described in Chapter 2. The cells were not permeablised and were stained with anti-human GM-CSF FITC conjugated antibody or a control FITC conjugated antibody. There is extensive staining over the surface of cells transfected with the G_4S construct which is not seen with pCR3.1 GM-CSF transfected cells.

It was assumed therefore that for this anchored GM-CSF to be detectable in the ELISA the SU domain of the GALV envelope must be being shed. A western was performed on the supernatant and the result is seen in **Figure 8.6**. This was performed following the protocol listed in Chapter 2. Specifically a 16.5% tricine gel was used, PVDF membrane, and 0.2μg/ml of the anti-human GM-CSF antibody (AF-215-NA, R&D) with a donkey anti-goat biotinylated secondary antibody at 1;10,000. As a positive control supernatant was also collected from a single HT1080 clone which had been stably transfected with pCR3.1 GM-CSF and selected in geneticin (HT1080-GM, discussed in more detail below). For a negative control supernatant was collected from cells transfected with pCR3.1 GALV.

The result confirmed a positive band in the G_4S lanes at 70+kd compared to the identified GM-CSF band in supernatant from HT1080-GM at ~ 24kd. This finding was compatible with the ELISA detecting GM-CSF anchored to GALV SU being shed into the supernatant.

8.2.5 Analysis of the furin sensitive linker construct

As expected, due to the ubiquitous expression of furin, transfection of HT1080 cells with pCR3.1 GM-F-GALV resulted in both GM-CSF production and syncitia formation. The degree of GALV expression would appear to match that seen with pCR3.1 GALV using

Figure 8.5: Immunofluorescence of HT1080 cells transiently transfected with pCR3.1 GM-G_4S-GALV. Cells were transfected with pCR3.1 GM-CSF (i), or pCR3.1 GM-G_4S-GALV(ii-iv). Non-permeabilised samples were stained with FITC conjugated Anti GM-CSF antibody (i, iii, iv) or FITC conjugated control antibody (ii). GM-CSF was identified anchored to the cell surface in pCR3.1 GM-G_4S-GALV transfected cells.

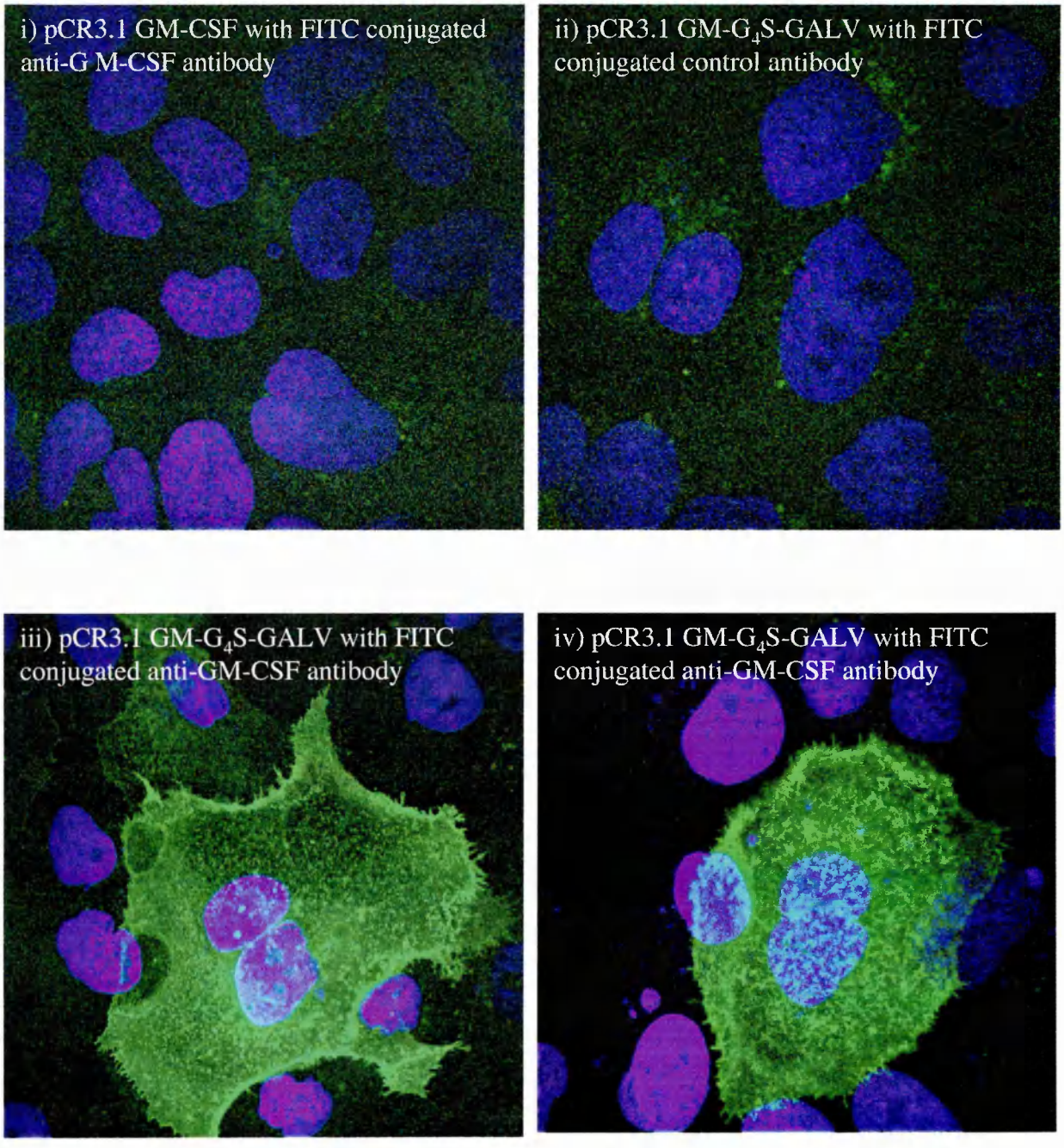

Figure 8.6: GM-CSF bound to GALV SU by the G_4S linker was detected in the supernatant by immunoblot. Supernatant from HT1080 cells stably expressing GM-CSF or transiently transfected with pCR3.1 GM-G4S-GALV or pCR3.1 GALV was probed for GM-CSF by Western blot. GM-CSF was identified from GM-G4S-GALV transfected cells as a significantly larger band compared to the GM-CSF expressing cell line. GALV acted as a negative control.

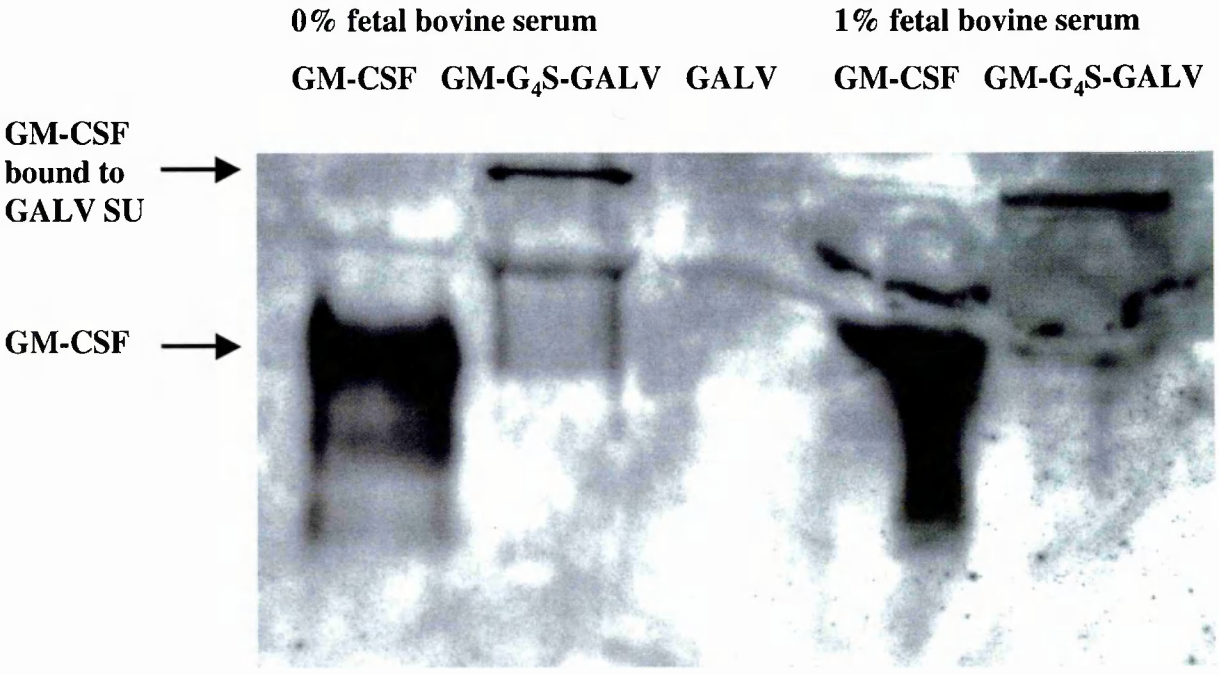

syncitia formation as a surrogate index, however the GM-CSF produced was consistently significantly higher than that seen with pCR3.1 GM-CSF. A number of experiments were designed to explain the increased GM-CSF production.

The first experiment was devised to indicate whether the process of syncitia formation caused a general enhancement in transcription and translation, coined a 'factory' effect. A cell line was produced which stably secreted GM-CSF. HT1080 cells were transfected with pCR3.1 GM-CSF and after 48 hours serially diluted and selected in geneticin 5μg/ml. Clonal populations were collected at 10 days as described in Chapter 2. Once bulked up 12 clones were selected for analysis by ELISA and the highest expressor selected, producing HT1080-GM. This cell line was then mixed at varying ratios with parental HT1080 and plated in 6 well plates. The following day these mixed cell populations were transiently transfected with no DNA, pCR3.1 β Gal or pCR3.1 GALV. After overnight incubation the cells were washed and fresh media added. Supernatant was collected after a further 48 hours, spun down and the supernatant collected for analysis by ELISA. The result can be seen in **Figure 8.7**. The data is representative of three similar experiments.
As can be seen if syncitia formation did induce a 'factory' effect higher levels of GM-CSF would be seen in GALV transfected groups. This was not the case.

Further evidence suggesting the increase in GM-CSF production with the furin construct was unrelated to syncitia formation was identified by transient transfection of non-fusing and fusing cell lines. Murine cell lines, due to critical amino acid differences in region A of PiT 1(see Chapter 1), do not fuse with GALV. Therefore transient transfection of B16 (murine melanoma) with pCR3.1 GM-F-GALV was compared with transfection of a moderate fusing cell line HT1080 and a highly fusing cell line 293A. Cells were plated in 6 well plates. The following day they were transiently transfected with pCR3.1 GM-CSF, pCR3.1 GM-F-GALV or pCR3.1 GALV. After overnight incubation the cells were washed and fresh media added. Supernatant was collected after a further 48 hours, spun down and the supernatant collected for analysis by ELISA. The result can be seen in **Figure 8.8**. The data is representative of three similar experiments.

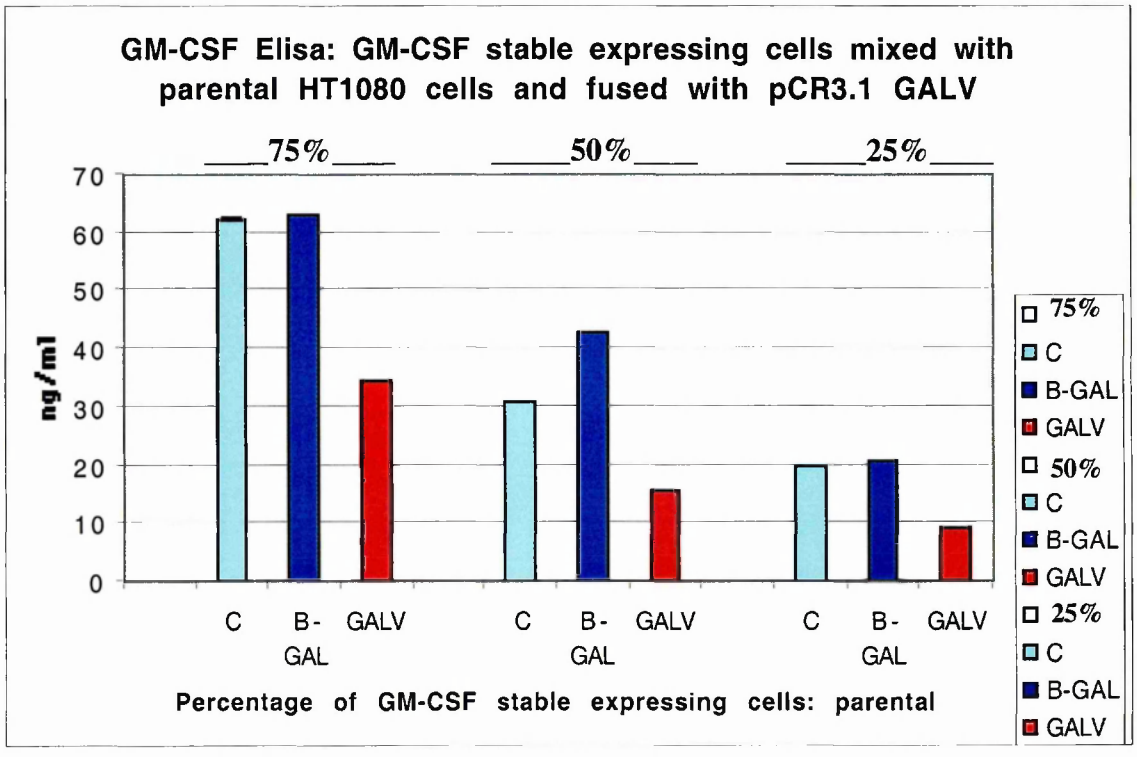

Figure 8.7: Syncitia formation alone does not induce an increase in GM-CSF secretion. Parental HT1080 cells were mixed with HT1080-GM clone at varying ratios. The cells were transiently transfected and incubated overnight, washed and fresh media applied. This was collected after a further 48 hours and analysed for GM-CSF content by ELISA.

pCR3.1 GALV transfection induced widespread syncitia formation. This did not result in an increase in GM-CSF release compared to untransfected controls (C) or ß-Galactosidase (B-GAL) transfection control.

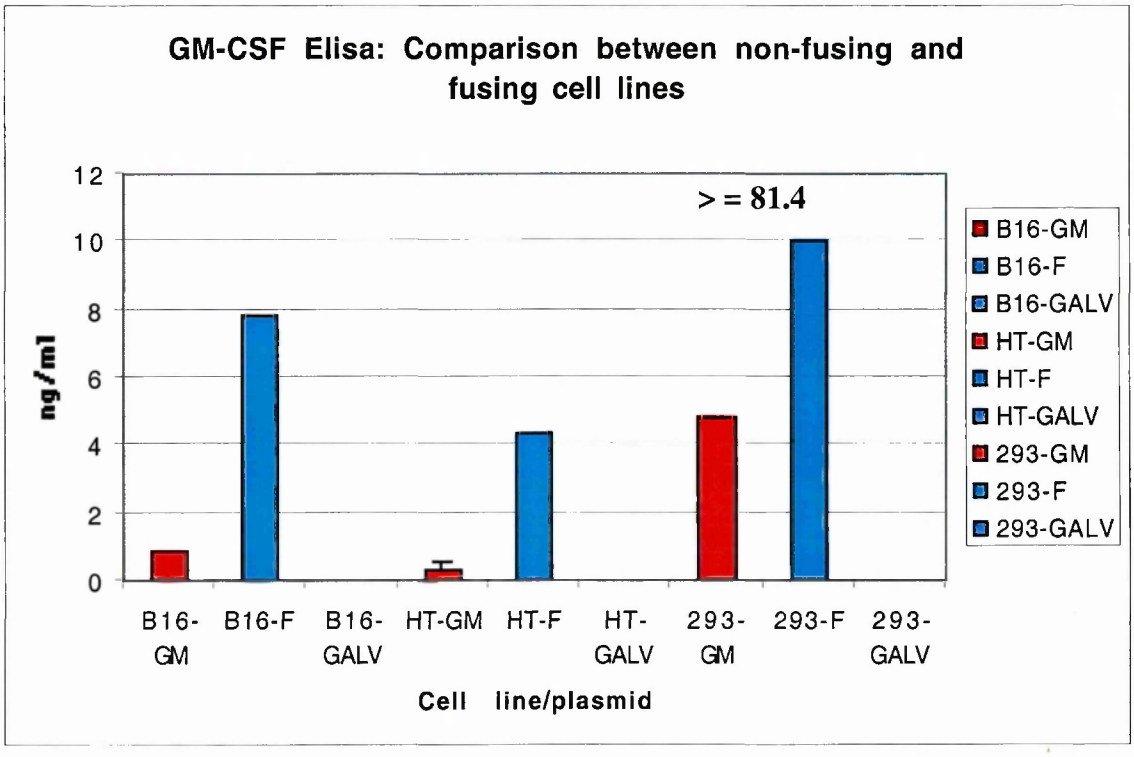

Figure 8.8: The pCR3.1 GM-FURIN-GALV construct produced higher levels of GM-CSF independent of fusion.

Cells were transiently transfected with pCR3.1 GM-CSF (-GM), pCR3.1 GM-FURIN-GALV (-F), or pCR3.1 GALV (-GALV). After overnight incubation cells were washed and fresh media applied. After a further 48 hours supernatant was collected for GM-CSF Elisa. A fusion index of the GALV transfected cells was recorded indicating that no syncitia were formed in B16 cells, as expected as they are of murine origin, moderate syncitia formation in HT1080 (+++ at 24, +++/++++ at 48 hours) and extensive syncitia formation in 293A cells (++++ at 24, +++++ at 48 hours).

The result indicated a consistent finding of a greater than 8 fold production of GM-CSF from cells transfected with the furin construct in comparison to pCR3.1 GM-CSF. This was unrelated to fusion.

Following these findings it seemed appropriate to explore whether enhancer elements within the GALV gene lead to high levels of transcription of GALV containing elements such as pCR3.1 GM-F-GALV. Quantitative analysis of mRNA by Northern blot was therefore conducted on 293A cells transiently transfected with the pCR3.1 plasmids developed in this chapter.

293A cells were plated in 25cm^2 flasks. The following day they were transfected using the Effectene protocol with pCR3.1 GM-CSF, pCR3.1 GM-F-GALV, pCR3.1 GM-MMP-GALV, pCR3.1 GM-G_4S-GALV, pCR3.1 GALV IRES GM or pCR3.1 GALV. After 48 hours mRNA was extracted according to the protocol previously described and underwent Northern blot analysis as described in Chapter 2. The probe used was GM-CSF: pCR3.1 GM-CSF was digested with BsiW 1 and the ~500 base pair fragment generated used in the described protocol.

The result can be seen in **Figure 8.9 I**. For comparison of mRNA levels to protein levels supernatant was collected from the samples at the time of mRNA preparation and ELISA for GM-CSF performed, **Figure 8.9 II**.

The Northern blot identified the predicted size of transcript from each group: pCR3.1 GM-CSF transfected samples acted as the positive control, pCR3.1 GALV samples as the negative control. The Linker containing constructs produced samples with a significantly larger transcript size than GM-CSF alone due to the prescence of the GALV sequence. The IRES construct generated two transcript sizes; one equivalent to GM-CSF mRNA alone, the other the largest transcript compatible with GALV, GM-CSF and IRES sequence.

Quantitatively there are differences in band intensity between the samples, most notably with the pCR3.1 GM-G_4S-GALV transfected samples giving the weakest band. However when subjected to digital densitrometry analysis the difference between the GM-CSF band and Furin band was < 1:1.5. Differential rates of transcription therefore does not explain the 7 fold increase in GM-CSF detected by ELISA as seen in **Figure 8.9 II**.

Figure 8.9: mRNA levels do not explain the increased GM-CSF secretion from PCR3.1 GM-FURIN-GALV. 293A cells were transiently transfected with the pCR3.1 plasmids indicated. mRNA was extracted at 48 hours for Northern blot analysis (I) and supernatant was collected for GM-CSF ELISA (II).

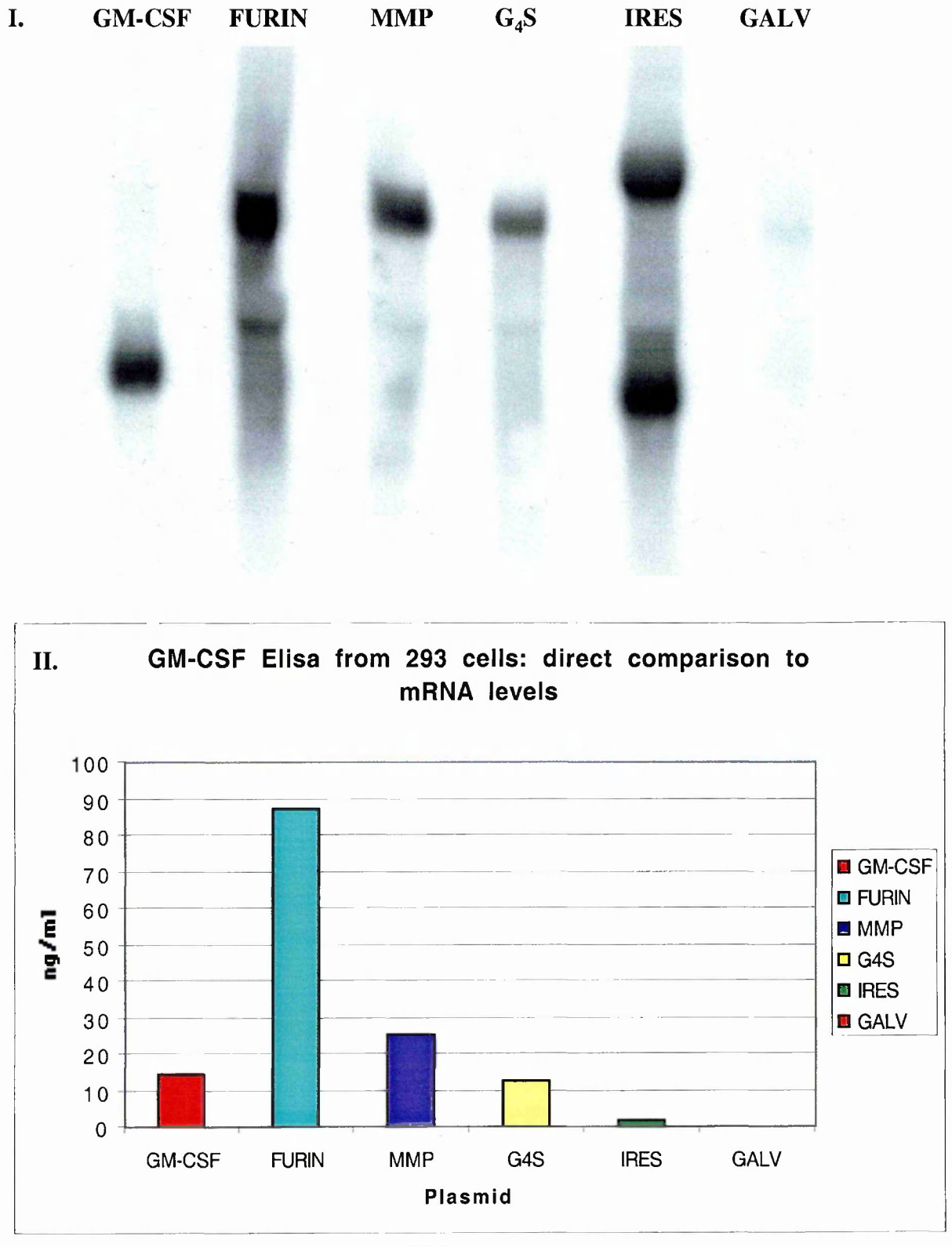

8.2.6 Analysis of the MMP sensitive linker construct

The initial data from Table 8.1 and Figures 8.2, 8.3 indicated transient transfection of HT1080 cells with pCR3.1 GM-MMP-GALV resulted in GM-CSF levels equivalent to pCR3.1 GM-CSF but decreased syncitia formation relative to pCR3.1 GALV. However transfection of cell lines with low MMP expression also produced syncitia formation equivalent to that seen in HT1080, with similar relative levels of GM-CSF detectable by ELISA (see **Figure 8.9 II** and **Figure 8.12 III**).

To confirm the MMP status of the cell lines used supernatant from cells was collected and a Matrix metalloproteinase-2 activity assay performed (Amersham pharmacia biotech). The findings were in keeping with previously published data indicating U87 were very high expressors, HT1080 high and TEL.CeB.6, A431M and 293A low expressors (see **Figure 8.11**).

To investigate the GM-CSF ELISA readings a Western was performed on supernatant collected from cells transiently transfected with pCR3.1 GM-CSF, pCR3.1 GM-MMP-GALV or pCR3.1 GALV. The low MMP expressor cell line 293A and high expressor line HT1080 were transfected. The protocol used was identical to that described as for assessment of the non-cleaveable linker. The result can be seen in **Figure 8.10.**

Bound GM-CSF to GALV SU is detected both from the 293A cells and HT1080 in samples from pCR3.1 GM-MMP-GALV transfectants. In addition free GM-CSF is also detected in these samples; relatively more so in the HT1080 samples compared to 293A.

Immunofluorescence was performed on TEL.CeB.6 cells transiently transfected with pCR3.1 GM-CSF, pCR3.1 GM-MMP-GALV or pCR3.1 GM-F-GALV. Fixed and permeabilised cells were stained with FITC-conjugated rat anti-human GM-CSF monoclonal antibody (Pharmingen) and DAPI. The result is seen in **Figure 8.12.** pCR3.1 GM-CSF transfected samples demonstrated no syncitia formation and no GM-CSF staining as the cytokine was being secreted. pCR3.1 GM-F-GALV transfected samples demonstrated extensive syncitia formation. In a few (~5%) of syncitia some positive GM-CSF staining was identified as illustrated in **8.12 II.** pCR3.1 GM-MMP-GALV transfected samples demonstrated syncitia formation with extensive GM-CSF staining. This confirmed the Western and ELISA findings suggesting some protease cleavage

Figure 8.10: GM-CSF can be identified bound to GALV SU and secreted free from cells transfected with pCR3.1 GM-MMP-GALV. 293A and HT1080 cells were transiently transfected with pCR3.1 constructs containing GM-CSF, GM-MMP-GALV or GALV. After 48 hours protein was collected from the supernatant and probed for GM-CSF by Western.

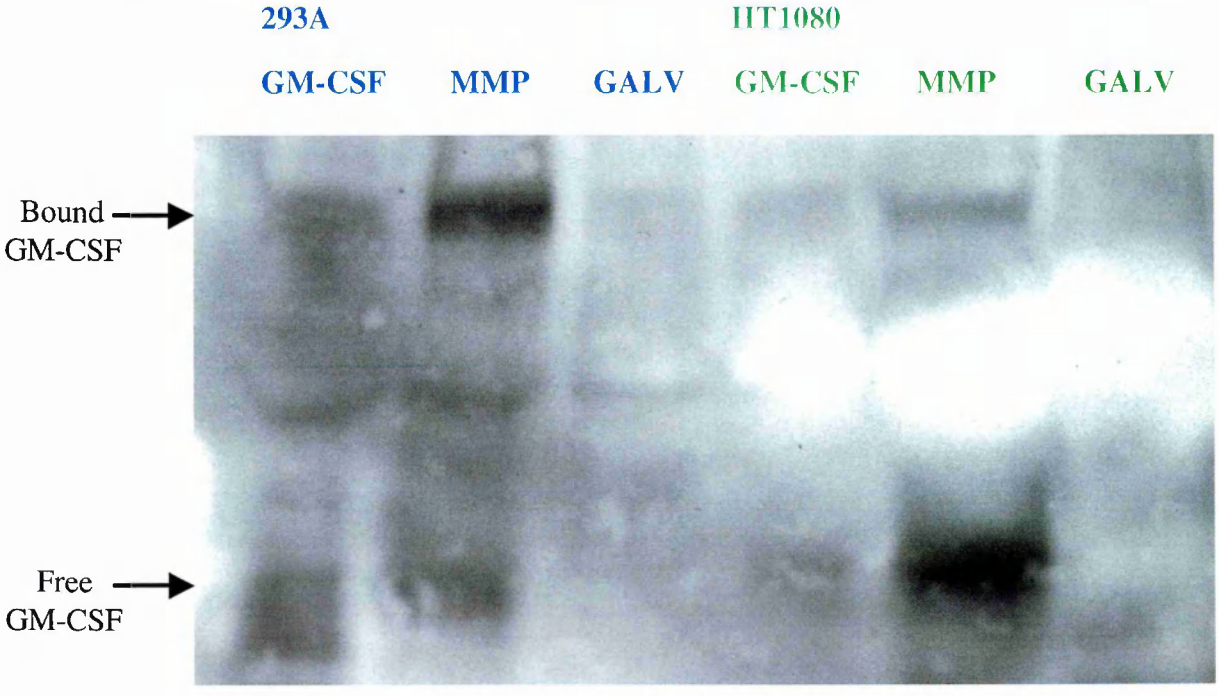

Figure 8.11: Pro-matrix metalloproteinase -2 (MMP-2) ELISA of a number of cell lines in vitro. U87 cells were the only ones to demonstrate active MMP-2 at 2ng/ml supernatant/3x10^5 cells.

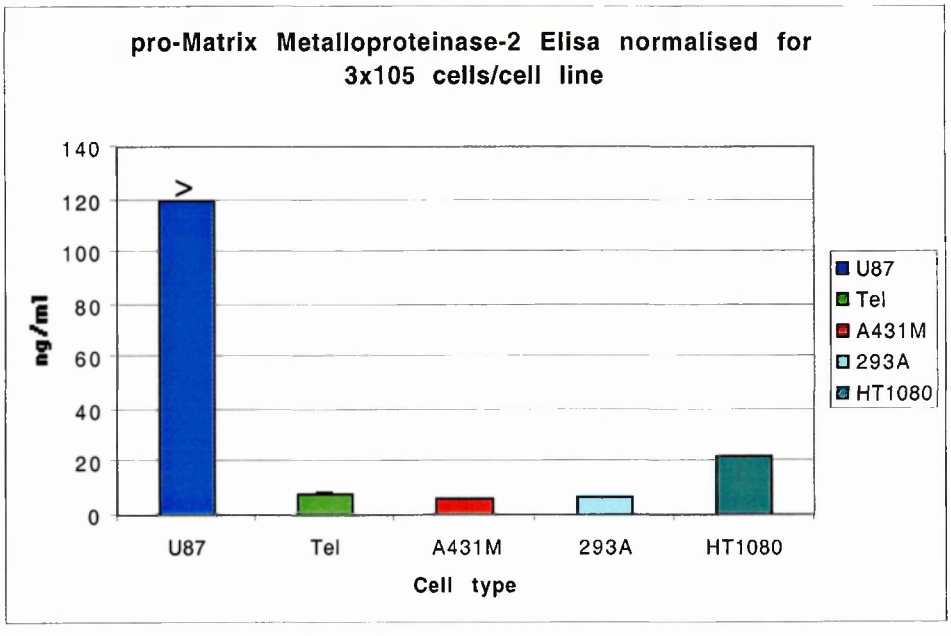

Figure 8.12: GM-CSF identified in syncitia induced by pCR3.1 GM-MMP-GALV. TEL.CeB.6 cells were transiently transfected with pCR3.1 GM-CSF (I), pCR3.1 GM-FURIN-GALV (II) or pCR3.1 GM-MMP-GALV (III). After 48 hours cells were fixed, permeabilised and stained with anti-GM-CSF antibody FITC labeled and DAPI.

GM-CSF can be identified in the syncitia induced by pCR3.1 GM-MMP-GALV, in a minority of syncitia induced by pCR3.1 GM-FURIN-GALV but not in cells transfected by pCR3.1 GM-CSF.

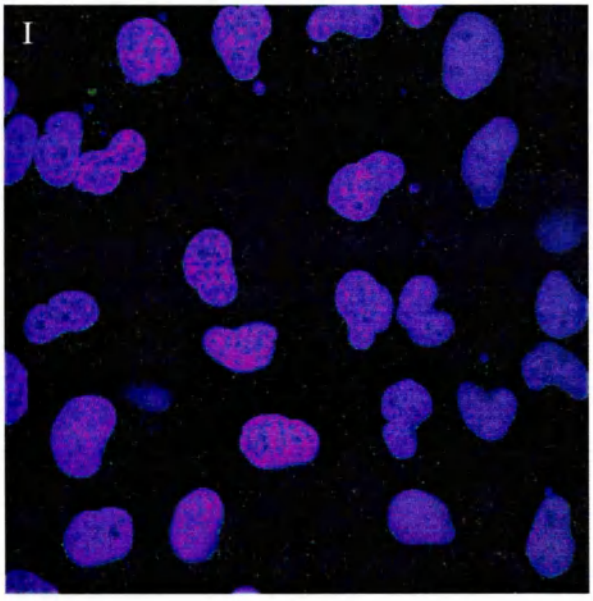

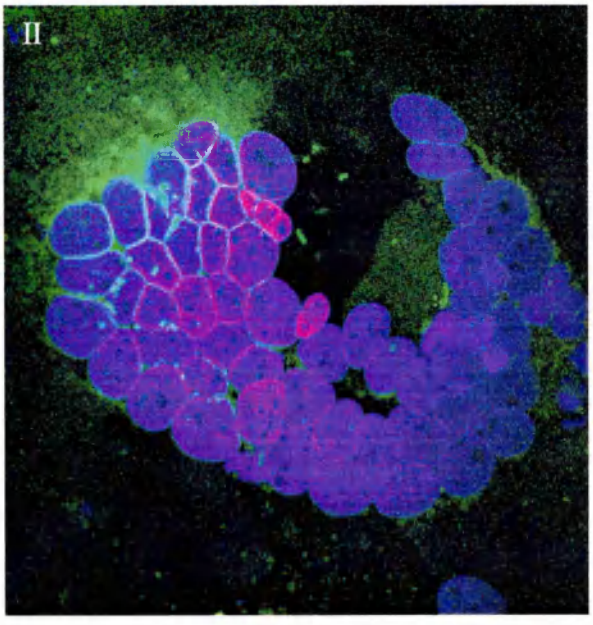

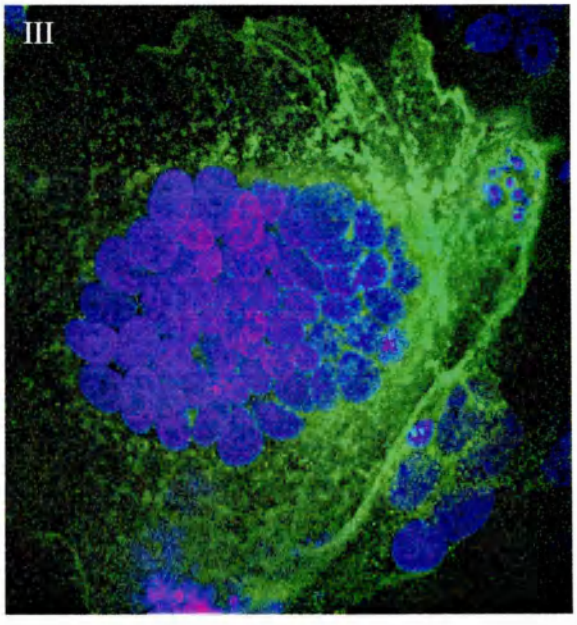

which allowed for syncitia development; but this process was inefficient and therefore some GM-CSF remained surface bound to GALV SU.

Further confirmation of the nature of the MMP linker in a cell-cell fusion model has been provided by a collaborator Dr L.Kirkham, Mayo Foundation. In this model epithelial growth factor (EGF) was added to the N-terminal of GALV using a MMP sensitive linker. Again fusion occurred in cell lines to a comparable level irrespective of their known MMP expression level. In addition, syncitia formation was blocked in susceptible cell lines following transfection of ligand MMP linked GALV constructs if experiments were conducted in the presence of 1,10-phenanthroline. This drug is a general metalloproteinase inhibitor which did not effect unmodified GALV fusion.

The conclusion from the experiments detailed above and our collaborator was that the 'MMP sensitive' linker was not specific for MMP but was capable of being cleaved by additional cell associated proteases.

8.2.7 Analysis of the IRES containing construct

This construct behaved as it was predicted to. Cap-dependent expression of GALV resulted in comparable fusion to pCR3.1 GALV. IRES-dependent expression of GM-CSF resulted in a lower relative value produced compared to pCR3.1 GM-CSF. This was not an unexpected finding and consistent with previous descriptions of IRES activity.

8.3 Discussion

The aim of the work detailed in this chapter was to express both GM-CSF and FMG (GALV) from a single vector. This was achieved by the mechanisms outlined. However the scheme illustrated in **Figure 8.1** for the MMP sensitive construct did not eventuate probably due to a lack of specificity of the consensus sequence used. This meant there was no targeted aspect to this strategy i.e. even in cell lines known to have low MMP expression GM-CSF – GALV cleavage occurred due to the action of non MMP cellular proteases. This promoted fusion and the release of GM-CSF. However this cleavage was inefficient resulting in a relative decrease in fusion and therefore decreased cytotoxicity induced by FMG. The IRES containing construct produced fusion comparable to wild type but produced relatively low levels of GM-CSF. Therefore on balance the furin sensitive

vector appears to be the most amenable of the co-expression constructs to further development. This was due to the fusion performance comparable to GALV alone combined with a significantly greater GM-CSF production than GM-CSF alone. This implies that this construct has the best profile for inducing the stated aims of this study; namely combining the pro-inflammatory cytotoxicity induced by FMG with high local levels of cytokine to promote the development of a tumour specific immune response.

The mechanism for enhanced GM-CSF production by the furin sensitive construct was not fully identified. However the majority of the increase was not explained by increased transcription as indicated by the Northern analysis. This would suggest the increased secretion identified occurred due to preferential translation and processing through the secretory pathway.

The protease insensitive linker, Gly-Gly-Gly-Gly-Ser highlighted the process of shedding. MLV type retroviruses have similar envelope glycoprotein structure. The SU and TM subunits of the envelope are held together by a labile disulfide bond (see Chapter 1). Disruption of this bond results in SU dissociating from the Env complex (Gliniak et al., 1991). Therefore even with the process of fusion being blocked by the N-terminal display of GM-CSF, GM-CSF was still detectable in the supernatant. It is probable that this GM-CSF – SU fusion protein would still retain the biological activities of GM-CSF (Maurice et al., 1999). This effect would therefore limit the ability to target GM-CSF release, using a retroviral FMG in a linker strategy, should targeting be required.

The data presented in this chapter formed part of the following paper:

Lack of specificity of cell surface protease targeting of a cytotoxic hyperfusogenic gibbon ape leukaemia virus envelope glycoprotein

Lucy A Kirkham, Andrew Bateman, Alan Melcher, Richard G Vile and Adele K Fielding

Journal of Gene Medicine: Accepted for publication April 2002

CHAPTER 9: CONCLUSIONS AND FUTURE DIRECTIONS

Chapter 9: Conclusions and future directions

The hypothesis to be tested in this thesis was that fusogenic membrane glycoproteins could be potential cytotoxic gene therapy agents in the treatment of cancer. The data presented would indicate that FMG, due to their novel mechanism of action, do merit further consideration for inclusion into gene therapy strategies.

The initial studies were designed to assess the cytotoxic effects of expressing FMG in tumour cells in vitro. Plasmid transfection of a variety of FMG in a wide range of tumour cell lines indicated the potential cytotoxicity and highlighted a number of important points. The cytotoxicity occurred secondary to multinucleated syncitia formation. For this to occur cells needed to express the appropriate viral receptor and be in close contact; as well some cells in the population needed to be adequately transfected and express the FMG. Experiments designed to assess the bystander effect of FMG expression indicated a level of 1:100 in selected cell lines in vitro. For suicide genes such as HSVtk the value was found to be 1:10. Direct comparison of FMG to suicide genes therefore indicated a superior cytotoxic effect of FMG in vitro due to this enhanced bystander effect. A further benefit over suicide genes was that following gene expression cytotoxicity would be initiated with no requirement for additional resource such as prodrug.

Studies of the mechanism of cytotoxicity indicated that there was no dependence on the stage of the cell cycle with FMG mediated cell death. This is in contrast to a number of suicide gene strategies which require cells to be in S phase of the cell cycle to be effective. This factor gains importance in the in vivo setting where tumour cell doubling time is significantly longer than that seen in vitro. Additional mechanistic assessments were made which indicated the predominant mode of cell death was through necrosis. A model was proposed whereby syncitia initially form in an organised manner with a structured arrangement of their cytoskeleton and organelles. After a period of time the syncitia become nonviable and die a bioenergetic form of cell death with necrosis. In certain cell lines autophagy could be identified within some syncitia and this would appear to provide further evidence for a state of energy depletion arising in syncitia.

Associated with the necrotic death stress signals could be identified namely gp96 up regulation and induction of inducible Hsp70. This stress response was identified in both the in vitro and in vivo settings. Release of heat shock proteins amongst other intracellular components from necrotically dying synctia are likely to be pro-inflammatory; potentially enhancing the efficacy of the gene therapy.

Plasmid delivey of FMG in vivo indicated the cytotoxic effects were not only confined to the in vitro setting. Consequently viral vectors expressing FMG were developed.
Development of a C type retroviral vector expressing GALV proved problematic for a number of reasons. GALV being a truncated C type retroviral envelope would be able to heterotrimerise with the envelope contained within the packaging cell line. In addition if the packaging cell line was of human origin then GALV expression led to direct cytotoxicity and again poor titres. If required to form the envelope, the truncated GALV was incorporated poorly into virions and titres were poor. This feature was also seen with a lentiviral vector expressing GALV. However the Lenti-GALV vector pseudotyped with VSV-G was capable of being produced at a titre of 10^6. This was sufficient to permit in vivo testing. Lenti-GALV injected daily for 3 days into HT1080 tumours was able to eradicate tumours in 10 out of 10 mice.
Production of recombinant adenoviruses expressing measles F and H was performed using standard methods. The recoverable titre of an adenoviral vector expressing F was consistently one log less than that for an H expressing vector. Preliminary experiments injecting Ad H and Ad F directly into HT1080 tumours seeded in nude mice did indicate syncitia formation occurred in vivo. These preliminary experiments indicated the extent of syncitia formation was not widespread suggesting a relatively low transduction efficiency. In light of this, in experiments designed to assess the efficacy of Ad FMG, tumours were seeded with HT1080 cells stably expressing F and injected with Ad H vector. In this aggressive tumour model tumour eradication was seen in a third of mice. In comparison no longterm survivors were seen in the control groups. This result along with the identification of syncitia formation in vivo was encouraging. However there was clearly lower levels of transfection by Ad vector (both Ad H and Ad GFP expressing) than expected. This effect hampered a full assessment of the direct cytotoxic activity in vivo

and highlighted the importance of the vector in any gene therapy strategy. Further studies are required to ascertain the cause of the low transfection efficiency. These will focus on whether it is the tumour model which becomes significantly less infectable with adenovirus in vivo, the recombinant Ad produced was in some way defective or some component of our in vivo protocol led to a reduced transfection efficiency.

Development of an adenoviral vector expressing GALV required the introduction of a strategy designed to cause transcriptional silencing of GALV in the human adenoviral producer cells. Without the silencing GALV expression would lead to extensive cytotoxicity of the 293 cells and failure to produce Ad GALV. The DNA recombinase Cre/ *lox* system was employed to act in conjunction with a transcriptional stop sequence upstream of the GALV gene. This permitted the production of an adenoviral vector containing a transcriptionally silent GALV. This vector was then used to transfect 293 Cre cells. The Cre excised the stop sequence and an adenoviral vector was produced capable of expressing GALV. This vector was tested in vitro and found to be capable of inducing syncitia formation. Future studies will focus on the efficacy of Ad GALV in suitable in vivo models.

Addition of adjuvants to a cytotoxic gene therapy strategy may be important for the successful outcome of the therapy. Various plasmid vectors were developed which expressed GALV in combination with GM-CSF. Expression of GALV covalently linked to GM-CSF by a non-cleaveable linker indicated that the hybrid protein was transported to the cell membrane and GM-CSF was identified anchored to the cell surface. The presence of the GM-CSF prevented GALV mediated fusion. Interestingly GM-CSF was also able to be detected in the supernatant. This was due to the process of shedding seen with retroviral envelopes whereby the SU component, with in this case GM-CSF attached, is shed into the media .

High levels of secreted GM-CSF and GALV were identified from a construct incorporating a furin sensitive site between the two proteins. This was more efficient at dual protein production than a construct containing an IRES site.

In an attempt to target FMG mediated fusion and GM-CSF release to tumours a construct was produced linking GM-CSF to GALV via a matrix metalloproteinase (MMP) sensitive

linker. It was identified that the linker sequence was not specific for extrinsic matrix metalloproteinases but was also sensitive to intracellular proteases. This resulted in GALV mediated fusion and GM-CSF secretion occuring in cell lines with no MMP production. However the intracellular cleavage was not 100% efficient and impaired syncitia formation resulted compared to GALV alone. The conclusion for the MMP sensitive linker strategy therefore was that it would not be useful for targeting.

To date the in vivo efficacy of FMG have been tested in immunodeficient mice. This has meant no in vivo assessment has been possible to characterise the immunostimulatory effects of FMG mediated cell death. It is proposed that FMG mediated cell death occuring by necrosis would lead to the generation of a tumour specific immune response, and with that, a likely improved therapeutic effect. Testing FMG in an immunocompetent model would also allow assessment of any adjuvant strategies including co-expression of FMG with cytokines. I therefore propose to develop an FMG model capable of fusing murine cells. There are a number of candidate genes which appear suitable. Experience has already been gained with VSV-G which has a very broad tropism; being capable of fusing murine and human cells amongst others. However the mechanism of fusion generally requires a drop in pH to initiate the required conformational change in the FMG. Probably a more useful FMG for gene therapy strategies would be one capable of fusion at neutral pH: suggesting FMG from retroviral, paramyxoviral or orthomyxoviral family members (Hernandez et al., 1996). Candidate FMG will therefore include those from the retrovirus MoMLV, and the paramyxovirus Sendai virus. Mutation of the wild type MoMLV FMG will be required to generate a hyperfusogenic envelope. One strategy to achieve this would be to modify the R peptide in a similar manner to the hyperfusogenic GALV used in this thesis. Broader tropism for the Sendai F and HN could also be achieved by obtaining a mutant F previously described (Paterson '00).

In addition to utilising FMG as cytotoxic gene therapy agents they may have a role as fusagens in the development of anti-tumour vaccines. Dendritic cell–tumour cell hybrids have been shown to be effective vaccines in murine tumour models (Gong et al., 1997) and patients with metastatic renal cell carcinoma (Kugler et al., 2000). Fusion has required

'electrofusion' or co-incubation of DC and tumour cells in the presence of polyethylene glycol. Expression of FMG by tumour cells or DC and co-incubation would be expected to produce hybrids in vitro. I propose to examine this and test a FMG induced hybrid vaccine in murine tumour models. DC-tumour cell hybrids may be more efficiently produced by this method than those previously utilised. In addition progression of the FMG induced hybrid cells to form syncitia would lead to necrosis; further promoting the development of a tumour specific immune response. Additional studies are proposed where DC expressing FMG could be injected directly into tumours in vivo. This strategy would avoid the process of extracting and culturing an individual's tumour prior to vaccine development.

In conclusion this project set out to assess whether fusogenic membrane glycoproteins were potential cytotoxic gene therapy agents. Studies have indicated FMG cytotoxicity in vitro and in vivo. In vitro data indicated a significant bystander effect which resulted in greater efficacy of tumour cell killing compared with suicide genes. In addition the mechanism of the cytotoxicity has been defined; being via a predominantly necrotic cell death process. This phenomenon coupled with the novel approach of fusion make FMG attractive agents to develop for cytotoxic gene therapy and anti-tumour vaccine strategies.

REFERENCES

References

(2000). Gene therapy--a loss of innocence, Nat Med *6*, 1.

Adams, J. M., and Cory, S. (1998). The Bcl-2 protein family: arbiters of cell survival, Science *281*, 1322-6.

Aghi, M., Kramm, C. M., and Breakefield, X. O. (1999). Folylpolyglutamyl synthetase gene transfer and glioma antifolate sensitivity in culture and in vivo, J Natl Cancer Inst *91*, 1233-41.

Aghi, M., Kramm, C. M., Chou, T. C., Breakefield, X. O., and Chiocca, E. A. (1998). Synergistic anticancer effects of ganciclovir/thymidine kinase and 5-fluorocytosine/cytosine deaminase gene therapies, J Natl Cancer Inst *90*, 370-80.

Aiello, L., Guilfoyle, R., Huebner, K., and Weinmann, R. (1979). Adenovirus 5 DNA sequences present and RNA sequences transcribed in transformed human embryo kidney cells (HEK-Ad-5 or 293), Virology *94*, 460-9.

Albert, M. L., Sauter, B., and Bhardwaj, N. (1998). Dendritic cells acquire antigen from apoptotic cells and induce class I- restricted CTLs, Nature *392*, 86-9.

Anderson, W. F. (2000). Gene therapy scores against cancer Nat Med *6*, 862-3.

Anlezark, G. M., Melton, R. G., Sherwood, R. F., Coles, B., Friedlos, F., and Knox, R. J. (1992). The bioactivation of 5-(aziridin-1-yl)-2,4-dinitrobenzamide (CB1954)-- I. Purification and properties of a nitroreductase enzyme from Escherichia coli--a potential enzyme for antibody-directed enzyme prodrug therapy (ADEPT), Biochem Pharmacol *44*, 2289-95.

Arnold-Schild, D., Hanau, D., Spehner, D., Schmid, C., Rammensee, H. G., de la Salle, H., and Schild, H. (1999). Cutting edge: receptor-mediated endocytosis of heat shock proteins by professional antigen-presenting cells, J Immunol *162*, 3757-60.

Asea, A., Kraeft, S. K., Kurt-Jones, E. A., Stevenson, M. A., Chen, L. B., Finberg, R. W., Koo, G. C., and Calderwood, S. K. (2000). HSP70 stimulates cytokine production through a CD14-dependant pathway, demonstrating its dual role as a chaperone and cytokine, Nat Med *6*, 435-42.

Ashkenazi, A., and Dixit, V. M. (1998). Death receptors: signaling and modulation, Science *281*, 1305-8.

Bae, Y., Kingsman, S. M., and Kingsman, A. J. (1997). Functional dissection of the Moloney murine leukemia virus envelope protein gp70, J Virol *71*, 2092-9.

Basu, S., Binder, R. J., Ramalingam, T., and Srivastava, P. K. (2001). CD91 is a common receptor for heat shock proteins gp96, hsp90, hsp70, and calreticulin, Immunity *14*, 303-13.

Basu, S., Binder, R. J., Suto, R., Anderson, K. M., and Srivastava, P. K. (2000). Necrotic but not apoptotic cell death releases heat shock proteins, which deliver a partial maturation signal to dendritic cells and activate the NF-kappa B pathway, Int Immunol *12*, 1539-46.

Bateman A, Harrington K. H., A Ahmed, A Melcher, M Gough, D Riddle, A Dietz, M Crittenden and R Vile (2002). Viral Fusogenic Membrane Glycoprotein kill solid tumour cells by non-apoptotic mechanisms which promote cross presentation of tumour antigens by Dendritic cells, Submitted to Cancer Research.

Battini, J. L., Danos, O., and Heard, J. M. (1995). Receptor-binding domain of murine leukemia virus envelope glycoproteins, J Virol *69*, 713-9.

Beier, D. C., Cox, J. H., Vining, D. R., Cresswell, P., and Engelhard, V. H. (1994). Association of human class I MHC alleles with the adenovirus E3/19K protein, J Immunol *152*, 3862-72.

Bentley, N. J., Eisen, T., and Goding, C. R. (1994). Melanocyte-specific expression of the human tyrosinase promoter: activation by the microphthalmia gene product and role of the initiator, Mol Cell Biol *14*, 7996-8006.

Bergelson, J. M., Krithivas, A., Celi, L., Droguett, G., Horwitz, M. S., Wickham, T., Crowell, R. L., and Finberg, R. W. (1998). The murine CAR homolog is a receptor for coxsackie B viruses and adenoviruses, J Virol *72*, 415-9.

Bergers, G., Javaherian, K., Lo, K. M., Folkman, J., and Hanahan, D. (1999). Effects of angiogenesis inhibitors on multistage carcinogenesis in mice, Science *284*, 808-12.

Bernt, K. M., Ni, S., Li, Z-Y., Shayakhmetov, D. M., and Lieber, A. (2003). The effect of sequestration by nontarget tissues on anti-tumour efficacy of systemically applied, conditionally replicating adenovirus vectors, Molecular Therapy *8*, 746-55.

Berwin, B., and Nicchitta, C. V. (2001). To find the road traveled to tumor immunity: the trafficking itineraries of molecular chaperones in antigen-presenting cells, Traffic *2*, 690-7.

Bett, A. J., Haddara, W., Prevec, L., and Graham, F. L. (1994). An efficient and flexible system for construction of adenovirus vectors with insertions or deletions in early regions 1 and 3, Proc Natl Acad Sci U S A *91*, 8802-6.

Bhardwaj, N. (1997). Interactions of viruses with dendritic cells: a double-edged sword, J Exp Med *186*, 795-9.

Binder, R. J., Anderson, K. M., Basu, S., and Srivastava, P. K. (2000a). Cutting edge: heat shock protein gp96 induces maturation and migration of CD11c+ cells in vivo, J Immunol *165*, 6029-35.

Binder, R. J., Han, D. K., and Srivastava, P. K. (2000b). CD91: a receptor for heat shock protein gp96, Nat Immunol *1*, 151-5.

Boehm, T., Folkman, J., Browder, T., and O'Reilly, M. S. (1997). Antiangiogenic therapy of experimental cancer does not induce acquired drug resistance, Nature *390*, 404-7.

Bonini, C., Ferrari, G., Verzeletti, S., Servida, P., Zappone, E., Ruggieri, L., Ponzoni, M., Rossini, S., Mavilio, F., Traversari, C., and Bordignon, C. (1997). HSV-TK gene transfer into donor lymphocytes for control of allogeneic graft-versus-leukemia, Science *276*, 1719-24.

Borner, C., and Monney, L. (1999). Apoptosis without caspases: an inefficient molecular guillotine?, Cell Death Differ *6*, 497-507.

Boyd, J. M., Malstrom, S., Subramanian, T., Venkatesh, L. K., Schaeper, U., Elangovan, B., D'Sa-Eipper, C., and Chinnadurai, G. (1994). Adenovirus E1B 19 kDa and Bcl-2 proteins interact with a common set of cellular proteins, Cell *79*, 341-51.

Bramson, J. L., Hitt, M., Gauldie, J., and Graham, F. L. (1997). Pre-existing immunity to adenovirus does not prevent tumor regression following intratumoral administration of a vector expressing IL-12 but inhibits virus dissemination, Gene Ther *4*, 1069-76.

Brody, B. A., Rhee, S. S., and Hunter, E. (1994). Postassembly cleavage of a retroviral glycoprotein cytoplasmic domain removes a necessary incorporation signal and activates fusion activity, J Virol *68*, 4620-7.

Bullough, P. A., Hughson, F. M., Skehel, J. J., and Wiley, D. C. (1994). Structure of influenza haemagglutinin at the pH of membrane fusion, Nature *371*, 37-43.

Burns, J. C., Friedmann, T., Driever, W., Burrascano, M., and Yee, J. K. (1993). Vesicular stomatitis virus G glycoprotein pseudotyped retroviral vectors: concentration to very high titer and efficient gene transfer into mammalian and nonmammalian cells, Proc Natl Acad Sci U S A *90*, 8033-7.

Cao, X., Zhang, W., Wang, J., Zhang, M., Huang, X., Hamada, H., and Chen, W. (1999). Therapy of established tumour with a hybrid cellular vaccine generated by using granulocyte-macrophage colony-stimulating factor genetically modified dendritic cells, Immunology *97*, 616-25.

Castellino, F., Boucher, P. E., Eichelberg, K., Mayhew, M., Rothman, J. E., Houghton, A. N., and Germain, R. N. (2000). Receptor-mediated uptake of antigen/heat shock protein

complexes results in major histocompatibility complex class I antigen presentation via two distinct processing pathways, J Exp Med *191*, 1957-64.

Cavazzana-Calvo, M., Hacein-Bey, S., de Saint Basile, G., Gross, F., Yvon, E., Nusbaum, P., Selz, F., Hue, C., Certain, S., Casanova, J. L., *et al.* (2000). Gene therapy of human severe combined immunodeficiency (SCID)-X1 disease, Science *288*, 669-72.

Chartier, C., Degryse, E., Gantzer, M., Dieterle, A., Pavirani, A., and Mehtali, M. (1996). Efficient generation of recombinant adenovirus vectors by homologous recombination in Escherichia coli, J Virol *70*, 4805-10.

Chaudry, G. J., and Eiden, M. V. (1997). Mutational analysis of the proposed gibbon ape leukemia virus binding site in Pit1 suggests that other regions are important for infection, J Virol *71*, 8078-81.

Chen, L., Anton, M., and Graham, F. L. (1996a). Production and characterization of human 293 cell lines expressing the site-specific recombinase Cre, Somat Cell Mol Genet *22*, 477-88.

Chen, L., Waxman, D. J., Chen, D., and Kufe, D. W. (1996b). Sensitization of human breast cancer cells to cyclophosphamide and ifosfamide by transfer of a liver cytochrome P450 gene, Cancer Res *56*, 1331-40.

Chen, P. H., Ornelles, D. A., and Shenk, T. (1993). The adenovirus L3 23-kilodalton proteinase cleaves the amino-terminal head domain from cytokeratin 18 and disrupts the cytokeratin network of HeLa cells, J Virol *67*, 3507-14.

Chen, W., Syldath, U., Bellmann, K., Burkart, V., and Kolb, H. (1999). Human 60-kDa heat-shock protein: a danger signal to the innate immune system, J Immunol *162*, 3212-9.

Chinnadurai, G., Chinnadurai, S., and Brusca, J. (1979). Physical mapping of a large-plaque mutation of adenovirus type 2, J Virol *32*, 623-8.

Chong, H., Starkey, W., and Vile, R. G. (1998). A replication-competent retrovirus arising from a split-function packaging cell line was generated by recombination events between the vector, one of the packaging constructs, and endogenous retroviral sequences, J Virol *72*, 2663-70.

Christodoulopoulos, I., and Cannon, P. M. (2001). Sequences in the cytoplasmic tail of the gibbon ape leukemia virus envelope protein that prevent its incorporation into lentivirus vectors, J Virol *75*, 4129-38.

Clayman, G. L., Frank, D. K., Bruso, P. A., and Goepfert, H. (1999). Adenovirus-mediated wild-type p53 gene transfer as a surgical adjuvant in advanced head and neck cancers, Clin Cancer Res *5*, 1715-22.

Cobleigh, M. A., Vogel, C. L., Tripathy, D., Robert, N. J., Scholl, S., Fehrenbacher, L., Wolter, J. M., Paton, V., Shak, S., Lieberman, G., and Slamon, D. J. (1999). Multinational study of the efficacy and safety of humanized anti-HER2 monoclonal antibody in women who have HER2-overexpressing metastatic breast cancer that has progressed after chemotherapy for metastatic disease, J Clin Oncol *17*, 2639-48.

Cocks, B. G., Chang, C. C., Carballido, J. M., Yssel, H., de Vries, J. E., and Aversa, G. (1995). A novel receptor involved in T-cell activation, Nature *376*, 260-3.

Coffey, M. C., Strong, J. E., Forsyth, P. A., and Lee, P. W. (1998). Reovirus therapy of tumors with activated Ras pathway, Science *282*, 1332-4.

Coffin, J. C. (1996). Retroviridae, Fields Virology, Vol 2 (Philadelphia, Lippincott-Raven).

Cohen, E. A., Subbramanian, R. A., and Gottlinger, H. G. (1996). Role of auxiliary proteins in retroviral morphogenesis, Curr Top Microbiol Immunol *214*, 219-35.

Coiffier, B., Lepage, E., Briere, J., Herbrecht, R., Tilly, H., Bouabdallah, R., Morel, P., Van Den Neste, E., Salles, G., Gaulard, P., *et al.* (2002). CHOP chemotherapy plus rituximab compared with CHOP alone in elderly patients with diffuse large-B-cell lymphoma, N Engl J Med *346*, 235-42.

Cosset, F. L., and Russell, S. J. (1996). Targeting retrovirus entry, Gene Ther *3*, 946-56.
Cosset, F. L., Takeuchi, Y., Battini, J. L., Weiss, R. A., and Collins, M. K. (1995). High-titer packaging cells producing recombinant retroviruses resistant to human serum, J Virol *69*, 7430-6.

Cotter, F. E. (1999). Antisense therapy of hematologic malignancies, Semin Hematol *36*, 9-14.

Cunningham, C. C., Holmlund, J. T., Schiller, J. H., Geary, R. S., Kwoh, T. J., Dorr, A., and Nemunaitis, J. (2000). A phase I trial of c-Raf kinase antisense oligonucleotide ISIS 5132 administered as a continuous intravenous infusion in patients with advanced cancer, Clin Cancer Res *6*, 1626-31.

Danks, M. K., Morton, C. L., Pawlik, C. A., and Potter, P. M. (1998). Overexpression of a rabbit liver carboxylesterase sensitizes human tumor cells to CPT-11, Cancer Res *58*, 20-2.

Davis, I. D. (2000). An overview of cancer immunotherapy, Immunol Cell Biol *78*, 179-95.

Delassus, S., Sonigo, P., and Wain-Hobson, S. (1989). Genetic organization of gibbon ape leukemia virus, Virology *173*, 205-13.

Denault, J. B., and Leduc, R. (1996). Furin/PACE/SPC1: a convertase involved in exocytic and endocytic processing of precursor proteins, FEBS Lett *379*, 113-6.

Denesvre, C., Sonigo, P., Corbin, A., Ellerbrok, H., and Sitbon, M. (1995). Influence of transmembrane domains on the fusogenic abilities of human and murine leukemia retrovirus envelopes, J Virol *69*, 4149-57.

Desai, S. B., and Libutti, S. K. (1999). Tumor angiogenesis and endothelial cell modulatory factors, J Immunother *22*, 186-211.

Diaz, R., and Vile, R. (1999). Molecular Immunotherapy by gene transfer, Vol 8 (New York, Kluwer Academic/Plenum).

Diaz, R. M., Eisen, T., Hart, I. R., and Vile, R. G. (1998). Exchange of viral promoter/enhancer elements with heterologous regulatory sequences generates targeted hybrid long terminal repeat vectors for gene therapy of melanoma, J Virol *72*, 789-95.

Dong, J. Y., Wang, D., Van Ginkel, F. W., Pascual, D. W., and Frizzell, R. A. (1996). Systematic analysis of repeated gene delivery into animal lungs with a recombinant adenovirus vector, Hum Gene Ther *7*, 319-31.

Dorig, R. E., Marcil, A., Chopra, A., and Richardson, C. D. (1993). The human CD46 molecule is a receptor for measles virus (Edmonston strain), Cell *75*, 295-305.

Dranoff, G., Jaffee, E., Lazenby, A., Golumbek, P., Levitsky, H., Brose, K., Jackson, V., Hamada, H., Pardoll, D., and Mulligan, R. C. (1993). Vaccination with irradiated tumor cells engineered to secrete murine granulocyte-macrophage colony-stimulating factor stimulates potent, specific, and long-lasting anti-tumor immunity, Proc Natl Acad Sci U S A *90*, 3539-43.

Eiden, M. V., Farrell, K. B., and Wilson, C. A. (1996). Substitution of a single amino acid residue is sufficient to allow the human amphotropic murine leukemia virus receptor to also function as a gibbon ape leukemia virus receptor, J Virol *70*, 1080-5.

Einfeld, D., and Hunter, E. (1988). Oligomeric structure of a prototype retrovirus glycoprotein, Proc Natl Acad Sci U S A *85*, 8688-92.

Emerman, M. (1996). HIV-1, Vpr and the cell cycle, Curr Biol *6*, 1096-103.

Fadok, V. A., Bratton, D. L., Frasch, S. C., Warner, M. L., and Henson, P. M. (1998). The role of phosphatidylserine in recognition of apoptotic cells by phagocytes, Cell Death Differ *5*, 551-62.

Fass, D., Davey, R. A., Hamson, C. A., Kim, P. S., Cunningham, J. M., and Berger, J. M. (1997). Structure of a murine leukemia virus receptor-binding glycoprotein at 2.0 angstrom resolution, Science *277*, 1662-6.

Fass, D., Harrison, S. C., and Kim, P. S. (1996). Retrovirus envelope domain at 1.7 angstrom resolution, Nat Struct Biol *3*, 465-9.

Federico, M. (1999). Lentiviruses as gene delivery vectors, Curr Opin Biotechnol *10*, 448-53.

Feldman, A. L., and Libutti, S. K. (2000). Progress in antiangiogenic gene therapy of cancer, Cancer *89*, 1181-94.

Feulgen R, V. K. (1924). Uber den Mechanismus der Nuclealfearbung. II. Mittheilung. Uber das verhalten der kerne partiell hydrolysierter mikroskopischer Praparate zur fuchsin-schwefligen Saure nach voraufgegangener Behandlung mit Phenylhydrazin., Z Physiol Chem *136*, 57-61.

Fielding, A. K., Chapel-Fernandes, S., Chadwick, M. P., Bullough, F. J., Cosset, F. L., and Russell, S. J. (2000). A hyperfusogenic gibbon ape leukemia envelope glycoprotein: targeting of a cytotoxic gene by ligand display, Hum Gene Ther *11*, 817-26.

Florkiewicz, R. Z., and Rose, J. K. (1984). A cell line expressing vesicular stomatitis virus glycoprotein fuses at low pH, Science *225*, 721-3.

Frankel, A. D., and Young, J. A. (1998). HIV-1: fifteen proteins and an RNA, Annu Rev Biochem *67*, 1-25.

Freeman, S. M., Abboud, C. N., Whartenby, K. A., Packman, C. H., Koeplin, D. S., Moolten, F. L., and Abraham, G. N. (1993). The bystander effect: tumor regression when a fraction of the tumor mass is genetically modified, Cancer Res *53*, 5274-83.

Fugier-Vivier, I., Servet-Delprat, C., Rivailler, P., Rissoan, M. C., Liu, Y. J., and Rabourdin-Combe, C. (1997). Measles virus suppresses cell-mediated immunity by interfering with the survival and functions of dendritic and T cells, J Exp Med *186*, 813-23.

Gagandeep, S., Brew, R., Green, B., Christmas, S. E., Klatzmann, D., Poston, G. J., and Kinsella, A. R. (1996). Prodrug-activated gene therapy: involvement of an immunological component in the bystander effect, Cancer Gene Ther *3*, 83-8.

Gaken, J., Jiang, J., Daniel, K., van Berkel, E., Hughes, C., Kuiper, M., Darling, D., Tavassoli, M., Galea-Lauri, J., Ford, K., *et al.* (2000). Fusagene vectors: a novel strategy for the expression of multiple genes from a single cistron, Gene Ther *7*, 1979-85.

Galanis, E., Bateman, A., Johnson, K., Diaz, R. M., James, C. D., Vile, R., and Russell, S. J. (2001). Use of viral fusogenic membrane glycoproteins as novel therapeutic transgenes in gliomas, Hum Gene Ther *12*, 811-21.

Gallucci, S., Lolkema, M., and Matzinger, P. (1999). Natural adjuvants: endogenous activators of dendritic cells, Nat Med *5*, 1249-55.

Gasson, J. C. (1991). Molecular physiology of granulocyte-macrophage colony-stimulating factor, Blood *77*, 1131-45.

Gaudin, Y. (2000). Reversibility in fusion protein conformational changes. The intriguing case of rhabdovirus-induced membrane fusion, Subcell Biochem *34*, 379-408.

Gething, M. J., and Sambrook, J. (1992). Protein folding in the cell, Nature *355*, 33-45.

Geutskens, S. B., van der Eb, M. M., Plomp, A. C., Jonges, L. E., Cramer, S. J., Ensink, N. G., Kuppen, P. J., and Hoeben, R. C. (2000). Recombinant adenoviral vectors have adjuvant activity and stimulate T cell responses against tumor cells, Gene Ther *7*, 1410-6.

Gliniak, B. C., Kozak, S. L., Jones, R. T., and Kabat, D. (1991). Disulfide bonding controls the processing of retroviral envelope glycoproteins, J Biol Chem *266*, 22991-7.

Gong, J., Chen, D., Kashiwaba, M., and Kufe, D. (1997). Induction of antitumor activity by immunization with fusions of dendritic and carcinoma cells, Nat Med *3*, 558-61.

Gordon, E. M., Chen, Z. H., Liu, L., Whitley, M., Wei, D., Groshen, S., Hinton, D. R., Anderson, W. F., Beart, R. W., Jr., and Hall, F. L. (2001). Systemic administration of a matrix-targeted retroviral vector is efficacious for cancer gene therapy in mice, Hum Gene Ther *12*, 193-204.

Gough, M. J., Melcher, A. A., Ahmed, A., Crittenden, M. R., Riddle, D. S., Linardakis, E., Ruchatz, A. N., Emiliusen, L. M., and Vile, R. G. (2001). Macrophages orchestrate the immune response to tumor cell death, Cancer Res *61*, 7240-7.

Grable, M., and Hearing, P. (1992). cis and trans requirements for the selective packaging of adenovirus type 5 DNA, J Virol *66*, 723-31.

Graham, F. L., Smiley, J., Russell, W. C., and Nairn, R. (1977). Characteristics of a human cell line transformed by DNA from human adenovirus type 5, J Gen Virol *36*, 59-74.

Greber, U. F., Willetts, M., Webster, P., and Helenius, A. (1993). Stepwise dismantling of adenovirus 2 during entry into cells, Cell *75*, 477-86.

Griffin, D.E., Bellini, W.J., (1996). Fields Virology, Third Edition edn (Philadelphia, Lippincott).

Gromme, M., Uytdehaag, F. G., Janssen, H., Calafat, J., van Binnendijk, R. S., Kenter, M. J., Tulp, A., Verwoerd, D., and Neefjes, J. (1999). Recycling MHC class I molecules and endosomal peptide loading, Proc Natl Acad Sci U S A *96*, 10326-31.

Grosjean, I., Caux, C., Bella, C., Berger, I., Wild, F., Banchereau, J., and Kaiserlian, D. (1997). Measles virus infects human dendritic cells and blocks their allostimulatory properties for CD4+ T cells, J Exp Med *186*, 801-12.

Guenechea, G., Gan, O. I., Inamitsu, T., Dorrell, C., Pereira, D. S., Kelly, M., Naldini, L., and Dick, J. E. (2000). Transduction of human CD34+ CD38- bone marrow and cord blood-derived SCID-repopulating cells with third-generation lentiviral vectors, Mol Ther *1*, 566-73.

Gurley, A. M., Hidvegi, D. F., Bacus, J. W., and Bacus, S. S. (1990). Comparison of the Papanicolaou and Feulgen staining methods for DNA quantification by image analysis, Cytometry *11*, 468-74.

Hall, A. R., Dix, B. R., O'Carroll, S. J., and Braithwaite, A. W. (1998). p53-dependent cell death/apoptosis is required for a productive adenovirus infection, Nat Med *4*, 1068-72.

Hallenbeck, P. L., Chang, Y. N., Hay, C., Golightly, D., Stewart, D., Lin, J., Phipps, S., and Chiang, Y. L. (1999). A novel tumor-specific replication-restricted adenoviral vector for gene therapy of hepatocellular carcinoma, Hum Gene Ther *10*, 1721-33.

Hamstra, D. A., Page, M., Maybaum, J., and Rehemtulla, A. (2000). Expression of endogenously activated secreted or cell surface carboxypeptidase A sensitizes tumor cells to methotrexate-alpha-peptide prodrugs, Cancer Res *60*, 657-65.

Hanahan, D., and Folkman, J. (1996). Patterns and emerging mechanisms of the angiogenic switch during tumorigenesis, Cell *86*, 353-64.

Hanahan, D., and Weinberg, R. A. (2000). The hallmarks of cancer, Cell *100*, 57-70.

Hanna, N. N., Mauceri, H. J., Wayne, J. D., Hallahan, D. E., Kufe, D. W., and Weichselbaum, R. R. (1997). Virally directed cytosine deaminase/5-fluorocytosine gene therapy enhances radiation response in human cancer xenografts, Cancer Res *57*, 4205-9.

Hardy, S., Kitamura, M., Harris-Stansil, T., Dai, Y., and Phipps, M. L. (1997). Construction of adenovirus vectors through Cre-lox recombination, J Virol *71*, 1842-9.

Harris, H., and Watkins, J. F. (1965). Hybrid cells derived from mouse and man: artificial heterokaryons of mammalian cells from different species, Nature *205*, 640-646.

Harris, S. R., and Thorgeirsson, U. P. (1998). Tumor angiogenesis: biology and therapeutic prospects, In Vivo *12*, 563-70.

Hearing, P., Samulski, R. J., Wishart, W. L., and Shenk, T. (1987). Identification of a repeated sequence element required for efficient encapsidation of the adenovirus type 5 chromosome, J Virol *61*, 2555-8.

Heise, C., Sampson-Johannes, A., Williams, A., McCormick, F., Von Hoff, D. D., and Kirn, D. H. (1997). ONYX-015, an E1B gene-attenuated adenovirus, causes tumor-specific cytolysis and antitumoral efficacy that can be augmented by standard chemotherapeutic agents, Nat Med *3*, 639-45.

Hengartner, M. O. (2000). The biochemistry of apoptosis, Nature *407*, 770-6.

Hermiston, T. (2000). Gene delivery from replication-selective viruses: arming guided missiles in the war against cancer, J Clin Invest *105*, 1169-72.

Hernandez, L. D., Hoffman, L. R., Wolfsberg, T. G., and White, J. M. (1996). Virus-cell and cell-cell fusion, Annu Rev Cell Dev Biol *12*, 627-61.

Higuchi, H., Bronk, S. F., Bateman, A., Harrington, K., Vile, R. G., and Gores, G. J. (2000). Viral fusogenic membrane glycoprotein expression causes syncytia formation with bioenergetic cell death: implications for gene therapy, Cancer Res *60*, 6396-402.

Hoess, R. H., and Abremski, K. (1984). Interaction of the bacteriophage P1 recombinase Cre with the recombining site loxP, Proc Natl Acad Sci U S A *81*, 1026-9.

Hoffmann, T. K., Meidenbauer, N., Dworacki, G., Kanaya, H., and Whiteside, T. L. (2000). Generation of tumor-specific T-lymphocytes by cross-priming with human dendritic cells ingesting apoptotic tumor cells, Cancer Res *60*, 3542-9.

http://seer.cancer.gov/Publications/CSR1973_1997/overview/.

Hu, W. S., and Pathak, V. K. (2000). Design of retroviral vectors and helper cells for gene therapy, Pharmacol Rev *52*, 493-511.

Inaba, K., Inaba, M., Romani, N., Aya, H., Deguchi, M., Ikehara, S., Muramatsu, S., and Steinman, R. M. (1992). Generation of large numbers of dendritic cells from mouse bone marrow cultures supplemented with granulocyte/macrophage colony-stimulating factor, J Exp Med *176*, 1693-702.

Jaattela, M. (1999). Escaping cell death: survival proteins in cancer, Exp Cell Res *248*, 30-43.

Jaffee, E. M., Hruban, R. H., Biedrzycki, B., Laheru, D., Schepers, K., Sauter, P. R., Goemann, M., Coleman, J., Grochow, L., Donehower, R. C., *et al.* (2001). Novel allogeneic granulocyte-macrophage colony-stimulating factor- secreting tumor vaccine for pancreatic cancer: a phase I trial of safety and immune activation, J Clin Oncol *19*, 145-56.

Januszeski, M. M., Cannon, P. M., Chen, D., Rozenberg, Y., and Anderson, W. F. (1997). Functional analysis of the cytoplasmic tail of Moloney murine leukemia virus envelope protein, J Virol *71*, 3613-9.

Kafri, T. (2001). Lentivirus vectors: difficulties and hopes before clinical trials, Curr Opin Mol Ther *3*, 316-26.

Kantarjian, H., Sawyers, C., Hochhaus, A., Guilhot, F., Schiffer, C., Gambacorti-Passerini, C., Niederwieser, D., Resta, D., Capdeville, R., Zoellner, U., *et al.* (2002). Hematologic and cytogenetic responses to imatinib mesylate in chronic myelogenous leukemia, N Engl J Med *346*, 645-52.

Karp, C. L., Wysocka, M., Wahl, L. M., Ahearn, J. M., Cuomo, P. J., Sherry, B., Trinchieri, G., and Griffin, D. E. (1996). Mechanism of suppression of cell-mediated immunity by measles virus, Science *273*, 228-31.

Kaufmann, S. H., Okret, S., Wikstrom, A. C., Gustafsson, J. A., and Shaper, J. H. (1986). Binding of the glucocorticoid receptor to the rat liver nuclear matrix. The role of disulfide bond formation, J Biol Chem *261*, 11962-7.

Kavanaugh, M. P., Miller, D. G., Zhang, W., Law, W., Kozak, S. L., Kabat, D., and Miller, A. D. (1994). Cell-surface receptors for gibbon ape leukemia virus and amphotropic murine retrovirus are inducible sodium-dependent phosphate symporters, Proc Natl Acad Sci U S A *91*, 7071-5.

Kawakami, T. G., Huff, S. D., Buckley, P. M., Dungworth, D. L., Synder, S. P., and Gilden, R. V. (1972). C-type virus associated with gibbon lymphosarcoma, Nat New Biol *235*, 170-1.

Kawashita, Y., Ohtsuru, A., Kaneda, Y., Nagayama, Y., Kawazoe, Y., Eguchi, S., Kuroda, H., Fujioka, H., Ito, M., Kanematsu, T., and Yamashita, S. (1999). Regression of hepatocellular carcinoma in vitro and in vivo by radiosensitizing suicide gene therapy under the inducible and spatial control of radiation, Hum Gene Ther *10*, 1509-19.

Kay, M. A., Glorioso, J. C., and Naldini, L. (2001). Viral vectors for gene therapy: the art of turning infectious agents into vehicles of therapeutics, Nat Med *7*, 33-40.

Kayaga, J., Souberbielle, B. E., Sheikh, N., Morrow, W. J., Scott-Taylor, T., Vile, R., Chong, H., and Dalgleish, A. G. (1999). Anti-tumour activity against B16-F10 melanoma with a GM-CSF secreting allogeneic tumour cell vaccine, Gene Ther *6*, 1475-81.

Kerkau, T., Bacik, I., Bennink, J. R., Yewdell, J. W., Hunig, T., Schimpl, A., and Schubert, U. (1997). The human immunodeficiency virus type 1 (HIV-1) Vpu protein interferes with an early step in the biosynthesis of major histocompatibility complex (MHC) class I molecules, J Exp Med *185*, 1295-305.

Kerr, J. F., Wyllie, A. H., and Currie, A. R. (1972). Apoptosis: a basic biological phenomenon with wide-ranging implications in tissue kinetics, Br J Cancer *26*, 239-57.

Ketner, G., Spencer, F., Tugendreich, S., Connelly, C., and Hieter, P. (1994). Efficient manipulation of the human adenovirus genome as an infectious yeast artificial chromosome clone, Proc Natl Acad Sci U S A *91*, 6186-90.

Khuri, F. R., Nemunaitis, J., Ganly, I., Arseneau, J., Tannock, I. F., Romel, L., Gore, M., Ironside, J., MacDougall, R. H., Heise, C., *et al.* (2000). A controlled trial of intratumoral ONYX-015, a selectively-replicating adenovirus, in combination with cisplatin and 5-fluorouracil in patients with recurrent head and neck cancer, Nature Medicine *6*, 879-885.

Kirn, D. H. (2000). A tale of two trials: selectively replicating herpesviruses for brain tumors, Gene Ther *7*, 815-6.

Kitanaka, C., and Kuchino, Y. (1999). Caspase-independent programmed cell death with necrotic morphology, Cell Death Differ *6*, 508-15.

Klatzmann, D., Cherin, P., Bensimon, G., Boyer, O., Coutellier, A., Charlotte, F., Boccaccio, C., Salzmann, J. L., and Herson, S. (1998a). A phase I/II dose-escalation study of herpes simplex virus type 1 thymidine kinase suicide gene therapy for metastatic melanoma. Study Group on Gene Therapy of Metastatic Melanoma, Hum Gene Ther *9*, 2585-94.

Klatzmann, D., Valery, C. A., Bensimon, G., Marro, B., Boyer, O., Mokhtari, K., Diquet, B., Salzmann, J. L., and Philippon, J. (1998b). A phase I/II study of herpes simplex virus type 1 thymidine kinase suicide gene therapy for recurrent glioblastoma. Study Group on Gene Therapy for Glioblastoma, Hum Gene Ther *9*, 2595-604.

Kleijmeer, M. J., Escola, J. M., UytdeHaag, F. G., Jakobson, E., Griffith, J. M., Osterhaus, A. D., Stoorvogel, W., Melief, C. J., Rabouille, C., and Geuze, H. J. (2001). Antigen loading of MHC class I molecules in the endocytic tract, Traffic *2*, 124-37.

Klein, C., Bueler, H., and Mulligan, R. C. (2000). Comparative analysis of genetically modified dendritic cells and tumor cells as therapeutic cancer vaccines, J Exp Med *191*, 1699-708.

Klionsky, D. J., and Emr, S. D. (2000). Autophagy as a regulated pathway of cellular degradation, Science *290*, 1717-21.

Kobune, F., Sakata, H., and Sugiura, A. (1990). Marmoset lymphoblastoid cells as a sensitive host for isolation of measles virus, J Virol *64*, 700-5.

Kochanek, S., Clemens, P. R., Mitani, K., Chen, H. H., Chan, S., and Caskey, C. T. (1996). A new adenoviral vector: Replacement of all viral coding sequences with 28 kb of DNA independently expressing both full-length dystrophin and beta-galactosidase, Proc Natl Acad Sci U S A *93*, 5731-6.

Kokoris, M., Sabo, P., and Black, M. (2000). In Vitro evaluation of Mutant HSV-1 Thymidine Kinases for Suicide Gene Therapy, Anticancer Research *20*, 959-964.

Kol, A., Lichtman, A. H., Finberg, R. W., Libby, P., and Kurt-Jones, E. A. (2000). Cutting edge: heat shock protein (HSP) 60 activates the innate immune response: CD14 is an essential receptor for HSP60 activation of mononuclear cells, J Immunol *164*, 13-7.

Kordower, J. H., Emborg, M. E., Bloch, J., Ma, S. Y., Chu, Y., Leventhal, L., McBride, J., Chen, E. Y., Palfi, S., Roitberg, B. Z., *et al.* (2000). Neurodegeneration prevented by lentiviral vector delivery of GDNF in primate models of Parkinson's disease, Science *290*, 767-73.

Krammer, P. H. (2000). CD95's deadly mission in the immune system, Nature *407*, 789-95.

Krasnykh, V. N., Douglas, J. T., and van Beusechem, V. W. (2000). Genetic targeting of adenoviral vectors, Mol Ther *1*, 391-405.

Kroemer, G., Dallaporta, B., and Resche-Rigon, M. (1998). The mitochondrial death/life regulator in apoptosis and necrosis, Annu Rev Physiol *60*, 619-42.

Kugler, A., Stuhler, G., Walden, P., Zoller, G., Zobywalski, A., Brossart, P., Trefzer, U., Ullrich, S., Muller, C. A., Becker, V., *et al.* (2000). Regression of human metastatic renal cell carcinoma after vaccination with tumor cell-dendritic cell hybrids, Nat Med *6*, 332-6.

Kuppen, P. J. K., van der Eb, M. M., Jonges, L. E., Hagenaars, M., Hokland, M. E., Nannmark, U., Goldfarb, R. H., Basse, P.H., Fleuren, G.H., Hoeben, R. C., and van de Velde, C. J. H. (2001). Tumor structure and extracellular matrix as apossible barrier for therapeutic approaches using immune cells or adenoviruses in colorectal cancer, Histochem Cell Biol (2001) *115*:67-72.

Lakso, M., Sauer, B., Mosinger, B., Jr., Lee, E. J., Manning, R. W., Yu, S. H., Mulder, K. L., and Westphal, H. (1992). Targeted oncogene activation by site-specific recombination in transgenic mice, Proc Natl Acad Sci U S A *89*, 6232-6.

Lamb, R. A., Joshi, S. B., and Dutch, R. E. (1999). The paramyxovirus fusion protein forms an extremely stable core trimer: structural parallels to influenza virus haemagglutinin and HIV-1 gp41, Mol Membr Biol *16*, 11-9.

Lamb, R. A., and Pinto, L. H. (1997). Do Vpu and Vpr of human immunodeficiency virus type 1 and NB of influenza B virus have ion channel activities in the viral life cycles?, Virology *229*, 1-11.

Lambin, P., Nuyts, S., Landuyt, W., Theys, J., De Bruijn, E., Anne, J., Van Mellaert, L., and Fowler, J. (2000). The potential therapeutic gain of radiation-associated gene therapy with the suicide gene cytosine deaminase, Int J Radiat Biol *76*, 285-93.

Lavillette, D., Maurice, M., Roche, C., Russell, S. J., Sitbon, M., and Cosset, F. L. (1998). A proline-rich motif downstream of the receptor binding domain modulates conformation and fusogenicity of murine retroviral envelopes, J Virol *72*, 9955-65.

Levitt, J. M., Howell, D. D., Rodgers, J. R., and Rich, R. R. (2001). Exogenous peptides enter the endoplasmic reticulum of TAP-deficient cells and induce the maturation of nascent MHC class I molecules, Eur J Immunol *31*, 1181-90.

Liang, X. H., Jackson, S., Seaman, M., Brown, K., Kempkes, B., Hibshoosh, H., and Levine, B. (1999). Induction of autophagy and inhibition of tumorigenesis by beclin 1, Nature *402*, 672-6.

Lin, A. H., Kasahara, N., Wu, W., Stripecke, R., Empig, C. L., Anderson, W. F., and Cannon, P. M. (2001). Receptor-specific targeting mediated by the coexpression of a targeted murine leukemia virus envelope protein and a binding-defective influenza hemagglutinin protein, Hum Gene Ther *12*, 323-32.

Lipsker, D., Ziylan, U., Spehner, D., Proamer, F., Bausinger, H., Jeannin, P., Salamero, J., Bohbot, A., Cazenave, J. P., Drillien, R., *et al.* (2002). Heat shock proteins 70 and 60 share common receptors which are expressed on human monocyte-derived but not epidermal dendritic cells, Eur J Immunol *32*, 322-32.

Majno, G., and Joris, I. (1995). Apoptosis, oncosis, and necrosis. An overview of cell death, Am J Pathol *146*, 3-15.

Manchester, M., Naniche, D., and Stehle, T. (2000). CD46 as a measles receptor: form follows function, Virology *274*, 5-10.

Mangel, W. F., McGrath, W. J., Toledo, D. L., and Anderson, C. W. (1993). Viral DNA and a viral peptide can act as cofactors of adenovirus virion proteinase activity, Nature *361*, 274-5.

Mann, R., Mulligan, R. C., and Baltimore, D. (1983). Construction of a retrovirus packaging mutant and its use to produce helper-free defective retrovirus, Cell *33*, 153-9.

Marais, R., Spooner, R. A., Light, Y., Martin, J., and Springer, C. J. (1996). Gene-directed enzyme prodrug therapy with a mustard prodrug/carboxypeptidase G2 combination, Cancer Res *56*, 4735-42.

Marcusson, E. G., Yacyshyn, B. R., Shanahan, W. R., Jr., and Dean, N. M. (1999). Preclinical and clinical pharmacology of antisense oligonucleotides, Mol Biotechnol *12*, 1-11.

Marin, M., Rose, K. M., Kozak, S. L., and Kabat, D. (2003). HIV-1 Vif protein binds the editing enzyme APOBEC3G and induces its degradation, Nat Med 9, 1398-1407.

Markert, J. M., Medlock, M. D., Rabkin, S. D., Gillespie, G. Y., Todo, T., Hunter, W. D., Palmer, C. A., Feigenbaum, F., Tornatore, C., Tufaro, F., and Martuza, R. L. (2000). Conditionally replicating herpes simplex virus mutant, G207 for the treatment of malignant glioma: results of a phase I trial, Gene Ther *7*, 867-74.

Markowitz, D., Goff, S., and Bank, A. (1988). Construction and use of a safe and efficient amphotropic packaging cell line, Virology *167*, 400-6.

Martinez-Salas, E. (1999). Internal ribosome entry site biology and its use in expression vectors, Curr Opin Biotechnol *10*, 458-64.

Martuza, R. L. (2000). Conditionally replicating herpes vectors for cancer therapy, J Clin Invest *105*, 841-6.

Matzinger, P. (1994). Tolerance, danger, and the extended family, Annu Rev Immunol *12*, 991-1045.

Matzinger, P. (1998). An innate sense of danger, Semin Immunol *10*, 399-415.

Maurice, M., Mazur, S., Bullough, F. J., Salvetti, A., Collins, M. K., Russell, S. J., and Cosset, F. L. (1999). Efficient gene delivery to quiescent interleukin-2 (IL-2)-dependent cells by murine leukemia virus-derived vectors harboring IL-2 chimeric envelope glycoproteins, Blood *94*, 401-10.

McCart, J. A., Puhlmann, M., Lee, J., Hu, Y., Libutti, S. K., Alexander, H. R., and Bartlett, D. L. (2000). Complex interactions between the replicating oncolytic effect and the enzyme/prodrug effect of vaccinia-mediated tumor regression, Gene Ther *7*, 1217-23.

McGrory, W. J., Bautista, D. S., and Graham, F. L. (1988). A simple technique for the rescue of early region I mutations into infectious human adenovirus type 5, Virology *163*, 614-7.

McGuire, W. P., Hoskins, W. J., Brady, M. F., Kucera, P. R., Partridge, E. E., Look, K. Y., Clarke-Pearson, D. L., and Davidson, M. (1997). Comparison of combination therapy with paclitaxel and cisplatin versus cyclophosphamide and cisplatin in patients with suboptimal stage III and stage IV ovarian cancer: a Gynecologic Oncology Group study, Semin Oncol *24*, S2-13-S2-16.

Meier, P., Finch, A., and Evan, G. (2000). Apoptosis in development, Nature *407*, 796-801.

Melcher, A., Gough, M., Todryk, S., and Vile, R. (1999). Apoptosis or necrosis for tumor immunotherapy: what's in a name?, J Mol Med *77*, 824-33.

Melcher, A., Todryk, S., Hardwick, N., Ford, M., Jacobson, M., and Vile, R. G. (1998). Tumor immunogenicity is determined by the mechanism of cell death via induction of heat shock protein expression, Nat Med *4*, 581-7.

Metcalf, D. (1985). The granulocyte-macrophage colony-stimulating factors, Science *229*, 16-22.

Miller, A. D. (1996). Cell-surface receptors for retroviruses and implications for gene transfer, Proc Natl Acad Sci U S A *93*, 11407-13.

Miller, A. D., and Buttimore, C. (1986). Redesign of retrovirus packaging cell lines to avoid recombination leading to helper virus production, Mol Cell Biol *6*, 2895-902.

Miller, A. D., Garcia, J. V., von Suhr, N., Lynch, C. M., Wilson, C., and Eiden, M. V. (1991). Construction and properties of retrovirus packaging cells based on gibbon ape leukemia virus, J Virol *65*, 2220-4.

Miller, C. R., Buchsbaum, D. J., Reynolds, P. N., Douglas, J. T., Gillespie, G. Y., Mayo, M. S., Raben, D., and Curiel, D. T. (1998). Differential susceptibility of primary and established human glioma cells to adenovirus infection: targeting via the epidermal growth factor receptor achieves fiber receptor-independent gene transfer, Cancer Res *58*, 5738-48.

Miller, D. G., and Miller, A. D. (1993). Inhibitors of retrovirus infection are secreted by several hamster cell lines and are also present in hamster sera, J Virol *67*, 5346-52.

Mittereder, N., March, K. L., and Trapnell, B. C. (1996). Evaluation of the concentration and bioactivity of adenovirus vectors for gene therapy, J Virol *70*, 7498-509.

Miyoshi, H., Blomer, U., Takahashi, M., Gage, F. H., and Verma, I. M. (1998). Development of a self-inactivating lentivirus vector, J Virol *72*, 8150-7.

Moolten, F. L. (1986). Tumor chemosensitivity conferred by inserted herpes thymidine kinase genes: paradigm for a prospective cancer control strategy, Cancer Res *46*, 5276-81.

Moolten, F. L. (1994). Drug sensitivity (suicide) genes for selective cancer chemotherapy, Cancer Gene Ther *1*, 279-87.

Morgenstern, J. P., and Land, H. (1990). Advanced mammalian gene transfer: high titre retroviral vectors with multiple drug selection markers and a complementary helper-free packaging cell line, Nucleic Acids Res *18*, 3587-96.

Morimoto, R. I. (1993). Cells in stress: transcriptional activation of heat shock genes, Science *259*, 1409-10.

Mroz, P. J., and Moolten, F. L. (1993). Retrovirally transduced Escherichia coli gpt genes combine selectability with chemosensitivity capable of mediating tumor eradication, Hum Gene Ther *4*, 589-95.

Mullen, C. A., Kilstrup, M., and Blaese, R. M. (1992). Transfer of the bacterial gene for cytosine deaminase to mammalian cells confers lethal sensitivity to 5-fluorocytosine: a negative selection system, Proc Natl Acad Sci U S A *89*, 33-7.

Mulsant, P., Gatignol, A., Dalens, M., and Tiraby, G. (1988). Phleomycin resistance as a dominant selectable marker in CHO cells, Somat Cell Mol Genet *14*, 243-52.

Murphy, F., Fauquet, C., and Bishop, D. (1995). Virus taxonomy: 6th report of the international committee on taxonomy of viruses, Archives of Virology *Supplement 10*, 193-201.

Muzio, M., Stockwell, B. R., Stennicke, H. R., Salvesen, G. S., and Dixit, V. M. (1998). An induced proximity model for caspase-8 activation, J Biol Chem *273*, 2926-30.

Nakayama, K. (1997). Furin: a mammalian subtilisin/Kex2p-like endoprotease involved in processing of a wide variety of precursor proteins, Biochem J *327*, 625-35.

Naldini, L., Blomer, U., Gallay, P., Ory, D., Mulligan, R., Gage, F. H., Verma, I. M., and Trono, D. (1996). In vivo gene delivery and stable transduction of nondividing cells by a lentiviral vector, Science *272*, 263-7.

Naniche, D., Varior-Krishnan, G., Cervoni, F., Wild, T. F., Rossi, B., Rabourdin-Combe, C., and Gerlier, D. (1993). Human membrane cofactor protein (CD46) acts as a cellular receptor for measles virus, J Virol *67*, 6025-32.

Nicotera, P., Leist, M., and Ferrando-May, E. (1998). Intracellular ATP, a switch in the decision between apoptosis and necrosis, Toxicol Lett *102-103*, 139-42.

O'Hara, B., Johann, S. V., Klinger, H. P., Blair, D. G., Rubinson, H., Dunn, K. J., Sass, P., Vitek, S. M., and Robins, T. (1990). Characterization of a human gene conferring sensitivity to infection by gibbon ape leukemia virus, Cell Growth Differ *1*, 119-27.

Ogura, H., Sato, H., Kamiya, S., and Nakamura, S. (1991). Glycosylation of measles virus haemagglutinin protein in infected cells, J Gen Virol *72*, 2679-84.

Ohashi, K., Burkart, V., Flohe, S., and Kolb, H. (2000). Cutting edge: heat shock protein 60 is a putative endogenous ligand of the toll-like receptor-4 complex, J Immunol *164*, 558-61.

Pannell, D., and Ellis, J. (2001). Silencing of gene expression: implications for design of retrovirus vectors, Rev Med Virol *11*, 205-17.

Parmiani, G., Rivoltini, L., Andreola, G., and Carrabba, M. (2000). Cytokines in cancer therapy, Immunol Lett *74*, 41-4.

Patterson, A. V., Zhang, H., Moghaddam, A., Bicknell, R., Talbot, D. C., Stratford, I. J., and Harris, A. L. (1995). Increased sensitivity to the prodrug 5'-deoxy-5-fluorouridine and modulation of 5-fluoro-2'-deoxyuridine sensitivity in MCF-7 cells transfected with thymidine phosphorylase, Br J Cancer *72*, 669-75.

Pawlik, T. M., Nakamura, H., Yoon, S. S., Mullen, J. T., Chandrasekhar, S., Chiocca, E. A., and Tanabe, K. K. (2000). Oncolysis of diffuse hepatocellular carcinoma by intravascular administration of a replication-competent, genetically engineered herpesvirus, Cancer Res *60*, 2790-5.

Pedersen, L., van Zeijl, M., Johann, S. V., and O'Hara, B. (1997). Fungal phosphate transporter serves as a receptor backbone for gibbon ape leukemia virus, J Virol *71*, 7619-22.

Pederson, L. C., Buchsbaum, D. J., Vickers, S. M., Kancharla, S. R., Mayo, M. S., Curiel, D. T., and Stackhouse, M. A. (1997). Molecular chemotherapy combined with radiation therapy enhances killing of cholangiocarcinoma cells in vitro and in vivo, Cancer Res *57*, 4325-32.

Peng, K.-W., and Vile, R. (1999). Vector development for cancer gene therapy, Tumor Targeting *4*, 3-11.

Peng, K. W., Vile, R., Cosset, F. L., and Russell, S. (1999). Selective transduction of protease-rich tumors by matrix- metalloproteinase-targeted retroviral vectors, Gene Ther *6*, 1552-7.

Peng, P., Menoret, A., and Srivastava, P. K. (1997). Purification of immunogenic heat shock protein 70-peptide complexes by ADP-affinity chromatography, J Immunol Methods *204*, 13-21.

Pennisi, E. (1998). Training viruses to attack cancers, Science *282*, 1244-6.

Pirkkala, L., Nykanen, P., and Sistonen, L. (2001). Roles of the heat shock transcription factors in regulation of the heat shock response and beyond, Faseb J *15*, 1118-31.

Polacino, P. S., Pinchuk, L. M., Sidorenko, S. P., and Clark, E. A. (1996). Immunodeficiency virus cDNA synthesis in resting T lymphocytes is regulated by T cell activation signals and dendritic cells, J Med Primatol *25*, 201-9.

Poste, G. (1970). Virus-induced polykaryocytosis and the mechanism of cell fusion, Adv Virus Res *16*, 303-56.

Poumbourios, P., Center, R. J., Wilson, K. A., Kemp, B. E., and Kobe, B. (1999). Evolutionary conservation of the membrane fusion machine, IUBMB Life *48*, 151-6.

Punnonen, J., Cocks, B. G., Carballido, J. M., Bennett, B., Peterson, D., Aversa, G., and de Vries, J. E. (1997). Soluble and membrane-bound forms of signaling lymphocytic activation molecule (SLAM) induce proliferation and Ig synthesis by activated human B lymphocytes, J Exp Med *185*, 993-1004.

Querido, E., Marcellus, R. C., Lai, A., Charbonneau, R., Teodoro, J. G., Ketner, G., and Branton, P. E. (1997a). Regulation of p53 levels by the E1B 55-kilodalton protein and E4orf6 in adenovirus-infected cells, J Virol *71*, 3788-98.

Querido, E., Teodoro, J. G., and Branton, P. E. (1997b). Accumulation of p53 induced by the adenovirus E1A protein requires regions involved in the stimulation of DNA synthesis, J Virol *71*, 3526-33.

Ram, Z., Culver, K. W., Oshiro, E. M., Viola, J. J., DeVroom, H. L., Otto, E., Long, Z., Chiang, Y., McGarrity, G. J., Muul, L. M., *et al.* (1997). Therapy of malignant brain tumors by intratumoral implantation of retroviral vector-producing cells, Nat Med *3*, 1354-61.

Rampling, R., Cruickshank, G., Papanastassiou, V., Nicoll, J., Hadley, D., Brennan, D., Petty, R., MacLean, A., Harland, J., McKie, E., *et al.* (2000). Toxicity evaluation of replication-competent herpes simplex virus (ICP 34.5 null mutant 1716) in patients with recurrent malignant glioma, Gene Ther *7*, 859-66.

Rao, L., Debbas, M., Sabbatini, P., Hockenbery, D., Korsmeyer, S., and White, E. (1992). The adenovirus E1A proteins induce apoptosis, which is inhibited by the E1B 19-kDa and Bcl-2 proteins, Proc Natl Acad Sci U S A *89*, 7742-6.

Reitz, M. S., Jr., Voltin, M., and Gallo, R. C. (1980). Characterization of a partial provirus from a gibbon ape naturally infected with gibbon ape leukemia virus, Virology *104*, 474-81.

Restifo, N. P. (2000). Building better vaccines: how apoptotic cell death can induce inflammation and activate innate and adaptive immunity, Curr Opin Immunol *12*, 597-603.

Rima, B. K., Earle, J. A., Baczko, K., ter Meulen, V., Liebert, U. G., Carstens, C., Carabana, J., Caballero, M., Celma, M. L., and Fernandez-Munoz, R. (1997). Sequence divergence of measles virus haemagglutinin during natural evolution and adaptation to cell culture, J Gen Virol *78*, 97-106.

Roberts, P. C., Kipperman, T., and Compans, R. W. (1999). Vesicular stomatitis virus G protein acquires pH-independent fusion activity during transport in a polarized endometrial cell line, J Virol *73*, 10447-57.

Rodriguez, R., Schuur, E. R., Lim, H. Y., Henderson, G. A., Simons, J. W., and Henderson, D. R. (1997). Prostate attenuated replication competent adenovirus (ARCA) CN706: a selective cytotoxic for prostate-specific antigen-positive prostate cancer cells, Cancer Res *57*, 2559-63.

Rogulski, K. R., Wing, M. S., Paielli, D. L., Gilbert, J. D., Kim, J. H., and Freytag, S. O. (2000). Double suicide gene therapy augments the antitumor activity of a replication-competent lytic adenovirus through enhanced cytotoxicity and radiosensitization, Hum Gene Ther *11*, 67-76.

Rogulski, K. R., Zhang, K., Kolozsvary, A., Kim, J. H., and Freytag, S. O. (1997). Pronounced antitumor effects and tumor radiosensitization of double suicide gene therapy, Clin Cancer Res *3*, 2081-8.

Rosenberg, S. A., Blaese, R. M., Brenner, M. K., Deisseroth, A. B., Ledley, F. D., Lotze, M. T., Wilson, J. M., Nabel, G. J., Cornetta, K., Economou, J. S., *et al.* (2000). Human gene marker/therapy clinical protocols, Hum Gene Ther *11*, 919-79.

Ross, P. J., and Parks R.J. (2003). Oncolytic adenovirus: getting there is half the battle, Molecular Therapy *8*, 705-6.

Roth, J. A., Nguyen, D., Lawrence, D. D., Kemp, B. L., Carrasco, C. H., Ferson, D. Z., Hong, W. K., Komaki, R., Lee, J. J., Nesbitt, J. C., *et al.* (1996). Retrovirus-mediated wild-type p53 gene transfer to tumors of patients with lung cancer, Nat Med *2*, 985-91.

Russell, S. J. (1994). Replicating vectors for gene therapy of cancer: risks, limitations and prospects, Eur J Cancer *8*, 1165-71.

Sallusto, F., and Lanzavecchia, A. (1994). Efficient presentation of soluble antigen by cultured human dendritic cells is maintained by granulocyte/macrophage colony-stimulating factor plus interleukin 4 and downregulated by tumor necrosis factor alpha, J Exp Med *179*, 1109-18.

Saraste, A. (1999). Morphologic criteria and detection of apoptosis, Herz *24*, 189-95.

Sauer, B. (1987). Functional expression of the cre-lox site-specific recombination system in the yeast Saccharomyces cerevisiae, Mol Cell Biol *7*, 2087-96.

Sauer, B. (1993). Manipulation of transgenes by site-specific recombination: use of Cre recombinase, Methods Enzymol *225*, 890-900.

Saunders, M., Dische, S., Barrett, A., Harvey, A., Griffiths, G., and Palmar, M. (1999). Continuous, hyperfractionated, accelerated radiotherapy (CHART) versus conventional radiotherapy in non-small cell lung cancer: mature data from the randomised multicentre trial. CHART Steering committee, Radiother Oncol *52*, 137-48.

Sauter, B., Albert, M. L., Francisco, L., Larsson, M., Somersan, S., and Bhardwaj, N. (2000). Consequences of cell death: exposure to necrotic tumor cells, but not primary tissue cells or apoptotic cells, induces the maturation of immunostimulatory dendritic cells [see comments], J Exp Med *191*, 423-34.

Savage, D. G., and Antman, K. H. (2002). Imatinib mesylate--a new oral targeted therapy, N Engl J Med *346*, 683-93.

Savill, J., and Fadok, V. (2000). Corpse clearance defines the meaning of cell death, Nature *407*, 784-8.

Scaffidi, C., Fulda, S., Srinivasan, A., Friesen, C., Li, F., Tomaselli, K. J., Debatin, K. M., Krammer, P. H., and Peter, M. E. (1998). Two CD95 (APO-1/Fas) signaling pathways, Embo J *17*, 1675-87.

Scheid, A., and Choppin, P. W. (1977). Two disulfide-linked polypeptide chains constitute the active F protein of paramyxoviruses, Virology *80*, 54-66.

Schlegel, R., Tralka, T. S., Willingham, M. C., and Pastan, I. (1983). Inhibition of VSV binding and infectivity by phosphatidylserine: is phosphatidylserine a VSV-binding site?, Cell *32*, 639-46.

Schneider-Schaulies, J. (2000). Cellular receptors for viruses: links to tropism and pathogenesis, J Gen Virol *81*, 1413-29.

Schuler, M., Rochlitz, C., Horowitz, J. A., Schlegel, J., Perruchoud, A. P., Kommoss, F., Bolliger, C. T., Kauczor, H. U., Dalquen, P., Fritz, M. A., *et al.* (1998). A phase I study of adenovirus-mediated wild-type p53 gene transfer in patients with advanced non-small cell lung cancer, Hum Gene Ther *9*, 2075-82.

Seya, T., Hirano, A., Matsumoto, M., Nomura, M., and Ueda, S. (1999). Human membrane cofactor protein (MCP, CD46): multiple isoforms and functions, Int J Biochem Cell Biol *31*, 1255-60.

Shand, N., Weber, F., Mariani, L., Bernstein, M., Gianella-Borradori, A., Long, Z., Sorensen, A. G., and Barbier, N. (1999). A phase 1-2 clinical trial of gene therapy for recurrent glioblastoma multiforme by tumor transduction with the herpes simplex thymidine kinase gene followed by ganciclovir. GLI328 European-Canadian Study Group, Hum Gene Ther *10*, 2325-35.

Shenk, T. S. (1996). Adenoviridae: the viruses and their replication, Fields Virology, Vol 2 (Philidelphia, Lippincott-Raven).

Simons, J. W., Mikhak, B., Chang, J. F., DeMarzo, A. M., Carducci, M. A., Lim, M., Weber, C. E., Baccala, A. A., Goemann, M. A., Clift, S. M., *et al.* (1999). Induction of immunity to prostate cancer antigens: results of a clinical trial of vaccination with

irradiated autologous prostate tumor cells engineered to secrete granulocyte-macrophage colony-stimulating factor using ex vivo gene transfer, Cancer Res *59*, 5160-8.

Singh-Jasuja, H., Scherer, H. U., Hilf, N., Arnold-Schild, D., Rammensee, H. G., Toes, R. E., and Schild, H. (2000). The heat shock protein gp96 induces maturation of dendritic cells and down-regulation of its receptor, Eur J Immunol *30*, 2211-2215.

Snitkovsky, S., and Young, J. A. (1998). Cell-specific viral targeting mediated by a soluble retroviral receptor- ligand fusion protein, Proc Natl Acad Sci U S A *95*, 7063-8.

Soiffer, R., Lynch, T., Mihm, M., Jung, K., Rhuda, C., Schmollinger, J. C., Hodi, F. S., Liebster, L., Lam, P., Mentzer, S., *et al.* (1998). Vaccination with irradiated autologous melanoma cells engineered to secrete human granulocyte-macrophage colony-stimulating factor generates potent antitumor immunity in patients with metastatic melanoma, Proc Natl Acad Sci U S A *95*, 13141-6.

Soldatenkov, V. A., and Smulson, M. (2000). Poly(ADP-ribose) polymerase in DNA damage-response pathway: implications for radiation oncology, Int J Cancer *90*, 59-67.

Sorscher, E. J., Peng, S., Bebok, Z., Allan, P. W., Bennett, L. L., Jr., and Parker, W. B. (1994). Tumor cell bystander killing in colonic carcinoma utilizing the Escherichia coli DeoD gene to generate toxic purines, Gene Ther *1*, 233-8.

Southern, P. J., and Berg, P. (1982). Transformation of mammalian cells to antibiotic resistance with a bacterial gene under control of the SV40 early region promoter, J Mol Appl Genet *1*, 327-41.

Srivastava, P. K., Menoret, A., Basu, S., Binder, R. J., and McQuade, K. L. (1998). Heat shock proteins come of age: primitive functions acquire new roles in an adaptive world, Immunity *8*, 657-65.

Srivastava, P. K., and Old, L. J. (1988). Individually distinct transplantation antigens of chemically induced mouse tumors, Immunol Today *9*, 78-83.

Sterman, D. H., Treat, J., Litzky, L. A., Amin, K. M., Coonrod, L., Molnar-Kimber, K., Recio, A., Knox, L., Wilson, J. M., Albelda, S. M., and Kaiser, L. R. (1998). Adenovirus-mediated herpes simplex virus thymidine kinase/ganciclovir gene therapy in patients with localized malignancy: results of a phase I clinical trial in malignant mesothelioma, Hum Gene Ther *9*, 1083-92.

Stojdl, D. F., Lichty, B., Knowles, S., Marius, R., Atkins, H., Sonenberg, N., and Bell, J. C. (2000). Exploiting tumor-specific defects in the interferon pathway with a previously unknown oncolytic virus, Nat Med *6*, 821-5.

Swisher, S. G., Roth, J. A., Nemunaitis, J., Lawrence, D. D., Kemp, B. L., Carrasco, C. H., Connors, D. G., El-Naggar, A. K., Fossella, F., Glisson, B. S., *et al.* (1999). Adenovirus-

mediated p53 gene transfer in advanced non-small-cell lung cancer, J Natl Cancer Inst *91*, 763-71.

Tailor, C. S., Nouri, A., and Kabat, D. (2000). Cellular and species resistance to murine amphotropic, gibbon ape, and feline subgroup C leukemia viruses is strongly influenced by receptor expression levels and by receptor masking mechanisms, J Virol *74*, 9797-801.

Tait, D. L., Obermiller, P. S., Hatmaker, A. R., Redlin-Frazier, S., and Holt, J. T. (1999). Ovarian cancer BRCA1 gene therapy: Phase I and II trial differences in immune response and vector stability, Clin Cancer Res *5*, 1708-14.

Takeuchi, Y., Cosset, F. L., Lachmann, P. J., Okada, H., Weiss, R. A., and Collins, M. K. (1994). Type C retrovirus inactivation by human complement is determined by both the viral genome and the producer cell, J Virol *68*, 8001-7.

Tatsuo, H., Ono, N., Tanaka, K., and Yanagi, Y. (2000). SLAM (CDw150) is a cellular receptor for measles virus, Nature *406*, 893-7.

Tatsuo, H., Ono, N., and Yanagi, Y. (2001). Morbilliviruses use signaling lymphocyte activation molecules (CD150) as cellular receptors, J Virol *75*, 5842-50.

Taylor, G. M., and Sanders, D. A. (1999). The role of the membrane-spanning domain sequence in glycoprotein- mediated membrane fusion, Mol Biol Cell *10*, 2803-15.

Thornberry, N. A., and Lazebnik, Y. (1998). Caspases: enemies within, Science *281*, 1312-6.

Thumm, M., Egner, R., Koch, B., Schlumpberger, M., Straub, M., Veenhuis, M., and Wolf, D. H. (1994). Isolation of autophagocytosis mutants of Saccharomyces cerevisiae, FEBS Lett *349*, 275-80.

Todryk, S., Melcher, A. A., Hardwick, N., Linardakis, E., Bateman, A., Colombo, M. P., Stoppacciaro, A., and Vile, R. G. (1999). Heat shock protein 70 induced during tumor cell killing induces Th1 cytokines and targets immature dendritic cell precursors to enhance antigen uptake, J Immunol *163*, 1398-408.

Tomonaga, M., Golde, D. W., and Gasson, J. C. (1986). Biosynthetic (recombinant) human granulocyte-macrophage colony- stimulating factor: effect on normal bone marrow and leukemia cell lines, Blood *67*, 31-6.

Tsukada, M., and Ohsumi, Y. (1993). Isolation and characterization of autophagy-defective mutants of Saccharomyces cerevisiae, FEBS Lett *333*, 169-74.

Turner, P. C. (2000). Ribozymes. Their design and use in cancer, Adv Exp Med Biol *465*, 303-18.

Udono, H., and Srivastava, P. K. (1993). Heat shock protein 70-associated peptides elicit specific cancer immunity, J Exp Med *178*, 1391-6.

van der Eb, M. M., Cramer, S. J., Vergouwe, Y., Schagen, F. H., van Krieken, J. H., van der Eb, A. J., Rinkes, I. H., van de Velde, C. J., and Hoeben, R. C. (1998). Severe hepatic dysfunction after adenovirus-mediated transfer of the herpes simplex virus thymidine kinase gene and ganciclovir administration, Gene Ther *5*, 451-8.

Vander Heiden, M. G., and Thompson, C. B. (1999). Bcl-2 proteins: regulators of apoptosis or of mitochondrial homeostasis?, Nat Cell Biol *1*, E209-16.

Vara, J. A., Portela, A., Ortin, J., and Jimenez, A. (1986). Expression in mammalian cells of a gene from Streptomyces alboniger conferring puromycin resistance, Nucleic Acids Res *14*, 4617-24.

Vile, R. G., Nelson, J. A., Castleden, S., Chong, H., and Hart, I. R. (1994). Systemic gene therapy of murine melanoma using tissue specific expression of the HSVtk gene involves an immune component, Cancer Res *54*, 6228-34.

Vile, R. G., and Russell, S. J. (1995). Retroviruses as vectors, Br Med Bull *51*, 12-30.

Vile, R. G., Russell, S. J., and Lemoine, N. R. (2000). Cancer gene therapy: hard lessons and new courses, Gene Ther *7*, 2-8.

Vogel, C. L., Cobleigh, M. A., Tripathy, D., Gutheil, J. C., Harris, L. N., Fehrenbacher, L., Slamon, D. J., Murphy, M., Novotny, W. F., Burchmore, M., *et al.* (2002). Efficacy and safety of trastuzumab as a single agent in first-line treatment of HER2-overexpressing metastatic breast cancer, J Clin Oncol *20*, 719-26.

Vogelstein, B., Lane, D., and Levine, A. J. (2000). Surfing the p53 network, Nature *408*, 307-10.

Voll, R. E., Herrmann, M., Roth, E. A., Stach, C., Kalden, J. R., and Girkontaite, I. (1997). Immunosuppressive effects of apoptotic cells, Nature *390*, 350-1.

von Kalle, C., Kiem, H. P., Goehle, S., Darovsky, B., Heimfeld, S., Torok-Storb, B., Storb, R., and Schuening, F. G. (1994). Increased gene transfer into human hematopoietic progenitor cells by extended in vitro exposure to a pseudotyped retroviral vector, Blood *84*, 2890-7.

Wang, E., Cross, R. K., and Choppin, P. W. (1979). Involvement of microtubules and 10-nm filaments in the movement and positioning of nuclei in syncytia, J Cell Biol *83*, 320-37.

Warren, T. L., and Weiner, G. J. (2000). Uses of granulocyte-macrophage colony-stimulating factor in vaccine development, Curr Opin Hematol *7*, 168-73.

Wassenberg, J. J., Dezfulian, C., and Nicchitta, C. V. (1999). Receptor mediated and fluid phase pathways for internalization of the ER Hsp90 chaperone GRP94 in murine macrophages, J Cell Sci *112*, 2167-75.

Webb, A., Cunningham, D., Cotter, F., Clarke, P. A., di Stefano, F., Ross, P., Corbo, M., and Dziewanowska, Z. (1997). BCL-2 antisense therapy in patients with non-Hodgkin lymphoma, Lancet *349*, 1137-41.

Weber, E., Anderson, W. F., and Kasahara, N. (2001). Recent advances in retrovirus vector-mediated gene therapy: teaching an old vector new tricks, Curr Opin Mol Ther *3*, 439-53.

Webster, A., Hay, R. T., and Kemp, G. (1993). The adenovirus protease is activated by a virus-coded disulphide-linked peptide, Cell *72*, 97-104.

Weiss, R. A., and Tailor, C. S. (1995). Retrovirus receptors, Cell *82*, 531-3.

Weissenhorn, W., Dessen, A., Calder, L. J., Harrison, S. C., Skehel, J. J., and Wiley, D. C. (1999). Structural basis for membrane fusion by enveloped viruses, Mol Membr Biol *16*, 3-9.

Weissenhorn, W., Dessen, A., Harrison, S. C., Skehel, J. J., and Wiley, D. C. (1997). Atomic structure of the ectodomain from HIV-1 gp41, Nature *387*, 426-30.

Welch, W. J., Kang, H. S., Beckmann, R. P., and Mizzen, L. A. (1991). Response of mammalian cells to metabolic stress; changes in cell physiology and structure/function of stress proteins, Curr Top Microbiol Immunol *167*, 31-55.

Wickham, T. J., Mathias, P., Cheresh, D. A., and Nemerow, G. R. (1993). Integrins alpha v beta 3 and alpha v beta 5 promote adenovirus internalization but not virus attachment, Cell *73*, 309-19.

Wild, T. F., Malvoisin, E., and Buckland, R. (1991). Measles virus: both the haemagglutinin and fusion glycoproteins are required for fusion, J Gen Virol *72*, 439-42.

Wildner, O., Blaese, R. M., and Morris, J. C. (1999). Therapy of colon cancer with oncolytic adenovirus is enhanced by the addition of herpes simplex virus-thymidine kinase, Cancer Res *59*, 410-3.

Wilson, I. A., Skehel, J. J., and Wiley, D. C. (1981). Structure of the haemagglutinin membrane glycoprotein of influenza virus at 3 A resolution, Nature *289*, 366-73.

Wyllie, A. H. (1980). Glucocorticoid-induced thymocyte apoptosis is associated with endogenous endonuclease activation, Nature *284*, 555-6.

Wyllie, A. H. (1993). Apoptosis (the 1992 Frank Rose Memorial Lecture), Br J Cancer *67*, 205-8.

Xie, M., Tanaka, K., Ono, N., Minagawa, H., and Yanagi, Y. (1999). Amino acid substitutions at position 481 differently affect the ability of the measles virus hemagglutinin to induce cell fusion in monkey and marmoset cells co-expressing the fusion protein, Arch Virol *144*, 1689-99.

Yanagi, Y. (2001). The cellular receptor for measles virus--elusive no more, Rev Med Virol *11*, 149-56.

Yang, C., and Compans, R. W. (1996). Analysis of the cell fusion activities of chimeric simian immunodeficiency virus-murine leukemia virus envelope proteins: inhibitory effects of the R peptide, J Virol *70*, 248-54.

Yang, C., and Compans, R. W. (1997). Analysis of the murine leukemia virus R peptide: delineation of the molecular determinants which are important for its fusion inhibition activity, J Virol *71*, 8490-6.

Yang, Y., Li, Q., Ertl, H. C., and Wilson, J. M. (1995). Cellular and humoral immune responses to viral antigens create barriers to lung-directed gene therapy with recombinant adenoviruses, J Virol *69*, 2004-15.

Yee, J. K., Friedmann, T., and Burns, J. C. (1994). Generation of high-titer pseudotyped retroviral vectors with very broad host range, Methods Cell Biol *43*, 99-112.

Yeh, W. C., Itie, A., Elia, A. J., Ng, M., Shu, H. B., Wakeham, A., Mirtsos, C., Suzuki, N., Bonnard, M., Goeddel, D. V., and Mak, T. W. (2000). Requirement for Casper (c-FLIP) in regulation of death receptor-induced apoptosis and embryonic development, Immunity *12*, 633-42.

Yu, D. C., Chen, Y., Seng, M., Dilley, J., and Henderson, D. R. (1999). The addition of adenovirus type 5 region E3 enables calydon virus 787 to eliminate distant prostate tumor xenografts, Cancer Res *59*, 4200-3.

Zerfass, K., Levy, L. M., Cremonesi, C., Ciccolini, F., Jansen-Durr, P., Crawford, L., Ralston, R., and Tommasino, M. (1995). Cell cycle-dependent disruption of E2F-p107 complexes by human papillomavirus type 16 E7, J Gen Virol *76*, 1815-20.

Zhang, L., and Ghosh, H. P. (1994). Characterization of the putative fusogenic domain in vesicular stomatitis virus glycoprotein G, J Virol *68*, 2186-93.

Zhang, W. W. (1999). Development and application of adenoviral vectors for gene therapy of cancer, Cancer Gene Ther *6*, 113-38.

Zhao, Y., Zhu, L., Benedict, C. A., Chen, D., Anderson, W. F., and Cannon, P. M. (1998). Functional domains in the retroviral transmembrane protein, J Virol *72*, 5392-8.

Zhu, N. L., Cannon, P. M., Chen, D., and Anderson, W. F. (1998). Mutational analysis of the fusion peptide of Moloney murine leukemia virus transmembrane protein p15E, J Virol *72*, 1632-9.

Zufferey, R., Dull, T., Mandel, R. J., Bukovsky, A., Quiroz, D., Naldini, L., and Trono, D. (1998). Self-inactivating lentivirus vector for safe and efficient in vivo gene delivery, J Virol *72*, 9873-80.

Zufferey, R., Nagy, D., Mandel, R. J., Naldini, L., and Trono, D. (1997). Multiply attenuated lentiviral vector achieves efficient gene delivery in vivo, Nat Biotechnol *15*, 871-5.

LIST of ABBREVIATIONS

Ad	adenovirus
APC	antigen presenting cell
ATP	adenosine triphosphate
BE	bystander effect
bp	base pair
BSA	bovine serum albumin
CD	cytosine deaminase
cDNA	complementary deoxyribonucleic acid
CARD	caspase activation and recruitment domain
CMV	cytomegalovirus
CPE	cytopathic effect
CTL	cytotoxic T lymphocyte
DAPI	4',6-Diamidine-2'-phenylindole dihydrochloride
dATP	deoxyadenosine triphosphate
dCTP	deoxycytosine triphosphate
dGTP	deoxyguanosine triphosphate
dTTP	deoxythymidine triphosphate
dNTPs	dATP, dCTP, dGTP, dTTP
DC	dendritic cell
DED	death-effector domain
DEPC	diethylpyrocarbonate
DISC	death-inducing signalling complex
DMEM	Dulbecco's modification of Eagle's medium
DMSO	dimethyl sulphoxide
DNA	deoxyribonucleic acid
ds	double stranded
EDTA	ethylenediaminetetraacetic acid
EGF	epidermal growth factor
ELISA	enzyme-linked immunosorbent assay
EM	electron microscopy
ER	endoplasmic reticulum
F	fusion
Facs	fluorescence activated cell sorting
FADD	Fas-associated death domain protein
5FC	5-fluorocytosine
FCS	foetal calf serum
FITC	fluorescein isothiocyanate
FMG	fusogenic membrane glycoproteins
g	relative centrifugal force
g	gramme
GALV	gibbon ape leukaemia virus
GAPDH	glyceraldehyde-3-phosphate dehydrogenase
GFP	green fluorescent protein
GM-CSF	granulocyte - macrophage colony-stimulating factor

H	haemagglutinin
HIV	human immunodeficiency virus
HSF	heat shock factor
HSP	heat shock protein
HSP-PC	heat shock protein-peptide complexes
HSVtk	Herpes simplex virus type 1 thymidine kinase
IRES	internal ribosome entry site
ITR	inverted terminal repeat
kb	kilobase
LDH	lactate dehydrogenase
LTR	long terminal repeat
M	molar
MHC	major histocompatibility complex
MLV	murine leukaemia virus
MMP	matrix metalloproteinase
moi	multiplicity of infection
MoMLV	Moloney murine leukaemia virus
MOPS	-3-(N-morpholino) propanesulphonic acid
mRNA	messenger ribonucleic acid
MV	measles virus
MW	molecular weight
PARP	poly(ADP-ribose) polymerase
PBS	phosphate buffered saline
PCR	polymerase chain reaction
pfu	plaque forming unit
PI	propidium iodide
PRO	proline rich region
RBD	receptor binding domain
RCV	replication competent virus
RCA	replication competent adenovirus
RNA	ribonucleic acid
RPMI	Roswell Park Memorial Institute 1640 (cell culture medium)
RT	room temperature
rtPCR	reverse transcriptase-PCR
RV	retrovirus
s.c.	subcutaneous
SDS	sodium dodecyl sulphate
SEER	surveillance, epidemiology and end results
SLAM	signalling lymphocytic activation molecule
Smac/DIABLO	second mitochondria-derived activator of caspases/Direct IAP-binding protein with low pI
SSC	standard saline citrate
SU	surface
TAE	Tris-acetate-EDTA buffer
TE	Tris-EDTA
TM	transmemebrane

Tris	tris[hydroxymethyl] aminomethane
TRITC	tetramethylrhodamine isothiocyanate
Tunel	terminal deoxynucleotidyl transferase-mediated deoxyuradine triphosphate nick end labeling
X-gal	5-bromo-4-chloro-3-indoyl-b-D-galactosidase
VSV	vesicular stomatitis virus
v/v	volume per volume
w/v	weight per volume